

Sustainable structural design of high-rise

*Life-cycle assessment of main load bearing structures
of high-rise buildings in the Netherlands*

G.J. Lankhorst

Sustainable structural design of high-rise

Life-cycle assessment of main load bearing structures of high-rise buildings in the Netherlands

by

G.J. Lankhorst

to obtain the degree of Master of Science
at the Delft University of Technology,
to be defended publicly on Thursday April 5, 2018 at 16:00 PM.

Student number: 4091558
Project duration: May 24, 2017 – April 5, 2018
Thesis committee: Prof. ir. R. Nijssse, TU Delft
Dr. ir. K. C. Terwel, TU Delft
Dr. ir. H. M. Jonkers, TU Delft
Ir. J. Arts, Royal HaskoningDHV

An electronic version of this thesis is available at <http://repository.tudelft.nl/>.

Cover image: Copyright by Milrose Consultants, inc.
url: <https://www.milrose.com/insights/code-question-is-my-building-considered-a-high-rise>
Cover design: Emma Wisse



Abstract

High-rise buildings are a potential solution to the environmental impact caused by the built environment and the increasing demand for space in urban areas[3][11][37][51]. As recent developments focus on reducing the impact by operational energy (OE) (heating, cooling, hot water and ventilation during use phase)[38][44][51], impact by the embodied energy (EE) (production, construction, maintenance and demolition of materials) becomes increasingly significant[39][51][58][64][65]. Structural materials account for the biggest part of embodied carbon (EC) in buildings[23]. The number of studies that address the environmental impact of high-rise building structures has grown only recently, research is still limited[21][51][52]. Moreover, it is doubtful to which extent these researches are applicable to the Netherlands.

This thesis aims to provide insight in the environmental impact of structural systems for high-rise buildings of 150, 200 and 250 meters in the Netherlands. Five different stability and three floor different systems were designed in cast-in-situ concrete, prefab concrete and steel. All of the models contained a concrete core. 2-dimensional static linear calculations were performed in order to determine the cross-sections and reinforcement. Through parametric modelling, an automated design and analysis work-flow was developed and a total number of 146 models was assessed.

The environmental impact was calculated by using the fast track life-cycle analysis (LCA) method. A cradle-to-gate analysis (production phase only, A1-3) was performed by using data from the Nationale Milieu Database (National Environmental Database) (NMD) and steel data from Bouwen met Staal, which contain the environmental impact for multiple impact categories, measured in environmental cost (shadow price). The construction and demolition phases were left out of scope.

It was found that all steel structures had a 6% to 35% higher cradle-to-gate environmental impact compared to concrete structures with the same stability and floor system. Furthermore, no significant differences were found between the cradle-to-gate impacts of cast-in-situ and prefab concrete models. Differences in impact between the materials are likely to be affected by inclusion of the construction phase (A4-5) and foundation structure. It is expected that the gap in environmental impact between steel and concrete is reduced by inclusion of these aspects. Floors were responsible for 32% up to 73% of the total environmental impact.

Regarding the stability systems, results showed that, when subjected to wind loads, systems with axially loaded elements scored significantly better than systems with elements loaded in bending. The outrigger structure decreased the total environmental impact of the concrete models by 5% to 16% and 20% to 26% of the steel models, compared to the tube structure. The braced tube only decreased the impact for the 200 and 250 meter models, with 7% to 12%, compared to the tube structures. The diagrid structure had the best performance at all heights and reduced the environmental impact by 17% to 28% for concrete and 28% to 41% for steel models, compared to the tube structures.

Acknowledgements

This thesis has been written as final part of my studies at Delft University of Technology, in order to obtain a Master's degree in Civil Engineering. The last year has been an exciting year for me, where I combined several of my main interests in Building Engineering and combined them into one thesis subject. This showed me the goals I want to pursue in the next coming years of my career.

I would like to thank my graduation supervisors and committee members Janko Arts, Karel Terwel, Henk Jonkers and Rob Nijse. First, I would like to thank Janko Arts for his practical approach, being supportive, keeping the final goal in sight and answering lots of my questions. Furthermore, I would like to thank Karel Terwel for both his academic and practical approach, knowledge, critical questions and his guidance, especially in the early phases of this thesis. Next I would like to thank Henk Jonkers for his extensive knowledge on sustainability and willingness to explain several concepts and answering my difficult questions. Lastly, I would like to thank Rob Nijse for his knowledge, questions and role as chairman of the graduation committee.

I would also like to thank my colleagues at Royal HaskoningDHV for the time and effort they took to answer my questions and the pleasant working environment.

Finally, I would like to thank my friends and family for their support and motivation during the writing of this thesis.

Gerran Lankhorst

Delft, March 2018

Contents

List of Figures	xi
List of Tables	xv
Nomenclature	xvii
1 Introduction	1
1.1 Relevance	2
1.1.1 Sustainability	2
1.1.2 High-rise buildings	2
1.1.3 Structural design	2
1.2 Current state of knowledge	4
1.3 Research objective and questions	5
1.3.1 Problem statement	5
1.3.2 Research objective	5
1.3.3 Research questions	5
1.3.4 Delimitations	5
1.4 Methodology	7
1.4.1 Phase 1: Literature review	7
1.4.2 Phase 2: Structural design	7
1.4.3 Phase 3: Environmental impact assessment	7
1.5 Report outline	8
2 Literature review	9
2.1 Definition of concepts	10
2.2 Structural design of high-rise buildings	11
2.2.1 Historical overview	11
2.2.2 Forces and response	11
2.2.3 Stability systems	12
2.2.4 Floor systems	17
2.3 Sustainable structural design	19
2.3.1 Minimizing material use / design for efficiency	19
2.3.2 Minimizing material production energy / design for materials	19
2.3.3 Minimizing embodied energy / design for energy	19
2.3.4 Maximizing structural system reuse / design for recycling/adaptability	19
2.3.5 Life-cycle analysis	20
2.4 Sustainable structural design of high-rise buildings	22
2.4.1 Van Hellenberg Hubar (2009)	22
2.4.2 Foraboschi, Mercanzin and Trabucco (2014)	22
2.4.3 Trabucco et al (2016), CTBUH	23
2.5 Summary	25
3 Structural design	27
3.1 General geometry	28
3.1.1 Floor-to-floor height and building height	28
3.1.2 Floor plans and core dimensions	28
3.2 Loads and performance criteria	30
3.2.1 Vertical loads	30
3.2.2 Wind loads	30
3.2.3 Load combinations	31
3.2.4 Performance criteria	32

3.3	Stability system design	33
3.3.1	1. Frame	34
3.3.2	2. Outrigger	35
3.3.3	3. Tube	36
3.3.4	4. Braced tube	37
3.3.5	5. Diagrid	38
3.3.6	Materials	39
3.3.7	Design restrictions	39
3.4	Floor design	40
3.4.1	Flat slab floor (FSF)	40
3.4.2	Hollow core slab floor (HCSF)	41
3.4.3	Composite floor (CF)	42
3.5	Modelling method	44
3.5.1	Calculation model for global design	44
3.5.2	Loads	50
3.5.3	Design checks	50
3.5.4	Calculation model for reinforcement design	53
3.5.5	Implementation in Grasshopper	56
3.6	Results	58
3.7	Summary	59
4	Life-cycle assessment	61
4.1	Methodology	62
4.1.1	Goal and scope	62
4.1.2	Functional unit	62
4.1.3	System boundaries	62
4.1.4	Life-cycle inventory	63
4.1.5	Quantification of materials	64
4.2	Results	65
4.2.1	Interpretation of results	70
4.3	Comparison with literature	73
4.4	Factors of influence	75
4.4.1	Sensitivity analysis on shadow prices of materials	75
4.4.2	Reuse of steel elements	77
4.4.3	Fire resistant material	78
4.4.4	Foundation structure	78
4.4.5	Transportation	78
4.4.6	Construction phase	79
4.5	Summary	81
5	Conclusion	83
6	Discussion	87
6.1	Research and results	88
6.2	Future research and potential	89
	Bibliography	91
A	Foundation stiffness	95
B	Floor design	99
B.1	Flat slab floor	100
B.1.1	One-way spanning design	100
B.1.2	Two-way spanning design	100
B.1.3	Anchorage lengths	102
B.2	Hollow core slabs	105
B.3	Composite floors	110

C	Fire safety design	115
D	Reinforcement design	123
D.1	Reinforcement design beams	124
D.2	Reinforcement design columns	126
D.3	Reinforcement design core	128
D.4	Data visualisation	131
E	Frame and tube behaviour	133
F	Validation of calculation models	139
F.1	Frame and tube models	140
F.1.1	Verification with hand calculation	143
F.2	Diagrid models	144
G	Results	147

List of Figures

1.1	Average breakdown of embodied carbon	3
2.1	Life cycle stages	10
2.2	The Home Insurance Building in Chicago.	11
2.3	Cross-wind response	12
2.4	Premium for height	12
2.5	Interior structures	13
2.6	Exterior structures	13
2.7	Shear lag	15
2.8	Shear wall-frame interaction forces due to restricted deformations[2]	15
2.9	Outrigger structure	15
2.10	Optimal locations for 1, 2 and 3 outriggers according to Smith[47].	16
2.11	Different optional floor systems for use in buildings.	18
2.12	The life cycle of a structure and the corresponding phases according to EN 15804[49].	21
2.13	Integral cost (environmental + actual cost) for several stability systems of 3 heights.	22
2.14	Embodied energy of the flooring system as a function of height	23
2.15	LCA results of the 60-storey equivalent scenario	24
3.1	Schematic impressions of the core sizes.	29
3.2	Distribution of the wind pressure over the height of the building[32].	31
3.3	Conceptual elevation view of the used stability systems.	33
3.4	Column configurations used in the frame models.	34
3.5	Configuration of the outrigger models.	35
3.6	Configuration of the tube models.	36
3.7	Tube column and beam cross-sections.	36
3.8	Elevation view of the braced tube model.	37
3.9	Force flow in the belt-truss when subjected to vertical loads.	37
3.10	Configuration of the diagrid models.	38
3.11	Design restrictions for the concrete models.	39
3.12	Graphic view of m_x of a flat slab floor model in SCIA.	41
3.13	An example of a possible hollow core slab floor configuration.	42
3.14	Sketch impression of the composite floor configuration on castellated beams.	43
3.15	Possible configuration of a composite floor, including primary and secondary beams.	43
3.16	2-dimensional model of the core and explanation of the Schueller rule.	44
3.17	2-dimensional model of the frame model.	45
3.18	2-dimensional models of the outrigger structures.	46
3.19	2-dimensional calculation model of the frame and tube model.	47
3.20	2-dimensional model the braced tube models.	48
3.21	2-dimensional model the diagrid models.	49
3.22	Figures showing the way of modelling the vertical loads in the 2-dimensional models.	50
3.23	Simplified model of the second order effect.	51
3.24	Determination of A_p for profiles subjected to fire conditions from 4 and 3 sides.	52
3.25	Shifting moment lines in beams due to differential column shortening.	53
3.26	Shifting moment lines in columns due to differential column shortening.	54
3.27	Sketch showing the way of modelling for designing the reinforcement of the core.	55
3.28	Flowchart of the entire work flow showing the links between the main model and sub-models.	57
3.29	Overview of all the model variations after structural calculations.	58

4.1	Typical distribution of environmental impact by materials for the three different floor types.	65
4.2	Environmental impact of the 150-meter models in environmental cost per material.	66
4.3	Environmental impact of the 200-meter models in environmental cost per material.	67
4.4	Environmental impact of the 250-meter models in environmental cost per material.	68
4.5	Environmental impact of all the models with hollow core slab floors.	69
4.6	Summary of the results with the best and worst scoring models per material per height.	72
4.7	Results of the sensitivity analysis on the three main materials.	76
4.8	Environmental impact by transportation for one design case.	80
A.1	Conceptual impression of the deflection by stiffness of the building and the foundation represented by springs.	97
A.2	Pile foundation design for the 200-meter prefab concrete tube model with 10 columns and a hollow core slab floor.	97
B.1	Simply supported beam with moment distribution for the one-way spanning zone of the slab modelled as a beam.	100
B.2	Table 25 from GTB 2013[5] which identifies the reinforcement design moments in a flat slab floor with two edges as hinged line supports.	101
B.3	Model identifying the chosen perimeter and virtual column measurements for the punching shear model.	102
B.4	Reinforcement drawing of the bottom reinforcement in the flat slab floor for the 150-meter models.	103
B.5	Reinforcement drawing of the top reinforcement in the flat slab floor for the 150-meter models.	104
B.6	Overview of the hollow core slab configurations for the 150-meter diagrid models. The THQ beams are indicated as THQ400-150 where 400 is the height (mm) and 150 the weight (kg/m) of the profile.	106
B.7	Overview of the hollow core slab configurations for the 200-meter diagrid models. The THQ beams are indicated as THQ400-150 where 400 is the height (mm) and 150 the weight (kg/m) of the profile.	107
B.8	Overview of the hollow core slab configurations for the 250-meter diagrid models. The THQ beams are indicated as THQ400-150 where 400 is the height (mm) and 150 the weight (kg/m) of the profile.	108
B.9	Overview of the hollow core slab configurations for the all other models. The THQ beams are indicated as THQ400-150 where 400 is the height (mm) and 150 the weight (kg/m) of the profile.	109
B.10	Overview of the composite floor configurations for the 150-meter diagrid models. The castellated beams are indicated as IPE300-600 where IPE300 is the original profile and 600 is the height of the castellated beam.	111
B.11	Overview of the composite floor configurations for the 200-meter diagrid models. The castellated beams are indicated as IPE300-600 where IPE300 is the original profile and 600 is the height of the castellated beam.	112
B.12	Overview of the composite floor configurations for the 250-meter diagrid models. The castellated beams are indicated as IPE300-600 where IPE300 is the original profile and 600 is the height of the castellated beam.	113
B.13	Overview of the composite floor configurations for all other models. The castellated beams are indicated as IPE300-600 where IPE300 is the original profile and 600 is the height of the castellated beam.	114
D.1	Table 11.6 from GTB 2013 for determining the required reinforcement of the concrete beams. A similar table is used for C55/67.	125
D.2	Design graph 103.a from GTB 2013 for determining the required reinforcement of the concrete columns. A similar design graph is used for C55/67.	127
D.3	Sketch showing the way of modelling for designing the reinforcement of the core.	128
D.4	The left side of the spreadsheet that is used to determine the applied reinforcement of the core.	129
D.5	The right side of the spreadsheet that is used to determine the applied reinforcement of the core.	130

D.6	Visual representation of the required reinforcement in concrete elements for a 150-meter frame model.	131
E.1	The 3-dimensional validation model in SCIA.	141
E.2	The 2-dimensional validation model with the rule by Schueller[46] to cover for the shear lag aspect.	141
E.3	Comparison of global deflection of the 3- and 2-dimensional models for 8 columns.	142
E.4	Comparison of global deflection and corner column support reaction of the 3- and 2-dimensional frame/tube models for 6, 8 and 10 columns.	142
E.5	Simplification of the tube structure for the purpose of a hand calculation.	143
E.6	The 3-dimensional validation model in SCIA.	144
E.7	The 2-dimensional validation model with increased areas of the corner columns.	145
E.8	Comparison of global deflection and corner column support reaction of the 3- and 2-dimensional diagrid models.	146

List of Tables

2.1	Impact categories and their corresponding environmental cost and units[49].	21
3.1	An overview of the core dimensions of several office buildings.	28
3.2	Assumptions for calculation of the wind loads.	30
3.3	Material properties as used in this thesis.	39
3.4	Maximum width of column elements in millimetre for different amount of columns.	39
3.5	Hollow core slab properties and area loads.	41
3.6	Composite floor slab properties.	43
3.7	Factors used for calculating axial forces in columns.	47
3.8	An overview of which forces are used from which model for reinforcement design.	53
3.9	Requirements to the minimum width and cover of simply supported and continuous beams.	54
3.10	Requirements to the minimum width and cover of columns for fire safety in mm.	55
4.1	Life-cycle inventory showing the used materials and their shadow prices.	64
4.2	Meaning of the abbreviations used in the results.	65
B.1	Anchorage lengths in mm for the different bar diameters for C35/45.	102
B.2	Hollow core slab properties and area loads.	105
B.3	Composite floor slab properties.	110
D.1	Requirements to the minimum width and cover of simply supported and continuous beams in mm.	124
D.2	Requirements to the minimum width and cover of columns for fire safety in mm.	128
F.1	Dimensions that are used in the frame/tube validation models.	140
F.2	Dimensions that are used in the diagrid validation models.	144

Nomenclature

BIM	Building Information Modelling
BF	Blast Furnace
CO_{2e}	carbon equivalent
CTBUH	Council of Tall Buildings and Urban Habitat
EA	Electric Arc Furnace
EC	embodied carbon
EE	embodied energy
EPC	energy performance coefficient
EPD	environmental product declaration
FEA	finite element analysis
GFA	gross floor area
GWP	global warming potential
GHG	greenhouse gases
LCA	life-cycle analysis
LCI	life-cycle inventory
LCIA	life-cycle impact assessment
MRPI	Milieu Relevante Product Informatie (Environmental Relevant Product Information)
NFA	net floor area
NMD	Nationale Milieu Database (National Environmental Database)
OE	operational energy
SSD	sustainable structural design
TU Delft	Delft University of Technology

1

Introduction

Chapter 1 gives an introduction into the subject and describes the relevance of this research. A gap in knowledge is identified out of which the research questions and objectives follow. At the end a description of the delimitations and research methodology is given.

1.1. Relevance

1.1.1. Sustainability

Climate change is a fact and the environment is at risk. The increased greenhouse gas emissions are the cause of an increasing temperature and rising sea level. It is estimated that in the coming century, the sea level will rise with 26 to 82 centimetres[50]. Next to the global warming potential, also depletion of resources, depletion of the ozone layer, and lots of other environmental effects are causing risks to our ecosystem and lives.

The built environment is a key contributor to global greenhouse gas emissions[38] and buildings are held accountable for 30-40% of all primary energy used worldwide[54]. Therefore, the industry is researching possible ways to reduce the environmental impact of buildings.

1.1.2. High-rise buildings

In 1950, 30% of the world population lived in urban areas, this increased to 47% in 2000. United Nations projects that by 2030 this will rise to 60%, which comes down to 5 billion people worldwide[55]. However, space in urban areas is limited and therefore expensive. High-rise buildings prove to be efficient in terms of spatial needs.

There has been debate about the material and energy efficiency of high-rise buildings[1][21][53]. The tall building industry has been reacting with a delay to the call for sustainability, compared to the rest of the building industry. However, it has been shown by a growing amount of examples that designing tall energy efficient buildings is possible[51]. Next to that, in terms of urban planning, vertical cities also have a potential to reduce the need for transportation[3]. Moreover, it depends on how you measure the environmental impact when you compare building typologies. If you compare the environmental impact of a multi-storey condominium versus an ordinary dwelling, the condominium has a higher impact per square meter. However, if you measure per inhabitant it might be the case that the condominium has the lowest impact[37].

Apart from reduction in energy, high-rise buildings also form potential energy producers. The use of photovoltaic cells is already common within the building industry. Also the use of aerodynamic shapes and wind turbines in building slots to generate energy at great heights, as in the Strata SE1 building in London and the Pearl River Tower in Guangzhou, is seen more often. A possible future development might be integrating solar updraft towers in high-rise buildings[11]. Here energy is generated by turbines in a tower where air is passing through using a chimney effect.

Newly build high-rise buildings are still in demand and previous mentioned developments show that this demand is not likely to decrease. Examples like the recently finished Ministry buildings in The Hague (146 meters), 'De Rotterdam' (149 meters), proposed 'Zalmhaventoren' (212 meters) and contests for higher high-rise buildings (250 meters) show us that demand for high-rise buildings is also still present in the Netherlands.

1.1.3. Structural design

From January 1 2021 and on, the Dutch government wants new buildings to be 'near energy neutral'. This concerns the operational energy (OE) which includes heating, cooling, hot water and ventilation. However, it does not address the total life cycle of a building. The embodied energy (EE), which includes material supply, production, transport, construction, transportation to the building site and construction works are not accounted for. This part is estimated to be responsible for 10% to 20%[43] or even up to 33%[38] of the total carbon produced to operate a building for a 50-year service life.

Most of the research that has been done on improving sustainability of buildings, focussed on reducing energy during the operational phase[38][44][51][58]. As future buildings will be designed to net-zero energy standards, the carbon associated with the initial construction will represent a very significant increasing part of the total carbon emitted[39][51][58][64][65], possibly increasing to 100%[43]. Moreover, countries are switching to renewable energy sources, which also lead to a reduction of emitted carbon in the operational phase.

Apart from the above mentioned improvements regarding operational energy efficiency of buildings, gov-

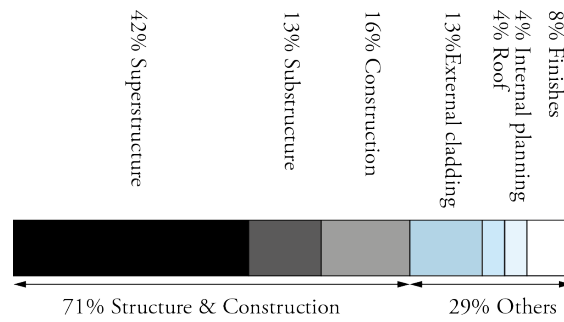


Figure 1.1: Average breakdown in building elements of embodied carbon in offices, hospitals and schools[18][23].

ernments are facing the challenge to reduce greenhouse emissions on the short term. Recently signed agreements, like the one in Paris in 2016, ensure that governments already have to make improvements in the next coming years. Improvements in operational energy efficiency may take many years to accumulate, while any reduction to the embodied energy of a building would contribute to the short term goals[38].

This research will focus solely on the structural design. This has to do with the fact that structure accounts for the biggest part of embodied carbon (EC) in buildings[23] as seen in figure 1.1. Additionally, it helps to focus attention on a well-defined quantity, while still having a significant impact[18].

1.2. Current state of knowledge

This section shows a short description of the literature that is reviewed in chapter 2. A more elaborated description can be found there, including explanations of several concepts and terminology.

As illustrated in section 1.1.2, the expectation is that the demand for high-rise buildings in urban areas will grow in the coming decades. However, next to the opportunities they create regarding energy production, they also have a big downside regarding material use. Tall buildings have to cope with large horizontal, due to wind and earthquakes, and vertical forces. This results in the 'premium for height', introduced by Fazlur Khan[25], described in section 2.2.3. As buildings grew taller and taller, more innovative stability systems were introduced.

Sustainable structural design has been introduced into the structural engineering discipline in the last decades. Many strategies are possible to decrease the environmental impact of structures of buildings. These strategies, formulated by Danatzko & Sezen[16] and Anderson & Silman[4], are described in section 2.3. Not all of these strategies are applicable, yet, to the design of tall buildings. For instance, reuse of materials for construction of new buildings is rather complicated, since tall buildings taller than 100 meters are often not demolished yet. A common tool for determining the environmental impact of the structure is the life-cycle analysis (LCA), as described in section 2.3.5. In the Netherlands it is common to address the environmental impact of the structure in environmental cost, or shadow prices, as explained in section 2.1.

The number of studies that address the environmental impact of high-rise building structures has grown only recently, research is still limited[21][51][52]. Several case-studies have been executed, but often fail to relate to the bigger picture[51]. In section 2.4, three researches are shown, including a research by Council of Tall Buildings and Urban Habitat (CTBUH) led by Trabucco[52] dating from 2016. This two-year study focusses on a variety of stability systems in steel and concrete for two buildings of 60 and 120 storeys in Chicago. Environmental impact is measured using global warming potential (GWP) and EE and the total life-cycle is addressed.

Secondly, a research by Foraboschi[21] dating from 2014, shows the relation between different floor systems and the environmental impact for a variety of heights in the range of 20 to 70 storeys. This study focusses more on the floor systems rather than the stability system, only two structural systems are regarded, since a big part of the material is incorporated in the floors. The environmental impact is measured cradle-to-gate in terms of EE for buildings in Italy.

Lastly, a research by Van Hellenberg Hubar[57] dating from 2009, shows the environmental impact for a couple of stability systems for the range of 70 to 136 meters. He addressed sustainability in a broader view, focussing on flexibility of the floor systems and also by combining environmental cost and actual cost.

1.3. Research objective and questions

1.3.1. Problem statement

In structural engineering, many engineers tend to underestimate their role in reducing the environmental cost in sustainable building design[63]. A change in attitude towards sustainability in structural design of high-rise is needed[16][45][51]. A better understanding of the environmental impact of structural systems, could create more awareness among structural engineers about their role in this part.

Reading section 1.2, it can be seen that no research has been done yet into the environmental impact in the 150 to 250 meters range for a wide range of stability systems. This is exactly the range which will be of interest for future high-rise projects in the Netherlands. Additionally, regulations, conditions, the building industry and environmental impact data in the Netherlands differ from North America and the rest of the world, which could lead to different results. This is supported by one of the conclusions in the research by Trabucco that the results are only applicable for the considered case study[52].

1.3.2. Research objective

Reading section 1.3.1, the following main research objective can be identified:

“Provide insight in the environmental impact of structural systems in cast-in-situ concrete, prefab concrete and steel of high-rise buildings in the range of 150 to 250 meters in the Netherlands.”

1.3.3. Research questions

Reading the problem statement, the following main research question can be formulated:

“To what extent is it possible to minimise the environmental impact of the main load bearing structure of high-rise, in the range of 150 to 250 meters in the Netherlands, by varying the structural system and the materials cast-in-situ concrete, precast concrete and steel?”

In order to answer the main research question, sub questions have been formulated:

- What are the possible main load bearing structures, loads and performance criteria for high-rise?
- What is sustainable structural design and how do you measure the environmental impact of the main load bearing structure?
- How is sustainable structural design related to high-rise and what is the current state of knowledge?
- What is the relation between different main load bearing structures and materials, for high-rise of 150 to 250 meters, and their environmental impact?

1.3.4. Delimitations

In order to keep this study manageable in terms of time and scope, delimitations are set. These delimitations are smartly chosen and consider the quality of the research. They are listed below.

Height The height of the considered buildings are 150, 200 and 250 meters, this follows from section 1.3.1.

Shape The shape of the considered buildings are rectangular and in compliance with Dutch regulations regarding daylight entry. Shape optimisation to reduce wind loads (e.g. aerodynamic shapes, building slots, rough corners and stepping geometry) will not be taken into account as each case would benefit from this approach.

Function The considered function of the buildings will be office. This has been chosen due to time limitations.

Core Assumed is that every building will have a concrete core, due to the fact that more disciplines benefit from this structure (e.g. fire safety for protected escape routes, vertical transportation, etc.). The size of the core is aimed to be in compliance with the needs for vertical transport and escape routes, based on Dutch reference projects.

Demolition Demolition of the high-rise buildings won't be taken into account in the calculation of the environmental impact of the building. Examples of demolished high-rise buildings (>150 meters) are very limited[38]. In the study by CTBUH[52], this aspect was covered by sending the building designs to a few demolition companies, only for the 246 meters scenario. This is not considered to be a realistic approach for this research, considering the time limitations.

Reuse Reuse strategies as being discussed in section 2.4, are not taken into account in this research. This has a couple of reasons. First, taking into account this strategy would rely on too much assumptions, because of the time limitations of this research. It could be considered as a graduation project on its own. Second, since demolition is not taken into account, reuse of the structure or components can also not be taken into account. Third, the examples of reused structural systems or components are very limited, especially for high-rise buildings. Fourth, examples of function changes are also very limited and require a higher investment, in both actual and environmental cost, at the start.

Structural design The structural design and calculations will be done according to the Dutch regulations regarding global strength and stiffness.

Loads Loading of the structure will consist of dead loads and live loads. Horizontal live loads will only consist of wind load, according to Dutch regulations. Earthquake loads are not considered, because of the lack of heavy earthquakes in the Netherlands.

Columns Internal columns, between the façade and the core, are not considered as an option in the design as this would decrease the flexibility of the space and the architectural value of the building.

Construction The construction phase of the building is not taken into account in the calculation of the environmental impact due to lack of data and available time.

Materials The considered materials in this research are cast-in-situ concrete, precast concrete and steel. Timber is not considered because of the lack of high-rise buildings in timber for these heights. However, it is a very interesting sustainable development and its options should be explored.

Foundation systems Design and calculation of the foundation is not taken into account in this research. Due to the wide variety of available foundation systems, this would significantly increase the number of design cases. Rotational spring stiffness of the foundation is taken into account when determining the stiffness and second order effect of the building.

Fire safety Structural fire safety is only taken into account on element level. This means that elements are required to remain their structural resistance for a period of time. For concrete this results in a minimum distance of the reinforcement. Steel members are clad with fire resistant material based on their profile factor and standard design tables by the manufacturer. Fire safety regarding smoke control, escape routes and crowd management will not be taken into account in the design.

Stability systems The following stability systems are considered: rigid frame with core, outrigger structure, framed tube with core, diagonal braced tube with belt-trusses and core and a diagrid structure with core. The excluded stability systems, as seen in section 2.2, are considered non-desirable regarding internal columns or inefficient in terms of required material for the considered heights.

Floor systems A flat slab floor, hollow core slab floor and composite floor are the considered options in this research. Post-tensioning will not be considered as an option due to the amount of extra required time in the construction phase. As is described in section 2.4, weight reducing systems as a BubbleDeck floor are less sustainable in terms of EE[21]. The Slimline floor is considered as a good alternative if function changes are taken into account[57]. However, function changes are excluded from this research. Additionally, the diaphragm action of the Slimline floor is not yet proven in high-rise buildings of this height and proved to be a problem at the European Patent Office building in Rijswijk.

1.4. Methodology

The research is divided into 3 phases which are explained in the paragraphs below.

1.4.1. Phase 1: Literature review

First, literature will be reviewed in order to retrieve more knowledge about the following three subjects: structural design of high-rise buildings, sustainable structural design (SSD) and current available research on environmental impact of high-rise building structures.

Regarding structural design of high-rise, information is gathered about materials, stability systems, floor systems, loads and fire safety. Additionally, floor plans and core sizes of several buildings are studied in order to create a rough design for use in this research. Next, a broad view on SSD is given including several strategies, different ways of measuring the environmental impact and a description on how to use LCA as a tool to measure the environmental impact of structures. At last, three different studies are discussed and summarised which elaborated on the environmental impact of high-rise building structures. The approach, conditions, results and conclusions are discussed and summarised, where-after the applicability to the considered cases in this thesis is discussed.

1.4.2. Phase 2: Structural design

After the literature study is done, the structural design phase is started. First, the geometry is designed based on daylight entry regulations and reference projects for determining the core dimensions. Three different heights are considered: 150, 200 and 250 meters.

The characteristics and conditions of the different stability systems are identified on a conceptual level. The main load bearing structures are designed for the design cases. The frame, tube and diagrid systems are split into sub-variations where column spacing is held variable, since the floor design for hollow core slab and composite floors heavily depends on the amount of supports in the façade. Floor systems are designed and dimensions are assigned to the supporting structure.

The 3-dimensional structural designs are converted into 2-dimensional parametric calculation models, because of the possibility for high-speed calculations and possible small geometric design changes. The weight of and loads on the floors are incorporated by introducing point and line loads in the calculation models. The 2-dimensional calculation models are evaluated and improved by comparing them to corresponding 3-dimensional models.

Cross-sections of the elements are estimated and designed while constantly monitoring the global and local stiffness and strength criteria. Reinforcement of the concrete elements is determined parametrically using design rules from GTB 2013[5]. Limitations are set to the maximum size of the cross-sections to ensure enough daylight entry into the building. When one or more of these criteria can not be satisfied, the design case is excluded from further use in the research.

The result of the structural design phase are building structure designs with the cross-sections optimised to the global and local stiffness and strength criteria.

1.4.3. Phase 3: Environmental impact assessment

Material quantities of the design cases are gathered and collected into spreadsheets. The environmental cost of the materials are gathered from the Nationale Milieu Database (National Environmental Database) (NMD) and Bouwen met Staal (Build with Steel), and assigned to the material quantities that are determined using results from phase 2. This results in an environmental impact per design case.

An analysis is made of the materials, elements and other factors that have a high impact on the environmental impact in order to discover possible trends. The results of this analysis are discussed and possible areas of improvement are proposed. Factors of influence on the results are discussed and a short sensitivity analysis is presented. Additionally, the GWP of the design cases is determined in order to relate the results of this research to other studies mentioned in section 2.4.

1.5. Report outline

The structure of this thesis follows the chronological order of the methodology as discussed in the previous section. In chapter 2 the literature review can be found. Chapter 3 describes the methodology, modelling methods and work-flow of the structural design phase. Chapter 4 describes the methodology used for the LCA and discusses the results and possible factors of influence. At last the conclusion and discussion can be found in chapter 5 and 6.

2

Literature review

Within this chapter, background information about structural design of high-rise buildings, sustainable structural design and life cycle assessment is presented. Furthermore, an overview of recent literature within the subject of sustainable structural design of high-rise buildings is given.

2.1. Definition of concepts

This paragraph presents a short overview of the used concepts in this thesis, in order to cover for misconceptions.

Operational energy (OE) is the energy used during the operational (use) phase of a building, see figure 2.1. This includes heating, cooling, hot water and ventilation.

Embodied energy (EE) is the energy used for the production, construction and end-of-life phase of a building, see figure 2.1. This includes energy used for the material extraction, material processing and product manufacturing, the transport of products to the construction site, the construction of a building and the demolition at the end of life. It is all the life-cycle energy excluding operational energy (OE).

Embodied carbon (EC) is the carbon produced by the embodied energy. The same amount of embodied energy can produce different amounts of embodied carbon depending on the fuel used and the carbon emitted or absorbed by the materials. It is more useful to measure in embodied carbon rather than embodied energy, because CO₂ significantly contributes to climate change. Furthermore, using carbon enables to compare the embodied with the operational emissions. Quantifying carbon therefore facilitates the assessment of the whole life-cycle impact of buildings[23].

Carbon equivalent (CO_{2e}) represents the equivalent of *greenhouse gases (GHG)* in carbon dioxide. CH₄, N₂O, SF₆, PFC and HFC are converted into CO_{2e} using conversion factors in order to obtain a common unit for the environmental impact.

Global warming potential (GWP) is the total embodied carbon of a building expressed in kg CO_{2e} per functional unit. A functional unit is a specified metric to normalize the carbon footprint of buildings, in order to compare ‘apples to apples’[18]. Common used functional units are floor area or number of occupants, where global warming potential (GWP) becomes kg CO_{2e}/m² or kg CO_{2e}/occupant respectively.

Environmental cost is an indication of the social cost to fight the consequences of a certain environmental impact. Several kinds of impact categories like emitted carbon, other GHG, resource depletion, ozone layer depletion, human toxicity and more are quantified into environmental cost in order to obtain a common unit. The environmental impact for different kinds of aspects are quantified for each material and then converted into environmental cost by addressing cost to each impact category. **Environmental cost** goes beyond GWP in measuring the environmental impact, because multiple impact categories are taken into account. Additionally, the environmental impact can be understood more easily as environmental impact is monetised and related to the **actual cost** of the structure.

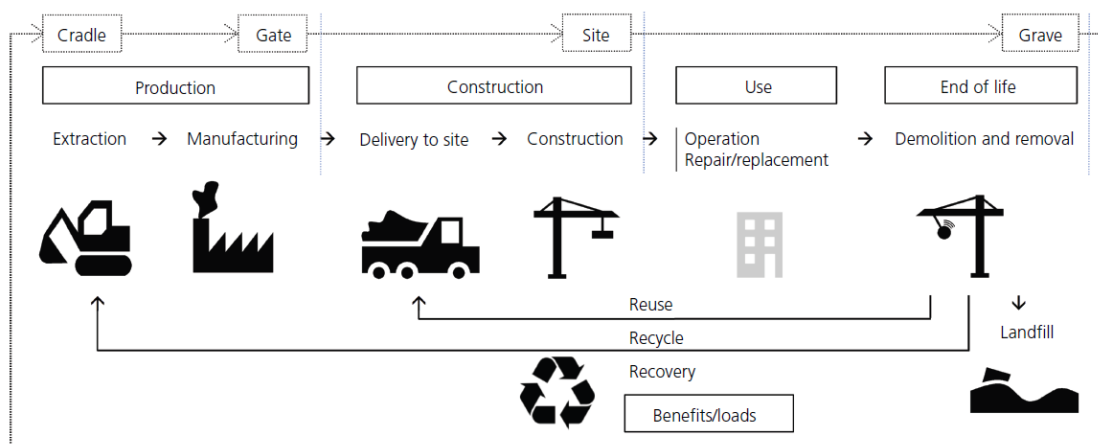


Figure 2.1: Life cycle stages: embodied and operational energy[14][17].

2.2. Structural design of high-rise buildings

In this section a short overview is given on aspects related to structural design of high-rise. Information is primarily gathered from Sarkisian[43], unless otherwise stated.

2.2.1. Historical overview

During the late 1800s, technological advancements led to the development of cast iron during the United States' industrial revolution. This material had a high strength and enabled prefabrication and fast erection on-site. Next to that, the fire of 1871 in Chicago created an opportunity to rethink design and construction in an urban environment. This led to the construction of the first skyscraper, the Home Insurance Building of 12 storeys in 1885 as depicted in figure 2.2.

Fuelled by identity and egos, a tall building boom in the late 1920s and early 1930s led to the construction of the Empire State Building. It remained the tallest building in the world for 41 years. In the Netherlands, it was not until the 1980s that the interest for high-rise buildings was beginning to develop. Rotterdam began to develop itself as the Dutch city for high-rise buildings, but also other cities followed.

Nowadays, focus is more on technology and the environment has been a growing aspect of attention. Buildings are still constructed higher and higher, suggesting that the limit has not yet been reached.

2.2.2. Forces and response

Tall buildings have to cope with large forces, both vertically and horizontally. Vertically, the gravity ensures that forces gradually increase from top to bottom. The forces depend on the weight of the structure and its intended function.

Horizontally, the largest forces originate from wind in the Netherlands. Wind causes large shear forces and base moments. Often it is the case that wind forces causes deflections that are governing for the design instead of strength of structural members. These deflections can be the global deflections at the top of the tower or inter-storey drift. Typically a 50-year return period is considered for serviceability. When considering wind for tall buildings, not only along-wind loading is important, but also cross-wind loading should be considered as seen in figure 2.3. This phenomenon is caused by the dynamic effects of wind on towers. Normal forces are applied to the perpendicular sides of towers when wind is applied and vortex shedding is developed.



Figure 2.2: The Home Insurance Building in Chicago.

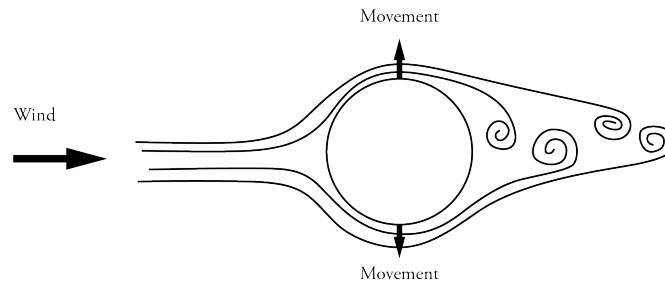


Figure 2.3: Cross-wind response of a tower.

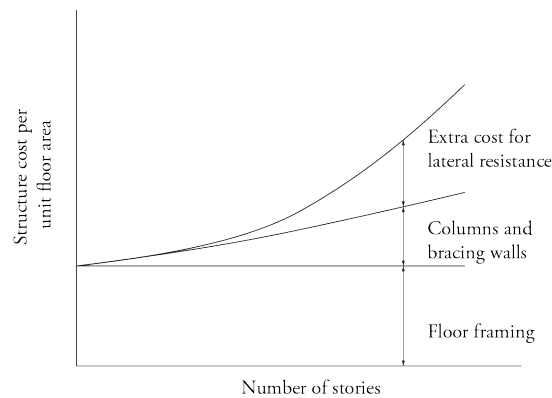


Figure 2.4: The premium for height by Fazlur Khan[18][25]

In seismic active areas, like Japan, earthquakes cause the biggest horizontal forces for a tall building. However, due to their flexible behaviour, tall buildings attract less force from the ground than those with a high stiffness, like low-rise buildings. In the Netherlands, areas prone to small earthquakes exist, like Groningen or Limburg. However, for tall buildings, these are not governing over wind loads in design due to the relatively long natural periods of the structures.

As said, tall buildings behave rather flexible. Often the flexible behaviour of tall buildings is expressed in their natural period, the time needed to sway for a certain natural mode. These natural periods are influenced by the stiffness, but also the mass of the building. Increasing the mass will cause the natural period to increase. Increasing the stiffness will cause the natural period to decrease.

2.2.3. Stability systems

There are many possible ways to achieve the required stiffness of a tall building. Depending on the height and the geometry, several options are available in terms of stability systems. These systems can be constructed with steel, concrete or a combination of the two.

Fazlur Khan[25] introduced the concept of “premium for height”, which is showed in figure 2.4. When the number of stories increases, the weight of the structure not only increases as a consequence of increased vertical loading, but also increases because of the increased lateral loading.

Ali & Moon[2] have made a classification proposal for the different stability systems of high-rise. It is based on interior and exterior structures where combinations of the two are possible. A structure is categorised as interior structure if the major part of the structure is placed inside the building. If the structure is primarily placed at the building perimeter, a structure can be classified as exterior structure.

Every stability system has an optimum height regarding material efficiency and serviceability requirements. In figure 2.5 and 2.6, the different classifications can be seen and their optimum heights, according to Ali & Moon[2]. Underneath, a selection of systems is explained to provide some more in-depth knowledge.

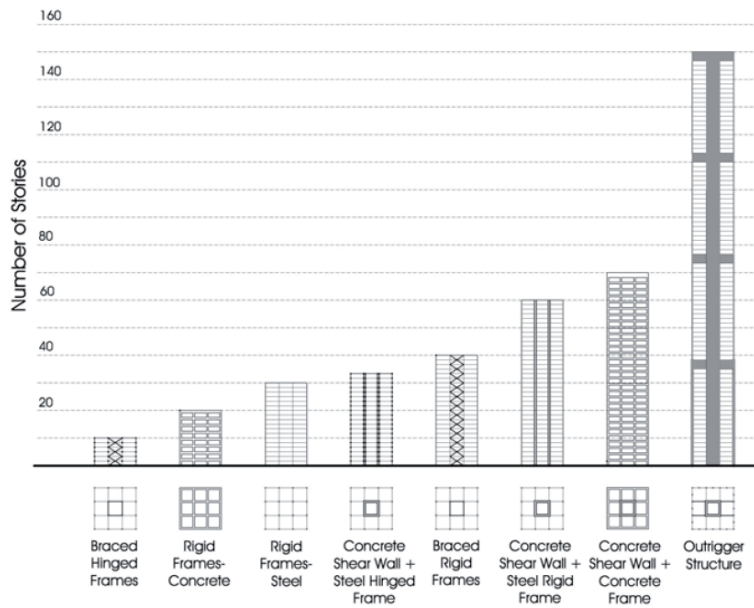


Figure 2.5: Interior structures, classification as proposed by Ali and Moon[2]

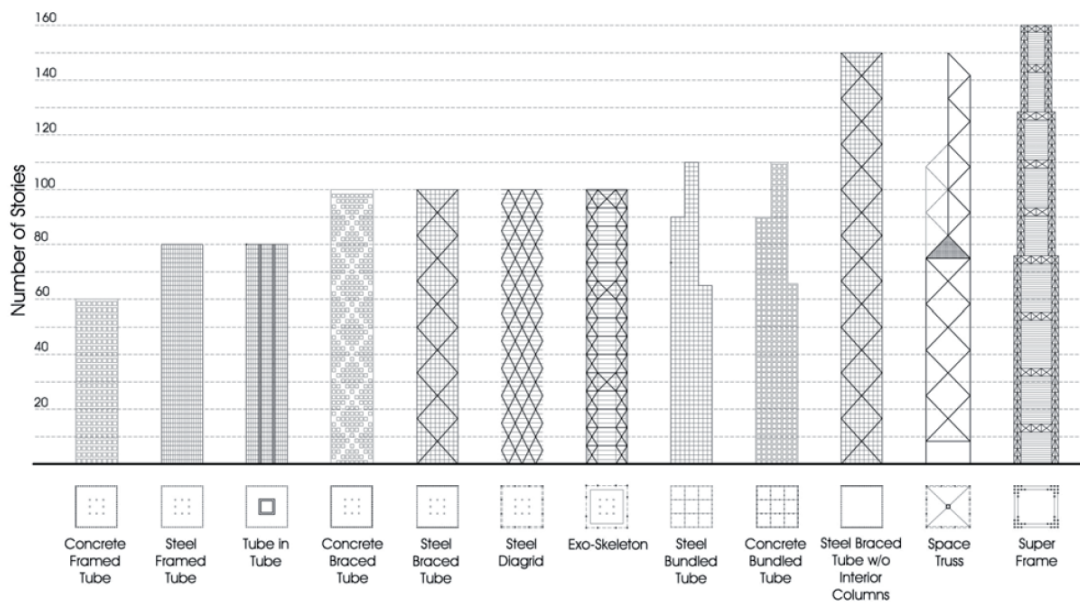


Figure 2.6: Exterior structures, classification as proposed by Ali and Moon[2]

Shear wall/truss with frame structure

This popular stability system can be executed in a couple of ways: concrete shear wall + steel hinged frame, braced rigid steel frames, concrete shear wall + steel rigid frame, concrete shear wall + concrete frame and concrete shear wall + composite frame. In all these cases, the core (or shear walls) is functioning as the main stabilising element in the structure and is loaded in bending. It behaves as a vertically cantilevered beam from the ground. The frame provides additional stiffness when the connections are made moment resisting. Then, the frame is primarily loaded in shear.

This type of stability system is very common as construction of this system is relatively straightforward and easy. Moreover, tall buildings require vertical transport which is often positioned in a core structure within the building. By combining these functions into the core, the scarce space in the building is used efficiently. Stiffness of this system can be further improved by using rigid connections and deeper beams.

Tube structure

This stability system consists of a moment-resisting frame at the perimeter of the building. It can either be executed in concrete, steel or composite. The connections are made moment-resisting, resulting in shear behaviour of the structure. The taller the building, the greater the need to use deeper rectangular sections for beams and columns and closer column spacing. Forces are unequally distributed on the columns due to shear lag as seen in figure 2.7. Shear lag is the unequal distribution of axial forces in columns caused by the inability of axial loads to flow around the corners of a tube, when subjected to lateral loads[2].

When a concrete core is added into the building as part of the stability system, a tube-in-tube structure is created. The outer tube wants to deform in shear while the concrete core primarily wants to deform in bending. However, due to diaphragm action of the floors, these two systems are coupled and are therefore restricted to undergo the same deformation[2]. This is illustrated in figure 2.8. This interaction is also present in a lower extent in the shear wall/truss with frame system as described in the previous section.

The tube-in-tube system has many similarities with the shear wall/truss with frame system. However, within the tube-in-tube system the columns are often spaced more closely. Additionally, concrete cross sections of the beams and columns are often more optimised to facilitate more stiffness to the building. This results in a change from frame behaviour more towards a perforated wall behaviour.

In the lower end of the building, the core is more dominant in the stiffness of the building, while in the upper part the rigid frame plays the dominant role. This effect is most extreme when considering a pure bending and shear beam. However, when looking to reality, the core needs openings for doors. Moreover, when designing the outer tube more towards a perforated wall than a column-beam structure, the two systems will most likely gradually crawl towards each other in their behaviour.

Outrigger structure

Outrigger structures typically consist of steel trusses or concrete walls, connecting the core to the perimeter columns. These outriggers are primarily loaded in shear and activate the perimeter columns, increasing the moment lever arm and therefore the stiffness of the whole system. The principle comes from sailing ships where the mast is stiffened by using outriggers[2]. It reduces the bending moment in the core which has a positive effect to possible uplifting forces in the foundation, this can be seen in figure 2.9. Typically, outriggers are 1 or 2 storeys high, resulting in less usable space. In order to distribute the high axial forces in the columns at the locations of the outriggers and increase the number of affected columns, belt trusses or walls can be used.

Due to the fact that the outriggers activate the columns axially, smaller cross sections can be achieved than a tube or frame structure would require. This has a positive effect on the column spacing and aesthetic and functional requirements. Moreover, the beams can be designed with pinned connections so that they do not contribute to the global stiffness of the building. This way cross sections can be kept relatively small in contrary to rigid-frame type connections. A major disadvantage is that outriggers interfere with the usable space within the building. However, this can be overcome by placing outriggers in mechanical floors[2].

The position of the outriggers has a big influence on the stiffness of the building. Figure 2.10 by Smith[47], gives an indication of the optimal positions for the outriggers for 1, 2 or 3 outriggers. Factor ω depends on

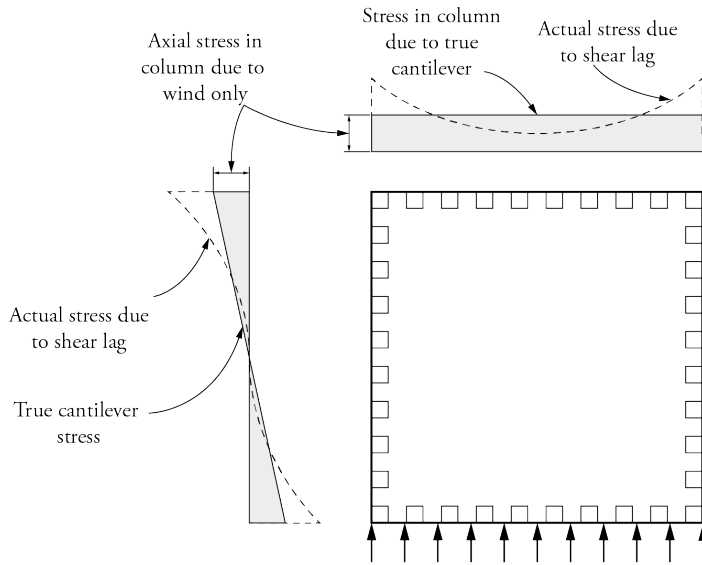


Figure 2.7: The phenomenon of shear lag illustrated[2].

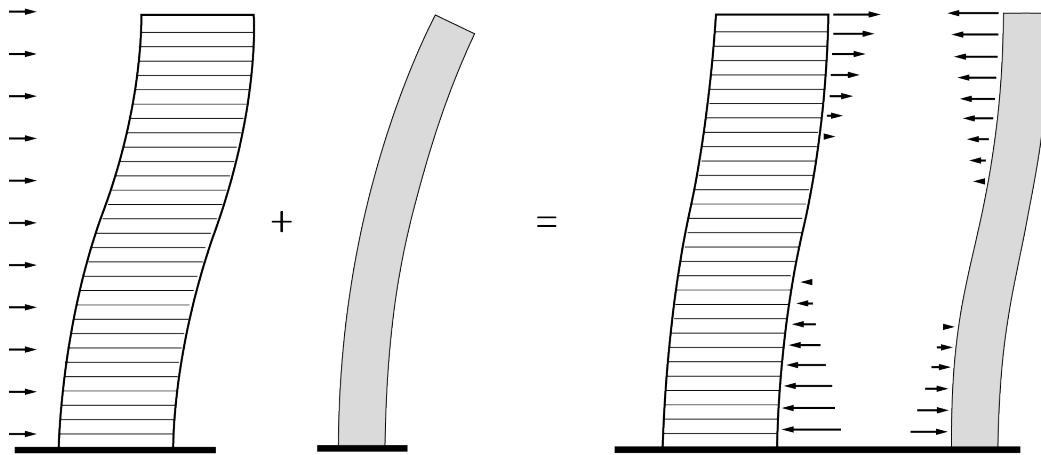


Figure 2.8: Shear wall-frame interaction forces due to restricted deformations[2]

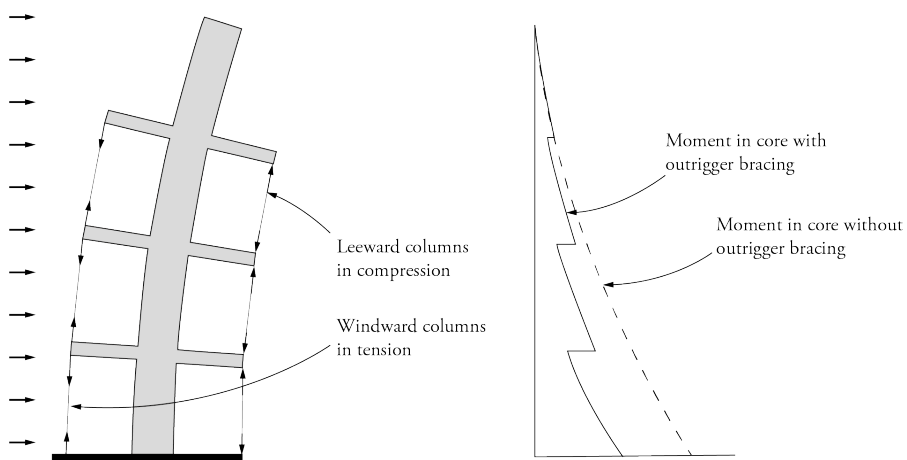


Figure 2.9: Core supported outrigger structures reduce the bending moment in the core[2]

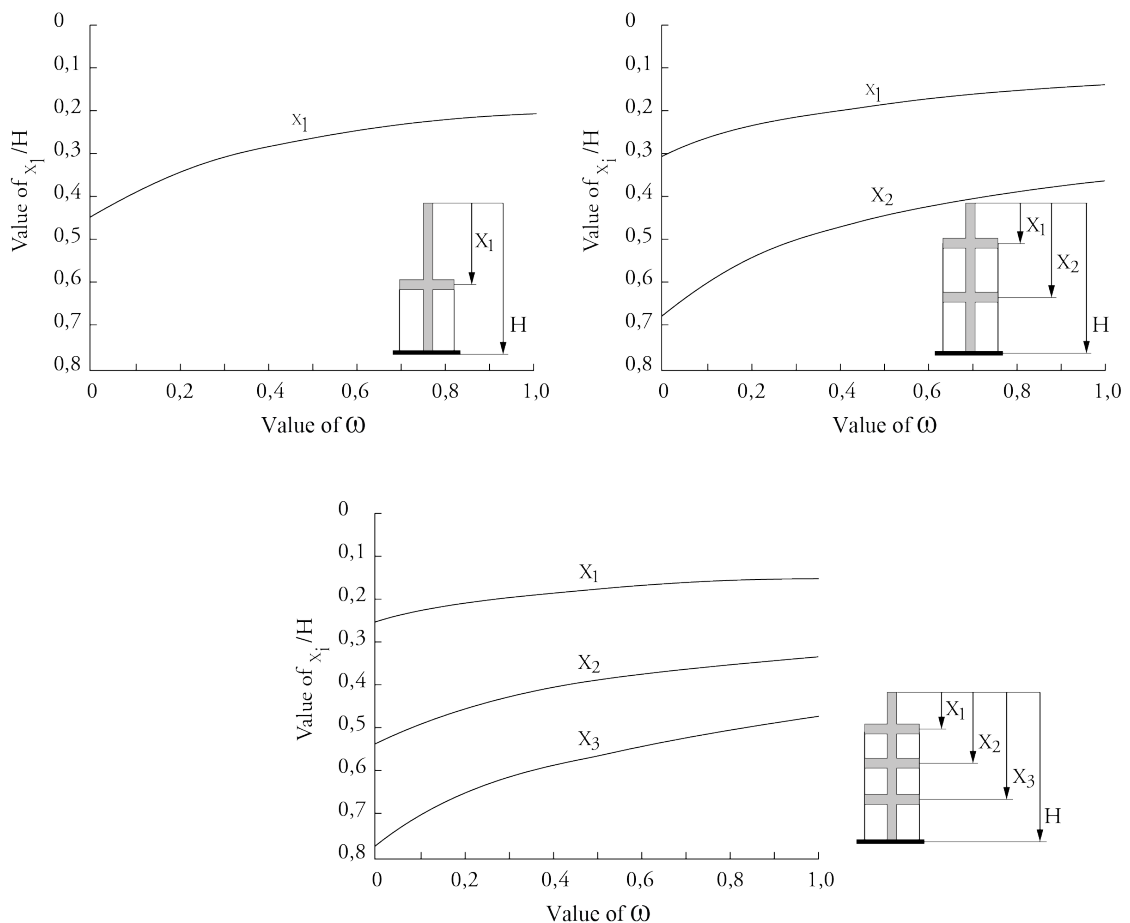


Figure 2.10: Optimal locations for 1, 2 and 3 outriggers according to Smith[47].

stiffness ratios between the columns and core; and the outriggers and core. An approximation can be made by hand calculations using the method from Smith.

Braced tube structure

The braced tube introduces diagonal elements to the tube system, creating a big truss. The use of these diagonals significantly increases the structural efficiency since the behaviour is dominated by axial forces instead of bending moment. This system is mostly seen in steel, but can also be executed in composite or concrete. When using concrete, a diagonal pattern of in-filled window spaces with diagonal placed reinforcement is used to create the braces. However, since high tension forces can occur in the diagonals of a braced tube system, it is highly likely that only the reinforcement steel is transferring the axial forces.

Moreover, due to the high axial forces in the braces, combined with the fact that axial loads in the corner columns due to gravity loads are small, there is a possibility that tension forces occur at the base of the building which are transferred to the foundation. This can be covered by transferring more gravity loads to the corner columns. One possible way to achieve this is by introducing belt trusses that transfer the vertical loads of the columns to the corner columns.

Diagrid structure

In a diagrid structure almost all conventional vertical columns are eliminated. This means that the diagrid members both carry horizontal and vertical forces due to their uniform triangulated configuration [2]. Members are primarily loaded in axial direction, creating a more material efficient system than conventional structures which transfer loads in bending.

The diagrid structure can be compared to an outrigger structure where columns are also loaded axially.

However, an outrigger structure still needs a core with significant shear rigidity in order to function. A diagrid structure provides both bending and shear rigidity, eliminating the need for a high shear rigidity core structure[2]. In order to further improve the total system's stiffness, such a core structure can still be added, resulting in a similar system to the tube-in-tube structure.

Usually, a tighter weave of the diagrid results in smaller structural members and even greater efficiency. The diagonal members usually span 1 or more floors. A diagrid structure is typically executed in steel, however concrete examples have also been build recently.

2.2.4. Floor systems

The primary objective of a floor is to transfer vertical loads to the core, walls and/or columns. Additionally, it should be able to act as a diaphragm in order to transfer lateral loads from the façade to the stabilising elements in the structure. Moreover, floors create physical barriers which should be fire resistant and provide sound insulation. At last, mechanical systems are often accommodated in, on and below the floor to serve the spaces with heating, ventilation and air conditioning systems.

Flat slab floor

A flat slab floor consists of a solid reinforced concrete plate and is shown in figure 2.11a. Spans of approximately 8.5-9.5 meters can be achieved by thickness's of 280-320 millimetres. The minimum thickness is 280 millimetres for residential buildings due to acoustic properties. The flat finishing at the bottom provides flexibility for installations to be installed, which can be directly attached to the floor.

When spanning over multiple columns, the most critical factor in the design of the floor is often punching shear. Some ways to improve this are adding beams or drop panels underneath the floor. However, this increases the complexity of construction, because of the additional form-work that is needed. Also post-tensioning can be applied to increase the span of the floor, or to reduce the thickness of the floor. A downside to post-tensioning is that construction speed is greatly reduced, which is a critical factor in tall building design.

Precast lattice girder floor

The precast lattice girder floor (in Dutch: breedplaatvloer), as seen in figure 2.11b consists of a precast concrete plank where bottom reinforcement is already in place. This type of floor is partly precast and partly constructed in-situ. The precast floors are installed in place and additional concrete is poured on top, including top reinforcement. Diagonal reinforcement ensures the cooperation between the precast and cast-in-situ concrete. Typically, these types of floors don't require additional form-work, speeding up the erection process. However, it does require additional crane movements.

BubbleDeck floor

A BubbleDeck floor uses plastic balls to replace concrete where it is not needed in order to reduce the weight of the floor and increase the bearing capacity. This type of floor, as seen in figure 2.11c, can be used in combination with a precast lattice girder floor. This provides both a lighter floor and a fast erection speed. Also pre-stressing can be applied to increase the spans.

Hollow core slab

The hollow core slab, shown in figure 2.11d, is an entirely precast floor made out of concrete. Inside the slab, tubes of concrete are left out to reduce the weight of the floor. Pre-stressing is applied to increase the bearing capacity and stiffness of the floor. These types of floors are used a lot in the industry and utility buildings. Diaphragm action can be achieved by adding an additional compression layer of cast-in-situ concrete incorporating extra reinforcement. The downside of this floor type is that it is less flexible and high amount of crane movements is needed. Hollow core slabs can be used in both concrete and steel structures.

Composite floor

A composite floor is a floor system where concrete and steel are combined, using the advantages of both materials. It consists of cast-in-situ concrete with reinforcement, poured on corrugated steel sheets which act as bottom reinforcement, as can be seen in figure 2.11e. The steel sheets are supported by steel beams. Composite action of the beams can be achieved by adding shear connectors between the beams and the slab. This enables the transfer of shear forces between the slab and the beams in order to create monolithically

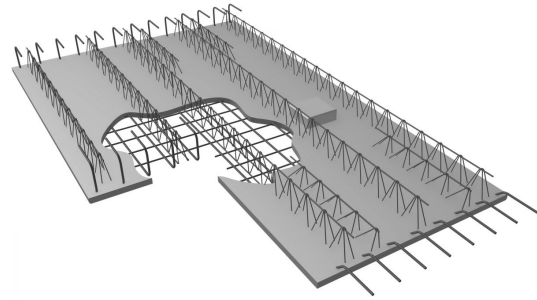
behaviour. The use of corrugated steel sheets enables a very fast erection speed, multiple sheets can be lifted at once and for limited spans, no additional form-work is needed. Composite floors are usually used in steel structures.

Slimline floor

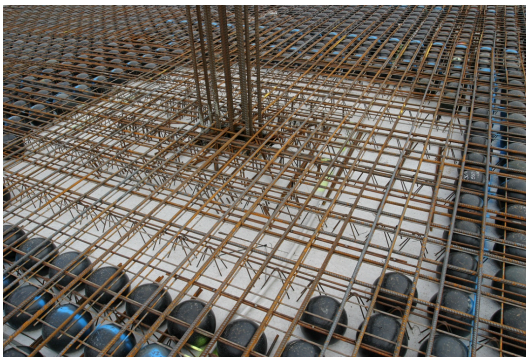
Another type of composite floors is a Slimline floor, shown in figure 2.11f. This type of floor is developed, targeting flexibility and sustainability, and is designed to easily access the mechanical systems which are placed inside the floor. It consists of closely spaced steel beams, placed between two concrete plates. Diaphragm action can be achieved by additional steel connectors between the different components, which is an important aspect in high-rise design.



(a) Flat slab floor.



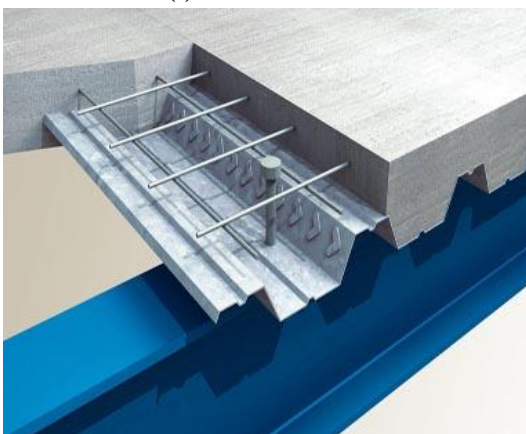
(b) Precast lattice girder floor.



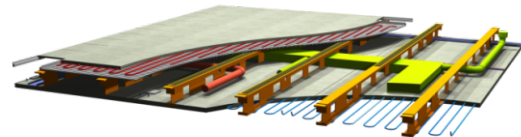
(c) BubbleDeck floor.



(d) Hollow core slab.



(e) Composite floor.



(f) Slimline floor.

Figure 2.11: Different optional floor systems for use in buildings.

2.3. Sustainable structural design

There are multiple definitions of sustainable structural design (SSD). Danatzko & Sezen [16] propose that the goal of SSD is the production of a structural system that meets the needs of the owner and user while minimizing the environmental impact and conserving resources where possible.

Within SSD, there are several strategies possible in order to meet this goal. Underneath five strategies are presented, as proposed by Danatzko & Sezen[16] and Anderson & Silman[4]. It must be stated that no single strategy is able to address the complexity surrounding SSD alone. It is always recommended to use a combination of several strategies, matching the sustainability goals of the project[16].

2.3.1. Minimizing material use / design for efficiency

The ultimate objective of this strategy is to reduce the amount of required raw materials and therefore reduce the project's impact on the environment. This can be achieved by efficiently combining materials with different structural properties, shape optimisation, dual-purpose structures and production processes reducing construction waste.

A structure consisting of the minimum amount of material can be labelled as sustainable design, because it has the least impact on the environment through lower raw material use. However, complexity of design and calculations rise, which in their turn might have negative impact on the length and cost of a project.

2.3.2. Minimizing material production energy / design for materials

This strategy focusses on the materials itself, minimising the environmental impact of the production process of different kinds of materials. It encourages engineers to make use of structural components consisting of responsibly-sourced, recycled or reused materials.

When the industry and engineers more fully define construction material properties, including its production energy, the sustainability of structural systems will increase. Using more sustainable materials does improve the sustainability of the structural system. However, this does not result in the most sustainable design. Especially, when the choice for a certain material in a structure is already made on beforehand.

2.3.3. Minimizing embodied energy / design for energy

This strategy corresponds to design strategies lowering both the embodied energy and the operational energy. It offers opportunities for sustainable designs to be developed as the focus shifts more to an effective use of the natural environment. Both the architect and engineer should assess the energy cost of construction versus the operational energy expenditure.

Ideally, this method results in a structure that satisfies the form both structurally as architecturally, finding a balance between the two to reduce the energy envelope of the structure. However, following this method could lead to a structurally inefficient structural design as it typically neglects optimising structural efficiency. This could decrease its overall sustainability.

2.3.4. Maximizing structural system reuse / design for recycling/adaptability

This strategy is more of a qualitative matter. It addresses the end-of-life of a structure and possibilities for reuse, which can be defined in two ways. First way of reuse is using already existing structures (e.g. the foundation of a former building) or reuse of structural members retrieved from former buildings (e.g. a steel beam). The second form of reuse addresses design for adaptability (e.g. replacing mechanical systems in floors) or design for reuse (e.g. making use of standardized connections).

This strategy contributes directly to financial gain and environmental sustainability. It reduces waste and the need for new raw materials. Next to that, it calls for architects and engineers to develop more standardized designs that allow for relocation of partial structural systems between project sites or possible structural element reuse. A downside of this strategy is that, designing a structure for multiple purposes or only using standardized elements, the efficiency and sustainability of the structure for its intended use are influenced negatively. Additionally, reuse of structural elements would require a thorough inspection before reuse could take place.

2.3.5. Life-cycle analysis

Life-cycle analysis (LCA) is more a tool than a real strategy, which is often used to justify or qualify the net-cost-to-benefit ratio, economic impact of a decision or to determine the sustainable properties of various aspects. Assessing a structural design through a multifaceted view enables the designer to produce a more sustainable design by including and balancing a greater number of aspects of the design.

A life-cycle analysis (LCA), employed for SSD, provides designers and owners a clear picture of what their structure can achieve during its lifetime. Additionally, an LCA calls for better inclusion of all representative parties, encouraging cross-disciplinary interaction. This interaction could lead to better overall sustainability through more effective designs. The downside of LCA is that the inaccuracy and uncertainty can be high when considering the structural system and sustainability.

Fast track method

LCA's can roughly be divided into two different categories[62]: the classical LCA and the 'fast track' LCA. Using the classical method, the environmental impact of the materials have to be determined from scratch. The focus is primarily on the life-cycle inventory (LCI) and life-cycle impact assessment (LCIA). The Fast Track method is commonly used as a fast way to perform an LCA, e.g. for comparing design alternatives. It uses the data that is produced by a classical LCA as input for the LCA.

In order to perform a fast track LCA, the following steps have to be followed according to Vögtlander[62]:

- Establish the scope and the goal of the analysis
- Establish the system, functional unit and system boundaries
- Quantify materials, use of energy, etc. in the system
- Enter the data into an Excel calculation sheet or computer program
- Interpret the results and draw conclusions

A thorough description of the scope, goal, system, functional unit and system boundaries is required for the following two reasons. In most cases the LCA can be improved or expanded. Additionally, in order to compare the study with other studies in literature. In both cases it has to be clear what exactly is being analysed and what is taken account of.

The system boundaries can be described in phases based on EN 15804[49]: the production phase (A1-3), construction phase (A4, A5), the use phase (B1-B5), end-of-life phase (C1-C4) and reuse/recycling phase (D), see figure 2.12. When assessing an environmental product declaration (EPD) for building structures, it is mandatory to include phases A1-A3, C3 and C4 and D according to Dutch legislation[49], which corresponds to a cradle-to-gate and end-of-life analysis.

For Dutch environmental impact assessments for buildings and products, the Nationale Milieu Database (National Environmental Database) (NMD) was created. The NMD contains information about the environmental impact of materials, processes and products for several impact categories. The data for building materials includes the production phase A1-A3. The user of this database can be sure that the different materials, processes and products are assessed in the same way and therefore can be used to e.g. compare design alternatives. The impact categories and their shadow prices, that are included in the NMD, are shown in table 2.1.

In order to perform an LCA, several tools and software products have been brought to the market. Among the international alternatives, there are also some Dutch tools. These are DuCo by IMd, GPR Gebouw, DGBC and the MRPI Free Tool. Until now, there has not been a tool that has been integrated into parametric design software.

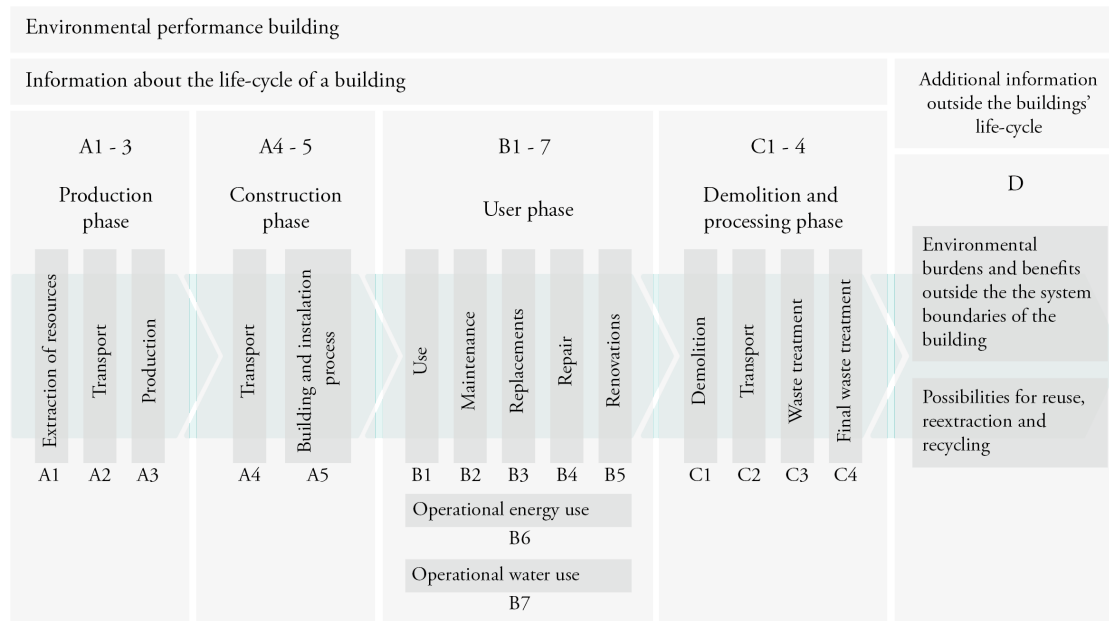


Figure 2.12: The life cycle of a structure and the corresponding phases according to EN 15804[49].

Impact category	Environmental cost per kg eq	Unit
Abiotic depletion	€0.16	kg Sb eq
Global warming potential	€0.05	kg CO ₂ eq
Ozone layer depletion	€30.00	kg CFC-11 eq
Human toxicity	€0.09	kg 1,4-DB eq
Fresh water aquatic ecotox.	€0.03	kg 1,4-DB eq
Marine aquatic ecotoxicity	€0.0001	kg 1,4-DB eq
Terrestrial ecotoxicity	€0.06	kg 1,4-DB eq
Photochemical oxidation	€0.06	kg C ₂ H ₄
Acidification	€4.00	kg SO ₂ eq
Eutrophication	€9.00	kg PO ₄ eq

Table 2.1: Impact categories and their corresponding environmental cost and units[49].

2.4. Sustainable structural design of high-rise buildings

Research into the environmental impact of different stability systems and materials for high-rise buildings is limited[21][51][52]. Underneath three different researches are briefly summarised and discussed.

2.4.1. Van Hellenberg Hubar (2009)

Van Hellenberg Hubar[57] graduated from Delft University of Technology (TU Delft) by looking into sustainability of structural and flooring systems of high-rise buildings in a broader view. He argued that flexibility is also an important aspect in sustainability, because the demand in the market might change. Therefore, it is important that a building should be flexible in terms of function change. Different types of floors were compared. Concluded was that an Infra+ floor (Slimline floor) would be the best solution regarding flexibility and sustainability, because of the easy access to the mechanical systems.

Furthermore, three different stability systems were compared for three different heights (70, 96 and 134 meters) using integral cost, as seen in figure 2.13. It was concluded that a concrete tube would be the best solution regarding integral cost. Moreover, it was concluded that using environmental cost, the comparison becomes sensitive to the assessment of environmental impacts into cost.

2.4.2. Foraboschi, Mercanzin and Trabucco (2014)

Foraboschi, Mercanzin and Trabucco[21] presented a research where the embodied energy (EE) of different structural systems and materials for different heights was compared according to the cradle-to-gate principle. A reference structure was dimensioned and detailed for buildings from 20 to 70 storeys (80 to 280 meters) situated in Genoa, Italy. Six types of floors were compared: a composite floor, flat slab and 4 weight-reducing concrete floors.

It was found that all weight-reducing systems increased the embodied energy, meaning that the weight-reducing materials, like the plastic used in BubbleDeck floors, include more embodied energy than the concrete that they replace. Figure 2.14 shows the EE per square meter for the different floor types where the third lightweight floor system is a BubbleDeck floor. Furthermore, two structural systems were compared, namely a reinforced concrete frame and a steel frame. It was found that reinforced concrete frames consume less energy than steel frames.

The research does not account for transportation to site, construction, demolition and recycling of the materials. This could have a significant impact on the results[12][13][43]. Additionally, only two structural systems were assessed as the focus was more on flooring systems.

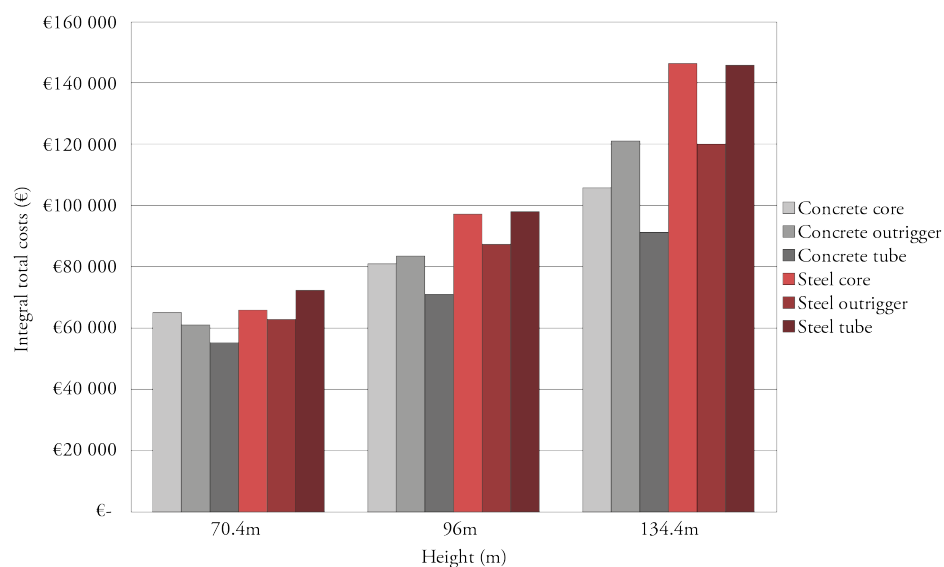


Figure 2.13: Integral cost per story for the different stability systems for 3 different heights according to Van Hellenberg Hubar[57].

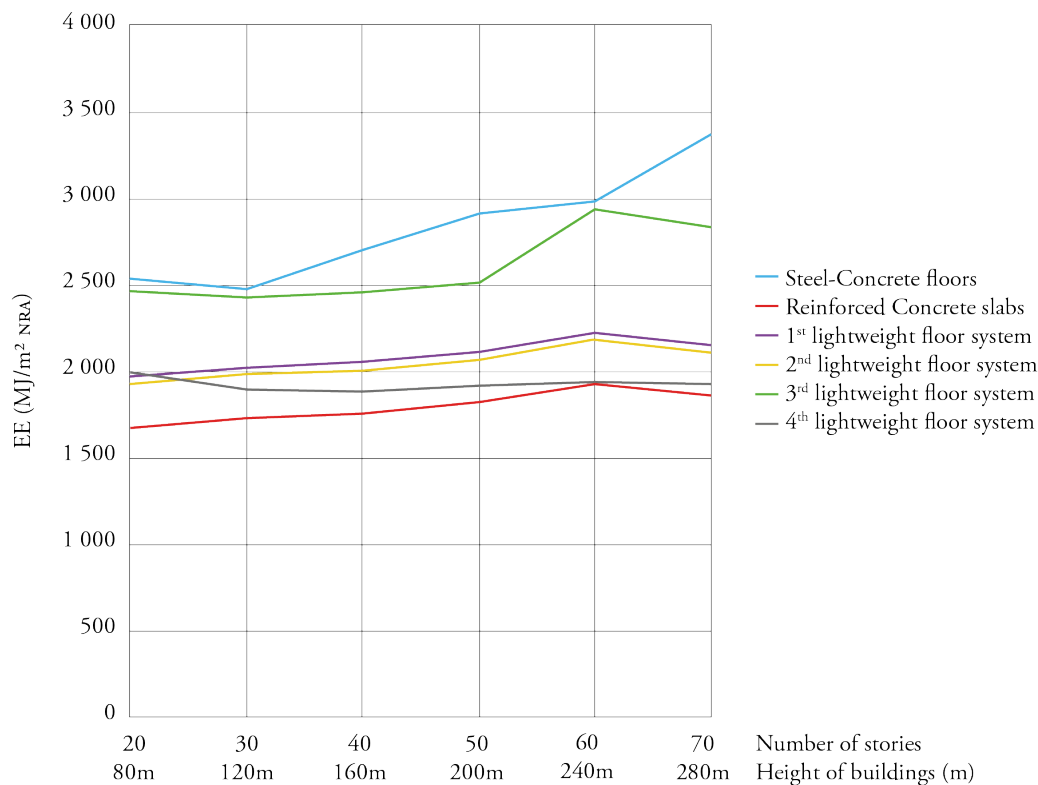


Figure 2.14: Total EE of the flooring system as a function of the height of the building (or of the number of stories), for each type of floor according to Foraboschi[21].

2.4.3. Trabucco et al (2016), CTBUH

Trabucco et al[52] recently finished a research initiated by the Council of Tall Buildings and Urban Habitat (CTBUH) on the LCA of tall building structural systems. This extensive research considered 8 different scenarios including concrete, steel and composite frame and diagrid structures for two different heights (60 and 120 storeys). The scenarios were compared using a complete LCA in terms of GWP and EE following regulations and conditions in Chicago.

A design brief was sent to several structural engineering companies which on their turn returned the fully designed structures to the research team. Transportation was included by modelling the transportation distances for an in 2009 completed tall office building in down-town Chicago. Data for the on-site construction operations were gathered by contacting suppliers to receive information of the energy consumption of the largest operating machines. End-of-life phase for the 60 storey models was modelled by contacting a demolition company on how a demolition project of this scale would be handled. Demolition for the 120 storey models was neglected as this operation seems impossible at this moment.

The research team agrees that LCA is still very sensitive to decisions that are made regarding the system boundaries and all the other conditions and limitations of the research. Therefore, the conclusions of the research can not be used to give conclusive results on the sustainability of different structural systems and materials in general.

Concluded was that all concrete scenarios had the highest score regarding GWP, see figure 2.15, while all steel scenarios had the highest EE. Additionally, significant reductions in GWP and EE can be achieved by reducing the structural spans of the floors, considering recyclability of steel or use special mix designs for concrete. Furthermore, transportation of construction materials and demolition waste accounted only for 1% to 2.5% in terms of the total GWP. It was not a very significant factor and therefore it might be beneficial to look for more sustainable materials that are situated at greater distances rather than use only local materials.

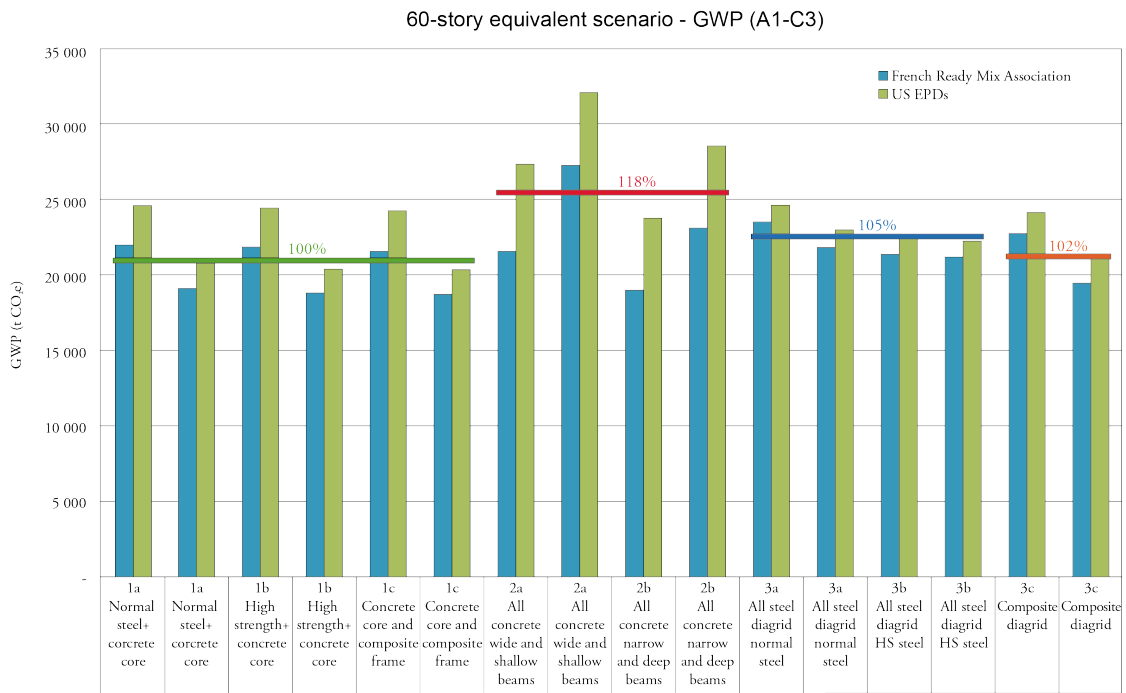


Figure 2.15: LCA results of the 60-storey equivalent scenario for GWP according to Trabucco[52].

While this is the most extensive generic research at the moment, the authors claim that the results are only applicable to the considered case study. It is doubtful whether this case study would be generally applicable for the Netherlands considering the fact that production, construction, regulations, wind and seismic conditions are all different.

2.5. Summary

In this chapter, literature was discussed. First definitions of **OE**, **EE**, **EC**, **CO₂e**, **GWP** and environmental cost were given. The definitions of these concepts are closely related and often misunderstood. These concepts are further used and discussed in this thesis.

Next, a broad view on structural design of high-rise buildings was given. High-rise buildings have to cope with significant larger horizontal and vertical forces than low-rise buildings. This results in the premium for height, introduced by Fazlur Khan[25]. Several stability systems were explained on how they provide lateral stability for high-rise buildings, according to the classification by Ali and Moon[2]. These include the shear wall/truss with frame structure, tube structure, outrigger structure, braced tube structure and diagrid structure. The first two systems are primarily loaded in bending and shear while the latter systems are primarily loaded to axial forces, when subjected to lateral loading. The shear lag aspect was introduced, which occurs in tube structures subjected to bending. This results in an inefficiency of lateral load transfer, which decreases the efficiency of the system. Furthermore, six types of common floor systems were explained including their advantages and disadvantages.

Furthermore, several strategies were introduced, related to **SSD**. Danatzko & Sezen propose that the goal of **SSD** is the production of a structural system that meets the needs of the owner and user while minimizing the environmental impact and conserving resources where possible[16]. Strategies to meet the goal, by Danatzko & Sezen and Anderson & Silman[4], are classified in: minimising material use/design for efficiency, minimising material production energy/design for materials, minimising embodied energy/design for energy, maximising structural system reuse/design for recycling/adaptability and **LCA**. The fast track **LCA** method[62] is explained as a relative fast way to perform an **LCA** making use of databases.

Lastly, three different researches are introduced on **SSD** of high-rise buildings. Among them is a graduation thesis by Van Hellenberg Hubar (2009)[57], which focused on sustainability as a broad concept. He focused on several floor systems and argued that the concrete tube structure is most beneficial regarding integral cost. A research by Foraboschi (2014)[21] also focusses on floor systems, among which four different types of weight-reducing systems for flat slab floors. **EE** is used to compare the floor systems for buildings of several heights and it was found that concrete frames had a lower **EE**. The last research was performed by the **CTBUH**, led by Trabucco (2016)[52]. This research focussed on several structural systems for a 60 storeys and 120 storeys building and the total life-cycle was addressed. Environmental impact was measured in **GWP** and **EE** and it was concluded that all concrete scenarios had the highest score regarding **GWP**, while all steel scenarios had the highest **EE**.

3

Structural design

This chapter describes the design processes and methodologies that have been used to create the structural designs used in this research. A detailed description is given of the geometrical aspects, the loads and performance criteria, design of the stability systems, design of the floor systems, the parametric design and analysis work-flow, and finally the results.

3.1. General geometry

The geometry of the models is defined by its height, Dutch regulations for daylight entry and required size for the core. Underneath is explained how the general geometry of the building is defined.

3.1.1. Floor-to-floor height and building height

The heights of the 3 model groups are approximately 150, 200 and 250 meters. It is assumed that the floor-to-floor height is 3.80 meters. This accommodates a minimal ceiling height of 2.60 meters (according to Dutch building regulations), ducting and mechanical systems, optional primary and secondary beams, floor and floor finish.

A floor-to-floor height of 3.8 meter results in the following number of stories and exact building heights accordingly: 40 floors and 152.0 meters, 52 floors and 197.6 meters, 64 floors and 243.2 meters, which also can be found in figure 3.1. These amounts of floors are chosen, because they are even numbers and easy to divide, which makes the design of the braced tube and diagrid easier.

3.1.2. Floor plans and core dimensions

The dimensions of the core have a big influence on the stiffness of the building, especially when the core is the primary stabilising element. However, the dimensions of the core are not solely determined by the structural engineer. Generally, one can say that the design team strives to make the core as small as possible. This follows from the fact that increasing the core results in less rentable space, called net floor area (NFA). Generally, a building requires a NFA of 75% or higher of the gross floor area (GFA) to be economically profitable. Recently, developers are demanding NFA ratios of 80% up to even 90%[43].

A core houses elevators, shafts for mechanical systems, stairs, structure and core program area. As buildings become higher, the need for vertical transportation also rises. Therefore, a core of a 150-meter building will not be the same as a 250-meter building core. The cores of the 3 model groups are based on reference projects as seen in table 3.1. Based on the area the following dimensions were chosen as seen in figure 3.1. A square core was chosen, because a long and narrow core would result in loss of stiffness and increased wind load in one direction if a rectangular floor plan was adapted; or loss of rentable space in the case a square plan was chosen.

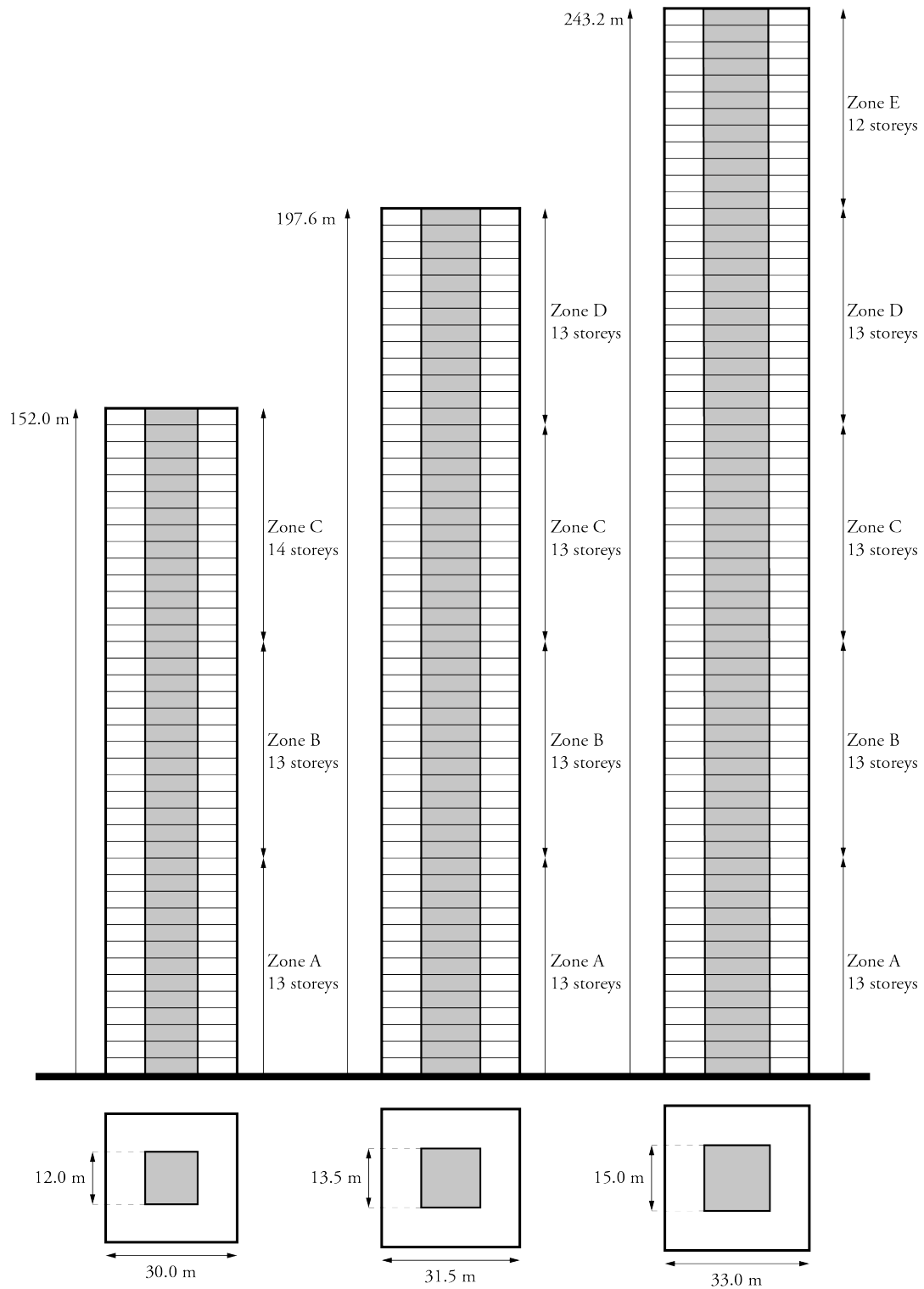
The design of the rest of the floor plan, the office space, is governed by Dutch regulations for daylight entry. These regulations require that each office space should be able to receive natural daylight. Detailed calculations, taking into account façade openings, should be done to proof that the regulations are met. However, as a rule of thumb, one could take a depth of 7.2 meters for office space and 1.8 meters for a hallway as a good approximation [56]. This results in a maximum depth of 9 meters. Therefore the dimensions of the floor plan of the model groups are solely dependant on the dimensions of the core. The floor plans and its dimensions can be seen in figure 3.1. The resulting NFA ratios are 84%, 82% and 79% for the 150-, 200- and 250-meter model groups.

Height zones

The structure of the building is divided into different height zones for dimensioning the vertical structure. The 150 m, 200 m and 250 m models are divided into 3, 4 and 5 vertical zones respectively, which can also be seen in figure 3.1. The column dimensions and core thickness's will decrease as the altitude increases. This reduces the overall weight which results in reduction of the dimensions and thickness's at the lower zones, and also a reduction in the second order effect, which is further explained in section 3.5.3.

Building	Height	Dimensions core	Area core
First	130 m	14 x 10 m	140 m ²
Maastoren	165 m	14 x 11 m	154 m ²
De Rotterdam	150 m	13 x 12 m	156 m ²

Table 3.1: An overview of the core dimensions of several office buildings.



Height	152.0 m	197.6 m	243.2 m
Nr. of storeys	40	52	64
Arera core	144.00 m ²	182.25 m ²	225.00 m ²
Net Floor area	84%	82%	79%
Slenderness	5.1	6.3	7.4

Figure 3.1: Conceptual impressions of the different floor plans, core sizes, heights and height zones of the model groups.

3.2. Loads and performance criteria

The considered loads are vertical dead and live loads; and horizontal wind loads, based on Eurocode 1[30]. The acting consequence class is CC3 for buildings higher than 70 meters, according to the Dutch national annex of Eurocode 0[29].

3.2.1. Vertical loads

A live load of 2.50 kN/m^2 is considered, this follows from Eurocode 1[31] as live load for the function office. Additionally, the following dead loads are also taken into account[43]:

- 1.00 kN/m^2 for partition walls
- 0.25 kN/m^2 for mechanical installations and ceiling
- 1.25 kN/m^2 for finishing top floor

This results in an additional 2.5 kN/m^2 dead load. When considering the possibility of a function change to for instance residences, the considered live load changes to 1.75 kN/m^2 according to the Eurocode. This leaves an additional 0.75 kN/m^2 for light-weight partition walls between residences, which is sufficient.

When considering the global strength and stiffness of the building, an additional façade dead load is assumed to be 1.0 kN/m^2 and evenly distributed over the floor area. This results in a façade weight of 1.97 kN/m^2 which is a realistic value for a light façade.

3.2.2. Wind loads

The wind load is calculated using Eurocode 1[32] and the corresponding National Annex for the Netherlands [33]. The wind load on the structure can be calculated with the following formula:

$$F_w = c_s c_d * c_f * q_p(z_e) * A_{ref} \quad (3.1)$$

Here, $c_s c_d$ is the structural factor; c_f the force coefficient; $q_p(z_e)$ the extreme wind pressure at height z_e ; and A_{ref} the reference surface where the wind pressure is acting on. The structural factor $c_s c_d$ takes dynamic effects into account caused by turbulence and non-simultaneously acting wind pressure on the surface. The force coefficient c_f takes aerodynamic effects into account and depends on the shape of the building.

In order to calculate the wind load in an early phase of a project, assumptions have to be made. An overview of these assumptions can be found in table 3.2.

The wind pressure is not equally distributed over the height, the pressure increases when height increases as well due to the logarithmic wind speed profile. In figure 3.2 the distribution of the wind pressure over the height of the building is shown. During this research, the height of the intermediate zones h_{strip} is equal to the inter-storey height. This results in a point load at every storey.

Originally, the Eurocode only considers wind loads for buildings until a height of 200 m. In order to calculate the wind loads for the 250 m models, formula 4.7 for turbulence intensity $I_v(z)$ has been adapted according to formula 3.8 from the Dubai Wind Code[19]. The Dubai Wind Code is entirely based on the

Parameter	Assumption	Comment
Wind area	II	Assumed to be Rotterdam
Terrain category	III	Assumed to be urban area
Natural frequency n_1	$n_1 = 46/h$	From Eurocode, appendix F
Mass M	40 000 000 kg (150 m) 55 000 000 kg (200 m) 75 000 000 kg (250 m)	Based on $+/- 11 \text{ kN/m}^2$
Structural damping δ_s	0.10	From table F.2 in Eurocode

Table 3.2: Assumptions for calculation of the wind loads.

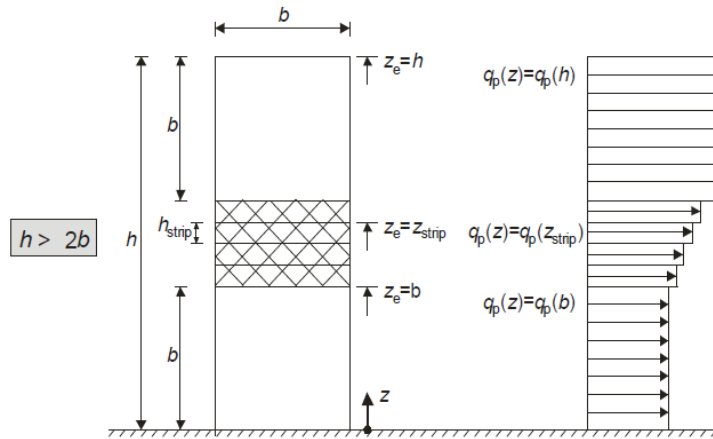


Figure 3.2: Distribution of the wind pressure over the height of the building[32].

Eurocode, but the height limit of 200 meters is removed. The additional formula that is used in addition to formula 4.7 in the Eurocode is:

$$z \geq 200m : I_v(z) = \frac{k_I}{c_0(z) * \ln(\frac{200}{z_0})} \quad (3.2)$$

The wind loads are calculated using a verified calculation sheet of Royal HaskoningDHV. The force coefficient c_f is calculated by hand by using section 7.6 of the Eurocode which presents the following formula:

$$c_f = c_{f,0} * \Psi_r * \Psi_\lambda \quad (3.3)$$

Here $c_{f,0}$ is the force factor for rectangular cross-sections with sharp corners without corrections for finishing effects; Ψ_r the reduction factor for rounded corners, depending on the Reynolds number; and Ψ_λ the finishing effects factor. The calculated values are respectively 2.1, 1.0, and 0.685 for 150 meters, 2.1, 1.0, and 0.694 for 200 meters, and 2.1, 1.0, and 0.701 for 250 meters. This results in c_f values of 1.44, 1.46 and 1.47 for 150, 200 and 250 meters respectively.

3.2.3. Load combinations

Acting load combinations are listed down below where G stands for gravity load, which includes dead load and superimposed dead load. Q_o stands for office live load and Q_w for wind load. The Ψ_0 -factors for the office live load and wind load are: $\Psi_{0;o} = 0.5$ and $\Psi_{0;w} = 0.0$. Additionally, when considering the office live load as main acting live load, only one floor has to be fully loaded. The rest of the floors are taken into account with the Ψ -factor meaning that only half of the live load is acting on these floors. The difference in total vertical load between $1.32 * G$ and $1.49 * G$ is more than half of the office live load acting on one floor, therefore this load case was not taken into account.

ULS load combinations

- LC1: $1.32 * G + \Psi_{0;o} * 1.65 * Q_o + 1.65 * Q_w$
- LC2: $1.49 * G + \Psi_{0;o} * 1.65 * Q_o$
- LC3: $0.90 * G + 1.65 * Q_w$

SLS load combinations

- LC4: $G + \Psi_{0;o} * Q_o + Q_w$
- LC5: $G + Q_w$

3.2.4. Performance criteria

When analysing the strength and stiffness of the building structure subjected to wind and gravity load, performance criteria should be taken into account. These criteria require the structure to have a certain level of strength and stiffness, both locally and globally.

Stiffness criteria are the maximum total deflection u_{total} , the inter-storey drift u_{storey} and local deflections of beams and floors w_{max} . The Eurocode does not specify limits for deflection, therefore the old limits originating from the Dutch code NEN 6702[27] are used. Here, the limits are defined as $u_{total} < 1/500 * h_{total}$, $u_{storey} < 1/300 * h_{storey}$ and $w_{max} < 0.004 * l$.

In the Netherlands the ground usually has a low stiffness, because it mostly consists of clay and peat in the first layers. Therefore, deep foundations are necessary for the ground to be able to bear the buildings. However, this means that buildings are not totally fixed at ground level, meaning that rotation is possible. In order to tackle this effect without having to make extended calculations using spring stiffnesses, it is assumed that half of the total deflection is already caused by the foundation. This is based on engineering experience and a quick foundation stiffness analysis for the 200-meter building, shown in appendix A. This means that the deflection limit used in the model is equal to 1/1000.

Fire safety

Fire safety is a huge concern when designing high-rise buildings, since it influences the design strategy of all disciplines. In the Netherlands, the structure of high-rise buildings should be fire resistant for 120 minutes according to the Eurocode. There are several ways to analyse the fire safety of building structures, from complex 3D fire simulations to simple component calculations.

This thesis uses the simple approach, where members itself will have to satisfy the criteria. For concrete, this usually comes down to adapting the concrete cover on the rebars. For steel, it usually results in adding a protective layer to the steel members, like a fire resistant paint.

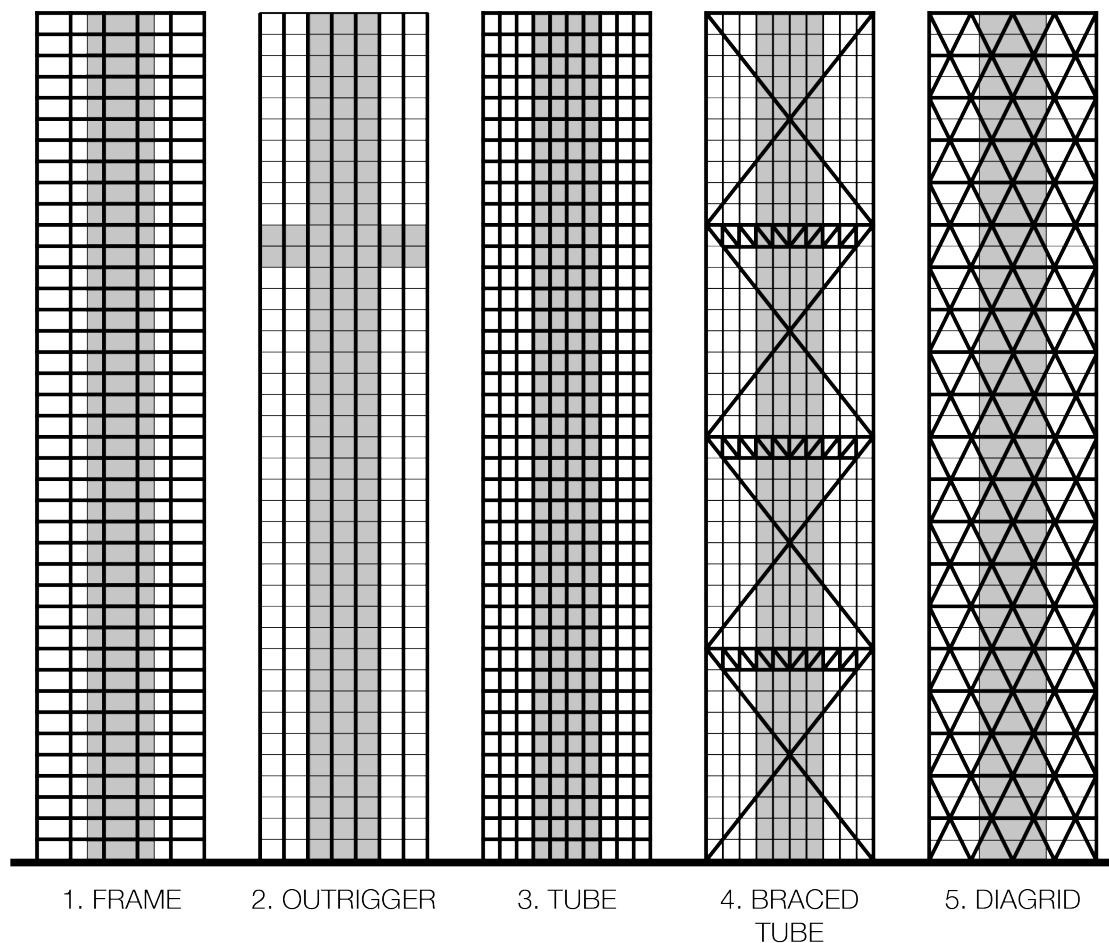


Figure 3.3: Conceptual elevation view of the used stability systems.

3.3. Stability system design

Five types of stability systems are compared: a rigid frame with core (*1. frame*), an outrigger structure (*2. outrigger*), a framed tube with core (*3. tube*), a diagonal braced tube with belt-trusses and core (*4. braced tube*) and a diagrid structure with core (*5. diagrid*). The structures situated in the façade work together with the concrete core in lateral stability.

The stability systems will be executed in three types of materials: cast-in-situ concrete, precast concrete and steel. In all cases the concrete core will be executed in cast-in-situ concrete, because of highly developed construction methods and reduced stiffness in joints when using prefab concrete (examples above 165 meters are not built yet[59]). In figure 3.3 an conceptual impression of the different stability systems can be seen.

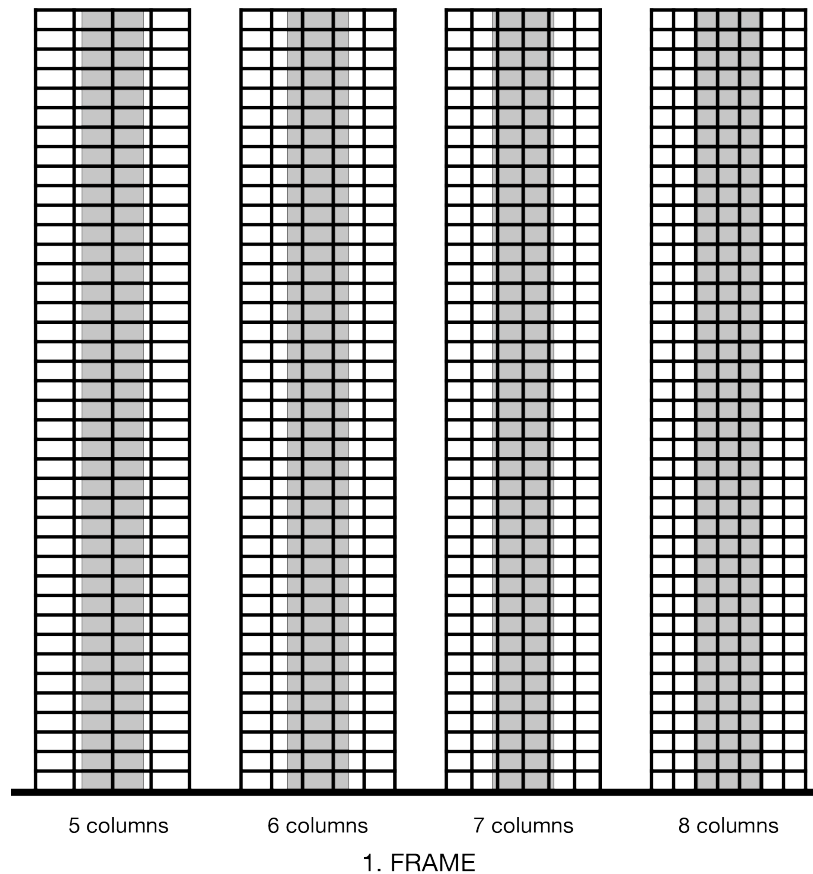


Figure 3.4: Elevation views of the four different column configurations used in the frame models for 150 meters.

3.3.1. 1. Frame

This stability system corresponds with the shear wall/truss with frame as discussed in subsection 2.2.3, it consists of a core and a moment resisting frame. Stability is achieved by bending of the core and shear of the frame. The beams are the critical factor here, as columns are usually widely spaced.

The number of columns (and the length and stiffness of the beams) has a big influence on both the stiffness and material use of the frame and on the floor design when considering e.g. a composite floor. Therefore, in this thesis four variations were made concerning the number of columns in the frame: 5 columns, 6 columns, 7 columns and 8 columns as is shown in figure 3.4. These four variations are all designed, including the floor systems and cross-sections, to achieve the lowest amount of material use and therefore the lowest possible environmental impact for this stability system.

For the concrete models, square and rectangular cross-sections are used for the columns and beams respectively, where the steel models make use of HD profiles for the columns and HEM profiles for the beams.

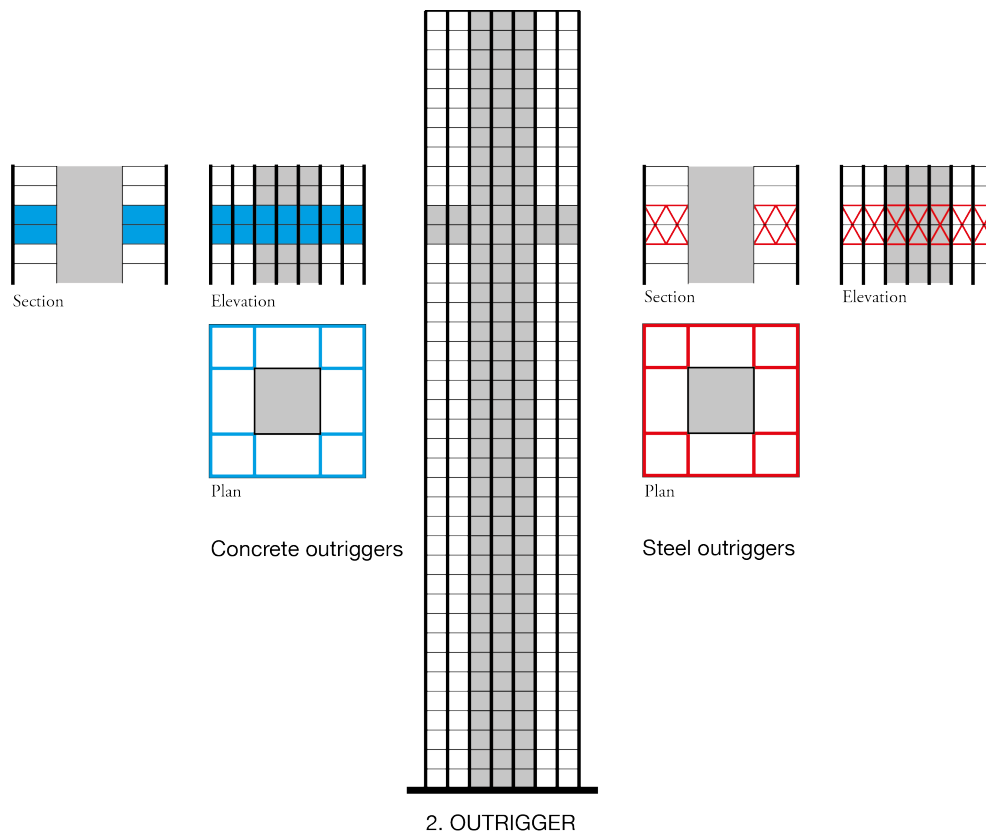


Figure 3.5: Elevation view of the outrigger model with shear walls. At the right side the outriggers and belt-truss for concrete (blue) and steel (red).

3.3.2. 2. Outrigger

Outriggers can be used with a variety of exterior structures like a frame, tube or mega-columns. In this thesis it is assumed that the core and outriggers are the only elements contributing to the global stiffness, meaning that the columns and beams will not contribute to the overall building stiffness itself by bending and shear. This means that the beams are only designed to distribute vertical loads to the columns, resulting in smaller concrete sections and the use of light IPE profiles for the steel beams.

It is chosen that the number of columns in the façade is 8 per side of the building. This reduces the span of the beams and therefore also reduces material use. The outriggers are designed as two-storey high concrete walls or steel trusses. There are 8 outriggers in total, 4 in each direction, as is shown in figure 3.5. In order to activate all of the perimeter columns, a belt wall or truss is used. It has been chosen to use one outrigger for the 150-meter model cases, two outriggers for the 200-meter model cases and 3 outriggers for the 250-meter model cases.

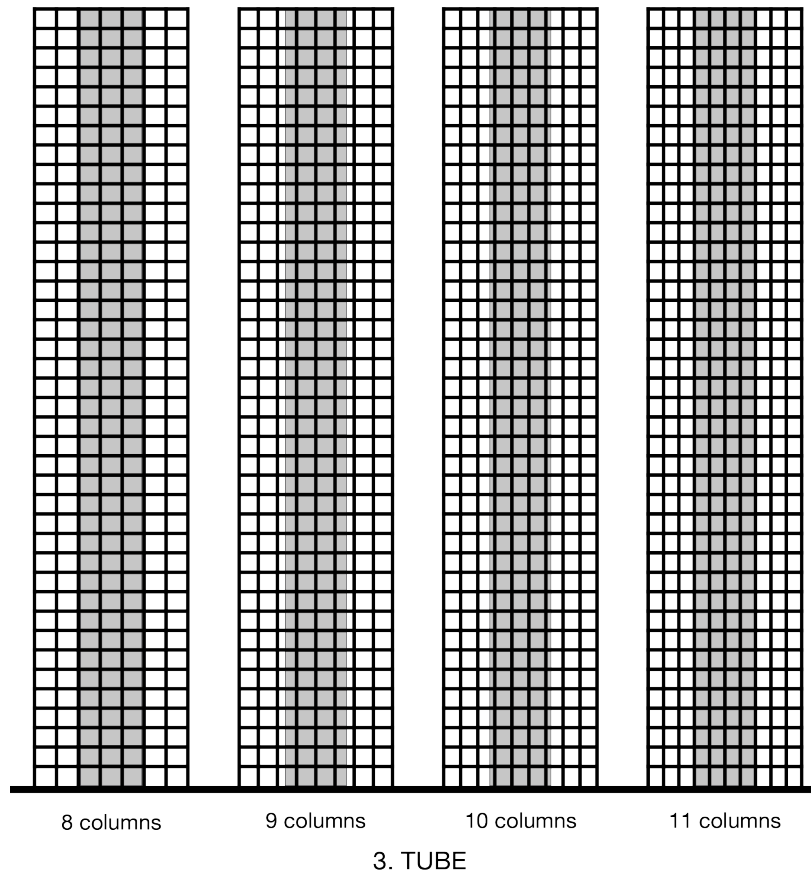


Figure 3.6: Elevation views of the four different column configurations used in the tube models for 150 meters.

3.3.3. 3. Tube

This stability system can be considered the same as *1. Frame*, however the columns are spaced more closely, increasing the stiffness of the frame significantly. As discussed at subsection 3.3.1, also here the number of columns is variable. Here the following variations are considered: 8 columns, 9 columns, 10 columns and 11 columns. This can be seen in figure 3.6.

For the concrete models, a distinction is made in the cross-sections comparing to the *1. Frame* models. Here, the cross-sections are wide and relatively thin rectangular sections for the columns and beams, increasing the stiffness of the frame while decreasing material use, as shown in figure 3.7. The steel models still use HD profiles for the columns and HEM profiles for the beams.

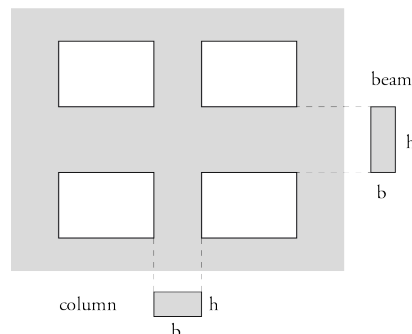


Figure 3.7: Cross-sections for the columns and beams that are used in the tube models instead of the square cross-sections used in the frame models.

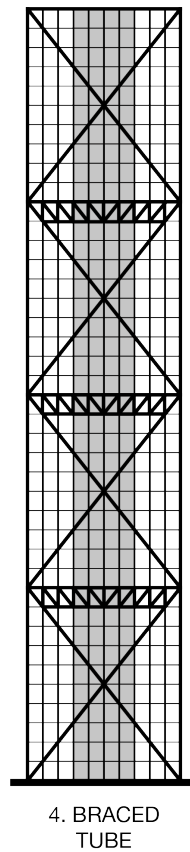


Figure 3.8: Elevation view of the braced tube model.

3.3.4. 4. Braced tube

A braced tube consists of a tube and a mega-truss which is primarily loaded in axial forces, creating an efficient load transfer path. In this thesis, it is assumed that the mega-truss is the only element of the exterior structure that provides stiffness to the building. This means that beams are only designed to transfer vertical loads to the columns, as is also being done at 2. *Outrigger* model cases. The number of columns for this model is chosen to be 11, following from the 3. *Tube* models.

A belt-truss is used to transfer vertical loads of the columns to the corner columns. This prevents that high tension forces will occur in the corners, causing uplift of the foundation. This is shown in figure 3.9. Furthermore, concrete models are excluded from this type of stability system due to structural implications.

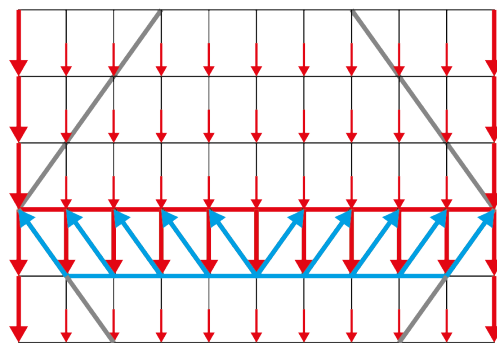
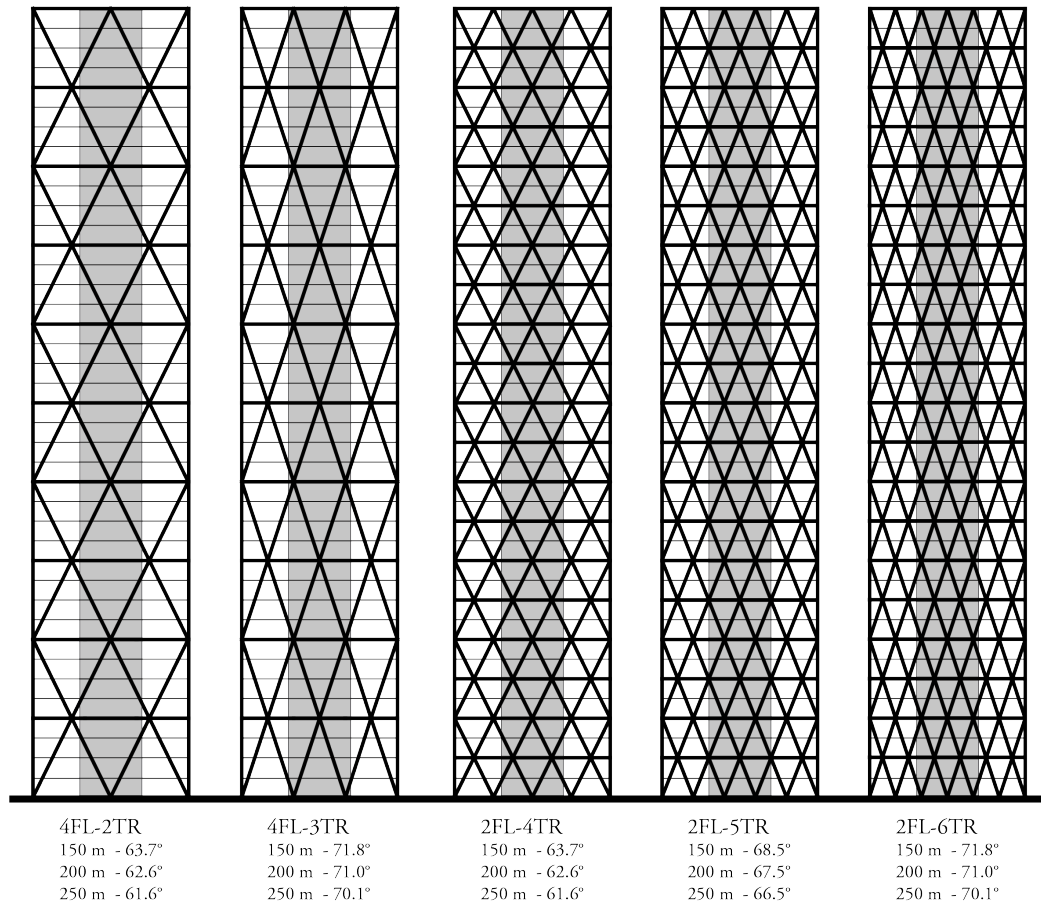


Figure 3.9: Force flow in the belt-truss when subjected to vertical loads. The green braces do not contribute in the vertical load paths.



5. DIAGRID

Figure 3.10: Elevation views of the five different diagrid configurations used in the diagrid models for 150 meters with the angles specified for each height. In **XFL-YTR**, **X** defines the height of the triangles and **Y** the number of triangles in the horizontal plane.

3.3.5. 5. Diagrid

The diagrid structure consists of diagonal members and vertical columns in the corners. The diagonal members are used for resisting both vertical and lateral forces. The configuration of the diagonal members can be done in several ways. Both the number of members per floor as the height of the members is variable. For lateral force design, the diagrid has a certain optimum angle. However, the floor configuration and the span of the secondary beams are also heavily influenced by the diagrid design. Therefore, several configurations are considered for all heights, following the used principle in the *1. Frame* and *3. Tube* model cases. In general, the optimal angle will range from 60° to 70° for diagrid structures with a slenderness ratio ranging from 4 to 9 [26]. It has been chosen to use 5 different diagrid configurations in this research, containing 2 variations in height and 3 variations in angle, see figure 3.10.

The diagrid will only be designed using precast concrete and steel. Cast-in-situ concrete has been excluded due to complex form-work that would be required to build this type of structure. Tension forces can occur in the diagrid beams due to the inclination of the columns. It has been chosen to solely use reinforcement to take the tension forces. Post-tensioning is certainly an option that should be considered when designing this type of structure. However, due to the high environmental impact of post-tensioning steel and time restrictions, it has been chosen to exclude this design option from this research.

The abbreviations mentioned in figure 3.10 define the geometry of the diagrid structure. In **XFL-YTR**, **X** defines the height of the triangles and **Y** the number of triangles in the horizontal plane. The resulting angles are listed in the caption of figure 3.10.

	C35/45	C55/67	S355
f_{cl} [N/mm^2]	35	55	355
f_{cd} [N/mm^2]	23.33	36.67	355
E [N/mm^2]	34000	38000	210000
E_{red} [N/mm^2]	11000	12000	
f_{ctm} [N/mm^2]	3.21	4.21	
ρ [kg/m^3]	2550 (reinforced)	2550 (reinforced)	7800

Table 3.3: Material properties as used in this thesis.

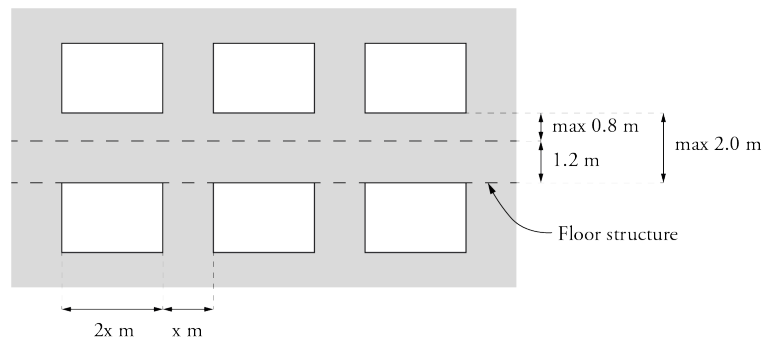


Figure 3.11: Design restrictions for the concrete models. Height of the beams is maximum 2.0 meters and horizontally, the ratio structure/opening should be at least 1/2.

3.3.6. Materials

As mentioned before, the materials that are used in the models of this thesis are cast-in-situ concrete, prefabricated concrete and steel. It was chosen to use C35/45 as cast-in-situ concrete, C55/67 as prefabricated concrete and S355 as steel grade. In every model, the core consists of cast-in-situ concrete. When doing calculations in concrete, the Young's modulus should be reduced to take creep and crack effects into account. The reduced Young's modulus is taken as roughly one third of the uncracked Young's modulus as this is common in the engineering industry. An overview of the material properties can be seen in table 3.3.

In all the models, the core is considered to be uncracked, meaning that the non-reduced Young's modulus can be used. This is checked during calculation of the models by evaluating if tensile stresses occur in Serviceability Limit State. The check is performed by using a reduced load combination where the live floor load for office (2.5 kN/m^2) and dead load for partition walls (1.0 kN/m^2) are left out:

$$DL_{floor} + DL_{facade} + LL_{wind} \quad (3.4)$$

3.3.7. Design restrictions

In order to prevent that very large cross-sections are required to satisfy the requirements, which could interfere with daylight entry through the façade, restrictions are set to the maximum sizes of the cross-sections. The maximum beam height is set to 2000 mm, resulting in a maximum height of the parapet of 800 mm. Furthermore, it is assumed that horizontally the structure/opening ratio is approximately 1 to 2 at maximum. This ratio is based on the Maastoren[56], a 165-meter office building in the Netherlands. This results in the maximum width for columns shown in table 3.4 and visualised in figure 3.11.

Nr of columns	5	6	7	8	9	10	11
150 m	2500	2000	1650	1450	1250	1100	1000
200 m	2600	2100	1750	1500	1300	1150	1050
250 m	2750	2200	1850	1550	1350	1200	1100

Table 3.4: Maximum width of column elements in millimetre for different amount of columns.

3.4. Floor design

As stated in section 1.3.4, the flat slab floor, hollow core slab floor and composite floor are considered as floor system options. As floors are one of the most critical factors in the environmental impact of high-rise buildings [21][52], these are carefully designed and optimised on strength, stiffness and material use. This section discusses the used methods for the design of the floors. An overview of all floor structures and more elaborate calculations can be found in appendix B. The different floor systems are used in the models as follows:

- Cast-in-situ concrete models: flat slab floor, hollow core slab
- Prefab concrete models: hollow core slab
- Steel models: composite floor, hollow core slab

3.4.1. Flat slab floor (FSF)

The flat slab floor is the heaviest floor of the three floor systems used. It solely consists of concrete with reinforcement added both in the top and the bottom of the floor. No weight reduction is used as this leads to a higher environmental impact due to the material that is used to reduce the weight [21].

The behaviour of the flat slab floor can roughly be divided in two different zones, namely one-way spanning behaviour and two-way spanning behaviour. This can be seen by observing m_x in figure 3.12. Here the moment distribution in x-direction, m_x is showed. It can be seen that the values in the left and right zones in the images are significantly higher than the values in the top and bottom zones. The one- and two-way spanning zones are also shown in figure 3.12.

The design of the flat slab floor is independent of the height of the building. The two-way spanning zones are equally sized in the 150-, 200- and 250-meter models, since the depth of the office space is kept constant at 9 meters. This means that the design of the flat slab floor for all model cases is approached the same, where the width of the one-way spanning zone is kept variable.

The behaviour of the supports depend on the bending capacity of the structure to which the floor is connected. The supports here are all modelled as hinged line supports. This prevents the occurrence of local bending moments in the core wall or torsional moments in the supporting façade beams. Eurocode 2[34][35] requires that accidental support moments of 33% of the maximum field moments have to be taken into account.

The concrete grade used is C35/45. A minimum fire resistance of 120 minutes is required. This means that the minimum plate thickness should be at least 200 millimetres and the minimum rebar distance (distance from bottom to centre-line reinforcement) 35 millimetres[10]. The height of the slab is chosen, based on the rule of thumb that l/d should satisfy $245/l$. Given the fact that a large cover is needed for fire safety reasons and heavy floors result in significantly larger dimensions of vertical members in high-rise, a slightly lower value was chosen:

$$d = 315mm \quad (3.5)$$

$$h = 315 + 35 = 350mm \quad (3.6)$$

$$q_w = 25 * 0.350 = 8.75kN/m^2 \quad (3.7)$$

$$q_k = 8.75 + 2.50 + 2.50 = 13.75kN/m^2 \quad (3.8)$$

$$q_d = 1.32 * (8.75 + 2.50) + 1.65 * 2.50 = 17.25kN/m^2 \quad (3.9)$$

The reinforcement of the one-way spanning zone of the slab is designed by considering a strip of 1 meter in width as a simply supported beam. Incidental support moments are taken into account as 33% of the maximum field moments. The two-way spanning zones are designed by using the column, reinforcement and middle strip approach used in the old Dutch norm NEN 6720[28]. Table 25 from GTB 2013[5] with 2 hinged line supports is used in order to calculate the bending moments. Additionally, it is required that support moments at the façade are minimum 33% of the field moments. This means that when table 25 presents values that fall below this minimum, these values are adapted in order to satisfy this criteria.

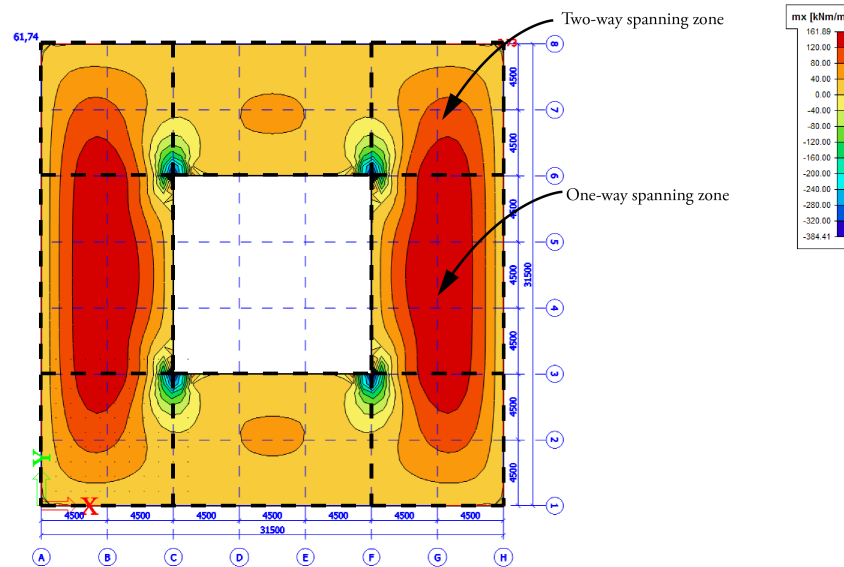


Figure 3.12: Graphic view of m_x of a flat slab floor model in SCIA.

Hollow core slab type	Height	Max span	Weight
VBI 200	200 mm	9.3m	3.02kN/m ²
VBI 260	260 mm	11.8m	3.76kN/m ²

Table 3.5: Hollow core slab properties and area loads.

3.4.2. Hollow core slab floor (HCSF)

The hollow core slab is a pre-stressed and prefabricated floor. The slabs have standardised sizes with each their own height, weight and maximum span. The properties of the slabs that are used in this research are listed in table 3.5 and are obtained from documentation from the supplier VBI[60][61]. A fire resistance of 120 minutes is taken into account for determining the maximum span. The slabs are spanning differently depending on their position. A part of the slabs is partly supported by a steel THQ beam, spanning from the core to a perimeter column. The THQ beam was chosen, because of its high torsional stiffness compared to other open sections. Combinations of VBI 200 and VBI 260 on the same floor are allowed in order to minimize material use and weight.

Diaphragm action is needed to achieve cooperation between the core and façade structure. When using a flat slab, the whole floor behaves monolithically. When using hollow core slabs, diaphragm action can be obtained by using a concrete screed layer. This concrete screed layer is estimated to have a height of 50 mm and includes a reinforcement net of Ø8-150. Additionally, extra reinforcement is needed at the building perimeter where tensile zones will occur when the building is loaded laterally. For this purpose, 3Ø25 is used, based on engineering judgement. A detailed overview of the used slabs and calculations of the steel beams can be found in appendix B. Following from 8 different column configurations and 5 different diaphragm configurations, a total of 27 different floor configurations can be found per building height variation.

The amount of pre-stress steel incorporated in the hollow core slabs is variable and depends on the span, loads and fire resistance. In order to prevent detailed calculations, the amount of pre-stress steel is estimated by consulting reference projects of Royal HaskoningDHV with similar spans and loads. This results in 3750 kg/m² (577 mm² per slab) of pre-stress steel for the VBI 200 slab and +/-5400 kg/m² (833 mm² per slab) for the VBI 260 slab.

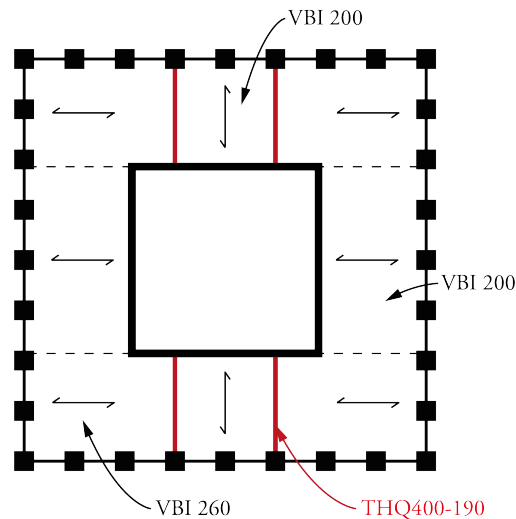


Figure 3.13: An example of a possible hollow core slab floor configuration.

3.4.3. Composite floor (CF)

The composite floor consists of a steel corrugated sheet with a concrete topping, supported by steel beams. The steel plate acts as primary reinforcement for the concrete floor. A reinforcement net of $\text{Ø}8\text{-}150$ is added in the top layer for monolithic behaviour, occasional support moments, crack width control and fire resistance. Additionally, reinforcement is added in the bottom gutter, close to the steel plate, to increase fire resistance. By adding $\text{Ø}16$ rebars, it is assumed that a fire resistance of 90 minutes can be achieved. The additional 30 minutes of fire resistance is achieved by adding fire resistant cladding. It was chosen to use the same material that is used for fire protection of the columns and beams, explained in section 4.4.3. A layer of 20 mm of PROMATECT-H is applied.

The configuration, span and therefore material use heavily depend on the configuration of the perimeter columns. Multiple floor designs are possible for the same column configuration. For each separate column configuration a unique floor design was made, where the focus was on minimising weight and material use. This is achieved by using temporary supports during construction and by allowing primary beams to be placed in an angle. Furthermore, the beams consist of IPE and HEA castellated beams to further minimize material use and allow mechanical installations to pass through the beams. Therefore, S355 is used which has no additional environmental impact compared to S235.

Further material minimisation could be achieved by using steel shear connectors in the concrete to enable composite action of the beams. However, calculation methods are more complex and therefore take considerably more time when evaluating a high amount of floor configurations. Therefore it was not considered in this thesis.

The composite floors are designed by using technical information documents and a calculation spreadsheet by the company Dutch Engineering, manufacturer of the ComFlor composite floors[20]. In Table 3.6 are the floor types and their properties listed that are used in the designs. The castellated beams are designed by using rules of thumb and simplified models for simply supported beams. A detailed overview of the floor designs, beam properties and design calculations can be found in appendix B. Following from 8 different column configurations and 5 different diagrid configurations, a total of 27 different floor configurations can be found per height class.

Floor type	Plate thickness	Floor thickness	Weight
ComFlor 46	0.9mm	120mm	2.70kN/m ²
ComFlor 75	0.9mm	140mm	2.62kN/m ²
	1.2mm	140mm	2.66kN/m ²
ComFlor 95	0.9mm	160mm	2.87kN/m ²
	1.2mm	160mm	2.90kN/m ²

Table 3.6: Composite floor slab properties.

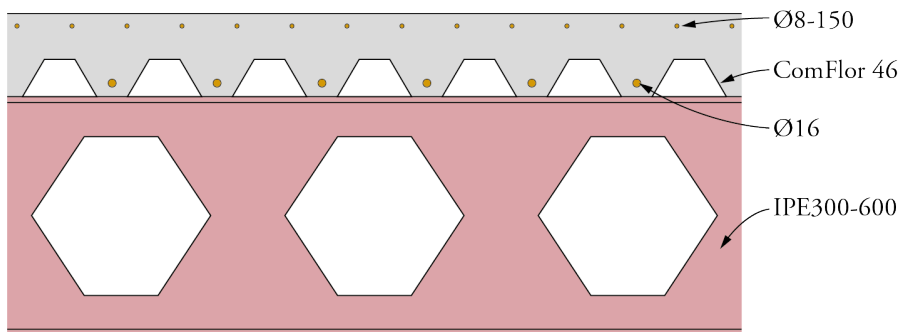


Figure 3.14: Sketch impression of the composite floor configuration on castellated beams.

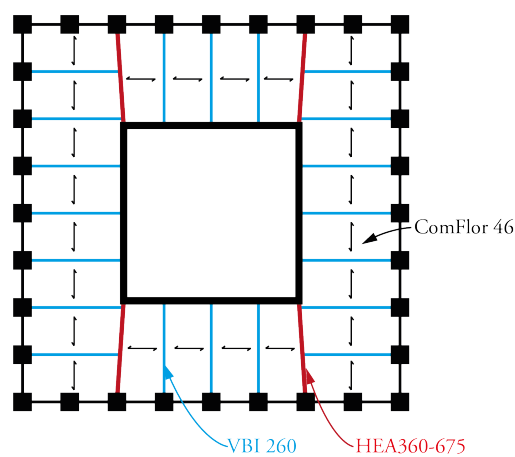


Figure 3.15: Possible configuration of a composite floor, including primary and secondary beams.

3.5. Modelling method

Reading section 3.1, 3.3 and 3.4, a total number of 3×62 models can be found, resulting in 186 models in total. This is also shown in section 3.6 in figure 3.29. The high number of models and the limited amount of time requires the design and computation time to be small. Therefore it was chosen to perform 2D frame calculations instead of 3D finite element analysis (FEA) calculations, as discussed in section 1.4.2. 2D frame models are fast in calculation while still being significantly accurate for the global design purposes in this thesis. The 2-dimensional models are discussed in the following sections.

Additionally, due to the high amount of the models and the high factor of repetition, it was chosen to make use of parametric models. It was chosen to use a combination of Rhinoceros[41], Grasshopper[42] and Karamba[24], a structural calculation plug-in for Grasshopper. A more elaborate description of the work flow can be found in 3.5.5.

It was chosen to include the façade structures two times in the 2-dimensional models, at the left and right side of the core. Another option was to only include the structure once and double the stiffness of all the elements. However, this would mean additional scripting in order to assign the right stiffness to the elements and also to retrieve the right forces in order to determine the reinforcement. Moreover, the required analysis time was only a matter of seconds so a shorter calculation time was not really desired.

Both the frame (and tube) and diagrid models have been validated using 3D models in both SCIA Engineering, Karamba and hand calculations. These comparisons can be found in appendix F.

3.5.1. Calculation model for global design

The core partially provides stiffness in all the models. When only considering the core, it can be modelled as a beam with bending stiffness EI_c and axial stiffness EA_c , cantilevered from the soil. The cross-section is defined by the dimensions of the core and the wall thickness t . The 2D model can be seen in figure 3.16. When applying the height zones to this model, thickness t will decrease step-wise when rising vertically.

In all the designs, the stiffness is also partially provided by a perimeter structure which creates tube-in-tube structures, except for the outrigger. The outer structure and the core are connected by the floors, which act as rigid diaphragms. Rigid diaphragms do not deform axially and transfer the lateral loads between the two structures. This ensures that the core and the outer tube undergo the same deformations. In 2D, these rigid diaphragms can be modelled as hinged connected beams, only subjected to axial forces and with an infinitely high axial stiffness.

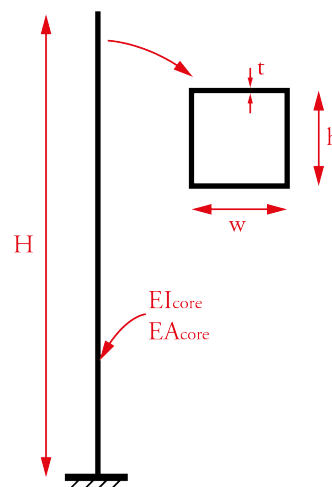


Figure 3.16: 2-dimensional model of the core and explanation of the Schueller rule.

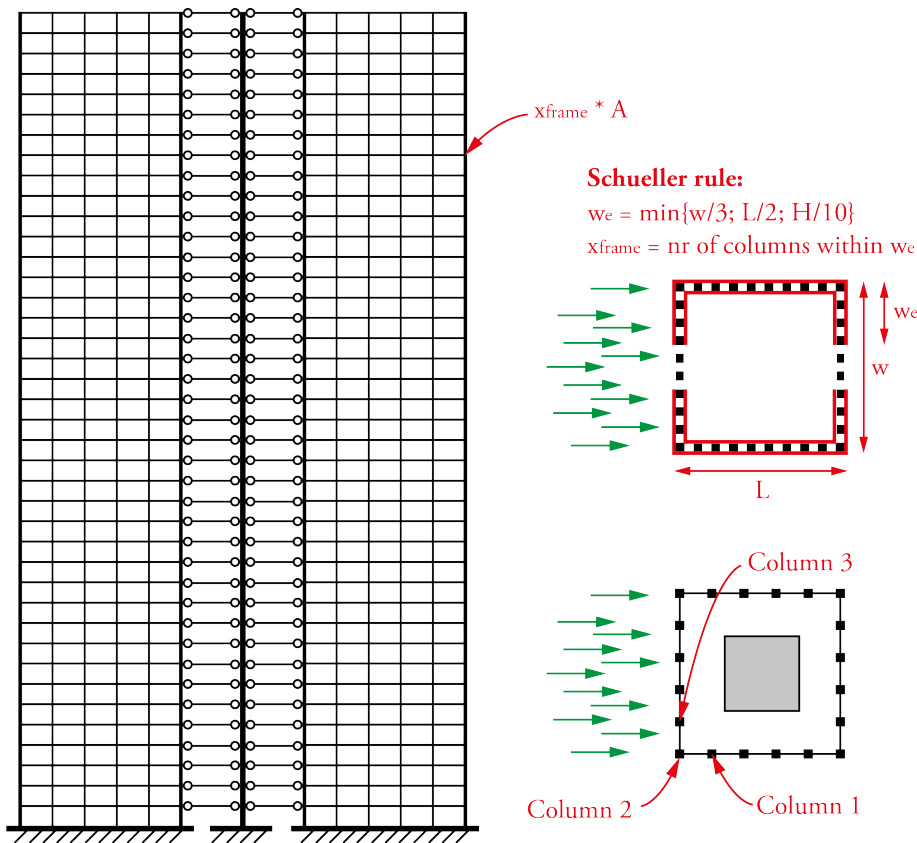


Figure 3.17: 2-dimensional model of the frame model.

1. Frame

The rigid frame models consist of perimeter columns rigidly connected with beams. Furthermore, due to shear lag, as explained in section 2.2.3, the tube can not use its full cross-section when subjected to lateral load. Cross-sections of the columns and thickness of the core vary per height zone, the cross-sections of the beams are kept constant over the height.

In order to cover the shear lag aspect when modelling the structure in 2D, the tube can be represented as a thin walled pipe with an effective width w_e [46]. The area of the corner columns is multiplied by the amount of columns that falls within the effective width. The model can be seen in figure 3.17, including an explanation of the Schueller rule.

Most of the times, $column_3$, indicated in figure 3.17, is governing for strength design of the columns. This follows from the fact that the axial load due to the wind load is higher in this column, because the lever arm is larger compared to $column_2$. However, due to the shear lag effect, the column force due to wind loads can not simply be obtained by using $F_{w;column3} = \sum F_w/n$, where n stands for the number of columns in the façade. Instead a factor, c_3 , is used, based on support reactions of 3D SCIA models that are used to verify the 2D models. The same holds for the corner column itself, $column_2$ where a factor c_2 is used. The values of these factors are showed in table 3.7. The actual axial force due to wind then becomes: $F_{wind;column,i} = F_{wind;corner} * c_i$.

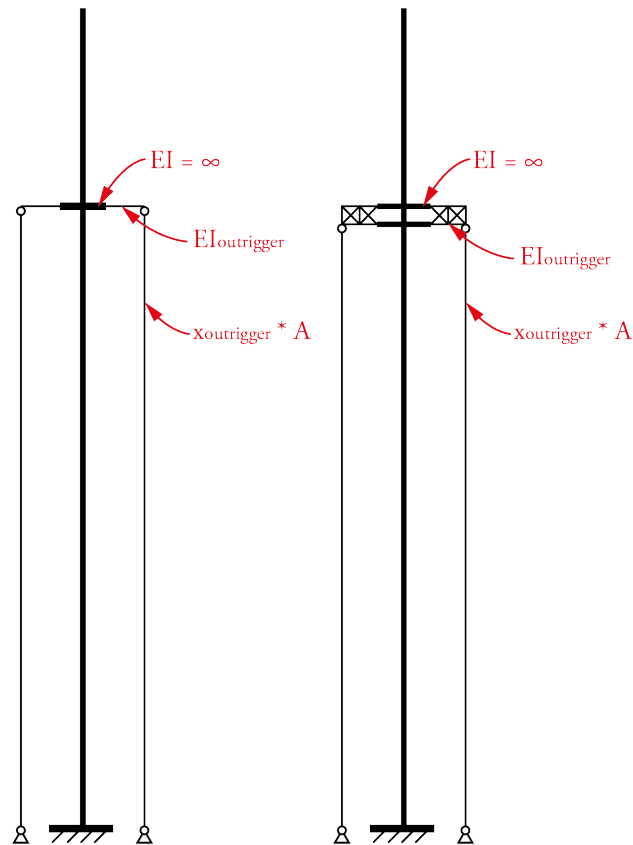


Figure 3.18: 2-dimensional models of the outriggers, showing the difference for the concrete and steel outriggers.

2. Outrigger

An outrigger structure activates the perimeter columns to increase the lever arm. The columns are subjected to axial loads and only deform axially. Depending on the amount of perimeter columns that are activated, the area of the columns is multiplied by a factor $x_{outrigger}$. The models in this thesis also contain a belt truss/wall. Therefore it is assumed that all of the columns are activated to cooperate in the lateral stability of the building, resulting in $x_{outrigger} = 8$. Beams in the building perimeter are pin connected to the columns and therefore do not contribute to the stiffness of the building. The beams are designed using rules of thumb resulting in rectangular cross-sections for concrete and IPE beams for steel models.

The outrigger structure itself is subjected to shear and bending forces, resulting in an inefficiency of transferring the axial forces from the columns to the core. Therefore, the outrigger structure is also modelled. Important to note is that the lever arm of the outrigger is an important aspect in the efficiency of the outrigger. A longer lever arm, increases the contribution of the columns to the stiffness of the building, but decreases the effective stiffness of the outrigger itself. When working in a 2D model, the core is modelled as a line element, resulting in a bigger lever arm than actually exists in reality. In order to cover this problem, the part of the outrigger in the 2D model that falls within the cross-section of the core, is modelled as a beam with an infinite high Young's modulus, $E_{outrigger;stiff} = \infty$.

The outriggers are modelled as they are in reality: a shear wall in concrete and a truss in steel. The cross-sections are multiplied by a factor 2, because there are 2 outriggers at each side of the core as is explained in section 3.3.2. The calculation models can be seen in figure 3.18.

As described in section 2.2.3, the location of the outriggers has a significant influence on the global stiffness of the building. The optimum locations can be determined by hand calculations by Smith[47]. However, since parametric models are used, a optimisation loop can be run in order to define the optimum locations. The used algorithm adjusts the position of the outriggers in order to find the solution that has the lowest deflection.

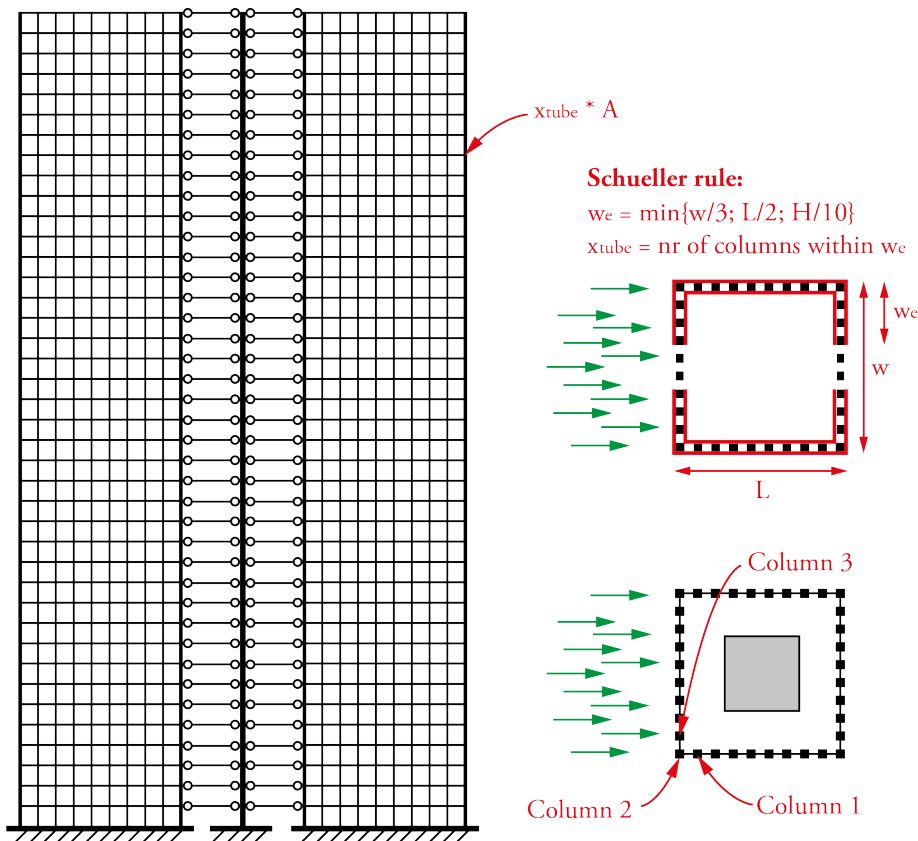


Figure 3.19: 2-dimensional calculation model of the frame and tube model.

3. Tube

The calculation models of the tube models are the same as the frame models explained in section 3.5.1. The difference between the two systems is the higher amount of columns (closer spacing) in the tube models and the deep rectangular cross sections for concrete, as explained in 3.3.3. Also here, column factors are used as indicated in 3.7. The corner column in the calculation model represents the whole façade perpendicular to the 2-dimensional plane. Therefore, the normal forces due to wind loads in $column_2$ and $column_3$ are derived by using factors c_2 and c_3 . These factors represent the part of the total normal force due to wind load in the corner column in the corner column that is actually acting on $column_2$ or $column_3$. The derived factors are based on support reactions of 3-dimensional SCIA models used for verification, as discussed in appendix F. The values of these factors are showed in table 3.7. The actual axial force due to wind then becomes: $F_{wind,column,i} = F_{wind,corner} * c_i$.

n	5	6	7	8	9	10	11
c_2	0.55	0.50	0.45	0.40	0.35	0.30	0.25
c_3	0.32	0.30	0.28	0.26	0.24	0.20	0.20

Table 3.7: Factors used for calculating axial forces in $column_2$ and $column_3$ due to wind loads, dependent on the amount of columns in the façade.

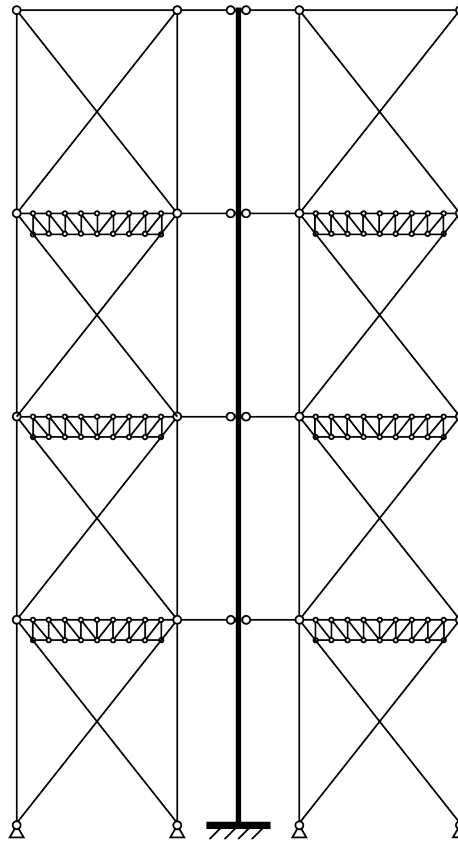


Figure 3.20: 2-dimensional model the braced tube models.

4. Braced tube

The braced tube consists of a tube structure where mega braces are added. These braces are subjected to axial forces and therefore behave stiffer than a frame subjected to shear forces. All connections are assumed to be hinges. Beams in the building perimeter are pin connected to the columns and therefore do not contribute to the stiffness of the building. Therefore, it is assumed that the column- and beam-structure does not contribute to the stiffness of the building and is only designed for gravity loads. Consequently, the 2D model of the braced tube consists of a cantilevered truss as can be seen in figure 3.20.

Due to low gravity loads in the corner columns, a belt truss is used to distribute the vertical loads to the corner columns. This prevents that tensile forces will occur at the base of the building.

The columns are designed for gravity forces, using simple calculations where floor loads are added to the self weight. Beams are designed using rules of thumb, using IPE beam cross sections. The mega columns in the corner consist of HD-profiles, where stiffness often governs over strength. When considering the higher models, bigger cross-sections than the standard sizes might be required. This aspect is covered by multiplying the amount of columns in the corner, where in reality custom profiles might be needed. However, since the columns are only subjected to axial forces, the required amount of material will be the same in the end.

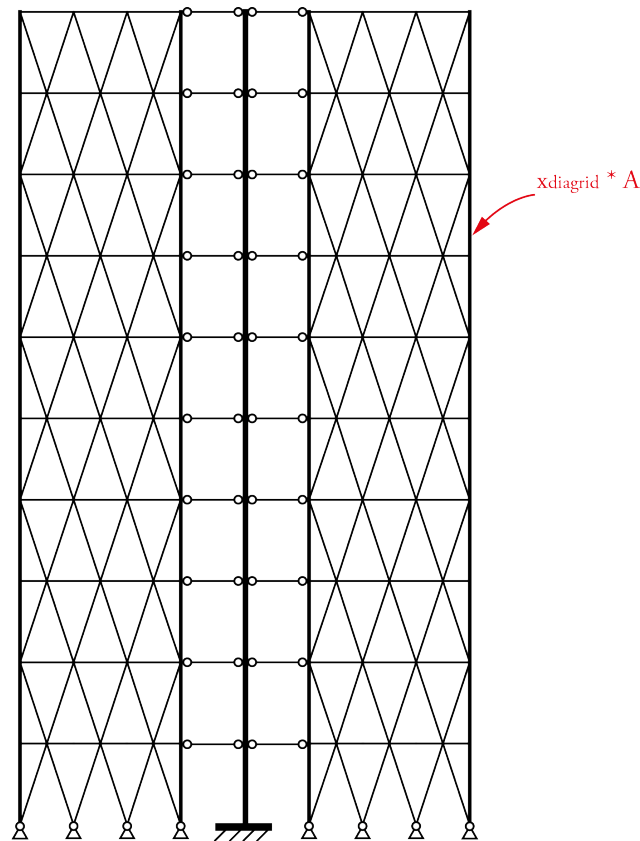


Figure 3.21: 2-dimensional model the diagrid models.

5. Diagrid

The diagrid consists of diagonal braces and horizontal beams which bear both the vertical and lateral loads. The members are primarily loaded axially. Members in the perpendicular façade also contribute to the stiffness of the building, just as is the case in the frame and tube models. After evaluation of 3-dimensional models, it appears that there is no shear lag present in the diagrid models. Therefore, the extra diagrid members in the perpendicular façade are added to the cross-section of the corner column by a factor $x_{diagrid}$. However, since the diagrid members are placed under an angle, an efficiency of 75% is used to determine the factor. Then the factor becomes $x_{diagrid} = 0.75 * n + 1$, where n is the number of diagrid members in the perpendicular façade divided by 2, and the 1 covers for the corner column.

The diagrid structure contains primary and secondary beams. The secondary beams are only subjected to gravity forces, which are then transferred to the diagrid members. The beams are not included in the 2D calculation models for global stiffness. The secondary beams are designed according to rules of thumb, resulting in deep rectangular cross-sections for concrete and IPE profiles for steel models. The primary beams are also subjected to tension forces due to gravity and lateral loading and therefore are included in the 2D calculation models. In the steel models, HEM profiles are used for the primary beams. The 2-dimensional diagrid model can be found in figure 3.21.

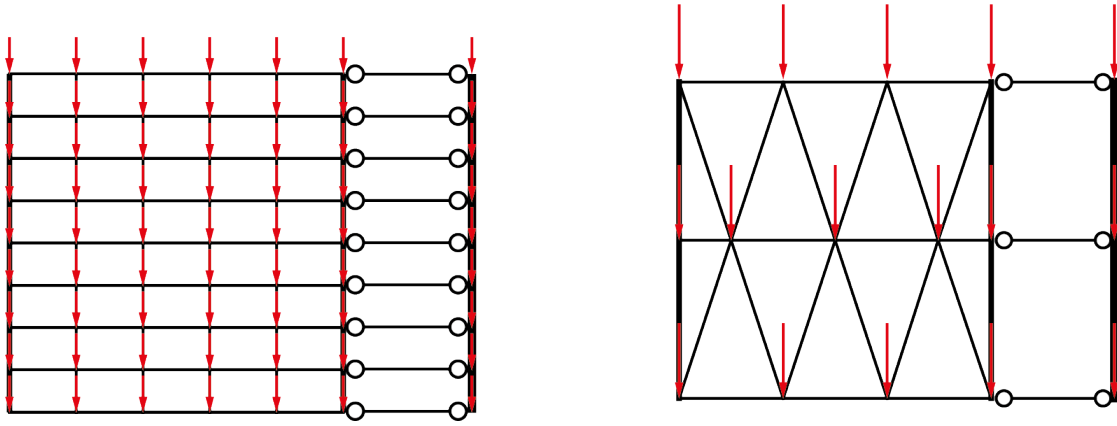


Figure 3.22: Figures showing the way of modelling the vertical loads in the 2-dimensional models.

3.5.2. Loads

Vertical loads on the floors also have to be included into the 2D models. However, since the floors are not modelled, the area loads need to be converted to fit in the calculation models. It has been chosen to model the area loads as point loads acting on the vertical members: columns and core. This is illustrated in figure 3.22.

The area loads that are used to determine the point loads consist of the floor loads, façade load and weight of the floor beams evenly distributed over the floor area. Since there are lots of different floor configurations, there is equal variety in point loads. The process of the calculation of the point loads is automated by linking spread sheets. The calculated loads then are used as input in the calculation models where the point loads are assigned to the nodes parametrically. The point loads in the corner columns are increased by the number of leftover columns in the perpendicular façade, divided by two. When the parametric models were created, the total weight of the floor loads was checked using hand calculations.

In reality, within the diagrid models, the floors also transfer their loads along the diagrid members, not solely in the nodes. In the 2D models this has been simplified in order to reduce complexity of the modelling and calculation processes. Instead, the floor loads in between diagrid nodes are added to the upper node, see figure 3.22.

3.5.3. Design checks

Second order effect

High-rise buildings are tall and have a relatively small width. Wind loads acting on the building cause big moments at the base of the building. Additionally, vertical forces also increase to high proportions at the base. Wind loads cause the building to deflect and because of that also the centre of mass of the building is displaced. This causes an additional moment at the base of the building, which causes additional deflection. This is called the second order effect and should be taken into consideration when designing high-rise buildings. Usually this causes the building to deflect 10% to 20% more.

When linear calculations are used, the second order effect is not taken into account automatically. Therefore, this is incorporated into the calculation models manually by means of a simplified model which is shown in figure 3.23.

The building is modelled as a single cantilevered beam. The base moment due to wind loads is M_1 and is obtained by multiplying the wind forces $F_{w,i}$ with their corresponding arm x_i . This causes the deflection u_w which is calculated by the 2D model. In order to obtain u_1 , the deflection caused by the foundation should also be added: $u_1 = u_w + u_f = u_w + 1/1000 * H$, where H is the height of the building.

It is assumed that the point of mass in the building is situated in the middle of the building and is deflected by $0.5 * u_1$. This causes the additional moment by multiplying the mass of the building with the lever arm: $M_2 = \sum F_{vert} * 0.5 * u_1$. Then, factor n , the ratio between M_1 and M_2 , can be determined by $n = M_1/M_2$.

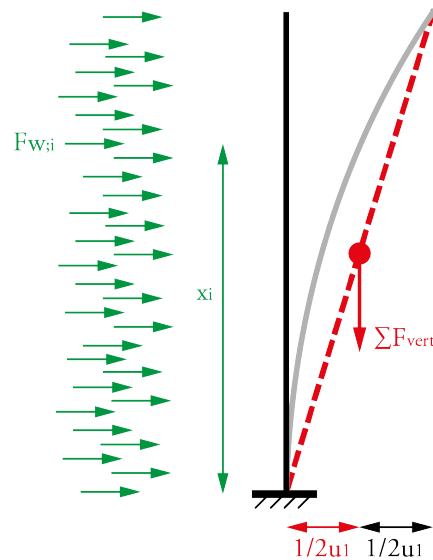


Figure 3.23: Simplified model of the second order effect.

This second order moment causes a second order deflection which causes a third order deflection and so on. Therefore, the second order factor N can be obtained by $N = n/(n - 1)$. The final deflection U can then be obtained by the following formula:

$$U = u_1 * N \leq \frac{1}{1000} * H \quad (3.10)$$

Core checks

The concrete core is checked on the maximum acting stress, considering LC1 and LC2. The maximum stress consists of stress from normal forces of vertical loads and stress from bending due to the wind loads. The stresses due to wind loads are multiplied by the second order factor.

Additionally, the concrete core is also checked on possible tension in SLS. It is assumed that the concrete core does not crack in SLS and therefore the normal Young's modulus can be used in SLS. This is verified by doing a check with LC5. LC3 is used to check if there is not too much tension in the core in ULS, that would lead to high reinforcement ratios. The dimensions of the core and the columns are designed in such a way that the highest unity check will result in the range of 0.8-0.9.

Column checks

The columns are evaluated and dimensioned on their maximal normal and bending forces, following from LC1 and LC2. The normal forces due to wind loads are multiplied by the second order factor. For column 1, the determination of the forces is simple and can be obtained directly from the model. For column 2 and 3, the factors that are determined in section 3.5.1 are used. Due to the increased cross-section in the corners for column 2, the self-weight first has to be subtracted and corrected for the normal column cross-section.

In this case, the cross sections are designed in such a way that the highest unity check will result in the range of 0.8-0.9. However, in some cases global stiffness is governing in the design of the columns.

Buckling of the concrete columns is taken into account when designing the reinforcement, explained in section 3.5.4. In the case of a steel column, buckling reduction factors are calculated using the formulas from Eurocode 3[36].

The columns are continuous and sideways supported by beams every storey. Therefore, L_{cr} was chosen to be half of the storey height. Additionally, the weak axis was chosen to calculate the capacity. Moreover, according to the Eurocode, the buckling curve for HD profiles is not specified. Regarding this aspect, a recommendation by Snijder[48] was followed to use buckling curve c with a corresponding α of 0.49.

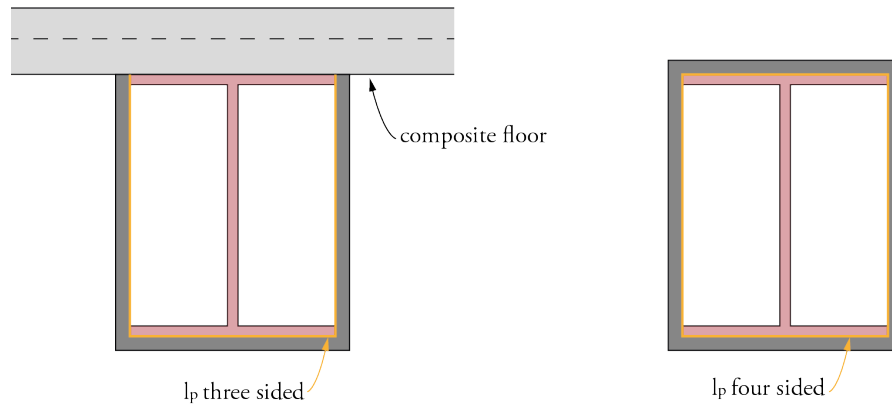


Figure 3.24: Determination of A_p for profiles subjected to fire conditions from 4 and 3 sides.

Beam checks

For the beams, deflection in LC4 is governing in most cases, which are checked using rules of thumb. In some cases where also normal forces are present, e.g. the diagrid or the belt truss in the braced tube models, also the stresses are checked in LC1 and LC2. For the concrete models, it is monitored that the amount of reinforcement does not become excessively high.

Fire safety

The fire resistance criteria are met by fulfilling minimum width and reinforcement distance for concrete, as discussed in section 3.5.4, and adding fire resistant material on the steel members. A choice was made to make use of the PROMATECT-H material from Promat and their design book[40].

Usually, the procedure is as follows: first the load during a fire load-case has to be determined. Then, by using the maximum bearing capacity at room temperature the η -factor can be determined, after which the critical steel temperature can be calculated. This is the temperature at which the element would fail during the fire load-case. Next, the steel temperature has to be calculated using the profile factor P and the estimated amount of fire resistant material. The profile factor P shows the relation between the speed of heating of the steel element and its geometry. The structure meets the requirements if the steel temperature remains lower than the critical steel temperature.

For the purpose of this thesis, it was chosen to use the standard design tables formulated in the design book by Promat[40]. These tables contain standard profiles and required applied thickness's of PROMATECT-H for standardised critical steel temperatures for 120 minutes of fire resistance for a standard fire curve, based on profile factor P . These standardised critical steel temperatures are 530 °C for columns and 575 °C for beams. These temperatures are based on recommendation by Bouwen met Staal[9].

Not all of the used sections in this thesis are listed in the tables, e.g. HD sections. Therefore, an approximation was made by determining the profile factors and interpolating the required thickness's based on the thickness's and profile factors listed in the tables from Promat. A minimum thickness of 20 mm based on data in the tables was assumed. The profile factors are calculated according to figure 3.24 and the following formula:

$$P = A_p/V \quad (3.11)$$

Here A_p is the surface area of the protected area. Tables containing the full data sheets for all used profiles can be found in appendix C.

	Calculation model 1 Global design	Calculation model 2 Reinforcement design
Due to wind load	N, M, V	
Due to vertical load	N	M, V

Table 3.8: An overview of which forces are used from which model for reinforcement design.

3.5.4. Calculation model for reinforcement design

The design of the reinforcement has been incorporated into the parametric model. No calculations have to be done manually, except the determination of the applied reinforcement. The model used for the global design uses a reduced Young's modulus for both the columns and beams, whereas in reality the Young's modulus of the columns in vertical direction has not changed. Additionally, vertical loads are modelled as point loads in the nodes in the model for global design. This means that moments due to vertical loads are not present in the beams and columns within this research.

Therefore, a second calculation model is created in Karamba to determine the bending moments and shear forces due to vertical loads. The results are combined with the bending moments and shear forces due to wind forces and normal forces from the global design model. The bending moments, shear forces and normal forces due to wind load, are multiplied by the second order factor. An explanation of which data is used from which model is shown in table 3.8. This section describes the used approached, a more elaborated explanation can be found in appendix D.

Within the calculation model for reinforcement design, only vertical loads are applied. These vertical loads are modelled as line loads on the beams in order to obtain the moments and shear forces that they cause. The corner columns do not have an increased area as only vertical loads are considered. This is only used in the model for global design for lateral stiffness. Lastly, the Young's modulus of the columns is not reduced and remains the original uncracked Young's modulus, since only vertical loads are considered.

Differential column shortening

When observing the moment lines of the beams and columns in the frame and tube models, one can see that these are shifting from the centre towards the corners, as can be seen in figure 3.25 and 3.26. The reason of this phenomenon is unevenly loaded columns, leading to differential column shortening, which results in imposed deformation and extra bending moments and shear forces. Differential column shortening occurs due to the fact that cross-sections are kept the same over the entire floor, and the columns are evenly distributed which means that corner columns receive less load.

This effect could be reduced by decreasing the cross-section of less loaded columns, or by shifting more load to the corner columns by changing the design. Another option would be using plastic calculations instead of linear elastic, resulting in redistribution of moments. All options would mean significant changes in the models and also would increase the complexity of the design process. Therefore, it was chosen to leave the model as it is and design the reinforcement in such a way that these extra bending moments are taken care of. This might lead to an overestimation of the required reinforcement in the beams. A more elaborate explanation of this aspect can be found in appendix E.

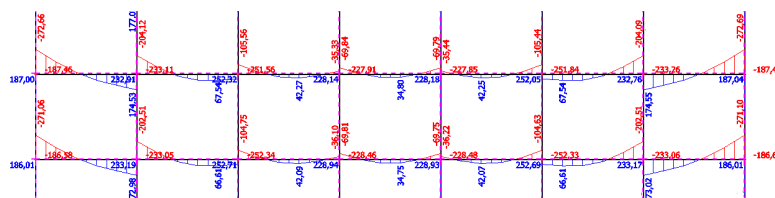


Figure 3.25: Shifting moment lines in the beams due to differential column shortening. These are results from a 3D SCIA model, only loaded with vertical loads.

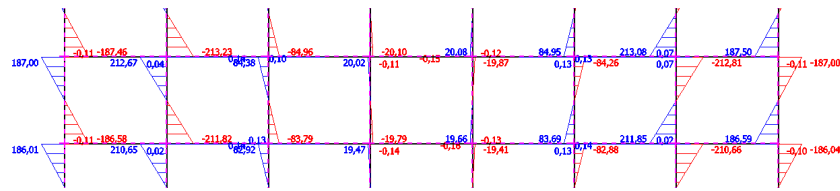


Figure 3.26: Shifting moment lines in the columns due to differential column shortening. These are results from a 3D SCIA model, only loaded with vertical loads.

Simply supported beam	b_{min}	200	240	300	500
	a_{min}	65	60	55	50
Continuous beam	b_{min}	200	300	450	500
	a_{min}	45	35	35	30

Table 3.9: Requirements to the minimum width and cover of simply supported and continuous beams in mm.

Reinforcement design beams

The design of the reinforcement of the beams is based on the approach that can be found in GTB 2013[5]. Table 11.6 from GTB 2013 is used to determine the required amount of reinforcement, based on the factor $M_{Ed}/(bd^2)$, taking into the minimum reinforcement.

First the bending moments due to LC1 and LC2 are determined. Bending moments due to wind loads are multiplied by the second order factor and then added to the bending moments due to vertical loads. Then, a distinction is made between positive moments and negative moments. Next, the maximum positive and the maximum negative moments are retrieved. The same holds for the shear forces. Upper reinforcement is designed using the negative moments and the lower reinforcement using the maximum positive moments.

In the case of the diagrid models, a tensile force is present in the diagrid beams due to vertical loading of the inclined elements. The tensile force is distributed over the top and bottom reinforcement in a 50/50 distribution. The extra required reinforcement is added to the required reinforcement due to bending moments.

The beams are split into two to four categories, depending on the range of the factor $M_{Ed}/(bd^2)$. Based on the chosen values of the factor for the categories, the beams are automatically assigned to the right category. The categorisation of the beams is then mirrored, in order to cope for wind loads in two directions, where the higher category is leading. Next, the amount and size of the bars that will be applied are determined. The focus here is to aim for the lowest amount of steel possible, keeping the bar to bar distance in mind.

At last, it is checked whether the minimum shear reinforcement is satisfactory. The minimum shear reinforcement and maximum distance are determined and being compared to the required shear reinforcement, with θ chosen as 21.8° . A diameter is chosen for the shear reinforcement and the spacing is automatically calculated. At last, the concrete compression zone is checked.

For fire safety reasons, a minimum cover on the rebars is required. This requirement depends on the width of the beam and its support conditions. In table 3.9 are the requirements for 120 minutes fire safety shown.

Reinforcement design columns

The design of the reinforcement in the columns is also based on the approach that can be found in GTB 2013[5]. Here, the amount of required reinforcement depends on two factors: $n = N_{Ed}/(f_{cd} * A_c)$ and $m = M_{Ed}/(f_{cd} * A_c * h)$. Using design graph 10.3.a from GTB 2013, the required mechanical reinforcement ratio ψ can be determined.

The moment, shear and normal forces are retrieved from the Karamba model. The moment values are increased by $1/30 * N_{Ed}$ in order to cover for imperfections. Values due to wind loads are multiplied by the second order factor. The values for n and m are calculated for each individual column. The design graph is digitalised into an Excel table and then imported into Grasshopper. Here, the n and m values of the columns

b_{min}	350	450
a_{min}	57	51

Table 3.10: Requirements to the minimum width and cover of columns for fire safety in mm.

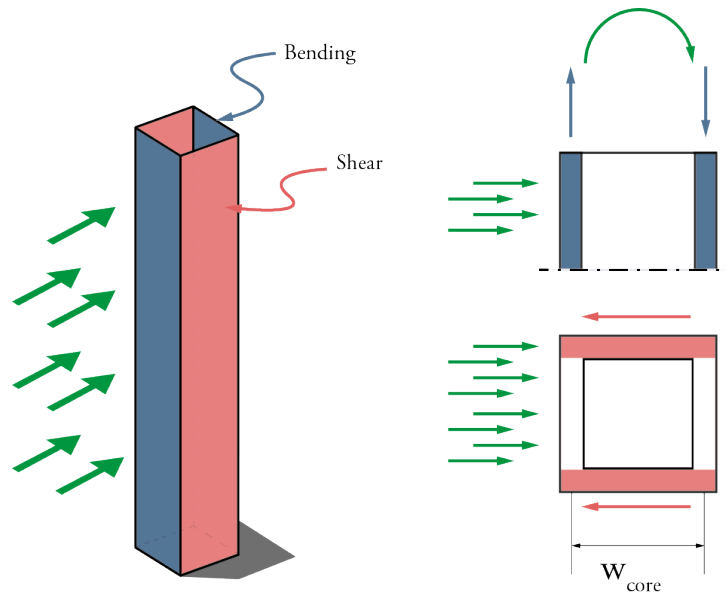


Figure 3.27: Sketch showing the way of modelling for designing the reinforcement of the core.

are cross-referenced with the values of the table with as result that ψ is automatically determined for each individual column.

The next step is that for each column it is determined whether a second order calculation should be performed or not. This is the case when $\lambda > \lambda_{lim}$. Here it is assumed that $\varphi_{ef} = 2.0$ so that $l_0 = 0.5 * l$; $A = 1.1$; and $C = 0.7$. Using the new calculated m value due to second order effects, a new reinforcement ratio ψ can be found. The columns also have to cope with large shear forces. The required shear reinforcement is determined in the same way as the beams.

For fire safety reasons, a minimum cover on the rebars is required. Additionally, a minimum of 8 rebars is required. In table 3.10 the requirements for 120 minutes fire safety are shown.

Reinforcement design core

The design of the reinforcement of the core is approached by splitting the core walls into two categories when subjected to lateral loading. The front and back wall are subjected to pure compression and tension forces due to the acting bending moment on the core. The side walls are subjected to pure shear due to the shear forces on the core. This approach is also generally applied in steel beam cross-sections. A graphic representation of this approach is shown in figure 3.27.

There are no requirements regarding the minimum amount of vertical and horizontal reinforcement according to the Eurocode. However, due to practical reasons a minimum reinforcement net of $\text{Ø}8\text{-}150/250$ is present, where 150 mm is the spacing for vertical reinforcement and 250 mm the spacing for horizontal reinforcement. Reinforcement is placed at the two sides of the walls with a minimum cover of 35 mm for fire safety reasons.

For the determination of the vertical reinforcement, also normal forces due to vertical loads are taken into account. LC3 is considered in this case as this load case results in the highest amount of tensile stress in the core. Considered is a one meter wide strip of the core wall, only subjected to normal forces. Forces are retrieved from the Karamba model and a n value is calculated for every story. Then, a ψ value is calculated,

using the column approach explained in the previous section. This ψ value is used to determine the required reinforcement, which is then exported to an Excel file where the applied vertical reinforcement is determined.

The determination of the horizontal reinforcement approaches the side walls as beams. The required shear reinforcement is determined using the same formula as is used with the beams. Here z is taken as the centre to centre distance of the front and back wall, which are subjected to normal forces. The required horizontal reinforcement is also exported to the spreadsheet to determine the applied reinforcement.

3.5.5. Implementation in Grasshopper

The entire process from modelling 3D geometry, to structural analysis of the 2D calculation models, to determining the environmental impact is entirely set up in a parametric way. This includes several spreadsheets that are imported in and exported out of the Grasshopper model.

Karamba is used to make structural calculations of the structures. Additional calculations are added as described in sections 3.5.1, 3.5.3 and 3.5.4. A flowchart showing entire work flow and links of the main and sub models can be seen in figure 3.28.

Inputs for the models are geometry parameters (dimensions building, column configuration, etc), structural parameters (cross-sections, materials, etc) and reinforcement parameters (cover, applied reinforcement, etc). The geometry parameters are defined by the model case, the structural and reinforcement parameters are variable and are optimised in order to minimise material use while still meeting the criteria. There is one Grasshopper model where the major part of analyses are done. In addition to that, there are two Excel spreadsheets which cover the design and analysis of the floors en core reinforcement. Finally, all material quantities are gathered into the environmental impact assessment spreadsheets, which determines the environmental impact.

The first step is generating the 3-dimensional and 2-dimensional geometry. The floor designs and wind calculations are based on this geometry and are executed in separate spreadsheets. The resulting loads are used as input in the Grasshopper model. Next, the global design calculation model is assembled where cross-sections, materials, loads and supports are assigned. Load cases are created and the building is divided into different height zones.

Now the first design loop is started where cross-sections are optimised to the global and local design criteria in ULS and SLS. The performance is checked and cross-sections are adapted manually accordingly. When criteria are not met, the structural parameters are changed manually up to the point that the criteria are satisfied. When it appears that significant high reinforcement ratios are required, it is possible to change the cross-section accordingly.

When the criteria are met, calculations of the second reinforcement design calculation model are started, as described in 3.5.4. Now the second design loop is started. The required reinforcement is determined by the model where after the applied reinforcement is determined manually. For the columns and beams, this is done within the Grasshopper model. The reinforcement of the core and floors is done in separate spreadsheets.

Finally, all the material quantities are automatically calculated in the Grasshopper model and spreadsheets and are then collected in the environmental impact spreadsheets. This last spreadsheet uses the shadow prices of materials as input to determine the environmental impact.

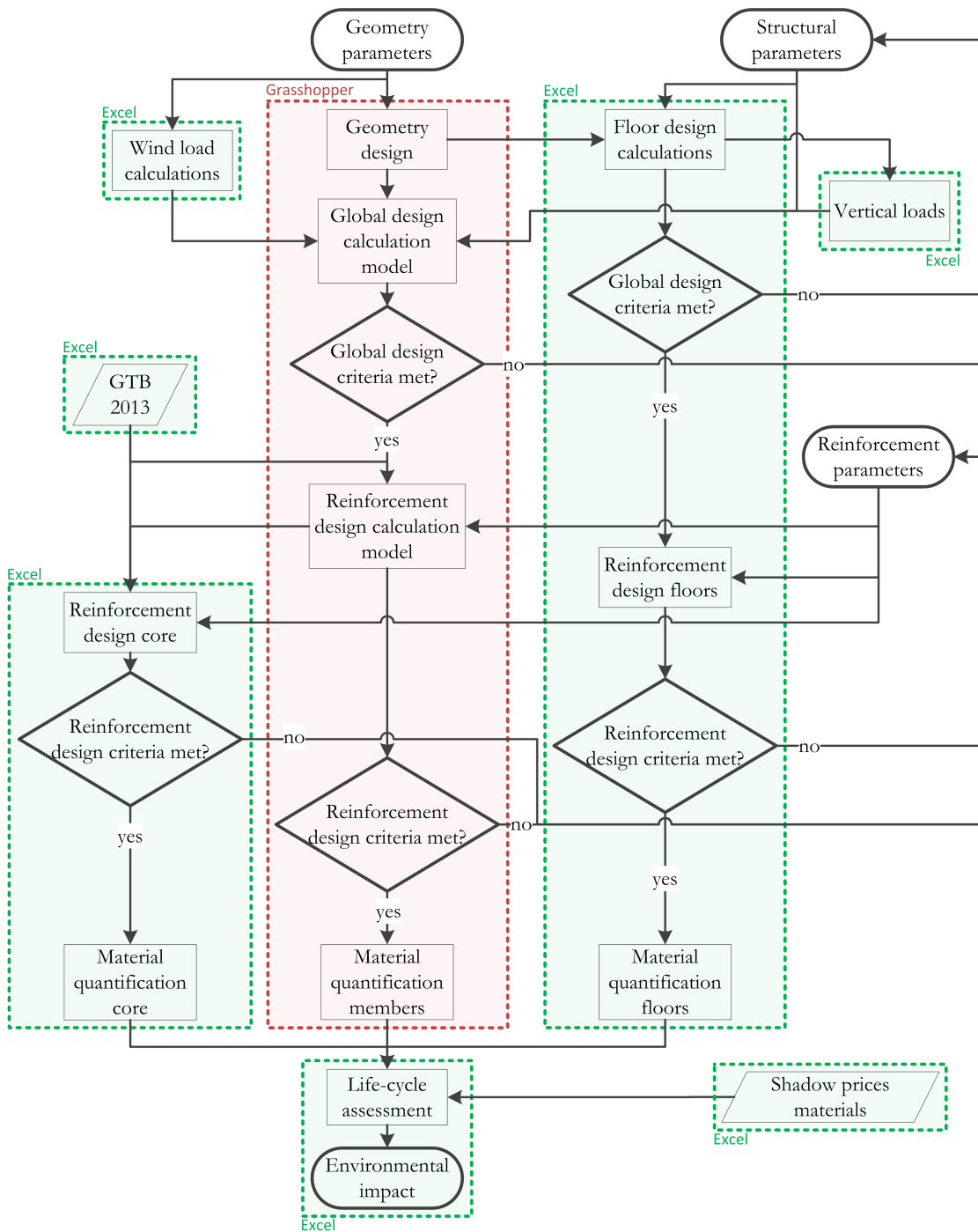


Figure 3.28: Flowchart of the entire work flow showing the links between the main model and sub-models.

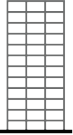

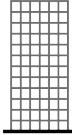
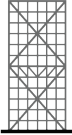
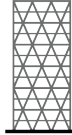
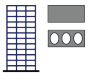
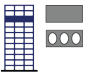
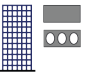
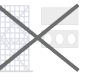

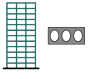

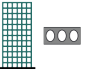

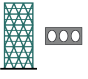

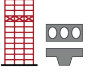
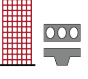
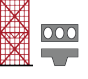
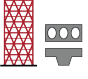

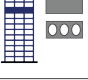
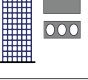


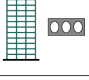

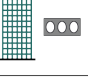

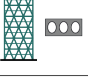
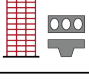

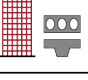
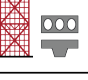
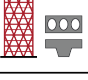


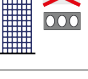




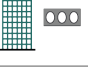

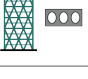

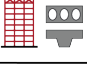
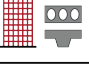
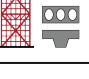
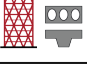
						
Stability system		1.FRAME	2.OUTRIGGER	3.TUBE	4.BRACED TUBE	5.DIAGRID
Subvariations		5CL, 6CL, 7CL, 8CL	8CL	8CL, 9CL, 10CL, 11CL	11CL	4FL-2TR, 4FL-3TR, 2FL-4TR, 4FL-5TR, 4FL-6TR
150 METERS	Cast-in-situ concrete					
	Prefab concrete					
	Steel					
200 METERS	Cast-in-situ concrete					
	Prefab concrete					
	Steel					
250 METERS	Cast-in-situ concrete					
	Prefab concrete					
	Steel					

Figure 3.29: Overview of all the model variations after structural calculations. Grey crosses represent models that were excluded on beforehand, red crosses represent models that were excluded during the calculations

3.6. Results

Results of the structural design phase can be found in appendix G where the dimensions are listed, along with the results of the environmental impact assessments. Figure 3.29 shows an overview of all the calculated models, in total a number of 145 models are designed. The grey crosses represent the variations that were excluded on beforehand, as can be read in section 3.3. The red crosses represent the variations that were excluded during the calculations.

The *1. Frame* structure is entirely excluded from the 250 models, since it was impossible to achieve the required stiffness within the design restrictions or by using default profiles. The same holds for the cast-in-situ models with flat slab floors.

The cross-sections were designed in a such a way that the required SLS criteria were satisfied and cross-sections would fulfil the ULS criteria. Stiffness was often governing over strength. In some models, the ULS criteria were met before the SLS criteria. In these cases, strength was governing over stiffness. This occurred in the 150-meter models at for instance the diagrid structures.

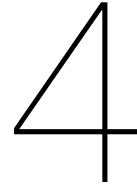
3.7. Summary

This chapter provided an overview of the used methodology, design approach, theories and assumptions for the structural designs of the considered buildings in this thesis. General geometry was described where the floor-to-floor height was set on 3.8 meters, resulting in three building heights of 152.0 meters, 197.6 meters and 243.2 meters. Dimensions of the building and core were chosen based on reference projects of high-rise buildings in the Netherlands. This resulted in slenderness ratios of 5.1, 6.3 and 7.4 for the 150-, 200-, and 250-meter models. Loads and performance criteria were obtained from the Eurocode, based on an office function. It was assumed that the foundation is responsible for half of the deflection of the building.

Five stability systems were introduced: 1. frame, 2. outrigger, 3. tube, 4. braced tube and 5. diagrid. The geometry of these systems and their sub variations were explained. In the 1. frame, 3. tube and 5. diagrid models, column spacing and inclination was kept variable. Several assumptions and approaches were explained in order to cover for aspects like shear lag.

Three types of structural materials were introduced: cast-in-situ concrete, prefab concrete and steel. The concrete structure is assumed to be cracked when subjected to lateral load, while the core is assumed to stay uncracked. Furthermore, three different floor types were introduced and discussed: the flat slab floor, hollow core slab floor and composite floor. These floors are designed using rules of thumbs, design tables from the G.T.B.[5] and information from suppliers.

Lastly, the calculation models were explained, showing the 2-dimensional models with their assumptions and way of modelling. Parametric modelling is used due to the high amount of models and structural analyses are performed in Karamba, a Grasshopper plug-in. The 2-dimensional models are verified using 3-dimensional models in SCIA. Reinforcement is automatically determined within the parametric models, using the approach in the Eurocode[34] and G.T.B.[5]. In addition to the Grasshopper model, several other spreadsheets are used to cover the whole iterative design process.



Life-cycle assessment

This chapter gives a comprehensive description of the process and methodologies of the life-cycle assessment where the environmental impact of the structural designs are calculated. Results and factors of influence are shown and discussed, giving a better understanding of the important factors within the environmental impact.

4.1. Methodology

In this research, several design alternatives are compared regarding their environmental impact. Following from section 2.3.5, it is chosen to conduct the life-cycle analysis (LCA) through the Fast Track method. In the next sections, a thorough description can be found of the goal, scope, functional unit, system boundaries, data selection, method of quantification and life-cycle inventory (LCI).

4.1.1. Goal and scope

The goal of this LCA is to compare several kinds of structural design options for three high-rise building structures of different heights on their environmental impact. As mentioned in chapter 1, solely the main load bearing structure, excluding foundation, is regarded in this assessment. Other building parts and materials are out of the scope of this research. The materials that are used for the structure are mentioned in section 3.3.6. Additional materials needed for the floor structures are mentioned in section 3.4.

Detailed specifications of the models can be found in chapter 3. The total number of assessed models is 145, equal to the number of models that is presented in section 3.6.

4.1.2. Functional unit

The main load bearing structure that is described in section 4.1.1, consists of:

- Core and shear walls
- Columns
- Beams
- Braces (if applied)
- Trusses (if applied)
- Floors (including supporting structure, if applied, e.g. beams)
- Fire resistant material (if applied)

The structural design options all have the same function and are designed to have the same performance according to the same conditions and regulations. This performance regards the structural performance of the main load bearing structure, e.g. global deformation, clarified in section 3.2.4.

4.1.3. System boundaries

The environmental impact of the structural design models is assessed according to the cradle-to-gate principle. This reduces the complexity of the calculations and makes it possible to assess a high amount of different variations. Section 2.3.5 describes the boundaries of a cradle-to-gate assessment which only includes the production phase (A1-3).

Construction phase

The construction phase (A4-A5) of this environmental impact assessment is excluded from the quantitative calculation. This follows from the fact that highly complex processes are required to construct a building of this size. There is a lack of data on the environmental impact of these processes. Moreover, these processes heavily depend on the on-site conditions.

In literature, there is inconsistency in estimates of the impact of the construction phase on the total environmental impact of the building structure. Sarkisian & Shook[45] estimate the to be construction phase 8% to 20% of the total embodied energy (EE) of the building structure for buildings between 0 and 80+ storeys. Chang et al[12] estimate that the construction phase is responsible for 10% of the total EE of a 19-storey reinforced concrete building structure.

The environmental impact of the building structure is negatively influenced by this phase. Differences in the environmental impact of the construction phase could relate to e.g. the speed of construction, need for heavy machinery, difficulty of construction, etc.

Use phase

In LCA's of building structure design alternatives, it is often assumed that the use phase (B1-7) has a negligible effect on the total environmental impact of the main load bearing structure. Trabucco et al[52] found no significant impacts during this phase regarding e.g. impact on daily energy consumption, maintenance and suitability to changes. A building structure is often designed for its assumed life-time, so direct impact of this phase on the environmental impact is assumed to be small.

On the other hand, the choice of a certain structural material, floor system or structural system, might have an indirect influence on the choice of alternatives in façade design or building services. A possible consequence is that the environmental impact of the total building (including e.g. heating, water use, etc.) is negatively influenced by this.

End-of-life phase and reuse/recycle/recovery

The end-of-life phase (C1-C4) consists of the demolition and removal of the building structure. Demolition of the building enables the materials and elements to be reused or recycled (D), if possible. The end-of-life phase has a negative impact on the environmental impact of the building structure, just as the construction phase, whereas reuse of materials and elements could have a positive impact.

As mentioned in section 2.3.4, designing for reuse and recycling of the building materials or elements can have a significant positive impact on the environmental impact of the structure. Construction waste and demand for construction materials are both reduced. However, tall buildings are very rarely demolished due to their high initial investments and often iconic status in the city skylines. Worldwide there have only been around 6 buildings of +/- 150 meters and higher that have been demolished, of the total of 3300 buildings that have been constructed as of September 2011[38]. This can be both seen as advantageous and disadvantageous regarding the environmental impact of the structure. It is a disadvantage, because the structural elements and materials of the building cannot be reused or recycled for new building elements. At the same time, it can also be seen as an advantage since the reuse of the building as a whole is more likely, eliminating the need for total demolition and replacement. In this case, upgrading and retrofitting of existing structures can be used to reduce the embodied carbon requirements over the building's lifetime[38].

Nevertheless, this phase might have a positive effect on the total environmental impact of the structure. This especially holds for steel due to the huge potential of reuse and recyclability of steel members. However, due to the high uncertainties, it was chosen to neglect this phase in this research.

4.1.4. Life-cycle inventory

Data from the Nationale Milieu Database (National Environmental Database) (NMD) (version January 2014) is used to assess the environmental impact in this research. A newer version was not available at the time. This database provides the environmental impact of materials for a variety of impact categories as described in section 2.3.5. The used materials in the models and their corresponding environmental impact is listed in table 4.1. The main focus is to compare the design alternatives on their environmental impact in terms of environmental cost, or shadow price. Additionally, results will also be generated where only the global warming potential (GWP) is considered. Through this way, a comparison of the results in this study can be made with other researches in literature.

In addition to the data from the NMD, also data about the environmental impact of steel from Bouwen met Staal is used. This LCA-data is collected in Milieu Relevante Product Informatie (Environmental Relevant Product Information) (MRPI) sheets and published on the website duurzaaminstaal.nl and originates from 2013[7][8]. Data is used for heavy sections and steel sheets for the composite floors. When comparing this data to the data found in the NMD, the resulting shadow prices are significantly lower in the MRPI sheets by Bouwen met Staal. At this point it is not clear what causes this difference. After consulting with several experts, it has been chosen to use the data by Bouwen met Staal as primary data set, since a new similar data set will be incorporated in a new version of the NMD. A further discussion on this topic can be found in section 4.4.1.

Important to note is that all data listed in figure 4.1 is straightly obtained except for C45/55 and the fire resistant material. C45/55 was not listed in the NMD and is used in the hollow core slabs. The environmental impact was obtained by using the average values of C35/45 and C55/67. Regarding the fire resistant material,

Material	Database material	Source	Density [kg/m ³]	Shadow price [€/kg]
C20/25	Concrete mortar C20/25 (CEMIII)	NMD	2400	0.00732
C35/45	Concrete mortar C35/45 (CEMIII)	NMD	2400	0.00750
C45/55	<i>Average of C35/45 and C55/67</i>	NMD	2400	0.00824
C55/67	Concrete mortar C55/67	NMD	2400	0.00898
FeB500	Concrete reinforcement steel (averaged)	NMD	7800	0.24711
PT steel	Prestressing steel (average)	NMD	7800	0.65682
S355	Steel, heavy construction products	Bouwen met Staal	7800	0.06750
Steel sheet	Steel, light construction products	Bouwen met Staal	7800	0.16750
Fire resistant material	<i>2x Gypsum-cardboard sheet</i>	NMD	870	0.06924

Table 4.1: Life-cycle inventory showing the used materials and their shadow prices.

which is also not listed in the [NMD](#), the environmental impact was obtained by multiplying the values for gypsum-cardboard sheet by 2. The fire resistant material consists for a large part of gypsum with additional fibres and other materials. [LCA](#) data was requested from the supplier, but was found to be not comparable to data in the [NMD](#) as several impact categories were missing. More research is required to determine the environmental impacts of several fire resistant materials.

4.1.5. Quantification of materials

The material quantities are collected through a developed integrated script in Grasshopper and additional spreadsheets, as seen in figure [3.28](#). The choice not to use one of the software tools mentioned in section [2.3.5](#) was based on the fact that these tools cannot be integrated with the Grasshopper environment that was used to model the structural behaviour. Moreover, because of the use of parametric software, quantification of the materials could easily be automated by integration into the structural models. This allows a faster, more fit-for-purpose and a more accurate calculation of the material quantities within the system.

Important to note is that the mass of reinforcement steel was multiplied by a factor 1.15 to cover for detailing, overlapping welds etc.

4.2. Results

This section shows an overview of the results of the environmental impact assessment. The full data sheets containing detailed results can be found in appendix G. Table 4.2 shows the abbreviations and their meaning that are used in the results.

Figures 4.2 to 4.4 show the results for 150-, 200- and 250-meter models respectively, only containing the best scoring sub-variations. This means that, for example for the 150-meter precast *I.frame* models with a hollow core slab, only one of the design variations is chosen regarding variations in amount of columns, e.g. 7 columns. This choice is based on the lowest overall environmental impact. Figure 4.1 shows the typical distribution of environmental impact by materials for the three types of floors.

Figure 4.5 shows the normalised results for the cast-in-situ concrete, precast concrete and steel models respectively. These only contain the models executed with a hollow core slab. The results seen in figures 4.2, 4.3 and 4.4 show that the models with the hollow core slabs have the least impact in all the categories. By using the same floor systems, a cross-material analysis can easily be made. Normalised means that the total environmental impact of the building structure is divided by the total gross floor area (GFA) of the building, resulting in environmental cost per square meter. This enables comparisons between different heights of the same system.

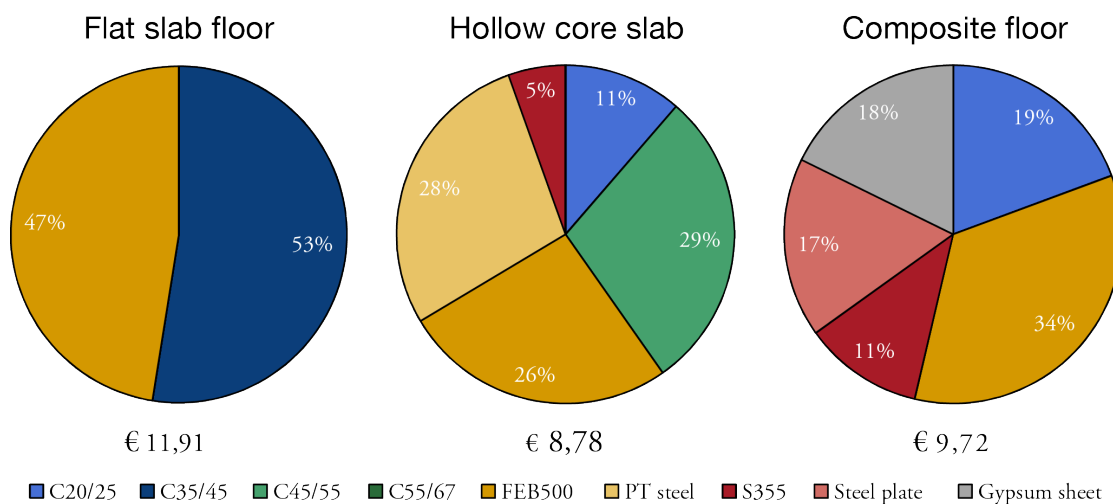


Figure 4.1: Typical distribution of environmental impact by materials for the three different floor types.

Abbreviation	Meaning
CIS	Cast-in-situ concrete
PF	Precast concrete
S	Steel
FSF	Flat slab floor
HCSF	Hollow core slab floor
CF	Composite floor

Table 4.2: Meaning of the abbreviations used in the results.

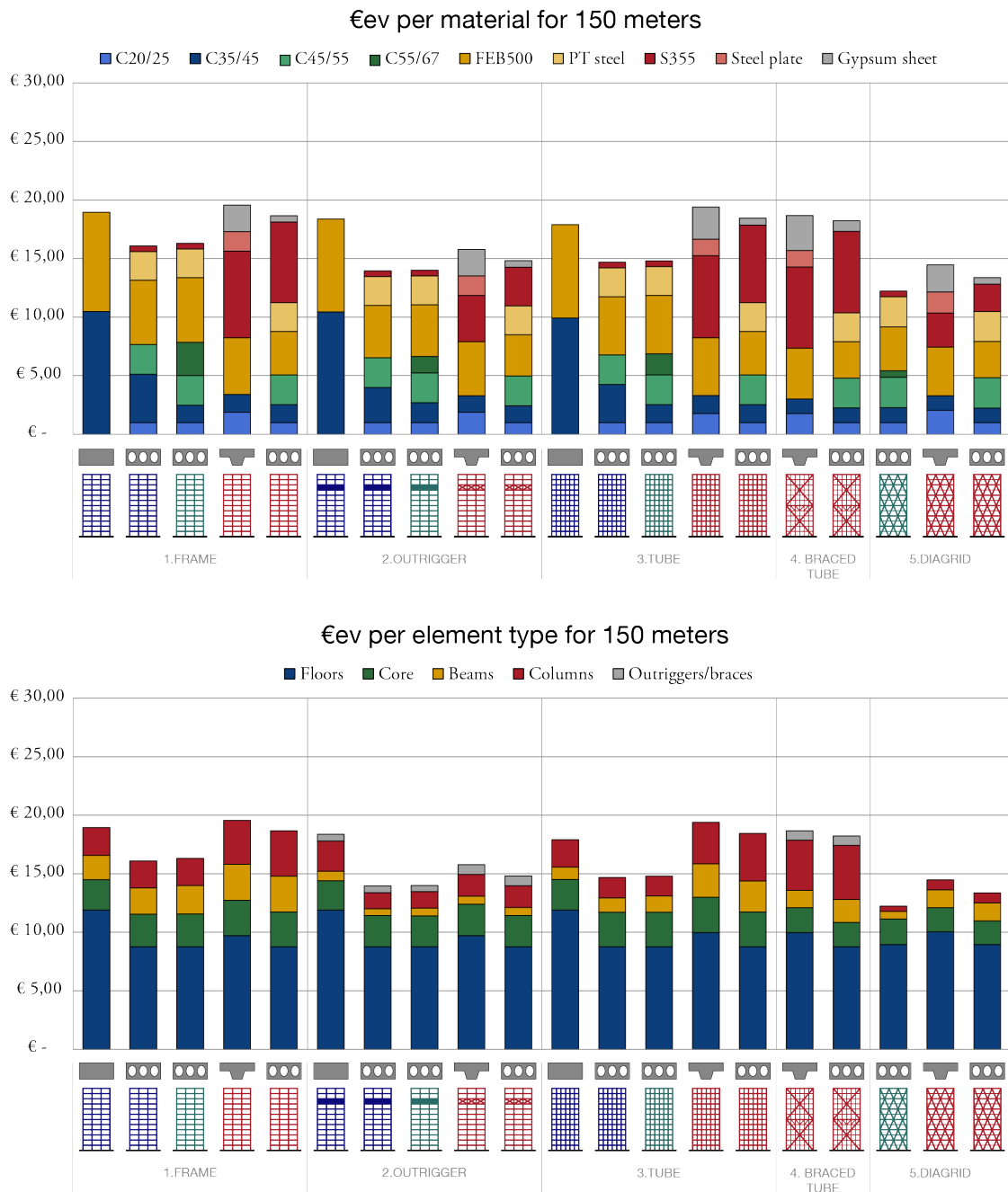


Figure 4.2: Environmental impact of the 150-meter models in environmental cost per material.

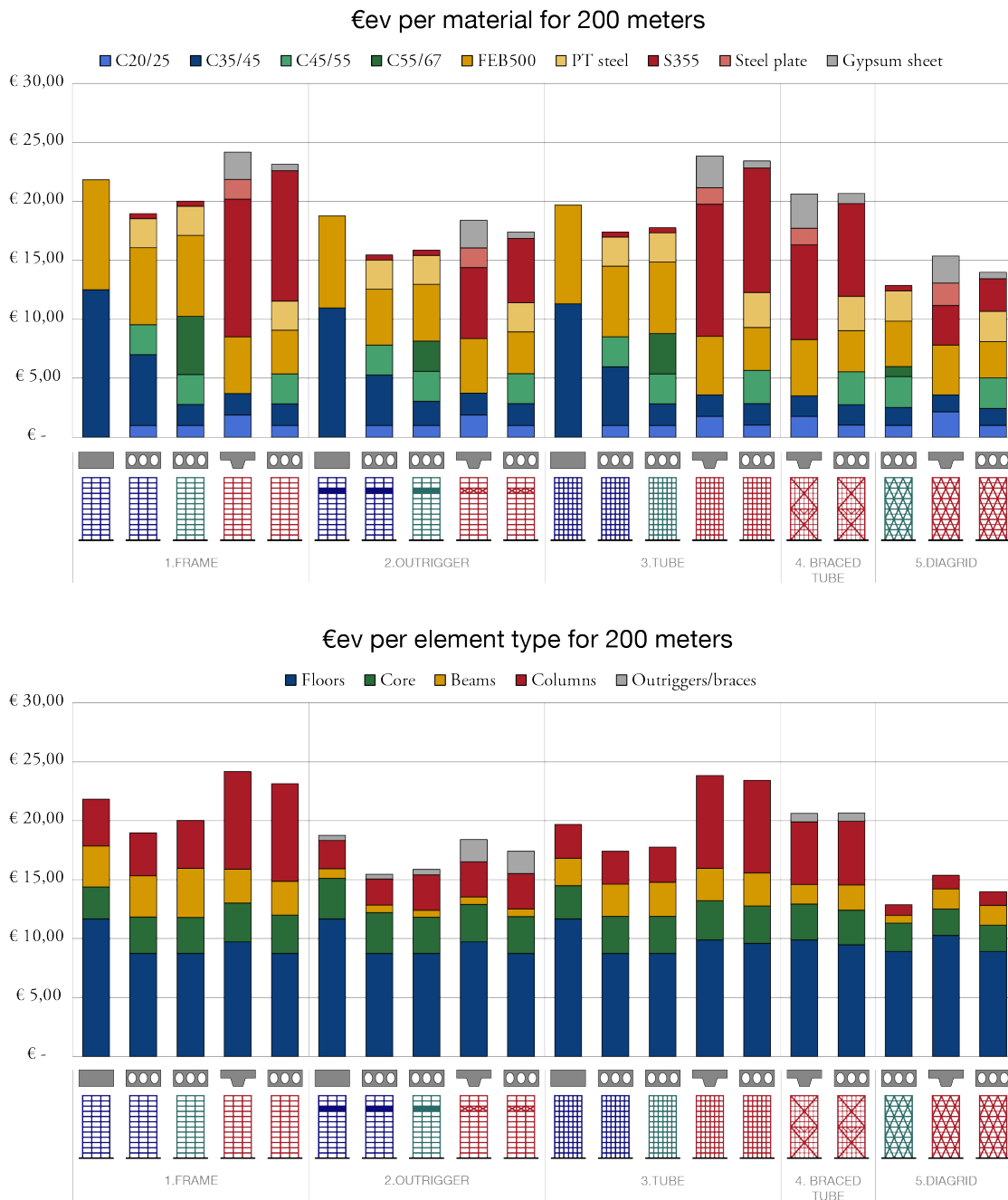


Figure 4.3: Environmental impact of the 200-meter models in environmental cost per material.

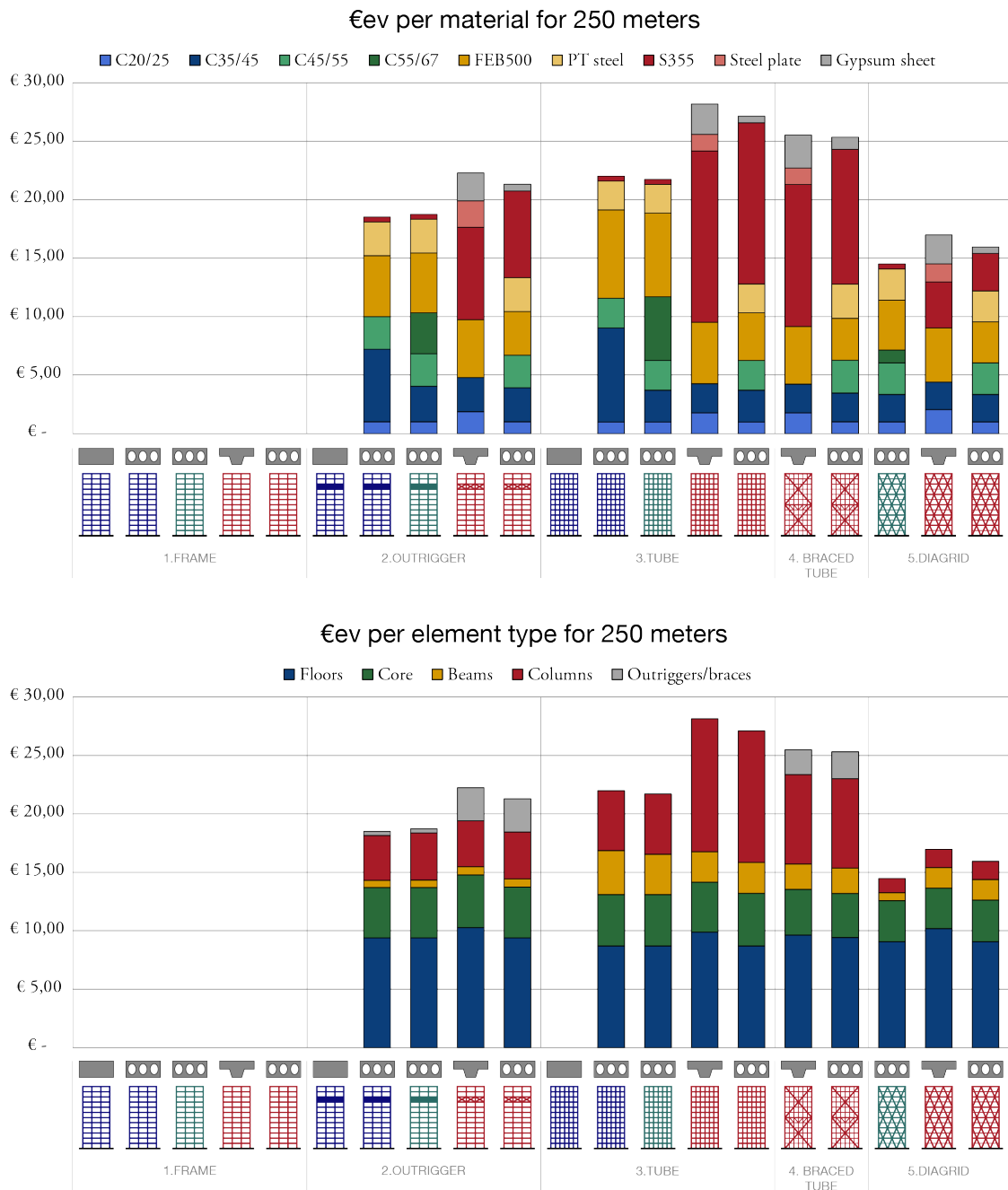


Figure 4.4: Environmental impact of the 250-meter models in environmental cost per material.

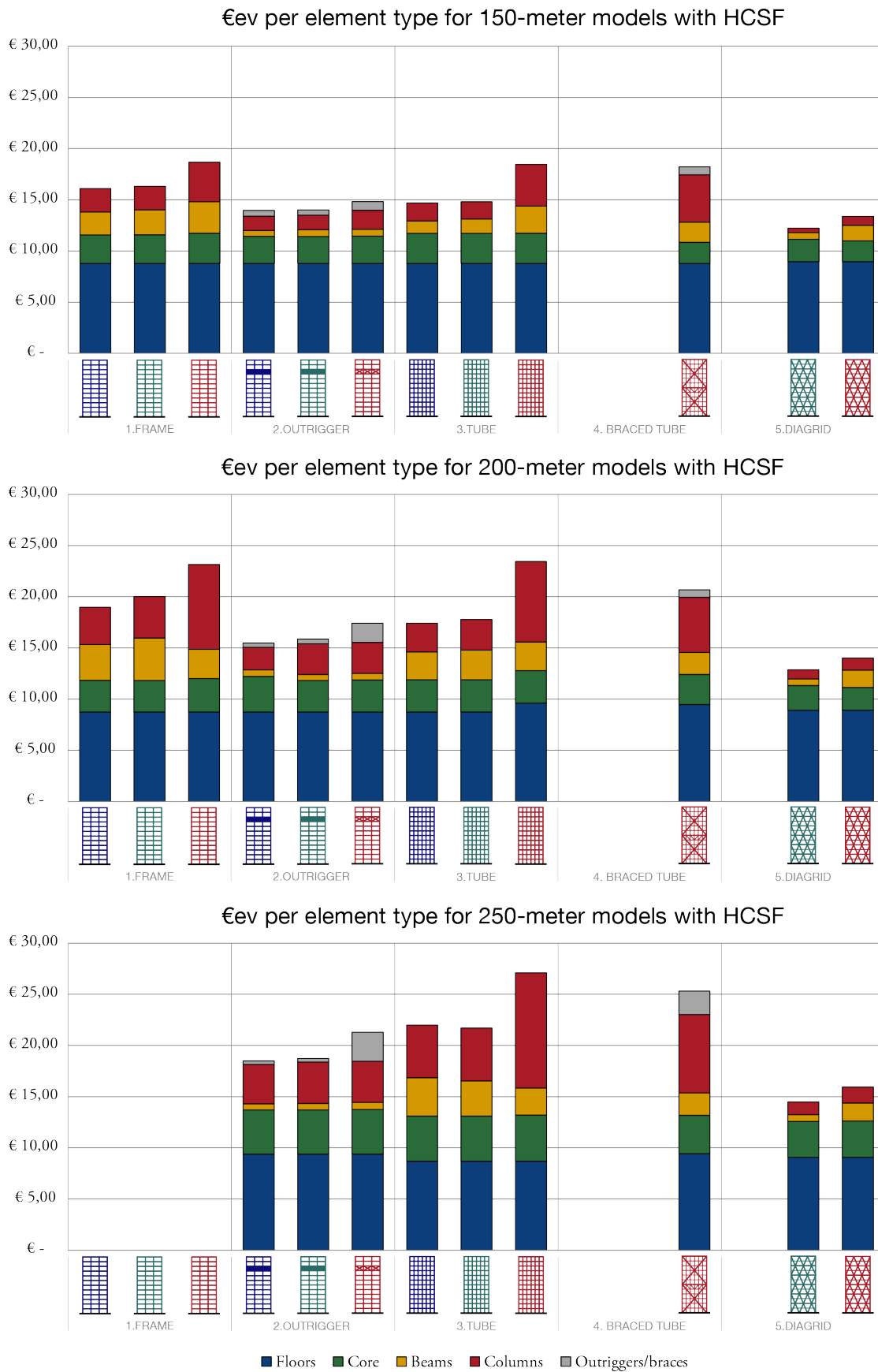


Figure 4.5: Environmental impact of all the models with hollow core slab floors, in environmental cost per square meter.

4.2.1. Interpretation of results

Materials

When comparing structural materials, one can see that the steel models generally score higher in terms of environmental impact than the concrete models with the same stability system. When comparing only the models with hollow core slab floors, the steel models generally score 6% to 35% higher than the concrete models with the same stability system. Observing the results, this can be blamed to the steel elements themselves. The impact of the columns and beams is higher in the steel models than within the concrete models. The steel models with the composite floors score higher, due to the higher impact of the floor system. At last the steel models both score higher and lower than the cast-in-situ concrete models with a flat slab floor, depending on the used stability system. A further discussion on the shadow price of steel and a selection of other materials can be found in section 4.4.1.

The environmental impacts of the cast-in-situ models compared to the prefab models are relatively close, when only observing the models with hollow core slab floors. The models with flat slab floors score significantly higher than the models with hollow core slab floors, due to the higher weight and initial impact of the flat slab floors. Within the structural designs, the cross-sections of the cast-in-situ concrete are generally bigger than within the prefab concrete models. However, prefab concrete has a higher shadow price per kg material than cast-in-situ concrete. A bigger difference in environmental impact might be found if transportation and construction are also included. A further discussion on this topic can be read in sections 4.4.5 and 4.4.6.

The fire resistant material that is used in the steel models with hollow core slab floors accounts for roughly 2% to almost 5% of the total impact. When composite floors are applied, this range increases to roughly 8% to 17%. One can say that, if the composite floors are left out of the equation, that fire resistant material has a relatively low impact on the total. However, there's uncertainty regarding the real shadow price of this material. A further discussion on this topic can be read in section 4.4.3.

Floors

The floors are in most cases responsible for the largest part of the environmental impact. This ranges from roughly 40% to 73% for the concrete models and 32% to 69% for the steel models. Within the steel models, the floors represent a slightly smaller part of the environmental impact due to the higher impact of the columns and beams.

The hollow core slab floors have the lowest impact of the three floor types in these design cases. When compared to the flat slab floors, the environmental impact is generally 17% to 26% lower. Both in the flat slab floor and hollow core slab floor the reinforcement and post tensioning steel is responsible for roughly 53% to 55% of the environmental impact of the floors. The total mass of reinforcement and post tensioning steel is lower in the flat slab floors, but the shadow price of the post tensioning steel is significantly higher than the impact of reinforcement steel.

The composite floors score 14% to 18% lower than the flat slab floors and 0% to 20% higher than the hollow core slab floors. The contribution of concrete to the environmental impact of the composite floors is relatively small in comparison to the other parts. A large part of the impact is due to steel sheets and beams, which represent 28% of the total impact. Reinforcement is an even bigger contributor with 34%. A part of the reinforcement is required due to structural criteria, but a large part is required due to fire safety reasons. Additionally, fire resistant material is responsible for 18% of the total impact of the composite floors. The high fire safety requirements therefore play a significant role in the environmental impact of the composite floors.

When solely comparing the results of models with different floor types, one can see that when lighter floor types are used, the environmental impact of the structure generally becomes lower. This follows from the fact that lighter floors result in lower vertical loads. One can say that lighter floor systems reduce the overall impact of the building. However, this also depends on the impact of the floor system itself. When using the lighter composite floor system, the environmental impact is increased when compared to the same building structure with hollow core slab floors.

Stability systems

Figure 4.5 gives an overview of the environmental impact per stability system by comparing only the systems with hollow core slab floors. By decreasing the scope to only one floor system, a good comparison can be made regarding individual performance of the stability systems and materials itself. Therefore the rest of this section only focuses on the models with hollow core slab floors.

Generally, the stability systems that are loaded axially perform better than systems loaded in bending and shear, such as the outrigger and diagrid. This coincides with the fact that axially loaded systems behave stiffer structurally than other systems. Another thing to notice is the decreasing material quantities in the core when stiffer structural systems are used. At last, the absolute value of the impact of the core also increases when lighter floor systems are used. This is a direct result of an increased demand for reinforcement due to lower normal forces in the core walls.

The premium for height as discussed in section 2.2.3 is clearly visible in all stability systems and materials. The environmental impact increases as the height of the models increases, indicating an increase in material use. For some systems the increase in impact is higher than others. Especially the diagrid shows a relative low increase compared to others. Here again, this probably has to do with the fact that this system behaves rather stiff. An explanation for the fact that the outrigger has a relative higher increase in impact could be explained by the fact that the outrigger system is still dependent on a stiff core structure.

The environmental impact of the frame structures are generally the highest of the five different stability systems. This type of stability system is the least stiff and therefore has to compensate this difference in stiffness by material use. This is not a very efficient way of improving the stiffness of the building and therefore, this structural system has the highest impact at the considered building heights. At 250 meters, it was impossible to design frame structures that would fulfil the strength, stiffness and design criteria.

The tube structure is similar to the frame structure, they both consist of a rigidly connected column-beam structure in the façade. However, the column spacing is reduced and the cross-sections of the concrete models is distributed more efficiently. For the concrete models, this results in a reduction, compared to the frame structures, of 5% to 9% for the 150-meter models and 8% to 11% for the 200-meter models. However, for the steel models there is no significant change in environmental impact of the tube structures compared to the frame structures. The reason that the concrete models show better results here is that the material is distributed more efficiently for global stiffness purposes.

For the comparisons with the other three types of stability systems, the tube structure is taken as a reference as this is a conventional way to achieve stability in high-rise buildings of this height range. Moreover, the frame structures are not available at 250 meters, which would make a comparison of different stability systems with varying heights more difficult.

The environmental impact of the 150-meter concrete outrigger structures is 5% lower, compared to the tube structure. At the 150-meter models in steel, the reduction in impact is 20%, which is significantly higher than the concrete models. At the 200-meter models the outrigger structure reduces the impact 11% for the concrete models and 26% for the steel models. At last, at 250-meter the reduction for concrete is 14% to 16% and 21% for steel. A justification for the higher reductions of environmental impact of the steel models could be the initial higher impact of the steel tube structures.

The braced tube structure does not have a significant advantage over the steel tube structure at 150 meters, in terms of environmental impact. At 200 meters, the braced tube has a reduced impact of 12% and at 250 meters, the reduction in impact is 7%. It can be seen that the braced tube structure shows a higher environmental impact than the outrigger structure. This has mainly to do with the fact that heavy belt-trusses are used to transfer vertical loads horizontally to the corner columns. This results in additional material use for the belt-truss itself. Changing the design regarding vertical load distribution might lead to more material efficiency and therefore a better design.

The diagrid shows the lowest scores in environmental impact in both concrete and steel for all heights. At 150 meters, the impact compared to the tube structure is decreased by 17% for concrete and 28% for steel.

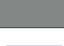




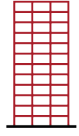





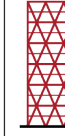





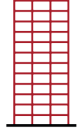





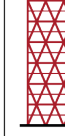

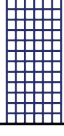



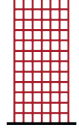





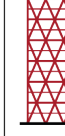
	Highest environmental cost			Lowest environmental cost		
	Cast-in-situ concrete	Prefab concrete	Steel	Cast-in-situ concrete	Prefab concrete	Steel
150 meters	  € 18,95	  € 16,32	  € 19,57	  € 13,96	  € 12,23	  € 13,38
200 meters	  € 21,84	  € 20,03	  € 24,19	  € 15,48	  € 12,88	  € 14,00
250 meters	  € 21,98	  € 21,71	  € 28,14	  € 18,50	  € 14,48	  € 15,94

Figure 4.6: Summary of the results with the best and worst scoring models per material per height.

At 200 meters, this increases to 28% for concrete and 40% for steel. At 250 meters, these reduction values slightly increase even more to 33% for concrete and 41% for steel. At average, using a diagrid structure instead of a tube structure reduces the environmental impact by 26% for concrete models and 36% for steel models.

Variations in environmental impact within the diagrid models (varying height and angle of the diagrid structure) are relatively larger than at other systems like the frame and tube. This is partly caused by the optimal angle for the diagrid. However, the spans of the beams have an even bigger influence on the total material quantities, this can be seen in the results in appendix G. The span of the beams is directly related to the density of the diagrid. Increasing the angle, reduces the span of the beams and therefore reduces the material use of the beams. Moreover, increasing the height of the diagrid members reduces the density of the diagrid and therefore increases the spans of the beams. However, the amount of primary beams is reduced by a factor 2 which would also decrease the amount of required material for the beams. Because of these reasons, the relation between the angle and height of the diagrid and its efficiency, as discussed in section 3.3.5, becomes subservient regarding required amount of material for high-rise buildings in the considered height range.

A comprehensive overview of the above discussed results can be seen in figure 4.6. Here, an overview is presented of the best and worst performing systems per material and height.

4.3. Comparison with literature

As discussed in chapter 2, not many research has been performed yet in this field. The studies that have been performed usually use **GWP** or **EE** as indicators of the environmental impact. Researches by Oldfield[38] and Trabucco[52] both contain data of the **GWP** of their models. As the **NMD** contains also the **GWP** data, but not the **EE** data, it was chosen to use Oldfield and Trabucco for a comparison. Results regarding the environmental impact measured in **GWP** can be found in appendix G. The research by Foraboschi[21] only contains information about the **EE** and was therefore not included in the comparison. A comparison with the research by Van Hellenberg Hubar[57] is also not considered due to large differences in scope of measuring the environmental impact and the relatively simple structural approach of the models.

Oldfield, 2012

The research of Oldfield focusses on the environmental impact of the St Mary Axe in London[38]. This building is 180 meters high, contains 41 storeys and has a **GFA** of 64.450 m². Oldfield quantified both the embodied carbon (**EC**) as operational energy (**OE**) of the whole building. He also addressed the **EC** of solely the structure which had an impact of 326 kg CO₂/m².

For comparison we take 200-meter steel diagrid models of this thesis with composite floors, 52 floors and a **GFA** of 51.597 m². The impact of these models measured in **GWP** range from 168 to 178 kg CO₂/m², roughly half of the impact of the impact of the St Mary Axe.

This could have three reasons: the first reason is that the models from this research contain a concrete core that also adds stiffness to the building, reducing the need for steel for global stiffness in the diagrid structure. Second, according to Trabucco[52], the difference might be justified by the fundamentally different shape of the building. Third, it is not entirely clear what the used impact is in the calculations for the **GWP** for steel. Values used in this thesis are relatively low compared to e.g. the values used in the research by Trabucco.

Trabucco, 2016

A second comparison can be made with the 60-storey models of the research by Council of Tall Buildings and Urban Habitat (**CTBUH**), by Trabucco[52]. These models have a **GFA** of 141.600 m² and are 246 meters in height. Due to the high difference in slenderness, it was chosen to compare the all steel diagrid from the research by Trabucco and the 250-meter steel diagrid models with composite floors from this research.

The used results from Trabucco also contain the construction phase (A4-5). Results for only the production phase (A1-3) were not listed in the paper and could therefore not be used. However, Trabucco stated that the impact of transport (A4) has a negligible impact of 1% to 2.5% on the total result. It is not known what the impact of construction (A5) is in this research. Suggested values from literature range from 10% to 20%[45].

The total impact of the all steel diagrid model of Trabucco is 243 kg CO₂/m² whereas the impact of the 250-meter steel diagrid models of this research range from 185 to 212 kg CO₂/m². This means that the results of this thesis are roughly one third lower than the results presented by Trabucco.

This difference in impact can be justified by a couple of reasons: first, the used results of the research by Trabucco also includes the construction phase. Additionally, the model in this research contains a concrete core which reduces the amount of required steel, as described in the comparison with Oldfield, which would increase the difference between Trabucco and the results in this study. Moreover, the used **GWP** values for steel by Trabucco are 33% higher than the values used in this thesis. At last, it remains unclear whether the foundation was taken into account.

Overall it was concluded that the concrete models had the highest scores regarding **GWP**, while all steel scenarios had the highest **EE**. When only considering the **GWP** results from this research, similar observations can be made as described in section 4.2.1. The steel models still score higher than the concrete models. This contradicts the conclusion by Trabucco that concrete models had the highest **GWP** values.

One of the possible reasons that could justify this difference is that the models in this thesis are significantly more slender than the models in the research by Trabucco. This means that the cross-sections in this

thesis are governed by the global stiffness of the building instead of strength as is probably the case in the research by Trabucco. Geometry deviates significantly as the floor plans in the research by Trabucco are approximately twice in size, resulting in slenderness ratios of 1:6.2 and 1:4.1 as a rectangular floor plan is used. The slenderness ratio for the 250-meter model in this research is 1:7.4. This means that the models show a more behaviour, resulting in higher amounts of required material.

Another reason can be found in the mix design of the concrete. The concrete mix designs that are used in the Netherlands usually contain more fly ash, which reduces the environmental impact of concrete significantly. This is already incorporated in the environmental impact values of the [NMD](#). The average value for concrete in this thesis is $0.10 \text{ kg CO}_2/\text{m}^3$ while the average values that are used in the research by Trabucco are $0.15 \text{ kg CO}_2/\text{m}^3$ and $0.19 \text{ kg CO}_2/\text{m}^3$. However, it is not known if these values already contain impact by the construction and demolition phase.

A last reason can be found in the fact that the research by Trabucco includes transportation, construction and demolition which are excluded in this research. Unfortunately, the results are only presented as total impacts, individual contributions of the different phases, materials or components can not be found in the paper. This means that a fair comparison cannot be made between these two researches regarding the comparisons between concrete and steel models.

Overall it can be stated that the results of this research are comparable with those found in literature. Large differences in impact can be justified by the differences in scope, geometry and impact of materials.

4.4. Factors of influence

This section describes factors that could have an influence on the results presented in section 4.2. These factors are described and analysed to determine what kind of influence these could have and what result this would have on possible conclusions.

4.4.1. Sensitivity analysis on shadow prices of materials

The shadow prices that are used in this thesis, listed in figure 4.1, originate from the NMD and partially from MRPI sheets from Bouwen met Staal. The used values are averages from the Dutch industry and can vary, depending on the used resources, location of the resources, type of used production processes and composition of the materials. A sensitivity analysis was made to gain more insight in the sensitivity of the end result with respect to the shadow price of certain materials.

It was chosen to perform this sensitivity analysis on the three main material categories: concrete (C20/25, C35/45, C45/55 and C55/67), reinforcement steel (FeB500 and post-tensioning steel) and steel (S355). The shadow prices are varied by +25% and -25%. Again, only the models with the hollow core slab floor were considered in order to make a fair comparison between the different materials and stability systems. The analyses were only performed on the 200-meter models, as the results of the three different height categories were found to be quite similar.

Case I: Concrete

The concrete mix design depends on numerous of factors, among which are strength, durability, workability, etc. Moreover, there is a tendency towards using more and more fly ash in the concrete mixes in order to reduce raw material use and environmental impact. The environmental impact of concrete mixes containing fly ash is significantly lower than solely using Portland cement. When comparing two CEM I concrete mixes to two CEM III concrete mixes with the same strength in the NMD, the CEM I concrete mixes have a 22% to 25% higher shadow price.

In this sensitivity analysis, the shadow prices of all the used concrete classes were adapted simultaneously. For the concrete models this means that the environmental impact of all element types is changed. For the steel models this only holds for the core and the floors, the steel structure remains unaffected. The results of the analysis are shown in figure 4.7.

As can be seen in figure 4.7, the concrete models are affected more than the steel models by changing the shadow price of concrete. The change of +/-25% of the concrete shadow price affects the concrete models by a variation of +/-12% to +/-13% of the total environmental impact. For steel this is +/-6% to +/-9%. This means that the difference between the steel and concrete models is reduced when the shadow price of concrete is increased and increased when the shadow price of concrete is reduced. However, the differences between the steel and concrete models are still ranging from 6% to 27% in favour of concrete in the case that the shadow price of concrete is increased by 25%. This means that concrete still has the lowest environmental impact in this scenario, considering the boundaries of this research.

Case II: Reinforcement steel

The production of reinforcement steel is similar to that of steel sections for beams and columns. The environmental impact of the end product largely depends on the use of scrap (secondary steel) in the production process. Ratios that are used in the NMD are not known, but the used ratios are based on national averages.

Within this analysis, the shadow prices of all reinforcement and post-tensioning steel were adapted simultaneously. This means that the impact by the hollow core slab floors is also reduced, but since this type of floors is used in all the models, differences between the different material categories still remain the same. Just as in the previous case, the concrete models are influenced more by changes in the shadow price of reinforcement steel than the steel models due to use of reinforcement steel in the columns and beams.

As can be seen in figure 4.7, the concrete models are affected more than the steel models by changing the shadow price of reinforcement steel. Here, the change of +/- 25% results in a variation in total impact of +/-12% at the concrete models and +/-7% to +/-10% at the steel models. These values are similar to the values

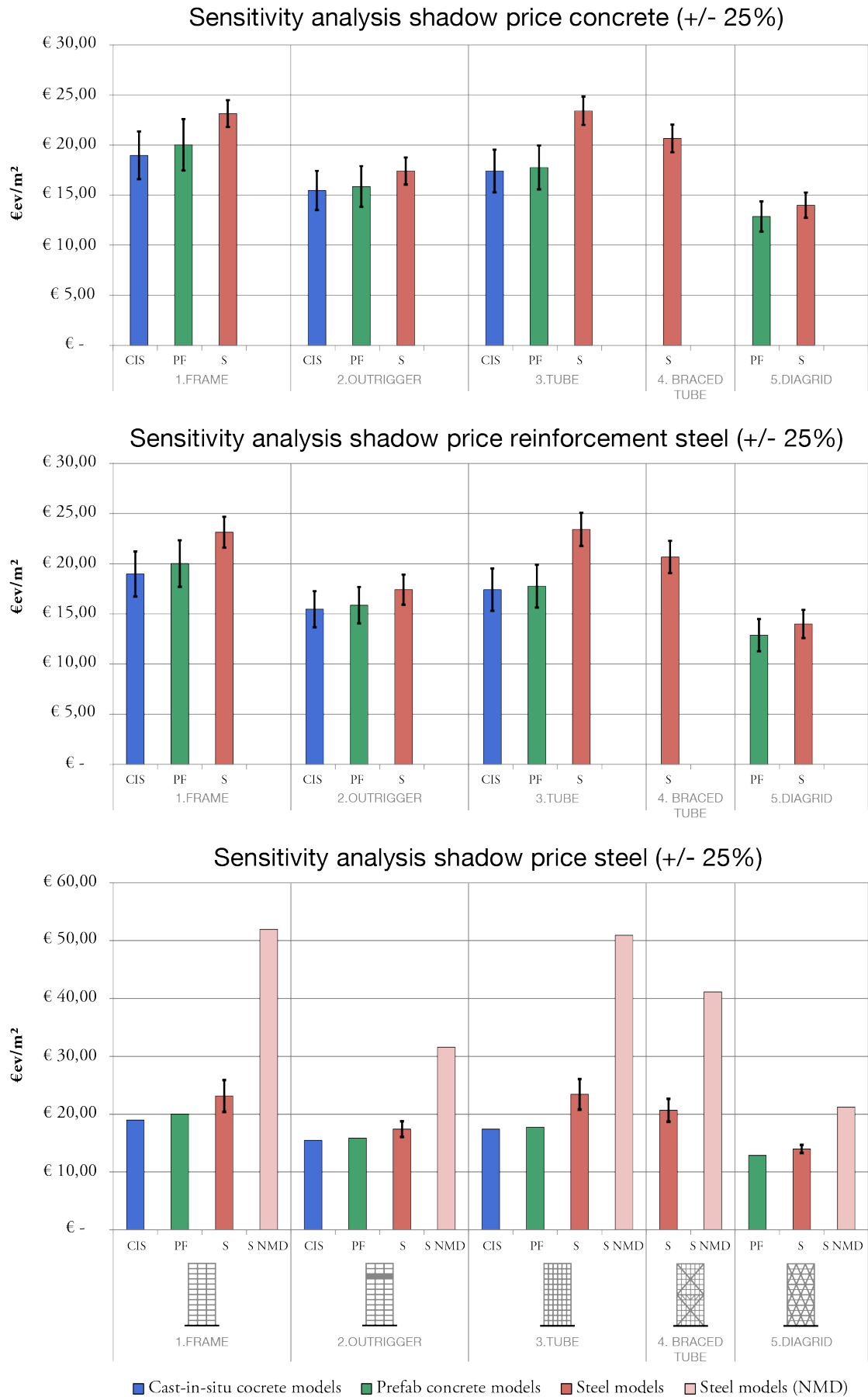


Figure 4.7: Results of the sensitivity analysis on the shadow price of three materials on the total environmental impact for 200-meter models with hollow core slabs.

that were found when the concrete shadow price was varied. The differences between the steel and concrete models range from 6% to 28% in favour of concrete when the shadow price of reinforcement steel is increased by 25%.

Case III: Steel

Just as the previous case, the environmental impact of the steel sections largely depends on the use of secondary steel in the production process. Roughly, there are two types of production processes that are used to produce steel. The first one is the Blast Furnace (BF) process[6], or basic oxygen steel making process, where steel is produced using iron ore and coal. Depending on the factory, roughly 20% to 30% scrap is added, mainly to regulate the temperature. During the process, slag and gas are produced. The slag can be used in concrete mixes, road construction, etc, the gas is used to produce electricity. The second type of production process is the Electric Arc Furnace (EAF) process[6]. Here, 100% scrap material is used to melt this directly into steel without the use of primary resources. Only oxygen and chalk are added in order to bind impurities. Also zinc coated steel is used in the electric oven where zinc is recovered and used in the production of new zinc.

Roughly 50% of the steel produced in Europe originates from EAF factories. The construction steel that is used in the Netherlands consists of 90% from EAF and 10% from BF according to Bouwen met Staal[6]. There is a worldwide tendency towards the EAF process, but the supply of scrap steel is the limiting factor.

The data published by Bouwen met Staal (2013) strongly deviates with the data that is obtained in the NMD (version January, 2014). When considering the shadow price of heavy construction steel, used for beams and columns, the cradle-to-gate shadow price using the data by Bouwen met Staal results in €0,0675/kg where using data from the NMD results in a shadow price of €0,2434. This means that when using the data from the NMD results in a 3.6 times higher impact by the steel members. After consultation with several experts, a choice was made to use the data as published by Bouwen met Staal. However, at this point it is still unknown what causes these large differences. A possible explanation might be found in different used EAF/BF ratios, but this can not be checked as these ratios are not stated in the NMD.

For this sensitivity analysis a similar approach was used as in the previous cases, but now also environmental impacts using data from the NMD are also used in the comparison to provide a complete image. As the concrete models do not contain significant amounts of steel, the sensitivity analysis on the shadow price of steel is only performed on the steel models.

As can be seen in figure 4.7, changing the shadow price of steel by +/-25% causes a change of +5% to +12% in the environmental impact of the steel models. When the shadow price is decreased by 25%, the environmental impact of the steel models is only 3% to 17% higher than the impact of the prefab concrete models. When the data from the NMD is used, the environmental impact of the steel models is 52% to 124% higher than the impact when using the data of Bouwen met Staal. In this case steel appears to be unfavourable in terms of environmental impact.

4.4.2. Reuse of steel elements

Reusing structural elements has a high potential for creating lower impact buildings. Elements like beams and columns are dismantled from the building, checked on quality and directly installed in a new building. Another possibility is recycling of the material, where used elements are used as raw material in the production process to create new elements. This already happens on large scale in steel, as explained in the previous section.

The possibility to dismantle and directly reuse steel members is one of its big advantages. Concrete elements often cannot be reused, but demolished can be recycled. As demolition is not within the scope of this research, reuse and recycling were not considered in this thesis. Possibility of recycling and reuse would be incorporated in a negative value in phase D, as explained in section 2.3.5 and figure 2.12, resulting in a lower shadow price of the material.

One of the possible scenarios in which steel would become more favourable over concrete in high-rise structures in terms over environmental impact, is when reuse of the structural elements after the building's life time would be considered to be possible. This would require high-rise buildings to be demolished in such a way that the elements would still be reusable, requiring the structure and connections to be demountable.

In low-rise buildings this already exists and is called 'modular' or 'circular' construction. Research would be required to investigate if this would also be beneficial in the case of high-rise buildings.

Another perspective on this issue is introduced by Oldfield[38]. He argues that demolishing the building and reusing its elements to build another building will always be less effective in terms of environmental impact than reusing the building as a whole. There are a considerable amount of cases where high-rise buildings are reused after its initial determined lifetime. In this case it would be required to research the maximum possible life span and the required retrofitting and maintenance of the concrete and steel structures.

4.4.3. Fire resistant material

There remains uncertainty regarding the environmental impact of fire resistant material. The shadow price for this material is not listed in the NMD and therefore had to be estimated. Also in literature there is little to be found on this subject. Trabucco[52] has accounted for fire resistant material, however what the impact of this material is on the total environmental impact remains unknown as data is not published.

When looking at the steel models with hollow core slab floors, the impact of the fire safety material is only responsible for 2% to 5% of the total impact. When focussing on the steel models with composite floors, this range rises to 8% to 17%. However, this heavily rests on the assumption that fire resistant material is needed to achieve 120 minutes of fire resistance for the composite floors. Whether this assumption is true can be discussed.

When it appears that the environmental impact of the fire resistant material is significantly higher, this would have a minor effect on the steel models with hollow core slab floors. However, it would have a significant effect on the steel models with composite floors, but, in this case it might be beneficial to refer to other solutions to achieve fire resistance that might have a lower impact.

4.4.4. Foundation structure

The foundation (or substructure) is now entirely out of scope of this research. However, it is quite possible that the impact of this part of the structure is quite significant. For the St Mary Axe the substructure was estimated to be responsible for approximately 28% of the total environmental impact of the structure[38].

Whether this ratio is directly applicable to high-rise buildings in the Netherlands is unknown. Ground conditions can vary hugely and have a big influence on the foundation design. It is known that the ground conditions in the Netherlands are not among the best to build tall buildings.

The foundation is responsible for distributing the high forces into the soil. The weight of the building usually plays a major role in dimensioning the foundation structure and therefore the material use in the foundation. This means that heavier buildings would also require heavier foundation systems. This could be an advantage for all the steel models, as these are significantly lighter than the concrete models. As an example, the 200-meter tube models weigh approximately 80 000 tonnes for cast-in-situ concrete with flat slab floors, 57 000 tonnes for prefab concrete with hollow core slabs and 37 000 tonnes for steel with composite floors.

However, following the assumptions and calculations from appendix A, weight of the building does not solely determine the material quantities of the foundation. Rotation stiffness is also a major factor of importance as described in section 3.2.4 and can be governing over strength in design.

In short, it is known that the foundation will have a very significant impact on the environmental impact of the structure. It is likely that including the foundation in the scope will have a beneficial effect for lighter buildings, like the steel models in this research. However, due to stiffness criteria it is not known to which degree the differences between concrete and steel models are reduced.

4.4.5. Transportation

As discussed in section 4.1.3, the construction phase is left out of the calculations. This includes transportation of the materials to the building site. According to Trabucco[52], transportation has a negligible effect on the total environmental impact of the structure. However, the impact of this phase hugely depends on the distances that are used. Moreover, it remains largely unknown whether there are big differences in impact

by construction between cast-in-situ concrete, prefab concrete and steel high-rise buildings. Therefore, it was chosen to perform a small study into this subject.

The model that is used in this study is the 200-meter outrigger model where a comparison is made between cast-in-situ concrete with flat slab floors, prefab concrete with hollow core slab floors, and steel with composite floors. Only transportation from the supplier to the building site is addressed, which corresponds to phase A4.

The [NMD](#) contains data for a Transport, Lorry >28t with shadow price per tonne kilometre (€0,01518 /tkm). This means that the impact is quantified for transporting 1000 kg over a distance of 1 km. It addresses the same impact categories as used for the [LCA](#) and can therefore be compared with the results. It is assumed that transport of the materials is governed by weight and not by volume.

The building location was assumed to be Rotterdam, as stated in section [3.2](#). Suppliers are unknown and are often determined by the contractor which often chooses the supplier based on cost. This means that suppliers can be located anywhere in the Netherlands. This especially goes for prefab concrete and steel. For cast-in-situ concrete and reinforcement steel, suppliers are often located close to the building site.

According to Stichting Bouwkwiteit, a fixed value of 150 km should be used as transport distance for the building materials, products and elements[49]. This value can be overruled when the actual suppliers are known. Because of the high uncertainty regarding the choice of suppliers, it has been chosen to use the fixed distance except for cast-in-situ concrete (C20/25 and C35/45) and reinforcement steel (FeB500). Here a value of 30 km is chosen which covers most of the suppliers in the neighbourhood of Rotterdam. Whether this is an accurate approach, can be discussed.

The results of this quick analysis can be seen in figure [4.8](#). The environmental cost are approximately €35 000, €81 000 and €24 000 for cast-in-situ concrete, prefab concrete and steel respectively. Prefab concrete scores considerably higher because of the high mass of prefab concrete that is transported over a long distance. Steel has the lowest impact by transportation, despite the long distance, because the required mass of steel for the structure is significantly lower.

When regarding the significance of transport to the total environmental impact, it can be stated that for steel and cast-in-situ concrete, transport has an almost negligible effect. Transport is responsible for 3.5% of the impact for the cast-in-situ concrete model and 2.4% for the steel model. This is comparable to values found in literature[52]. However, when looking at the prefab concrete model, transport is responsible for 9.0% of the total impact, due to the large transport distance. It can be stated that for concrete, the transport distance has a significant effect on the environmental impact of the transportation phase. Including transportation into the [LCA](#) probably has a slightly beneficial equalising effect for steel structures.

4.4.6. Construction phase

In addition to transportation (A4) discussed in the previous section, also construction (A5) is included in the construction phase. According to Sarkisian, the construction phase does have a significant impact on the total environmental impact of the structure. The whole construction phase (A4-5) can be accountable for approximately 10% to 25% of the total [EC](#)[45].

The impact of the construction phase depends on a number of factors: use of heavy machinery and equipment (e.g. concrete pumps, cranes, welding machines, etc.), transport of heavy machinery, equipment and materials to the building site, transport of workers to the building site and supporting processes (e.g. formwork, temporary heating, etc.)[15]. These factors also have a relation with building erection speed. Construction of a building with prefabricated elements is faster which probably has a positive influence on the environmental impact.

According to Sarkisian, on average, the impact of the construction phase is twice as high for reinforced concrete buildings than all steel buildings (10% versus 20%)[45]. However, it is unknown to which degree prefabricated concrete elements are taken into account. Additionally, some structural systems are more difficult to construct than others. It might be the case that e.g. a prefabricated concrete diagrid structure is more complex to build than a conventional frame structure. It is not known what the impact of complexity is on

the impact of the construction phase.

It is clear that the construction phase does have a significant influence on the total environmental impact of the structure. However, there a lot of uncertainties to give an estimation on how this would influence the results of this research. It is likely that steel will have an advantage over cast-in-situ concrete, for precast concrete this remains unknown.

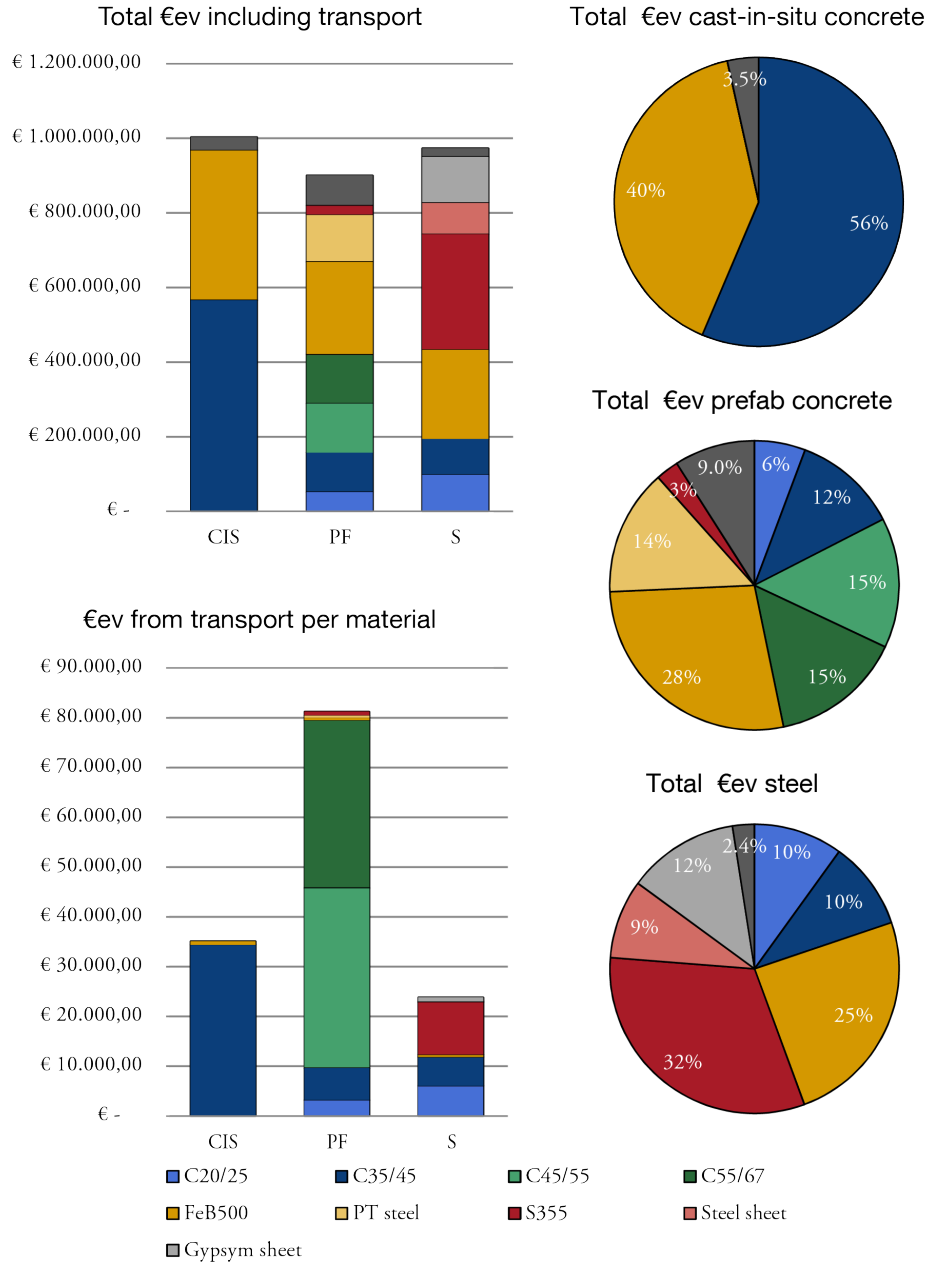


Figure 4.8: Environmental impact for the 200-meter tube models in cast-in-situ concrete (with flat slab floor), prefab concrete (with hollow core slab floor) and steel (with composite floor), including transportation.

4.5. Summary

This chapter showed the method, results and interpretation of the results of the [LCA](#) part of this thesis. The fast track [LCA](#) method was used to obtain the environmental impacts of the different structural designs. Only the production phase was considered (A1-3, cradle-to-gate), as demolition was excluded and no consistent data was found for the construction phase. Data on the environmental impacts of steel products are obtained from Bouwen met Staal (Build with Steel), all other materials were obtained from the [NMD](#). The material quantities were automatically determined within the parametric models.

Results showed that all the steel models generally score 6% to 35% in terms of cradle-to-gate environmental impact than the concrete models with the same stability system. This is due to a relative high shadow price of steel. The impact of cast-in-situ concrete and prefab concrete models are relatively close to each other. The impact of fire resistant material is only significant when models with composite floors are considered.

Of the three floor systems, the flat slab floor shows the highest environmental impact. The environmental impact of the hollow core slab floor is generally 17% to 26% lower. The environmental impact of the composite floor is generally 14% to 18% lower than the flat slab floor. Here, fire resistant material and reinforcement are responsible for the largest part of the environmental impact. Floors had a high share in the total environmental impact of 32% up to 73%.

The frame and tube structures have the highest environmental impacts of all stability systems. The outrigger structures reduce the impact by 5% 16% for the concrete models and 20% to 26% for the steel models, compared to the tube structures. For the braced tube structures, the reduction in impact compared to the tube structures is 7% to 12%. The diagrid shows the lowest environmental impacts. Here, the impact is reduced by 17% to 28% for the concrete models and 28% to 41% for the steel models, compared to the tube structures.

Several factors of influence on the results were discussed, among which are sensitivity of shadow prices, reuse of steel elements, fire resistant material, inclusion of foundation structure, inclusion of transportation and inclusion of the construction phase. Variations of 25% in the shadow prices of steel, concrete and reinforcement steel do not show significant changes in results and conclusions. Reuse of steel elements, inclusion of the foundation structure, inclusion of transportation and inclusion of the construction phase are likely to have a significant impact on the total environmental impact. It is expected that differences in impact between concrete and steel models are equalised by inclusion of these aspects in the [LCA](#).

5

Conclusion

This chapter describes the main conclusions of this thesis and provides an answer to the main research question. First a short summary is provided, after which the main findings are presented in several categories. Finally, the main conclusions are drawn.

Reduction of the environmental impact of the built environment is needed. Together with the increasing demand for urban area, high-rise buildings prove to be a potential solution. With buildings becoming near energy neutral, the focus shifts from reducing the impact by operational energy (OE) to reducing the impact by embodied energy (EE), caused by production, construction and demolition of materials, specifically the material needed for structure. Until now, limited research has been conducted on the environmental impact of high-rise structures, particularly in western Europe and the Netherlands.

This research aimed to provide an insight into the environmental impact of several structural systems and materials for the 150 to 250 meters range in the Netherlands. Three buildings of 150, 200 and 250 meters were designed and analysed using parametric models and static linear calculations. Five types of stability systems (frame, outrigger, tube, braced tube and diagrid), including three floor types (flat slab floor, hollow core slab floor and composite floor), were designed for all three heights in cast-in-situ concrete, precast concrete and steel.

The environmental impact was determined using the fast track life-cycle analysis (LCA) method. Only the production phase was considered (A1-3, cradle-to-gate), as demolition was excluded and no consistent data was found for the construction phase. The impact was calculated using environmental cost, shadow prices, a Dutch assessment method that includes multiple impact categories. LCA data was obtained from the Nationale Milieu Database (National Environmental Database) (NMD) and Bouwen met Staal (Build with Steel). A total of 145 models was assessed.

Main findings

The main findings of this research are described in detail in chapter 2. Down below these are categorised and summarised:

Materials

- Steel structures have a higher cradle-to-gate impact than the competing concrete structures. When considering the same floor systems, the impact was generally 6% to 35% higher, depending on the used stability system.
- No significant differences in cradle-to-gate impact were found between cast-in-situ and precast concrete.
- Fire resistant material generally is responsible for a small part of the total environmental impact. In the steel models with hollow core slabs this is 2% to 5%. In steel models with composite floors fire resistant material takes up a very significant part of 8% to 17% of the total environmental impact.
- An increase or decrease of 25% of the shadow price of steel, changes the total environmental impact of the steel models by 5% to 12%. A reduction of 25% of the shadow price of steel does not make the steel models more favourable than the concrete models in terms of environmental impact.
- An increase or decrease of 25% of the shadow price of concrete or reinforcement steel, changes the total environmental impact by 12% to 13% for concrete models and 6% to 10% for steel models. An increase of 25% of the shadow price of concrete or reinforcement steel does not make the steel models more favourable than the concrete models in terms of environmental impact.
- Inclusion of the construction phase and the foundation structure will have a significant impact on the total environmental impact. Differences in impact between steel and concrete are likely to be reduced by inclusion of these aspects.

Floors

- Floor structures are responsible for a major part of the total impact by the structure. For the concrete models this is roughly 40% to 73%. For steel models, this is 32% to 69%.
- Flat slab floors have the highest impact of the three different floor systems. Composite floors generally have a reduced impact of 14% to 18% compared to the flat slab floor where a large part of the impact is due to fire safety material (18%) and reinforcement (34%). The hollow core slab floor scores lowest in terms of environmental impact, generally 17% to 26% lower than the flat slab floor.

Stability systems

- Frame structures have the highest cradle-to-gate environmental impact of the five considered types of stability systems. At 250 meters, the frame structure was not sufficient to satisfy the criteria.
- Tube structures only reduce the impact for the concrete models due to more efficient cross-section design. The reduction in impact is 5% to 11% compared to the frame structures.
- The outrigger models decrease the environmental impact by 5% to 16% on average for the concrete models and 20% to 26% for steel models, compared to the tube structures.
- The braced tube only decreased the impact for the 200- and 250-meter models, with 7% to 12% compared to the tube structures.
- The diagrid structure decreased the impact even further to 17% to 28% on for concrete and 28% to 41% for steel models, compared to the tube structures.
- No significant differences in impact were found regarding the variations in stability systems and height of the building, other than an overall increased impact per square meter.
- Required material quantities for beams in the diagrid structure were found to be more dominant than required materials for the diagrid structure for lateral stiffness purposes.

Life-cycle assessment

- Using LCA-data for steel from solely the NMD results in considerably higher impacts than using data for steel published by Bouwen met Staal. The environmental impact increases by 52% to 124% depending on the used stability and floor system.

Conclusions

Summarising all of the above, the following conclusions can be drawn based on the outcomes and within the limits of this research:

Materials

- Steel structures have a 6% to 35% higher cradle-to-gate environmental impact compared to concrete structures in high-rise buildings. It is likely that the inclusion of the construction phase and foundation structure will lead to a decrease of this gap. However, at this point it is not known if this would lead to a scenario where the impact by steel structures would become lower than the concrete structures.
- Regarding the case of cast-in-situ versus precast concrete, no clear winner can be appointed, as the cradle-to-gate environmental impact scores are close to each other. It is likely that the inclusion of the construction phase will influence the results. The outcome hugely depends on numerous of (project specific) factors and can therefore not be predicted on beforehand based on the results from this thesis.
- Fire resistant material has a relatively low impact on the total environmental impact when the use of composite floors is not considered. More research is required to determine the actual environmental impact of fire resistant materials and fire safety measures for composite floors.
- Variation of +/- 25% of the shadow prices of concrete, reinforcement steel and steel can lead to an increase or reduction of the gap in environmental impact between the steel and concrete models. However, it does not result in a lower cradle-to-gate impact by the steel models compared to the concrete models, when the same stability system is considered.

Floors

- Floor systems are still responsible for the largest part, 32% to 73%, of the total environmental impact of high-rise structures. Decreasing the impact by the stability system increases the significance of reducing the impact by floors. Using a lighter floor system does lead to a decreasing demand of material for the structure, but does not necessarily lead to a lower total environmental impact, due to the impact by the floor itself.
- Flat slab floors have the highest environmental impact of the three systems, where after composite floors come next and hollow core slab floors have the lowest impact. Further research is needed whether this still holds when the construction phase is included in the LCA.

Stability systems

- The frame and tube structures lead to the highest cradle-to-gate environmental impacts for all heights. Using an outrigger structure decreases the impact by 5% to 16% for concrete and 20% to 26% for steel models, compared to the tube structure. The braced tube structure only decreases the impact at 200 and 250 meters by 7% to 12%, compared to the tube structure. The diagrid structure has the lowest impact for all considered heights and reduces the impact by 17% to 28% for concrete and 28% to 41% for steel models, compared to the tube structure.
- When designing diagrid structures for relatively low heights, one should also consider the required material for the beams in addition to the angle and density of the diagrid, in order to obtain the most material efficient solution.

Life-cycle assessment

- Fast track [LCA](#) is a relatively simple, yet sensitive way to determine the environmental impact of building structures. The results hugely depend on the used data, of which several possibilities roam around. More transparency and cooperation might lead to a fairer comparison and achieving the common goal of lower environmental impact by building structures.

Overall it can be concluded that structural designers and engineers already have the possibility to make a difference in reducing the environmental impact of high-rise buildings. This research showed that the cradle-to-gate environmental impact by steel structures is slightly higher than the concrete models. More importantly, it is evident that by using less obvious and already existing design solutions for the considered height range, like the diagrid structure, reductions in impact can be made in a relatively easy way.

6

Discussion

This chapter describes a discussion on aspects that might influence the results and conclusions described in this thesis. Furthermore, several areas of improvement or new areas of research are described that could have a positive contribution to sustainability of high-rise buildings.

6.1. Research and results

The results and conclusions of this thesis can be generally applied for high-rise buildings in the Netherlands within the delimitations listed in section 1.3.4. It must be noted that significant alterations in geometry might influence the results. Five other aspects that might influence the results are listed below.

Modelling and calculation methods

A relatively basic approach was used for the structural design and calculations. The 3-dimensional structures were translated into 2-dimensional structures, requiring simplifications and assumptions, resulting in inaccuracies. The effect of these inaccuracies was only partially investigated and it is therefore not completely known how they influence the results. Opposed to that, the inaccuracies were minimised by carefully verifying the results of the 2-dimensional models with corresponding 3-dimensional models in finite element analysis (FEA) software and alterations were made accordingly. Additionally, due to the use of parametric models, inaccuracies and possible minor errors exist in all of the models. Moreover, the geometry of the models is relatively simple to translate into 2-dimensional models. Therefore, it is expected that the conclusions will not change significantly when 3-dimensional models are used.

Sensitivity to data

During the process of writing this thesis, a switch was made from using life-cycle analysis (LCA) data for steel from the Nationale Milieu Database (National Environmental Database) (NMD) to data published by Bouwen met Staal. This significantly influenced the results and conclusions. The results of this research hugely depend on the used LCA-data. Minor changes in this data for a selection of materials was discussed and it was showed that these would not change the results significantly.

Exclusion of foundation

As discussed in section 4.4.4, the foundation has a significant impact on the environmental impact of the structure. It remains to some extent unpredictable on how including the foundation would influence the relative impacts between the cast-in-situ concrete, prefab concrete and steel structures. If one reasons that lighter structures require a less heavy foundation, the relative impacts would decrease. This would mean that cast-in-situ concrete would become less favourable in relation to prefab concrete, while steel would become more favourable. On the other hand, as stated in section 3.2.4, rotational stiffness of the foundation plays a major role in tall building design. Following this logic, the foundation could be considered to be more or less the same for all variations. The reality will most likely be situated somewhere in between.

Exclusion of construction phase

In sections 4.4.5 and 4.4.6, the possible influence of inclusion of the construction phase on the results was discussed. The influence of the transportation is project specific as it relies heavily on the choice of suppliers. Regarding cast-in-situ versus precast concrete, it is most likely that the impact by transportation is higher for prefab concrete as suppliers often are situated at longer distances. Steel buildings are significantly lighter and therefore need less transport, but suppliers can still be located relatively far away. The influence of construction remains difficult to predict as it depends on numerous of factors and is also project specific. The construction phase does have a significant impact on the total environmental impact and it is most likely that it will have an equalising effect on the gap in impact between steel and concrete structures. Moreover, the construction phase is probably the deciding factor when comparing cast-in-situ and prefab concrete.

Exclusion of demolition phase

The end-of-life phase was excluded from the scope of this thesis since demolition of high-rise buildings above 150 meters is almost non-existent. In the case that demolition of high-rise buildings would be considered possible and desirable, steel would most likely become the most favourable material due to its high recycling and reuse potential. However, it is more desirable to focus on extending the building's lifetime instead of demolition and reconstruction of the building.

6.2. Future research and potential

Sustainability of high-rise building structures is a very broad subject and there are still a lot of areas of improvement and new things to be discovered.

Timber high-rise structures

Timber structures have proven to significantly decrease the environmental impact in low-rise structures. Timber is a lightweight and natural material and could be a solution to the depletion of natural resources for the other materials. Therefore, it might be interesting to investigate whether high-rise building structures of timber would result in a lower environmental impact by the structure.

Reuse of building or structural elements

As indicated in section 4.4.2, reuse of the structural elements after demolition of the building could have a significant impact on the results. There are two sides of the same coin: first one should try to extend the building's life time by retrofitting and maintaining the structural integrity. This would require research into the maximum life span of the materials in high-rise structures. And second, if it is evident that high-rise building structures do have a maximum life span, possibilities of demolition should be investigated. This would require high-rise buildings to be demountable, which would have influence on the overall design and the design of connections. Moreover, sustainable demolishing techniques should be developed.

Construction phase

The influence of the construction phase was also discussed in sections 4.4.5 and 4.4.6. The construction phase consists of impact by transportation (A4) and construction (A5). The impact by the construction phase can be significant, especially for high-rise structures where the use of heavy machinery is more common and building methods are often more complex. The construction phase is especially a point of interest in the comparison of cast-in-situ and prefab concrete.

Influence of foundation

As stated in section 4.4.4, the foundation structure (or substructure) can have a significant impact on the environmental impact of the structure. The design of high-rise buildings foundations depends both on required strength and stiffness. Moreover, it could have an influence on the results when comparing cast-in-situ concrete, prefab concrete and steel building structures.

Fire resistant materials

The impact of fire resistant material can be significant, especially when using composite floors. As stated in section 4.4.3 the environmental impact of these materials are not known yet. Moreover, it is not clear at this point which of the fire mitigation strategies results in the lowest impact and whether there are other, more environmental friendly, options.

Light floor systems with low impact

Floor structures are responsible for a large part of the environmental impact of the structure. Using lighter floors reduces the amount of required material for the structure, but does not necessarily lead to a lower overall impact. More research should be done into existing and new lightweight floor systems with reduced environmental impact. An example is the Sustainable Form Inclusion System™ (SFIS) where plastic waste, e.g. empty water bottles, is put as displacement for concrete in order to reduce the weight of the slab.

Internal columns

Internal columns were not considered in this research, as it is common belief in the real estate market nowadays that internal columns decrease the architectural quality and rent-ability of the office spaces. However, floor structures are responsible for a major part of the environmental impact by the structure. Reducing the span by using internal columns could lead to a significant reduction of the impact. A possible downside of using internal columns could be that tension forces could occur in the foundation due to decreased vertical loads in the columns.

More detailed analysis of wind in relation to material use

Within this thesis, wind loads were calculated using the Eurocode and by applying the same assumptions on all models. It would be interesting to relate these assumptions according to the specific model. Possible parameters that could be relaxed would be, e.g. floor height (depending on floor system, reducing affected area by wind loads), weight and natural period (both influencing wind forces). Moreover, several kinds of wind mitigation strategies could be investigated, e.g. building slots or rough corners.

Integral design for environmental impact

At this time, researches into the environmental impact of building components are mostly done in a single disciplinary approach. The proposed optimum solutions by one discipline might lead to restrictions or difficulties for another and eventually not to the most sustainable integral design. More insight is needed in how these sustainability measures relate to each other.

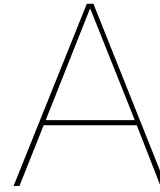
Bibliography

- [1] Mir Ali and Paul Armstrong. Overview of sustainable design factors in high-rise buildings. *Proc. of the CTBUH 8th World Congress*, 2008.
- [2] Mir Ali and Kyoung Sun Moon. Structural Developments in Tall Buildings: Current Trends and Future Prospects. *Architectural Science Review*, 50(3):205–223, 2007. doi: doi:10.3763/asre.2007.5027.
- [3] Mir M. Ali and Kheir Al-Kodmany. Tall Buildings and Urban Habitat of the 21st Century: A Global Perspective. *Buildings*, 2(4):384–423, 2012. ISSN 2075-5309. doi: 10.3390/buildings2040384.
- [4] John E. Anderson and Robert Silman. The role of the structural engineer in green building. *Structural Engineer*, 87(3):28–31, 2009.
- [5] Betonvereniging. G.T.B. 2013, 2013.
- [6] Bouwen met Staal. Duurzaam in staal. URL <http://www.duurzaaminstaal.nl>.
- [7] Bouwen met Staal. MRPI sheet for heavy steel construction products. Technical report, Zoetermeer, 2013.
- [8] Bouwen met Staal. MRPI sheet for light steel construction products. Technical report, Zoetermeer, 2013.
- [9] Bouwen met Staal. *Veilige waarden voor de kritieke staaltemperatuur bij ontwerp en aanbesteding*. Zoetermeer, 2015.
- [10] C.R. Braam. Vlakke plaatvloeren. *Cement*, 2:88–94, 2008.
- [11] Philip Castillo and Meiring Beyers. New Solar Initiatives in Supertall Buildings: The Spire at Ras Al Khaimah. *CTBUH Journal 2010*, (III):20–27, 2010.
- [12] Yuan Chang, Robert J. Ries, and Shuhua Lei. The embodied energy and emissions of a high-rise education building: A quantification using process-based hybrid life cycle inventory model. *Energy and Buildings*, 55:790–798, 2012. doi: 10.1016/j.enbuild.2012.10.019.
- [13] T.Y. Chen, J. Burnett, and C.K. Chau. Analysis of embodied energy use in the residential building of Hong Kong. *Energy*, 26(4):323–340, 2001. doi: 10.1016/S0360-5442(01)00006-8.
- [14] D. Clark. *What Colour Is Your Building?* Royal Institute of British Architects, London, 2013.
- [15] Raymond J Cole. Construction of Alternative Structural Systems. *Building and Environment*, 34:335–348, 1999.
- [16] Joseph M. Danatzko and Halil Sezen. Sustainable Structural Design Methodologies. *Practice Periodical on Structural Design and Construction*, 16(NOVEMBER):186–190, 2011. doi: 10.1061/(ASCE)SC.1943-5576.0000095.
- [17] C.a De Wolf, F.b Yang, D.c Cox, A.d Charlson, A.S.e Hattan, and J.f Ochsendorf. Material quantities and embodied carbon dioxide in structures. *Proceedings of the Institution of Civil Engineers: Engineering Sustainability*, 169(4):150–161, 2016. ISSN 1478-4629. doi: 10.1680/ensu.15.00033. URL <https://www.scopus.com/inward/record.uri?eid=2-s2.0-84981318480&partnerID=40&md5=fd52d26e7aa5749319880e5dd8eb2e0d>.
- [18] Catherine De Wolf. *Material quantities in building structures and their environmental impact*. PhD thesis, Massachusetts Institute of Technology, 2014.

- [19] Dubai Municipality. *Dubai wind code*. 2013.
- [20] Dutch Engineering. Staal-beton vloersystemen, ComFlor staalplaat-betonvloeren. 2013.
- [21] Paolo Foraboschi, Mattia Mercanzin, and Dario Trabucco. Sustainable structural design of tall buildings based on embodied energy. *Energy and Buildings*, 68:254–269, 2014. doi: 10.1016/j.enbuild.2013.09.003.
- [22] H Ham and C Terwel. *Structural calculations of High Rise Structures*. 2017.
- [23] S. C. Kaethner and J. A. BurrIDGE. Embodied CO₂ of structural frames. *The Structural Engineer*, May (5):33–40, 2012. ISSN 14665123.
- [24] Karamba. Karamba, 2017. URL <http://www.karamba3d.com>.
- [25] Fazlur R. Khan and Walter P. Moore. *Tall Building Systems and Concepts*. American Society of Civil Engineers, 1980.
- [26] Kyoung Sun Moon. Optimal Grid Geometry of Diagrid Structures for Tall Buildings. *Architectural Science Review*, 51(3):239–251, 2008. ISSN 00038628. doi: 10.3763/asre.2008.5129. URL <http://www.tandfonline.com/doi/abs/10.3763/asre.2008.5129>.
- [27] NEN 6702. Technical principles for building structures - TGB 1990 - Loadings and deformations, 2007.
- [28] NEN 6720. Regulations for concrete - Structural requirements and calculation methods, 2008.
- [29] NEN-EN 1990 NB. National Annex to NEN-EN 1990+A1+A1/C2: Eurocode: Basis of structural design, 2011.
- [30] NEN-EN 1991-1-1. Eurocode 1: Actions on structures - Part 1- 1: General actions - Densities, self-weight, imposed loads for buildings, 2011.
- [31] NEN-EN 1991-1-1 NB. National Annex to NEN-EN 1991-1-1+C1: Eurocode 1: Actions on structures - Part 1-1: General actions - Densities, self-weight, imposed loads for buildings, 2011.
- [32] NEN-EN 1991-1-4. Eurocode 1: Actions on structures -Part 1-4: General actions -Wind actions, 2011.
- [33] NEN-EN 1991-1-4 NB. National Annex to NEN-EN 1991-1-4+A1+C2: Eurocode 1: Actions on structures - Part 1-4: General actions - Wind actions, 2011.
- [34] NEN-EN 1992-1-1. Eurocode 2: Design of concrete structures – Part 1-1: General rules and rules for buildings, 2011.
- [35] NEN-EN 1992-1-1 NB. National Annex to NEN-EN 1992-1-1+C2 Eurocode 2: Design of concrete structures - Part 1-1: General rules and rules for buildings, 2011.
- [36] NEN-EN 1993-1-1. Eurocode 3: Design of steel structures - Part 1- 1: General rules and rules for buildings, 2011.
- [37] Jonathan Norman, Heather Maclean, and Christopher Kennedy. Comparing High and Low Residential Density: Life-Cycle Analysis of Energy Use and Greenhouse Gas Emissions. *Journal of Urban Planning and Development*, 132(1):10, 2006. URL <http://link.aip.org/link/JUPDDM/v132/i1/p10/s1{&}Agg=doi>.
- [38] Philip Oldfield. Embodied Carbon and High-Rise. In *CTBUH 2012 9th World Congress, Shanghai*, pages 614–622, 2012.
- [39] Hyo Seon Park, Bongkeun Kwon, Yunah Shin, Yousok Kim, Taehoon Hong, and Se Woon Choi. Cost and CO₂ emission optimization of steel reinforced concrete columns in high-rise buildings. *Energies*, 6: 5609–5624, 2013. doi: 10.3390/en6115609.
- [40] Promat. *Handboek Bouwkundige Brandpreventie*. Houten, 2016.

- [41] Robert McNeel & Associates. Rhinoceros, 2017. URL <https://www.rhino3d.com/>.
- [42] David Rutten. Grasshopper 3D, 2017. URL <http://www.grasshopper3d.com/>.
- [43] Mark Sarkisian. *Designing Tall Buildings, Structure as Architecture*. Routledge, New York, 2nd edition, 2016.
- [44] Mark Sarkisian and David Shook. Structural Innovations Inspired by Growth, Genetics, and Emergence Theory. In *37th LABSE Symposium Madrid 2014*, volume 102, pages 1634–1641, 2014. doi: 10.2749/222137814814067923.
- [45] Mark Sarkisian and David Shook. Embodied Carbon in Structures and Cities. In *37th LABSE Symposium Madrid 2014*, volume 102, pages 3166–3173, 2014.
- [46] W. Schueller. *The Vertical Building Structure*. Van Nostrand Reinhold, New York, 1990.
- [47] Bryan Stafford Smith and Alex Coull. *Tall Building Structures: Analysis and Design*. 1991. ISBN 0471512370.
- [48] H H Snijder, N Popa, and R C Spoorenberg. Buckling Curves for Heavy Wide Flange Steel Columns. 2010.
- [49] Stichting Bouwkwiteit. Bepalingsmethode Milieuprestatie Gebouwen en GWW-werken. Technical Report November, 2014.
- [50] The Intergovernmental Panel on Climate Change (IPCC). *Climate Change 2014: Mitigation of Climate Change*. 2014. ISBN 9781107654815. doi: 10.1017/CBO9781107415416.
- [51] Dario Trabucco and Antony Wood. LCA of tall buildings: Still a long way to go. *Journal of Building Engineering*, 7:379–381, 2016. doi: 10.1016/j.job.2016.07.009.
- [52] Dario Trabucco, Antony Wood, Olivier Vassart, and Nicoleta Popa. A Whole LCA of the Sustainable Aspects of Structural Systems in Tall Paper Type. *International Journal of High-Rise Buildings*, 5(2): 71–86, 2016.
- [53] G.J. Treloar, R. Fay, B. Ilozor, and P.E.D. Love. An analysis of the embodied energy of office buildings by height. *Facilities*, 19(5/6):204–214, 2001. doi: 10.1108/02632770110387797.
- [54] UNEP. *Buildings and Climate Change: Status, Challenges and Opportunities*. United Nations Environmental Programme, Nairobi, 2007.
- [55] United Nations. Future World Population Growth to be Concentrated in Urban Areas. *United Nations Population Division Report*, March, 2001.
- [56] J.P. Van Der Windt. Een factor van betekenis. *Cement*, 7:8–13, 2006.
- [57] Sebastiaan Van Hellenberg Hubar. *Duurzaamheid, flexibiliteit en kosten van hoogbouw*. PhD thesis, Delft University of Technology, 2009.
- [58] F. Van Herwijnen. Duurzaam construeren met materialen. Technical report, VNconstructeurs, Gorinchem, 2013.
- [59] Dick Van Keulen. EEM en prefab beton. *Cement*, 3:60–65, 2014.
- [60] VBI. Productdatablad Kanaalplaatvloer 200. 2017.
- [61] VBI. Productdatablad Kanaalplaatvloer 260. 2017.
- [62] Joost G. Vogtländer. *A practical guide to LCA for students designers and business managers*. VSSD, 2010. ISBN 90-6562-311-6.
- [63] Nengmou Wang and Hojjat Adeli. Sustainable building design. *Journal of Civil Engineering and Management*, 20(1):1–10, 2014. doi: 10.3846/13923730.2013.871330.

-
- [64] Mark D. Webster. Relevance of structural engineers to sustainable design of buildings. *Structural Engineering International: Journal of the International Association for Bridge and Structural Engineering (IABSE)*, 3:181–185, 2004. doi: 10.2749/101686604777963874.
- [65] Y. G. Yohanis and B. Norton. Life-cycle operational and embodied energy for a generic single-storey office building in the UK. *Energy*, 27:77–92, 2002. doi: 10.1016/S0360-5442(01)00061-5.



Foundation stiffness

This appendix elaborates on assumptions regarding the rotational stiffness of the foundation structure. In the Netherlands, soil is soft compared to other countries, meaning that horizontal displacements at the top of the building are partially caused by a rotation of the foundation structure. This effect is taken into account by assuming a certain value that is added to the total deflection of the building itself. A small study was performed to provide a theoretical and practical basis for this assumption.

The total deflection at the top of the building is partially caused by the stiffness of the building itself and partially by the rotational stiffness of the foundation structure which consists of piles. This is shown in figure A.1. The stiffness of the piles depends on the elastic and plastic deformation of the piles and on elastic and plastic soil settlements. Foundation piles transfer their loads to the ground through the tip and friction along the shaft of the piles. The spring stiffness of the piles depends on numerous of factors among which are pile geometry, material and site specific soil conditions. For this study, the 200-meter prefab tube model is used with 10 columns and a hollow core slab floor.

A conservative approximation of the pile stiffness is: 100 000 kN/m. However, higher values can be realised up to 200 000 kN/m or even more. For this specific study, a value of 150 000 kN/m was chosen. Using this value resulted in a balance in piles needed for rotational stiffness and vertical load transfer due to the weight of the building. Additionally, it was chosen to use prefab piles of 450 mm in width and length with a maximum bearing capacity of 2500 kN. The minimum distance between piles was taken as $3.0 * D = 1.35$ meters.

Each individual pile is represented as a spring with a certain arm to the centre line of the building. Multiplying the arm by the spring stiffness gives a contribution to the rotational stiffness of the building. By adding all these individual contributions together, the total rotational spring stiffness can be found. The total deflection can then be found by dividing the total moment due to wind by the rotational spring stiffness and multiplying this value by the height of the building, under the assumption that the angles are small.

$$k_{\phi} = \sum_{i=1}^n k_i * x_i \quad (\text{A.1})$$

$$u_{foundation} = \frac{M_{wind}}{k_{\phi}} * h \quad (\text{A.2})$$

The design of the pile foundation has been done in Rhinoceros in order to be able to compute the deflection due to rotation of the foundation by a simple Grasshopper script. This script automatically measures the distance of the pile to the centre line of the building and then computes the deflection. In figure A.2 the design of the foundation is shown for the assumption that the foundation is responsible for half of the total deflection ($1/1000 * H$). The red areas indicate where the upper structure, columns and core walls, is situated.

This pile foundation design contains 773 piles and fulfils the requirements regarding ULS bearing capacity. Only a small amount of extra piles was needed for rotational stiffness. A second study was performed in order to determine the amount of required piles for a foundation which would only be responsible for one third of the total building deflection ($1/1500 * H$). Here, amount of required piles increases with 28% to 1069, which means that a significant part (almost one third) of the piles is not needed for ULS bearing capacity, but for rotational stiffness of the building. This would result in a reduction of required material for the building structure, but it would significantly increase material use for the foundation structure. In this case it would be questionable if this would result in a reduction of overall material use. Therefore it was chosen to use the conservative approach where the foundation is responsible for half of the total building deflection ($1/1000 * H$).

In reality, when a building of this size would be build, it is highly possible that a few sub levels, or a parking garage, would be added beneath the ground surface. It would be beneficial to increase width and depth of these underground levels in order to increase the lever arms of the foundation piles. In this case a larger rotational spring stiffness could be realised when required. However, the design of such a structure heavily depends on project specific factors and was therefore not taken into account.

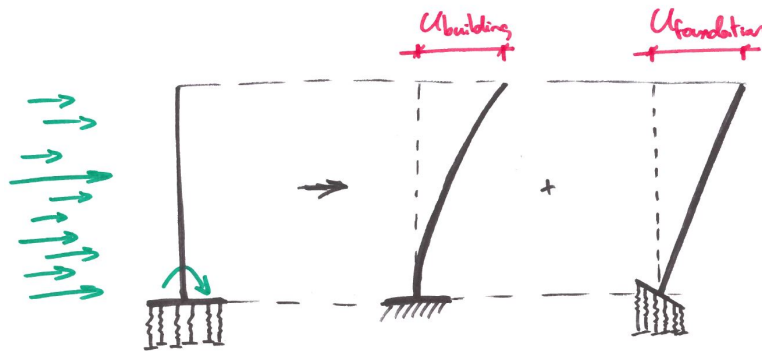


Figure A.1: Conceptual impression of the deflection by stiffness of the building and the foundation represented by springs.

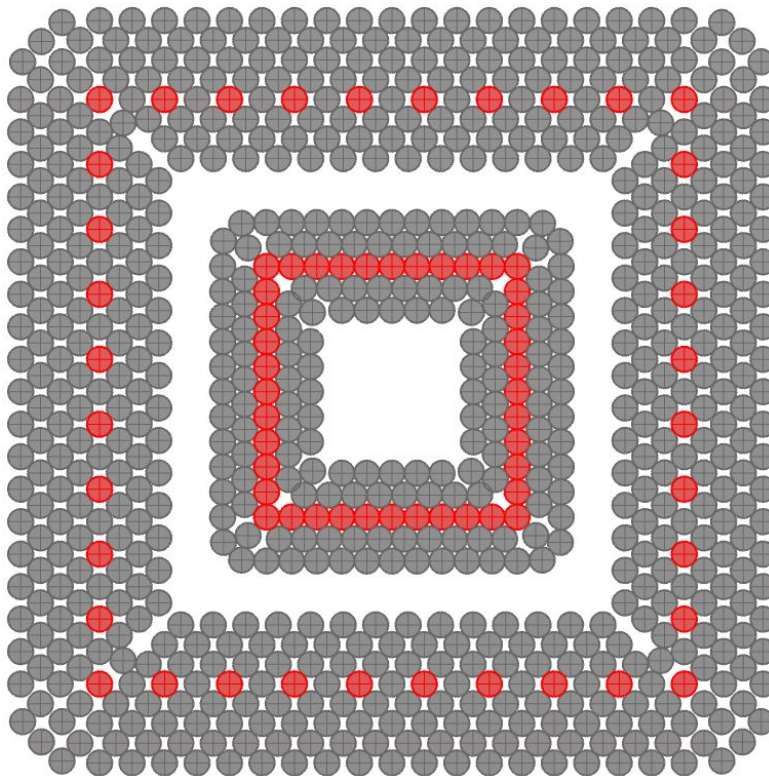


Figure A.2: Pile foundation design for the 200-meter prefab concrete tube model with 10 columns and a hollow core slab floor. The circles have a radius of $1.5 \cdot D$ and cannot overlap each other in order to satisfy the minimum distance of $3.0 \cdot D$. The red areas indicate where the upper structure is situated.

B

Floor design

This appendix elaborates on the specific calculation methods and design of the floor systems used in this thesis. It contains information about the required calculations and provides an complete overview of all the different floor designs.

B.1. Flat slab floor

B.1.1. One-way spanning design

The reinforcement of the slab is designed by considering a strip of 1 meter in width as a beam. The behaviour is displayed in figure B.1. The support and field moments can be calculated by using the following formulas where L is the length of the span.

$$M_{field;x} = 1/8 * q * L^2 \quad (B.1)$$

$$M_{support;x} = 1/24 * q * L^2 \quad (B.2)$$

The reinforcement net is chosen while considering the minimum reinforcement ratio of 0.17% and $M_{field;y} = 0.2 * M_{field;x}$. This results in a reinforcement net of Ø12-150 in x-direction and Ø10-250 in y-direction for the bottom part. It is assumed that the bottom reinforcement is present over the entire length for anchorage and moment line displacement. Additional reinforcement for the bottom in x-direction is Ø16 and Ø10 every 300 mm, which comes down to 25Ø16 and 25Ø10 over the entire width of the zone. The top reinforcement is only present at the supports. Both at the side of the core and the side of the façade a reinforcement net of Ø10-150 in x-direction and Ø6-250 in y-direction is used.

B.1.2. Two-way spanning design

The two-way spanning zones are designed by using the column, reinforcement and middle strip approach used in the old Dutch norm NEN 6720[28]. Table 25 from GTB 2013[5] with 2 hinged line supports is used in order to calculate the bending moments. Additionally, it is required that support moments at the façade are minimum 33% of the field moments. This means that when table 25 presents values that fall below this minimum, these values are adapted in order to satisfy this criteria.

The bottom reinforcement consists of a reinforcement net of Ø12-200. Additional reinforcement is required in the middle of the floor and the heavy loaded zones between the core and the façade. In the middle zones of the floor 12Ø6 is placed, meaning one bar every 400 mm. In the heavy loaded zones additional 12Ø8 is placed in the column strips and 6Ø12 in the reinforcement strips. Both result in extra bars every 400 mm.

The top reinforcement is only placed at the support zones. At the façade a net is used of Ø10-150 and at the the heavier loaded area at the core a net of Ø16-150. Additional reinforcement is also required here: 16Ø10 in the column strips and 9Ø16 in the reinforcement strips which means extra bars every 300 mm.

At the corners of the core, high shear stresses occur in the slab. These shear stresses are evaluated using the punching shear theory in Eurocode 2[34]. The most unfavourable case is a fully loaded slab supported by core walls with a minimum thickness of 300 mm. This 300 mm is used as the column size in the calculation. Bending in two directions is occurring and a possible hole for elevators is present at the other side of the core wall. This means that only 75% of the full perimeter is taken into account for determining the shear resistance, as shown in figure B.3. The β -factor is calculated using the following formulas:

$$u_1^* = 3\pi d + 3c = 3.867m \quad (B.3)$$

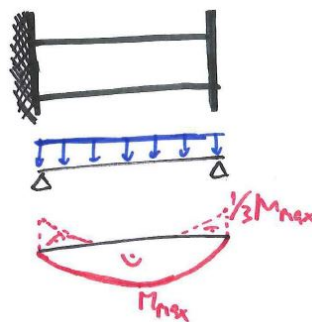
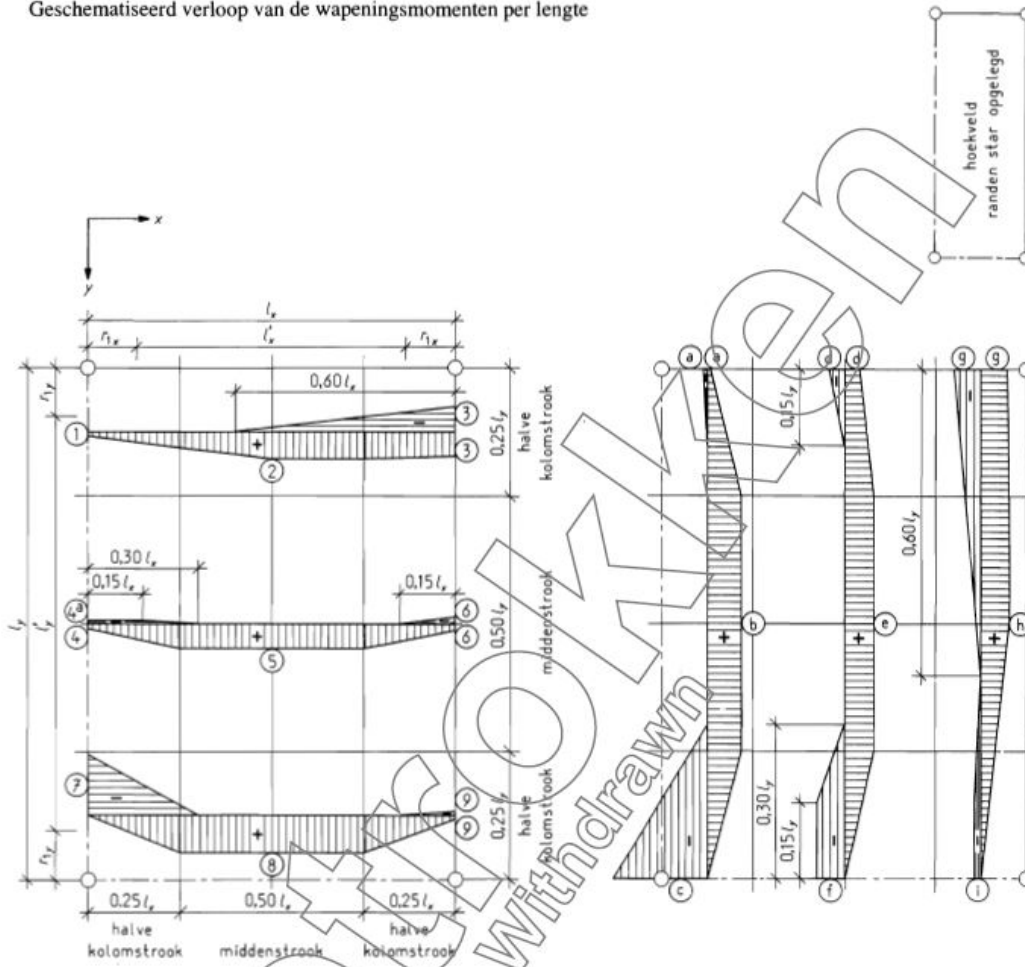


Figure B.1: Simply supported beam with moment distribution for the one-way spanning zone of the slab modelled as a beam.

Geschematiseerd verloop van de wapeningsmomenten per lengte



Momentencoefficiënten

l_y/l_x	$m_{xx}^* = 0,001 p_d l_x^2 \times$									$m_{yy}^* = 0,001 p_d l_y^2 \times$									
	1	2	3	4	5	6	7	8	9	a	b	c	d	e	f	g	h	i	
1,0	0	-61	±56	0	-34	+56	±21	-190	+86	0	0	+86	-190	±21	+56	-34	±56	+61	0
1,2	0	+73	±68	0	-21	+68	±19	-199	+105	0	0	+100	-252	±35	+76	-61	±71	+77	-10
1,4	+14	+89	±82	+15	-12	+82	±22	-202	+123	±12	±11	+113	-312	±50	+96	-90	±90	+95	-24
1,6	+23	+108	±99	+33	0	+98	±28	-200	+141	±21	±16	+123	-360	±65	+114	-117	±110	+115	-40
1,8	+33	+128	±115	+56	0	+115	±36	-193	+157	±31	±20	+132	-418	±80	+132	-143	±131	+136	-56
2,0	+45	+147	±131	+82	0	+135	±44	-185	+173	±42	±25	+139	-461	±95	+148	-166	±151	+155	-72

Figure B.2: Table 25 from GTB 2013[5] which identifies the reinforcement design moments in a flat slab floor with two edges as hinged line supports.

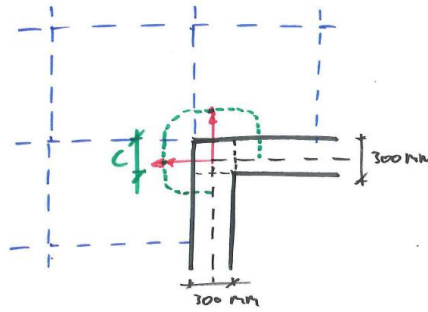


Figure B.3: Model identifying the chosen perimeter and virtual column measurements for the punching shear model.

$$u_1 = 4\pi d + 4c = 5.158m \quad (\text{B.4})$$

$$\beta = u_1/u_1^* = 1.33 \quad (\text{B.5})$$

The acting shear force is following from the support reaction in the corner in the SCIA model which is $R_z = 2917kN$. The acting shear stress follows from:

$$v_{Ed} = \beta * V_{Ed}/(u_1 * d) = 2.60N/mm^2 \quad (\text{B.6})$$

The resisting shear stress can be calculated by the following formulas:

$$v_{Rd} = 0.12 * k(100 * \rho_l * f_{ck})^{1/3} = 0.96N/mm^2 \geq v_{min} \quad (\text{B.7})$$

$$v_{min} = 0.035 * k^{3/2} f_{ck}^{1/2} = 0.50N/mm^2 \quad (\text{B.8})$$

This means that the shear stress criteria is not satisfied. The shear resistance can be improved by using drop panels or adding shear reinforcement. A choice was made for the latter as increasing the height of the slab did not seem to improve the shear resistance enough. The additional shear reinforcement is taken into account in the environmental impact calculations by increasing the reinforcement steel in the slabs by 5%.

B.1.3. Anchorage lengths

The required amounts of steel in the zones have been calculated and now the anchorage lengths are determined. Table 15.1b from GTB 2013[5] is used here to determine the anchorage lengths. The slab height is higher than 250 mm, which means that the adhesion conditions in the top layer are relatively bad compared to the bottom layer ($\eta_1 = 0.7$ for the top layer and $\eta_1 = 1.0$ for the bottom layer). Table B.1 shows the anchorage lengths that are derived for C35/45. Additionally, $d = 315$ millimetres is added to the anchorage length to retrieve the total length of the rebars.

	6	8	10	12	16	20	25	32
$\eta_1 = 1.0$	194	258	323	387	516	645	807	1032
$\eta_1 = 0.7$	277	369	461	553	737	922	1152	1475

Table B.1: Anchorage lengths in mm for the different bar diameters for C35/45.

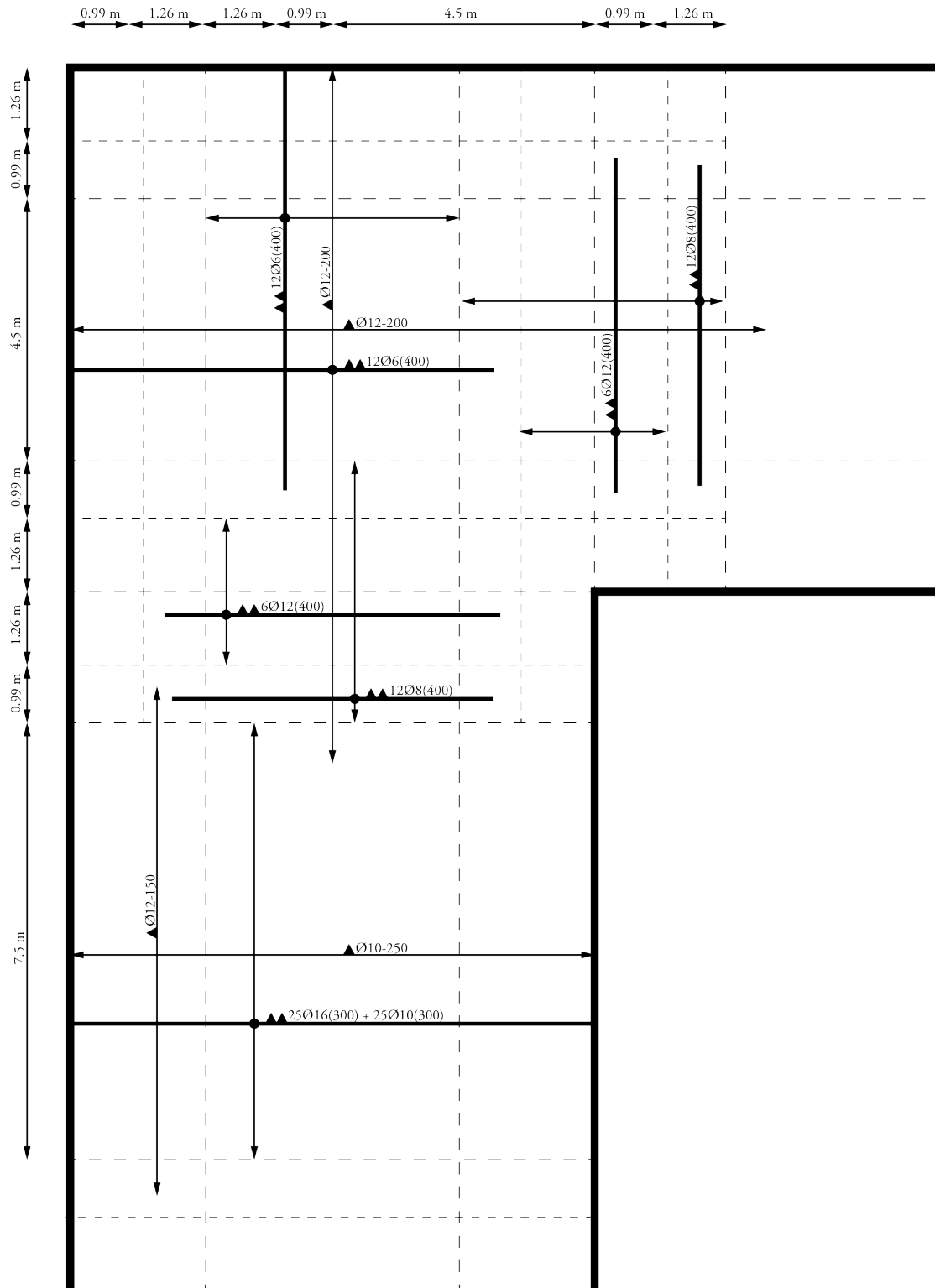


Figure B.4: Reinforcement drawing of the bottom reinforcement in the flat slab floor for the 150-meter models.

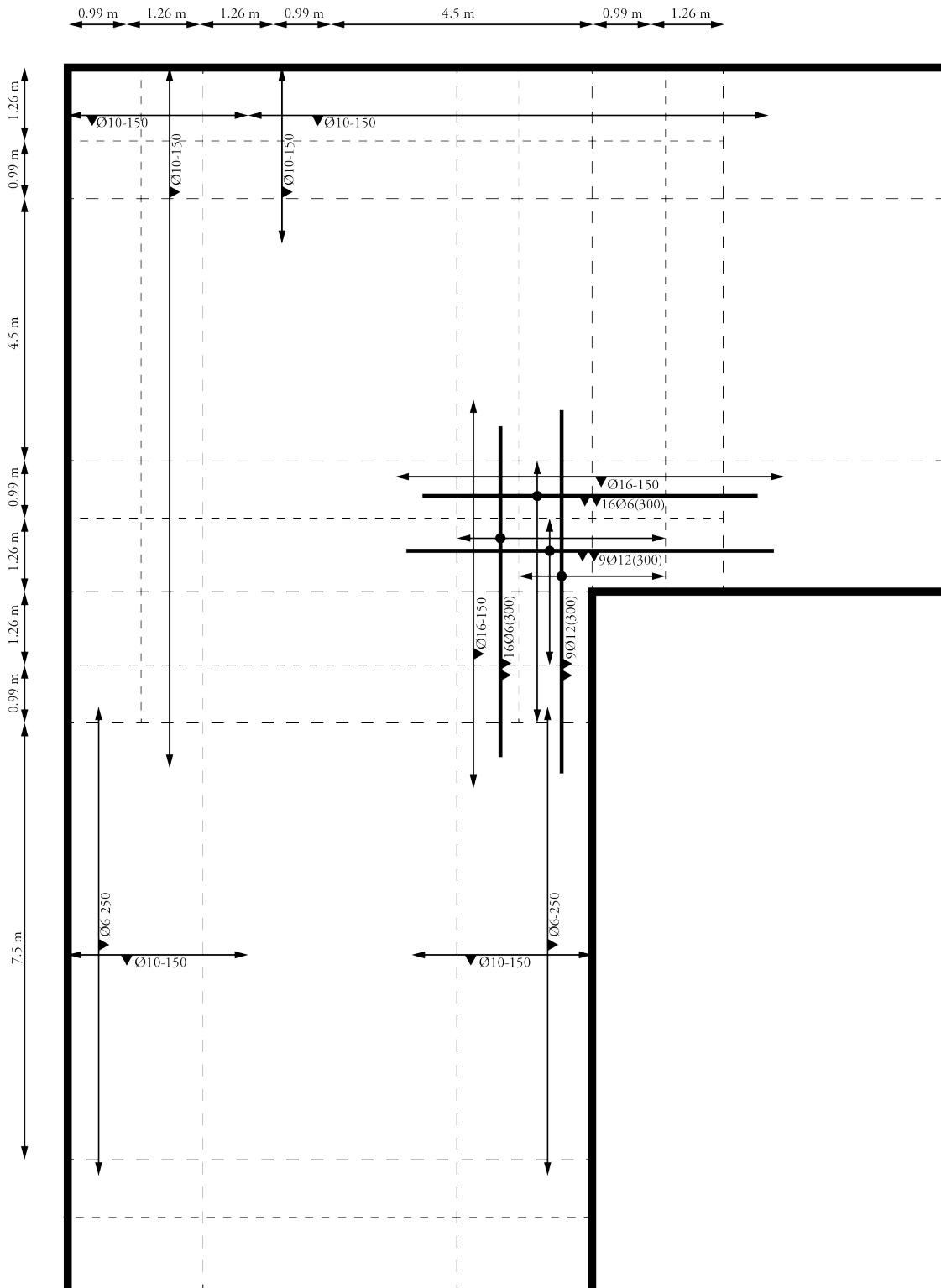


Figure B.5: Reinforcement drawing of the top reinforcement in the flat slab floor for the 150-meter models.

B.2. Hollow core slabs

The design of the hollow core slabs is related to the positioning of the supporting beams. These supporting beams are necessary in order to be able to construct floors without unnecessary long spans in the corners of the building. Two types of hollow core slabs are used, as shown in table B.2. The maximum span is based on information from the supplier VBI[60][61] and satisfies the deflection and fire resistance criteria.

The amount of pre-stress steel incorporated in the hollow core slabs is variable and depends on the span, loads and fire resistance. In order to prevent detailed calculations, the amount of pre-stress is estimated by consulting reference projects of Royal HaskoningDHV with similar spans and loads. This resulted in 3750 kg/m² (588 mm² per slab) of pre-stress steel for the VBI 200 slab and +/- 5400 kg/m² (833 mm² per slab) for the VBI 260 slab. This is on the conservative side, because the spans are at the limits of the capacity of the slab considering the relative high loads and the required fire resistance of 120 minutes.

Part of the hollow core slabs are support by steel THQ beams which span from the core to a column in the perimeter of the building. The THQ beam was chosen because of its high torsional stiffness as the beams are only loaded from one side. If necessary, torsion moments can be prevented by coupling the slab with the beam with a steel rebar at the lower bottom of the slab to the far web of the beam. When doing this, one should take into account that the effective span of the slab is increased. The beams are placed perpendicular to the core wall. Hollow core slabs can be cut in an angle, but that requires a minimum depth of 1 meter of uncut slab.

Diaphragm action is needed to achieve cooperation between the core and façade structure. When using a flat slab, the whole floor behaves monolithically. When using hollow core slabs, diaphragm action can be obtained by using a concrete screed layer. This concrete screed layer is estimated to have a height of 50 mm and includes a reinforcement net of Ø8-150. Additionally, extra reinforcement is needed at the building perimeter where tensile zones will occur when the building is loaded laterally. For this purpose, 3Ø25 is used, based on engineering judgement. The screed layer consists of C20/25 which is also used to fill the joints between the hollow core slabs.

Due to the different column configurations and different floor plans for the three height categories, nearly each design case has an unique floor design. An overview of the floor designs can be found in figures B.6 to B.9. Here the geometry is shown where black points represent the column locations. Furthermore, the types of floors and supporting beams are listed.

The supporting beams are designed as simply supported beams, using the forget-me-not formula for simply supported beams for deflection:

$$u = \frac{5 * ql^4}{384 * EI} \quad (B.9)$$

Hollow core slab type	Height	Max span	Weight
VBI 200	200 mm	9.3m	3.02kN/m ²
VBI 260	260 mm	11.8m	3.76kN/m ²

Table B.2: Hollow core slab properties and area loads.

150 METERS

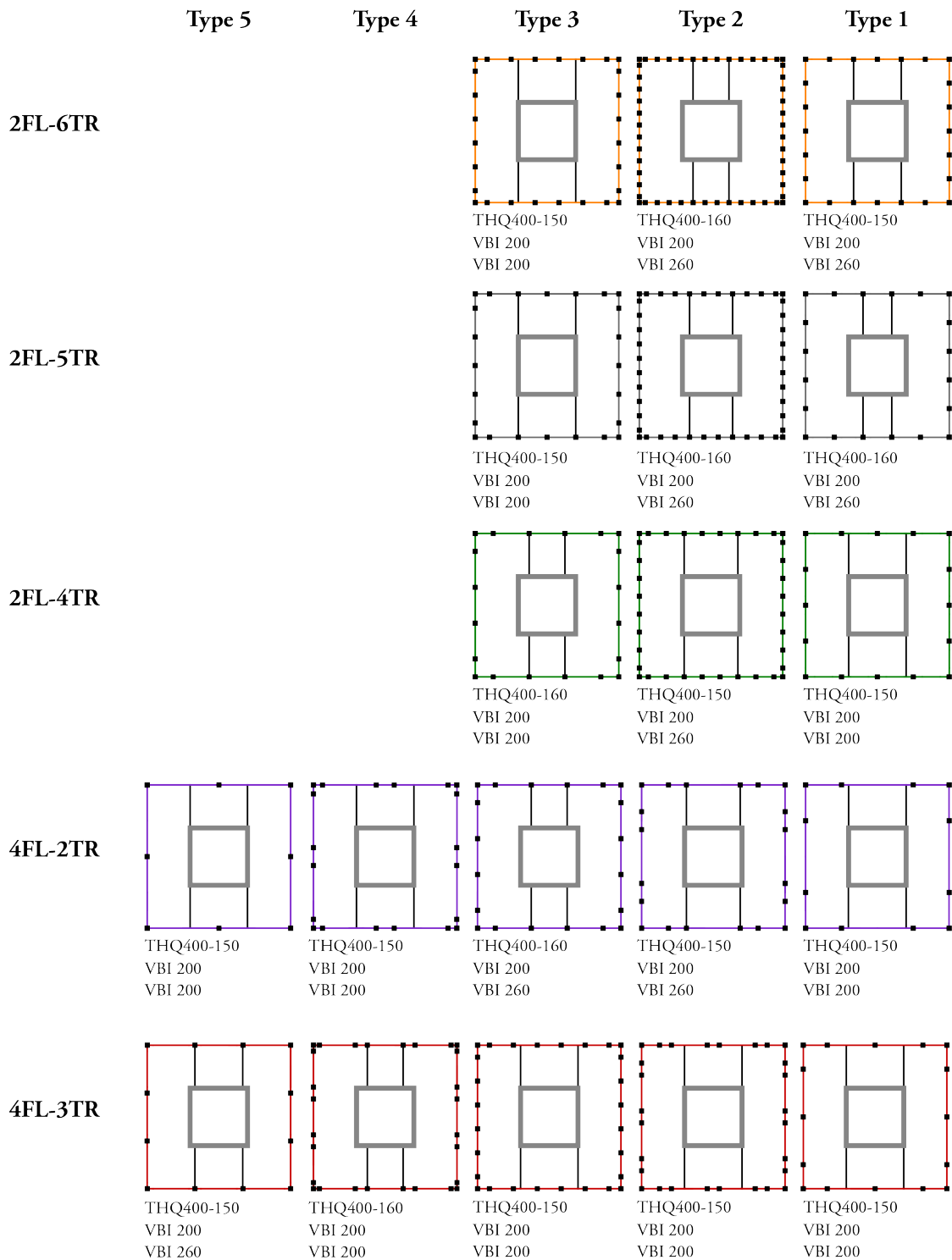


Figure B.6: Overview of the hollow core slab configurations for the 150-meter diagrid models. The THQ beams are indicated as THQ400-150 where 400 is the height (mm) and 150 the weight (kg/m) of the profile.

200 METERS

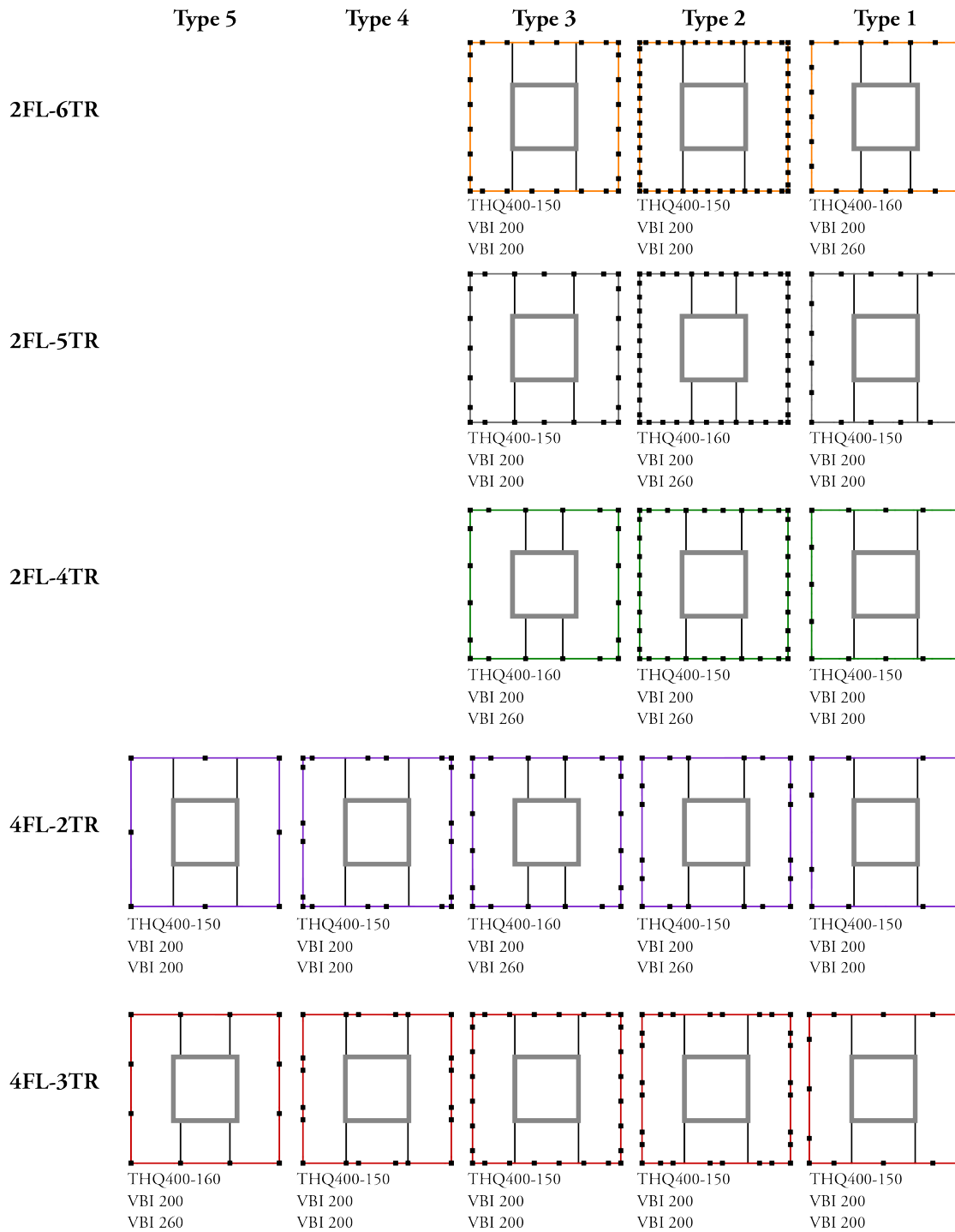


Figure B.7: Overview of the hollow core slab configurations for the 200-meter diagrid models. The THQ beams are indicated as THQ400-150 where 400 is the height (mm) and 150 the weight (kg/m) of the profile.

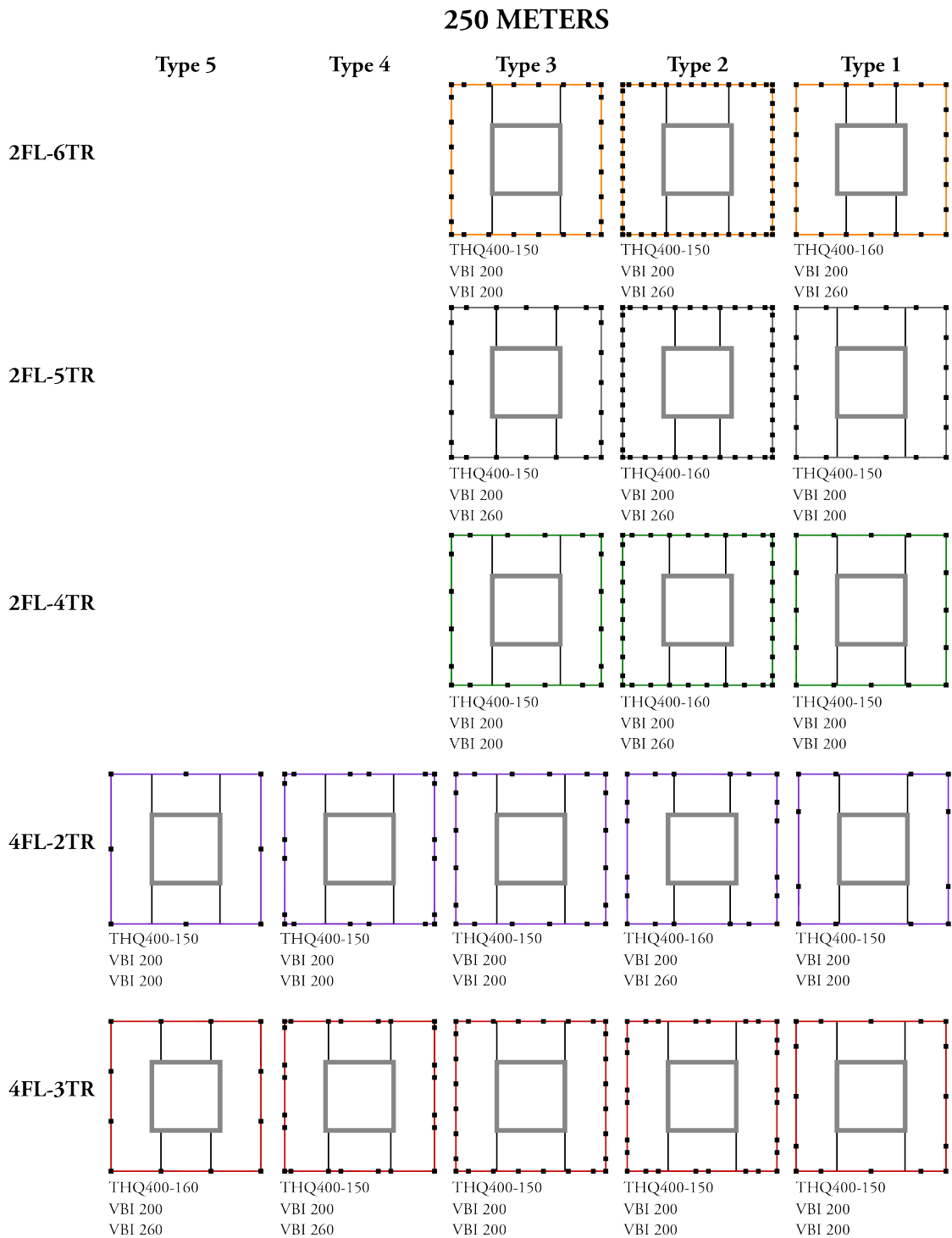


Figure B.8: Overview of the hollow core slab configurations for the 250-meter diagrid models. The THQ beams are indicated as THQ400-150 where 400 is the height (mm) and 150 the weight (kg/m) of the profile.

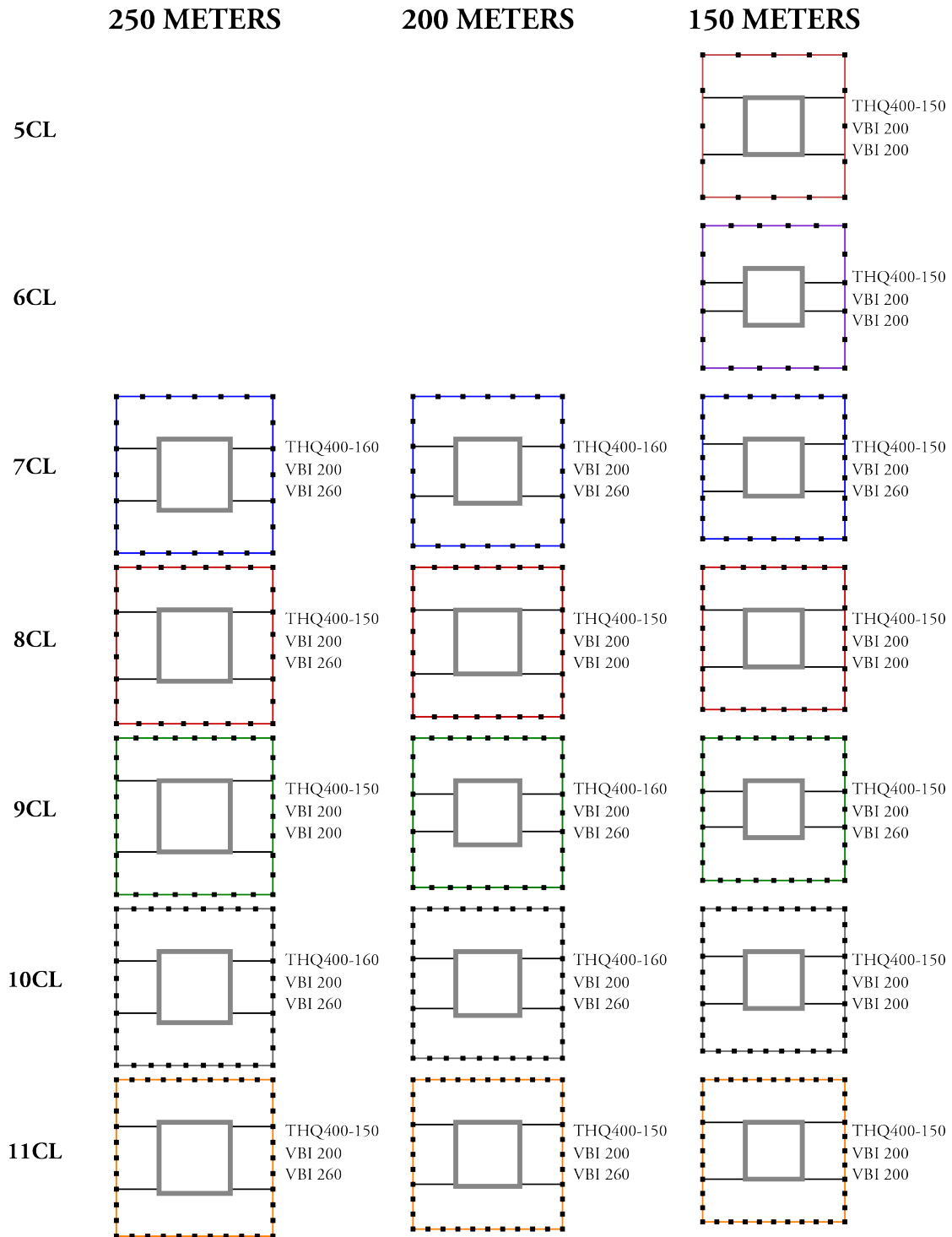


Figure B.9: Overview of the hollow core slab configurations for the all other models. The THQ beams are indicated as THQ400-150 where 400 is the height (mm) and 150 the weight (kg/m) of the profile.

B.3. Composite floors

The composite floor consists of a steel corrugated sheet with a concrete topping, supported by steel beams. The steel plate acts as primary reinforcement for the concrete floor. A reinforcement net of Ø8-150 is added in the top layer for monolithic behaviour, occasional support moments, crack width control and fire resistance. Additionally, reinforcement is added in the bottom gutter, close to the steel plate, to increase fire resistance. By adding Ø16 rebars, it is assumed that a fire resistance of 90 minutes can be achieved. The additional 30 minutes of fire resistance is achieved by adding fire resistant cladding. It was chosen to use the same material that is used for fire protection of the columns and beams. A layer of 20 mm of PROMATECT-H is applied.

The configuration, span and therefore material use heavily depend on the configuration of the perimeter columns. Multiple floor designs are possible for the same column configuration. For each separate column configuration a unique floor design was made, where the focus was on minimising weight and material use. This is achieved by using temporary supports during construction and by allowing primary beams to be placed in an angle. Furthermore, the beams consist of IPE and HEA castellated beams to further minimize material use and allow mechanical installations to pass through the beams. Therefore, S355 is used which has no additional environmental impact compared to S235.

Further material minimisation could be achieved by using steel shear connectors in the concrete to enable composite action of the beams. However, calculation methods are more complex and therefore take considerably more time when evaluating a high amount of floor configurations. Therefore it was not considered in this thesis.

The composite floors are designed by using technical information documents and a calculation spreadsheet by the company Dutch Engineering, manufacturer of the ComFlor composite floors[20]. In table B.3 are the floor types and their properties listed that are used in the designs. The castellated beams are designed by using rules of thumb and forget-me-nots, like equation B.9, for simply supported beams. In some cases, secondary beams are supported by a primary beam. In this case the total deflection of the primary beam + half of the deflection of the secondary beam is used in order to calculate the maximum displacement of the floor field.

Due to the different column configurations and different floor plans for the three height categories, nearly each design case has an unique floor design. An overview of the floor designs can be found in figures B.10 to B.13. Here, the geometry is shown, the types of floors and the types of castellated beams. The upper two beams in the lists are secondary beams and the last the primary beams.

Floor type	Plate thickness	Floor thickness	Weight
ComFlor 46	0.9mm	120mm	2.70kN/m ²
ComFlor 75	0.9mm	140mm	2.62kN/m ²
	1.2mm	140mm	2.66kN/m ²
ComFlor 95	0.9mm	160mm	2.87kN/m ²
	1.2mm	160mm	2.90kN/m ²

Table B.3: Composite floor slab properties.

150 METERS

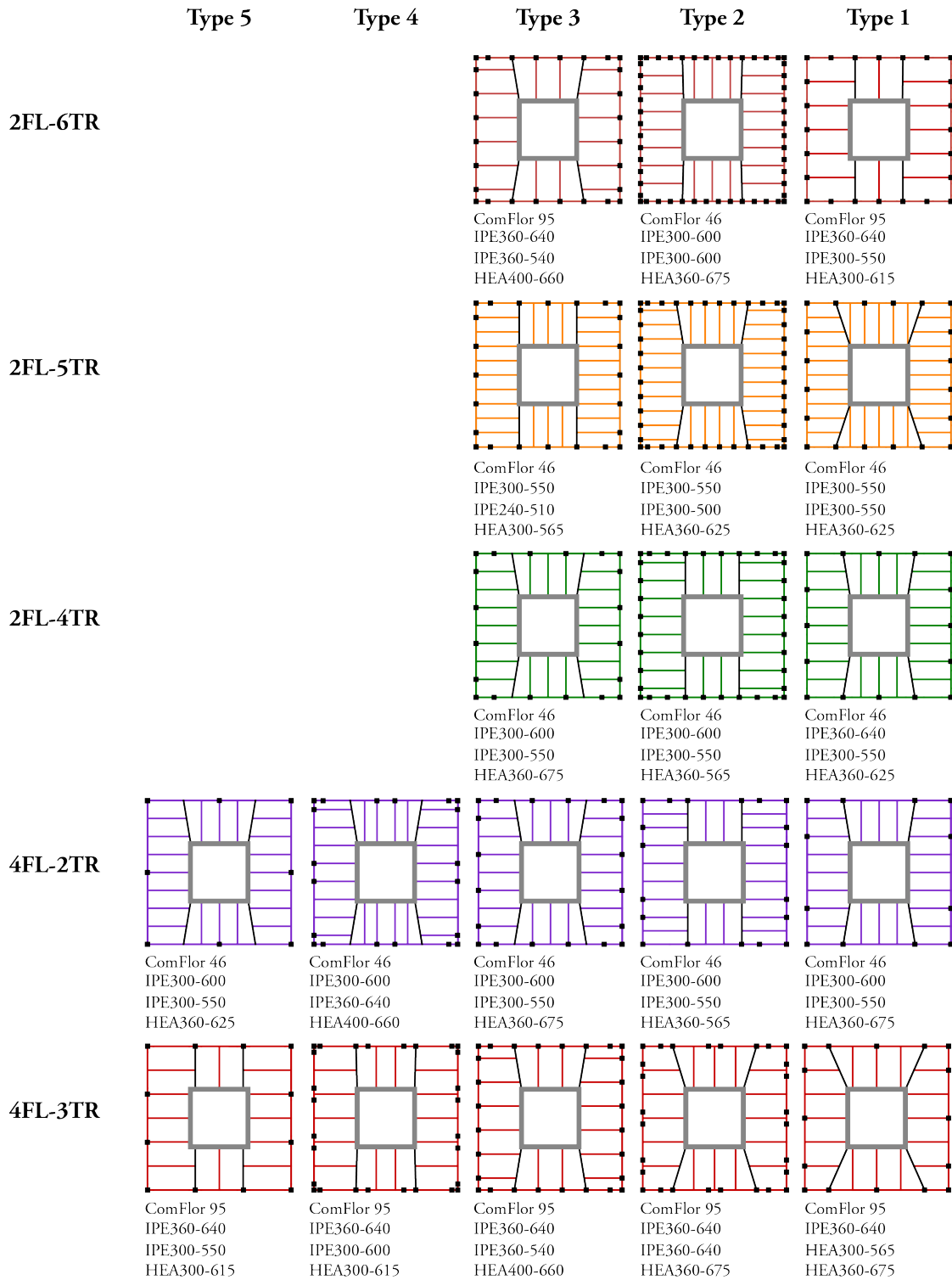


Figure B.10: Overview of the composite floor configurations for the 150-meter diagrid models. The castellated beams are indicated as IPE300-600 where IPE300 is the original profile and 600 is the height of the castellated beam.

200 METERS



Figure B.11: Overview of the composite floor configurations for the 200-meter diagrid models. The castellated beams are indicated as IPE300-600 where IPE300 is the original profile and 600 is the height of the castellated beam.

250 METERS

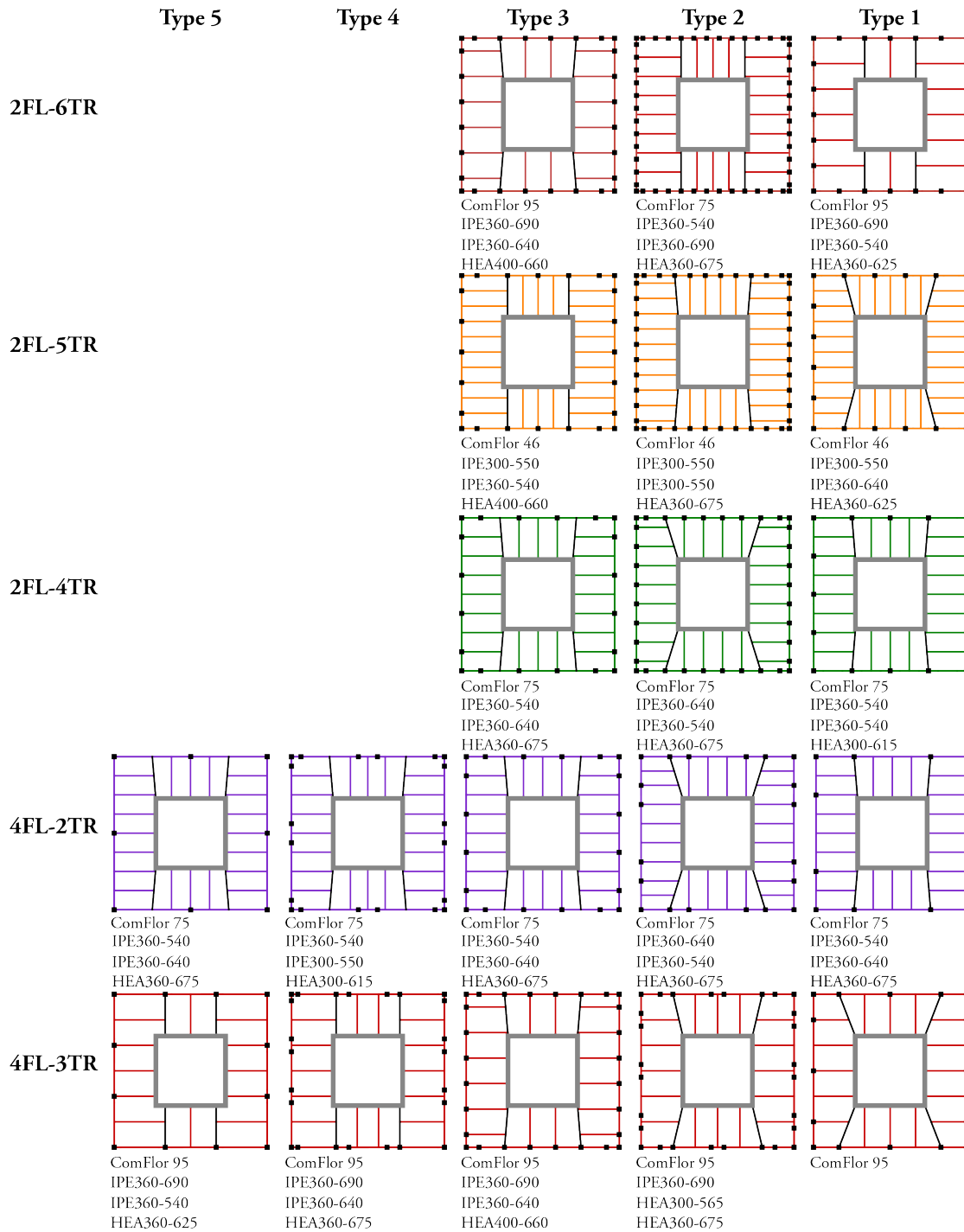


Figure B.12: Overview of the composite floor configurations for the 250-meter diagrid models. The castellated beams are indicated as IPE300-600 where IPE300 is the original profile and 600 is the height of the castellated beam.

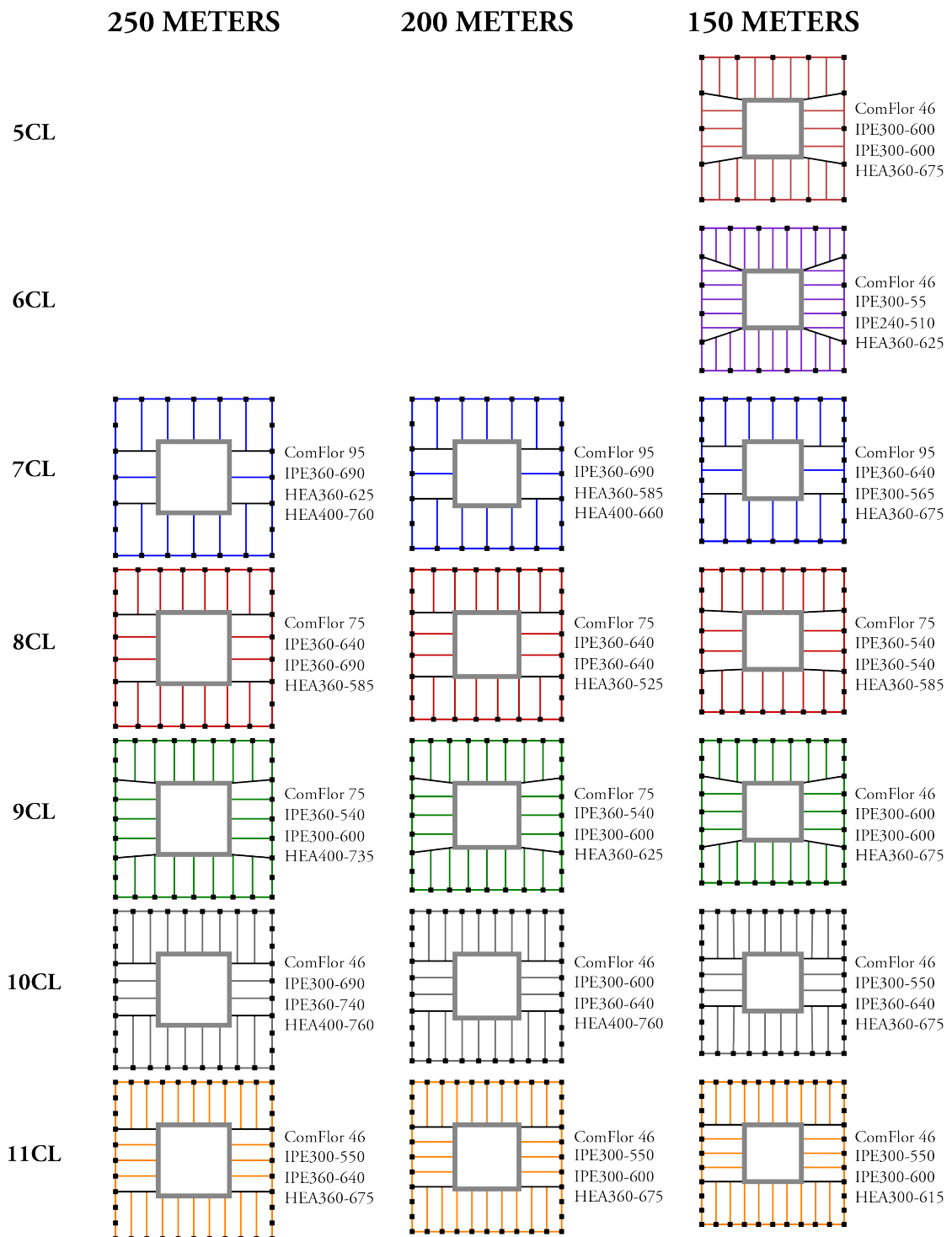
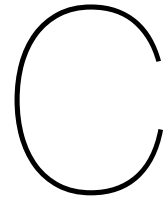


Figure B.13: Overview of the composite floor configurations for all other models. The castellated beams are indicated as IPE300-600 where IPE300 is the original profile and 600 is the height of the castellated beam.

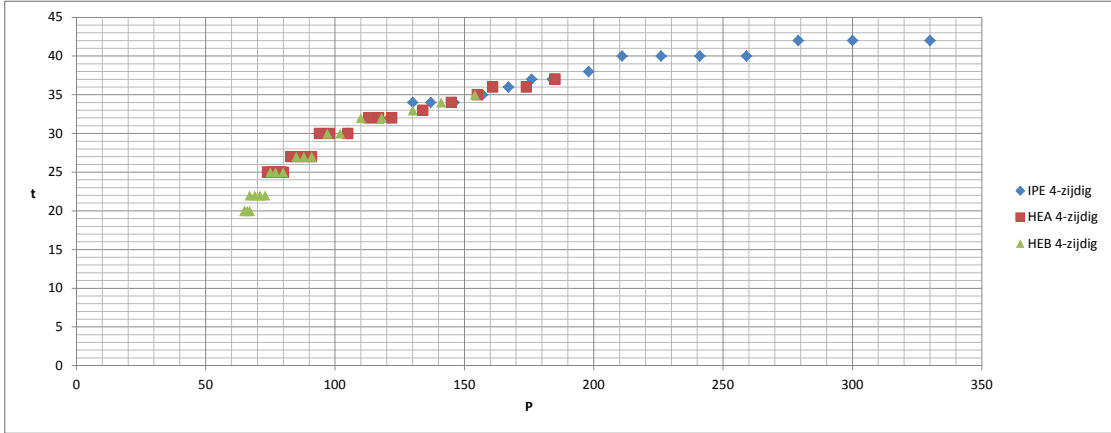


Fire safety design

This appendix contains the tables that were used to determine the required thickness and volume of the fire resistant material PROMATECT-H. Information of IPE, HEA and HEB sections were given by the design guide of the manufacturer[40]. The information for the HEM and HD profiles were retrieved by interpolating those requirements based on the profile factor.

PROMATECT-H KOLOM 530 C 4-ZIJDIG

ρ_{Promatect-h} 870 kg/m³



IPE	profiel nr	h mm	b mm	P 4-zijdig koker	PROMATECT-H mm	B1 mm	B2 mm	V m ³ /m	M kg/m
	80	80	46	330	42	56	174	0,019	16,8
	100	100	55	300	42	65	194	0,022	18,9
	120	120	64	279	42	74	214	0,024	21,0
	140	140	73	259	40	83	230	0,025	21,8
	160	160	82	241	40	92	250	0,027	23,8
	180	180	91	226	40	101	270	0,030	25,8
	200	200	100	211	40	110	290	0,032	27,8
	220	220	110	198	38	120	306	0,032	28,2
	240	240	120	184	37	130	324	0,034	29,2
	270	270	135	176	37	145	354	0,037	32,1
	300	300	150	167	36	160	382	0,039	34,0
	330	330	160	157	35	170	410	0,041	35,3
	360	360	170	146	34	180	438	0,042	36,6
	400	400	180	137	34	190	478	0,045	39,5
	450	450	190	130	34	200	528	0,050	43,1
	500	500	200	121	32	210	574	0,050	43,7
	550	550	210	113	32	220	624	0,054	47,0
	600	600	220	105	30	230	670	0,054	47,0

HEA	profiel nr	h mm	b mm	P 4-zijdig koker	PROMATECT-H mm	B1 mm	B2 mm	V m ³ /m	M kg/m
	100	96	100	185	37	110	180	0,021	18,7
	120	114	120	185	37	130	198	0,024	21,1
	140	133	140	174	36	150	215	0,026	22,9
	160	152	160	161	36	170	234	0,029	25,3
	180	171	180	155	35	190	251	0,031	26,9
	200	190	200	145	34	210	268	0,033	28,3
	220	210	220	134	33	230	286	0,034	29,6
	240	230	240	122	32	250	304	0,035	30,8
	260	250	260	117	32	270	324	0,038	33,1
	280	270	280	113	32	290	344	0,041	35,3
	300	290	300	105	30	310	360	0,040	35,0
	320	310	300	98	30	310	380	0,041	36,0
	340	330	300	94	30	310	400	0,043	37,1
	360	350	300	91	27	310	414	0,039	34,0
	400	390	300	87	27	310	454	0,041	35,9
	450	440	300	83	27	310	504	0,044	38,2
	500	490	300	80	25	310	550	0,043	37,4
	550	540	300	79	25	310	600	0,046	39,6
	600	590	300	79	25	310	650	0,048	41,8
	650	640	300	78	25	310	700	0,051	43,9
	700	690	300	76	25	310	750	0,053	46,1
	800	790	300	76	25	310	850	0,058	50,5
	900	890	300	74	25	310	950	0,063	54,8
	1000	990	300	74	25	310	1050	0,068	59,2

HEB	profiel nr	h mm	b mm	P 4-zijdig koker	PROMATECT-H mm	B1 mm	B2 mm	V m ³ /m	M kg/m
	100	100	100	154	35	110	180	0,020	17,7

120	120	120	141	34	130	198	0,022	19,4
140	140	140	130	33	150	216	0,024	21,0
160	160	160	118	32	170	234	0,026	22,5
180	180	180	110	32	190	254	0,028	24,7
200	200	200	102	30	210	270	0,029	25,1
220	220	220	97	30	230	290	0,031	27,1
240	240	240	91	27	250	304	0,030	26,0
260	260	260	88	27	270	324	0,032	27,9
280	280	280	85	27	290	344	0,034	29,8
300	300	300	80	25	310	360	0,034	29,1
320	320	300	77	25	310	380	0,035	30,0
340	340	300	75	25	310	400	0,036	30,9
360	360	300	73	22	310	414	0,032	27,7
400	400	300	71	22	310	454	0,034	29,2
450	450	300	69	22	310	504	0,036	31,2
500	500	300	67	22	310	554	0,038	33,1
550	550	300	67	20	310	600	0,036	31,7
600	600	300	67	20	310	650	0,038	33,4
650	650	300	66	20	310	700	0,040	35,1
700	700	300	65	20	310	750	0,042	36,9
800	800	300	66	20	310	850	0,046	40,4
900	900	300	65	20	310	950	0,050	43,8
1000	1000	300	65	20	310	1050	0,054	47,3

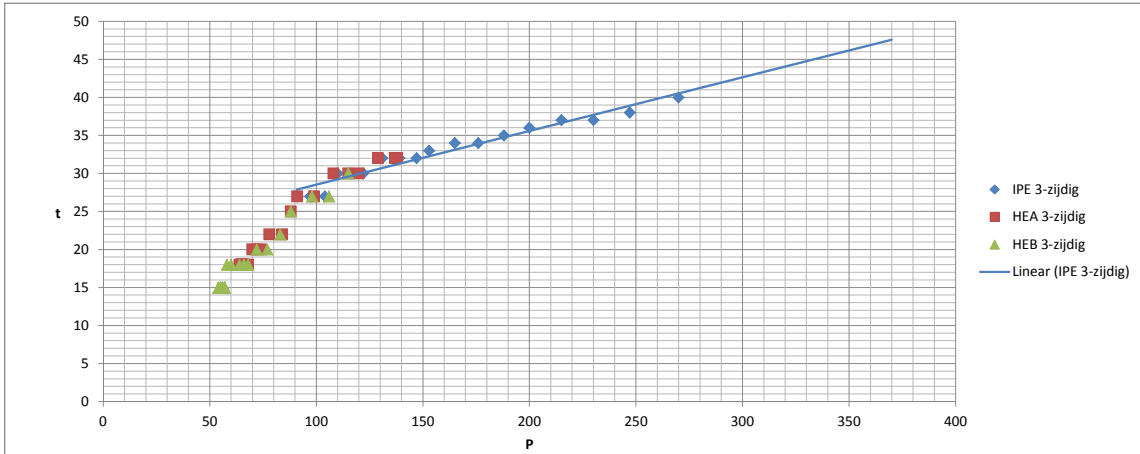
HEM	profiel nr	h mm	b mm	P 4-zijdig koker	PROMATECT-H mm	B1 mm	B2 mm	V m ³ /m	M kg/m
	100	120	106	85	27	116	184	0,01620	14,1
	120	140	126	80	25	136	200	0,01680	14,6
	140	160	146	76	25	156	220	0,01880	16,4
	160	180	166	71	22	176	234	0,01804	15,7
	180	200	186	68	22	196	254	0,01980	17,2
	200	220	206	65	22	216	274	0,02156	18,8
	220	240	226	62	20	236	290	0,02104	18,3
	240	270	248	52	20	258	320	0,02312	20,1
	260	290	268	51	20	278	340	0,02472	21,5
	280	310	288	50	20	298	360	0,02632	22,9
	300	340	310	43	20	320	390	0,02840	24,7
	320	359	309	43	20	319	409	0,02912	25,3
	340	377	309	43	20	319	427	0,02984	26,0
	360	395	308	44	20	318	445	0,03052	26,6
	400	432	307	45	20	317	482	0,03196	27,8
	450	478	307	47	20	317	528	0,03380	29,4
	500	524	306	48	20	316	574	0,03560	31,0
	550	572	306	50	20	316	622	0,03752	32,6
	600	620	305	51	20	315	670	0,03940	34,3
	650	668	305	52	20	315	718	0,04132	35,9
	700	713	304	53	20	314	763	0,04308	37,5
	800	814	303	55	20	313	864	0,04708	41,0
	900	910	302	57	20	312	960	0,05088	44,3
	1000	1008	302	59	20	312	1058	0,05480	47,7

HD 260	profiel nr	A mm ²	h mm	b mm	tw mm	tf mm	O mm	P m-1	PROMATECT-H mm	B1 mm	B2 mm	V m ³ /m	M kg/m
	93	11840	260	260	10,0	17,5	1040	88	27	270	324	0,03208	27,9
	114	14570	268	262	12,5	21,5	1060	73	22	272	322	0,02614	22,7
	142	18030	278	265	15,5	26,5	1086	60	20	275	328	0,02412	21,0
	172	21960	290	268	18,0	32,5	1116	51	20	278	340	0,02472	21,5
	225	28660	309	271	24,0	42,0	1160	40	20	281	359	0,02560	22,3
	299	38050	335	278	31,0	55,0	1226	32	20	288	385	0,02692	23,4
HD 320	profiel nr	A mm ²	h mm	b mm	tw mm	tf mm	O mm	P m-1	PROMATECT-H mm	B1 mm	B2 mm	V m ³ /m	M kg/m
	127	16130	320	300	11,5	20,5	1240	77	25	310	380	0,03450	30,0
	158	20120	330	303	14,5	25,5	1266	63	20	313	380	0,02772	24,1
	198	25230	343	306	18,0	32,0	1298	51	20	316	393	0,02836	24,7
	245	31500	359	309	21,0	40,0	1336	42	20	319	409	0,02912	25,3
	300	38210	375	313	27,0	48,0	1376	36	20	323	425	0,02992	26,0
HD 360	profiel nr	A mm ²	h mm	b mm	tw mm	tf mm	O mm	P m-1	PROMATECT-H mm	B1 mm	B2 mm	V m ³ /m	M kg/m
	179	22830	368	373	15,0	23,9	1482	65	20	383	418	0,03204	27,9
	196	25030	372	374	16,4	26,2	1492	60	20	384	422	0,03224	28,0
HD 400	profiel nr	A mm ²	h mm	b mm	tw mm	tf mm	O mm	P m-1	PROMATECT-H mm	B1 mm	B2 mm	V m ³ /m	M kg/m
	187	23760	368	391	15,0	24,0	1518	64	20	401	418	0,03276	28,5
	216	27550	375	394	17,3	27,7	1538	56	20	404	425	0,03316	28,8
	237	30090	380	395	18,9	30,2	1550	52	20	405	430	0,03340	29,1
	262	33460	387	398	21,1	33,3	1570	47	20	408	437	0,03380	29,4
	287	36630	393	399	22,6	36,6	1584	43	20	409	443	0,03408	29,6

314	39920	399	401	24,9	39,6	1600	40	20	411	449	0,03440	29,9
347	44200	407	404	27,2	43,7	1622	37	20	414	457	0,03484	30,3
382	48710	416	406	29,8	48,0	1644	34	20	416	466	0,03528	30,7
421	53710	425	409	32,8	52,6	1668	31	20	419	475	0,03576	31,1
463	58950	435	412	35,8	57,4	1694	29	20	422	485	0,03628	31,6
509	64900	446	416	39,1	62,7	1724	27	20	426	496	0,03688	32,1
551	70140	455	418	42,0	67,6	1746	25	20	428	505	0,03732	32,5
592	75490	465	421	45,0	72,3	1772	23	20	431	515	0,03784	32,9
634	80800	474	424	47,6	77,1	1796	22	20	434	524	0,03832	33,3
677	86340	483	428	51,2	81,5	1822	21	20	438	533	0,03884	33,8
744	94810	498	432	55,6	88,9	1860	20	20	442	548	0,03960	34,5
818	104330	514	437	60,5	97,0	1902	18	20	447	564	0,04044	35,2
900	114920	531	442	65,9	106,0	1946	17	20	452	581	0,04132	35,9
990	126240	550	448	71,9	115,0	1996	16	20	458	600	0,04232	36,8
1086	138580	569	454	78,0	125,0	2046	15	20	464	619	0,04332	37,7
1202	153050	580	471	95,0	130,0	2102	14	20	481	630	0,04444	38,7
1299	165470	600	476	100,0	140,0	2152	13	20	486	650	0,04544	39,5

PROMATECT-H LIGGER 575 C 3-ZIJDIG

ppromatect-h 870 kg/m³



IPE	profiel	h	b	P 3-zijdig	PROMATECT-H	B1	B2	V	M
	nr	mm	mm	koker	mm	mm	mm	m ³ /m	kg/m
	80	80	46	270	40	125	56	0,012	10,6
	100	100	55	247	38	143	65	0,013	11,6
	120	120	64	230	37	162	74	0,015	12,8
	140	140	73	215	37	182	83	0,017	14,4
	160	160	82	200	36	201	92	0,018	15,5
	180	180	91	188	35	220	101	0,019	16,5
	200	200	100	176	34	239	110	0,020	17,4
	220	220	110	165	34	259	120	0,022	18,9
	240	240	120	153	33	278	130	0,023	19,7
	270	270	135	147	32	307	145	0,024	21,1
	300	300	150	139	32	337	160	0,027	23,2
	330	330	160	131	32	367	170	0,029	25,2
	360	360	170	122	30	395	180	0,029	25,3
	400	400	180	116	30	435	190	0,032	27,7
	450	450	190	110	30	485	200	0,035	30,5
	500	500	200	104	27	532	210	0,034	29,9
	550	550	210	97	27	582	220	0,037	32,5
	600	600	220	91	27	632	230	0,040	35,1

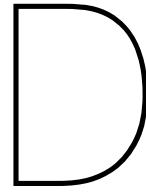
HEA	profiel	h	b	P 3-zijdig	PROMATECT-H	B1	B2	V	M
	nr	mm	mm	koker	mm	mm	mm	m ³ /m	kg/m
	100	96	100	138	32	133	110	0,012	10,5
	120	114	120	137	32	151	130	0,014	12,0
	140	133	140	129	32	170	150	0,016	13,6
	160	152	160	120	30	187	170	0,016	14,2
	180	171	180	115	30	206	190	0,018	15,7
	200	190	200	108	30	225	210	0,020	17,2
	220	210	220	99	27	242	230	0,019	16,8
	240	230	240	91	27	262	250	0,021	18,2
	260	250	260	88	25	280	270	0,021	18,1
	280	270	280	84	22	297	290	0,019	16,9
	300	290	300	78	22	317	310	0,021	18,1
	320	310	300	74	20	335	310	0,020	17,1
	340	330	300	72	20	355	310	0,020	17,7
	360	350	300	70	20	375	310	0,021	18,4
	400	390	300	68	18	413	310	0,020	17,8
	450	440	300	66	18	463	310	0,022	19,4
	500	490	300	65	18	513	310	0,024	20,9
	550	540	300	65	18	563	310	0,026	22,5
	600	590	300	65	18	613	310	0,028	24,1
	650	640	300	65	18	663	310	0,029	25,6
	700	690	300	64	18	713	310	0,031	27,2
	800	790	300	66	18	813	310	0,035	30,3
	900	890	300	65	18	913	310	0,038	33,4
	1000	990	300	66	18	1013	310	0,042	36,6

HEB	profiel nr	h mm	b mm	P 3-zijdig koker	PROMATECT-H mm	B1 mm	B2 mm	V m ³ /m	M kg/m
	100	100	100	115	30	135	110	0,011	9,9
	120	120	120	106	27	152	130	0,012	10,2
	140	140	140	98	27	172	150	0,013	11,6
	160	160	160	88	25	190	170	0,014	12,0
	180	180	180	83	22	207	190	0,013	11,6
	200	200	200	77	20	225	210	0,013	11,5
	220	220	220	72	20	245	230	0,014	12,5
	240	240	240	68	18	263	250	0,014	12,2
	260	260	260	66	18	283	270	0,015	13,1
	280	280	280	64	18	303	290	0,016	14,0
	300	300	300	60	18	323	310	0,017	15,0
	320	320	300	58	18	343	310	0,018	15,6
	340	340	300	57	15	360	310	0,015	13,4
	360	360	300	56	15	380	310	0,016	14,0
	400	400	300	56	15	420	310	0,017	15,0
	450	450	300	55	15	470	310	0,019	16,3
	500	500	300	54	15	520	310	0,020	17,6
	550	550	300	55	15	570	310	0,022	18,9
	600	600	300	56	15	620	310	0,023	20,2
	650	650	300	56	15	670	310	0,025	21,5
	700	700	300	55	15	720	310	0,026	22,8
	800	800	300	57	15	820	310	0,029	25,4
	900	900	300	57	15	920	310	0,032	28,1
	1000	1000	300	57	15	1020	310	0,035	30,7

HEM	profiel nr	h mm	b mm	P 3-zijdig koker	PROMATECT-H mm	B1 mm	B2 mm	V m ³ /m	M kg/m
	100	120	106	65	18	143	116	0,00724	6,3
	120	140	126	61	18	163	136	0,00832	7,2
	140	160	146	58	18	183	156	0,00940	8,2
	160	180	166	54	15	200	176	0,00864	7,5
	180	200	186	52	15	220	196	0,00954	8,3
	200	220	206	49	15	240	216	0,01044	9,1
	220	240	226	47	15	260	236	0,01134	9,9
	240	270	248	39	15	290	258	0,01257	10,9
	260	290	268	39	15	310	278	0,01347	11,7
	280	310	288	38	15	330	298	0,01437	12,5
	300	340	310	33	15	360	320	0,01560	13,6
	320	359	309	33	15	379	319	0,01616	14,1
	340	377	309	34	15	397	319	0,01670	14,5
	360	395	308	34	15	415	318	0,01722	15,0
	400	432	307	36	15	452	317	0,01832	15,9
	450	478	307	38	15	498	317	0,01970	17,1
	500	524	306	39	15	544	316	0,02106	18,3
	550	572	306	41	15	592	316	0,02250	19,6
	600	620	305	42	15	640	315	0,02393	20,8
	650	668	305	44	15	688	315	0,02537	22,1
	700	713	304	45	15	733	314	0,02670	23,2
	800	814	303	48	15	834	313	0,02972	25,9
	900	910	302	50	15	930	312	0,03258	28,3
	1000	1008	302	52	15	1028	312	0,03552	30,9

IPE 180	profiel nr	A1 mm ²	A2 mm ²	h mm	b mm	O mm	P m-1	PROMATECT-H mm	B1 mm	B2 mm	V m ³ /m	M kg/m
	240	2700	2100	240	91	571	238	38	283	101	0,02535	22,1
	270	2900	1900	270	91	631	263	40	315	101	0,02924	25,4
	300	3000	1800	300	91	691	288	42	347	101	0,03339	29,0
	370	3400	1900	370	91	831	314	44	419	101	0,04132	35,9
	420	3700	1900	420	91	931	333	46	471	101	0,04798	41,7
IPE 240	profiel nr	A mm ²	A2 mm ²	h mm	b mm	O mm	P m-1	PROMATECT-H mm	B1 mm	B2 mm	V m ³ /m	M kg/m
	300	4300	3500	300	120	720	185	35	340	130	0,02835	24,7
	360	4700	3200	360	120	840	213	37	402	130	0,03456	30,1
	400	4900	2900	400	120	920	236	38	443	130	0,03861	33,6
	460	5300	3200	460	120	1040	245	38	503	130	0,04317	37,6
	510	5600	3200	510	120	1140	259	40	555	130	0,04960	43,2
IPE 300	profiel nr	A mm ²	A2 mm ²	h mm	b mm	O mm	P m-1	PROMATECT-H mm	B1 mm	B2 mm	V m ³ /m	M kg/m
	375	5900	4800	375	150	900	168	34	414	160	0,03359	29,2
	450	6400	4300	450	150	1050	196	36	491	160	0,04111	35,8
	500	6800	4000	500	150	1150	213	37	542	160	0,04603	40,0

	550	7200	4300	550	150	1250	217	37	592	160	0,04973	43,3
	600	7500	4300	600	150	1350	229	37	642	160	0,05343	46,5
IPE 360	profil nr	A mm ²	A2 mm ²	h mm	b mm	O mm	P m-1	PROMATECT-H mm	B1 mm	B2 mm	V m³/m	M kg/m
	480	8200	6300	480	170	1130	156	34	519	180	0,04141	36,0
	540	8700	5800	540	170	1250	172	34	579	180	0,04549	39,6
	640	9500	5800	640	170	1450	190	36	681	180	0,05551	48,3
	690	9900	5800	690	170	1550	197	36	731	180	0,05911	51,4
	740	10300	5800	740	170	1650	205	37	782	180	0,06453	56,1
HEA 180	profil nr	A mm ²	A2 mm ²	h mm	b mm	O mm	P m-1	PROMATECT-H mm	B1 mm	B2 mm	V m³/m	M kg/m
	215	4800	4300	215	180	610	134	32	252	190	0,02221	19,3
	257	5000	4000	257	180	694	154	33	295	190	0,02574	22,4
	285	5200	3800	285	180	750	167	34	324	190	0,02849	24,8
	357	5600	4000	357	180	894	186	35	397	190	0,03444	30,0
	407	5900	4000	407	180	994	201	36	448	190	0,03910	34,0
HEA 240	profil nr	A mm ²	A2 mm ²	h mm	b mm	O mm	P m-1	PROMATECT-H mm	B1 mm	B2 mm	V m³/m	M kg/m
	290	8100	7200	290	240	820	107	30	325	250	0,02700	23,5
	345	8500	6800	345	240	930	122	30	380	250	0,03030	26,4
	385	8800	6500	385	240	1010	132	32	422	250	0,03501	30,5
	445	9300	6800	445	240	1130	140	32	482	250	0,03885	33,8
	495	9700	6800	495	240	1230	149	33	533	250	0,04343	37,8
HEA 300	profil nr	A mm ²	A2 mm ²	h mm	b mm	O mm	P m-1	PROMATECT-H mm	B1 mm	B2 mm	V m³/m	M kg/m
	390	13200	11700	390	300	1080	87	25	420	310	0,02875	25,0
	465	13800	11000	465	300	1230	99	27	497	310	0,03521	30,6
	520	14300	10500	520	300	1340	108	30	555	310	0,04260	37,1
	565	14700	11000	565	300	1430	111	30	600	310	0,04530	39,4
	615	15200	11000	615	300	1530	117	30	650	310	0,04830	42,0
HEA 360	profil nr	A mm ²	A2 mm ²	h mm	b mm	O mm	P m-1	PROMATECT-H mm	B1 mm	B2 mm	V m³/m	M kg/m
	440	15200	13400	440	300	1180	83	22	467	310	0,02737	23,8
	525	16000	12500	525	300	1350	95	27	557	310	0,03845	33,4
	585	16600	11900	585	300	1470	103	27	617	310	0,04169	36,3
	625	17000	12500	625	300	1550	105	27	657	310	0,04385	38,1
	675	17500	12500	675	300	1650	110	30	710	310	0,05190	45,2
HEA 400	profil nr	A mm ²	A2 mm ²	h mm	b mm	O mm	P m-1	PROMATECT-H mm	B1 mm	B2 mm	V m³/m	M kg/m
	550	19100	16500	550	300	1400	79	22	577	310	0,03221	28,0
	660	20300	15300	660	300	1620	91	27	692	310	0,04574	39,8
	735	21200	14400	735	300	1770	99	27	767	310	0,04979	43,3
	760	21500	15300	760	300	1820	99	27	792	310	0,05114	44,5
	810	22100	15300	810	300	1920	103	27	842	310	0,05384	46,8



Reinforcement design

This appendix contains a more elaborate description of the used methods and formulas to determine the reinforcement in the concrete elements in this thesis. This includes an overview of the used formulas and G.T.B. tables and design graphs.

D.1. Reinforcement design beams

The design of the reinforcement of the beams is based on the approach that can be found in GTB 2013[5]. Table 11.6 from GTB 2013, shown in figure D.1, is used to determine the required amount of reinforcement, based on the factor $M_{Ed}/(bd^2)$, taking into the minimum reinforcement $A_{s,min}$.

$$A_{s,min} = 0.26 * f_{ctm} * b_t * d / f_{yk} \quad (D.1)$$

First the bending moments due to LC1 and LC2 are determined. Bending moments due to wind loads are multiplied by the second order factor and then added to the bending moments due to vertical loads. Then, a distinction is made between positive moments and negative moments. Next, the maximum positive and the maximum negative moments are retrieved. The same holds for the shear forces. Upper reinforcement is designed using the negative moments and the lower reinforcement using the maximum positive moments.

In the case of the diagrid models, a tensile force is present in the diagrid beams due to vertical loading of the inclined elements. The tensile force is distributed over the top and bottom reinforcement in a 50/50 distribution. The extra required reinforcement is added to the required reinforcement due to bending moments.

The beams are split into 2 to 4 categories, depending on the range of the factor $M_{Ed}/(bd^2)$. Based on the chosen values of the factor for the categories, the beams are automatically assigned to the right category. The categorisation of the beams is then mirrored, in order to cope for wind loads in two directions, where the higher category is leading. Next, the amount and size of the bars that will be applied are determined. The focus here is to aim for the lowest amount of steel possible, keeping the bar to bar distance in mind.

At last, it is checked whether the minimum shear reinforcement is satisfactory. The minimum shear reinforcement $\rho_{w,min}$ and maximum distance s_{max} are determined and being compared to the required shear reinforcement, using the following formulas. θ is chosen to be 21.8°.

$$\rho_{w,min} = (0.08 * \sqrt{f_{ck}}) / f_{yk} \quad (D.2)$$

$$s_{max} = \max[300; 0,75 * d(1 + \cot(\alpha))] \quad (D.3)$$

$$A_{s,w/s;min} = \rho_{w,min} * A_c * s_{max} \quad (D.4)$$

$$A_{s,w/s;req} = \frac{V_{Ed}}{z * \cot(\theta) * f_{ywd}} \quad (D.5)$$

A diameter is chosen for the shear reinforcement and s is automatically calculated. The concrete compression zone can then be checked by the following formulas.

$$V_{Rd,max} = b_w * z * v * f_{cd} / (\cot(\theta) + \tan(\theta)) \quad (D.6)$$

$$v = 0.6 * (1 - \frac{f_{ck}}{250}) \quad (D.7)$$

For fire safety reasons, a minimum cover on the rebars is required. This requirement depends on the width of the beam and its support conditions. In table D.1 are the requirements for 120 minutes fire safety shown.

Simply supported beam	b_{min}	200	240	300	500
	a_{min}	65	60	55	50
Continuous beam	b_{min}	200	300	450	500
	a_{min}	45	35	35	30

Table D.1: Requirements to the minimum width and cover of simply supported and continuous beams in mm.

GTB 2010 - 11.6

buiging zonder normaalkracht
bij rechthoekige doorsneden

C35/45 B500



$\frac{M_{Ed}}{b d^2} \text{ (kNm/m}^3\text{)}$	k_s	$100 \rho_1$	k_x	k_z	$\frac{M_{Ed}}{b d^2} \text{ (kNm/m}^3\text{)}$	k_s	$100 \rho_1$	k_x	k_z
100	0,434	0,02	0,006	0,998	4600	0,385	1,20	0,297	0,884
200	0,433	0,05	0,011	0,996	4700	0,383	1,23	0,305	0,882
300	0,432	0,07	0,017	0,993	4800	0,382	1,26	0,312	0,879
400	0,431	0,09	0,023	0,991	4900	0,381	1,29	0,320	0,876
500	0,430	0,12	0,029	0,989	5000	0,379	1,32	0,327	0,873
600	0,429	0,14	0,035	0,986	(0,8)5100	0,378	1,35	0,335	0,870
700	0,428	0,16	0,041	0,984	5200	0,377	1,38	0,343	0,867
800	0,427	0,19	0,047	0,982	5300	0,375	1,41	0,351	0,864
900	0,426	0,21	0,053	0,980	5400	0,374	1,44	0,359	0,861
1000	0,425	0,24	0,058	0,977	5500	0,373	1,48	0,367	0,857
1100	0,424	0,26	0,064	0,975	5600	0,371	1,51	0,375	0,854
1200	0,423	0,28	0,071	0,973	5700	0,370	1,54	0,383	0,851
1300	0,422	0,31	0,077	0,970	5800	0,369	1,57	0,391	0,848
1400	0,421	0,33	0,083	0,968	5900	0,367	1,61	0,399	0,845
1500	0,420	0,36	0,089	0,965	6000	0,366	1,64	0,407	0,842
1600	0,419	0,38	0,095	0,963	6100	0,364	1,67	0,416	0,838
1700	0,418	0,41	0,101	0,961	6200	0,363	1,71	0,424	0,835
1800	0,417	0,43	0,107	0,958	(0,9)6300	0,362	1,74	0,433	0,832
1900	0,416	0,46	0,114	0,956	6400	0,360	1,78	0,442	0,828
2000	0,415	0,48	0,120	0,953	6500	0,359	1,81	0,450	0,825
2100	0,413	0,51	0,126	0,951	6600	0,357	1,85	0,459	0,821
2200	0,412	0,53	0,133	0,948	6700	0,356	1,88	0,468	0,818
2300	0,411	0,56	0,139	0,946	6800	0,354	1,92	0,477	0,814
2400	0,410	0,59	0,145	0,943	6900	0,353	1,96	0,486	0,811
2500	0,409	0,61	0,152	0,941	7000	0,351	1,99	0,495	0,807
2600	0,408	0,64	0,158	0,938	7100	0,349	2,03	0,505	0,804
2700	0,407	0,66	0,165	0,936	7200	0,348	2,07	0,514	0,800
2800	0,406	0,69	0,171	0,933	7300	0,346	2,11	0,524	0,796
2900	0,405	0,72	0,178	0,931	(1,0)7400	0,345	2,15	0,534	0,792
3000	0,404	0,74	0,185	0,928	7500	0,343	2,19	0,543	0,789
3100	0,402	0,77	0,191	0,926	7600	0,341	2,23	0,553	0,785
3200	0,401	0,80	0,198	0,923	7700	0,340	2,27	0,563	0,781
3300	0,400	0,82	0,205	0,920	7800	0,338	2,31	0,574	0,777
3400	0,399	0,85	0,212	0,918	7900	0,336	2,35	0,584	0,773
3500	0,398	0,88	0,219	0,915	8000	0,334	2,39	0,595	0,769
3600	0,397	0,91	0,225	0,912	8100	0,332	2,44	0,605	0,765
(0,7)3700	0,395	0,94	0,232	0,910	8200	0,331	2,48	0,616	0,760
3800	0,394	0,96	0,239	0,907	8205	0,330	2,48	0,617	0,760
3900	0,393	0,99	0,246	0,904					
4000	0,392	1,02	0,254	0,901					
4100	0,391	1,05	0,261	0,899					
4200	0,389	1,08	0,268	0,896					
4300	0,388	1,11	0,275	0,893					
4400	0,387	1,14	0,282	0,890					
4500	0,386	1,17	0,290	0,887					

Figure D.1: Table 11.6 from GTB 2013 for determining the required reinforcement of the concrete beams. A similar table is used for C55/67.

D.2. Reinforcement design columns

The design of the reinforcement in the columns is also based on the approach that can be found in GTB 2013[5]. Here, the amount of required reinforcement depends on two factors: $n = N_{Ed}/(f_{cd} * A_c)$ and $m = M_{Ed}/(f_{cd} * A_c * h)$. Using design graph 10.3.a from GTB 2013 shown in figure D.2, the mechanical reinforcement ratio ψ can be determined. Reinforcement ratio ρ can then be determined by the following formula:

$$\rho = \psi * f_{cd}/f_{yd} \quad (D.8)$$

The moment, shear and normal forces are retrieved from the Karamba model. The moment values are increased by $1/30 * N_{Ed}$ in order to cover for imperfections. Values due to wind loads are multiplied by the second order factor. The values for n and m are calculated for each individual column. The design graph is digitalised into an Excel table and then imported into Grasshopper. Here, the n and m values of the columns are cross-referenced with the values of the table with as result that ψ is automatically determined for each individual column.

The next step is that for each it is determined whether a second order calculation should be performed or not. This is the case when $\lambda > \lambda_{lim}$. This is done by using the following formulas. Here it is assumed that $\varphi_{ef} = 2.0$ so that $l_0 = 0.5 * l$; $A = 1.1$; and $C = 0.7$.

$$\lambda = 3.46 * l_0/h \quad (D.9)$$

$$\lambda_{lim} = 20ABC/\sqrt{n} \quad (D.10)$$

$$A = 1/(1 + 0.2 * \varphi_{ef}) \quad (D.11)$$

$$B = \sqrt{1 + 2\omega} \quad (D.12)$$

$$\omega = \frac{A_s * f_{yd}}{A_c * f_{cd}} \quad (D.13)$$

$$C = 1.7 - r_m \quad (D.14)$$

$$r_m = M_{01}/M_{02} \quad (D.15)$$

The second order eccentricity depends on the second order effect and uneven creep distribution and can be calculated by the following formulas:

$$K_r = \frac{n_u - n}{n_u - n_{bal}} \leq 1 \quad (D.16)$$

$$n_u = 1 + \omega \quad (D.17)$$

$$n_{bal} = 0.4 \quad (D.18)$$

$$K_\varphi = 1 + \beta\varphi_{ef} \geq 1 \quad (D.19)$$

$$\beta = 0.35 + f_{ck}/200 - \lambda/150 \quad (D.20)$$

$$e_2 = 0.1 * (K_r * K_\varphi * f_{yd}) * l_0^2/(0.45 * d * E_s) \quad (D.21)$$

The maximum acting design moment including the second order effect can then be calculated by:

$$M_{0e} = 0.6 * M_{02} + 0.4 * M_{01} \leq 0.4 * M_{02} \quad (D.22)$$

$$M_2 = N_{Ed} * n_2 \quad (D.23)$$

$$M_{Ed} = \max[M_{02}, M_{0e} + M_2, M_{01} + 0.5 * M_2] \quad (D.24)$$

Using the new m value, a new reinforcement ratio ψ can be found. The columns also have to cope with large shear forces. The required shear reinforcement is determined in the same way as the beams.

For fire safety reasons, a minimum cover on the rebars is required. Additionally, a minimum of 8 rebars is required. In table D.2 the requirements for 120 minutes fire safety are shown.

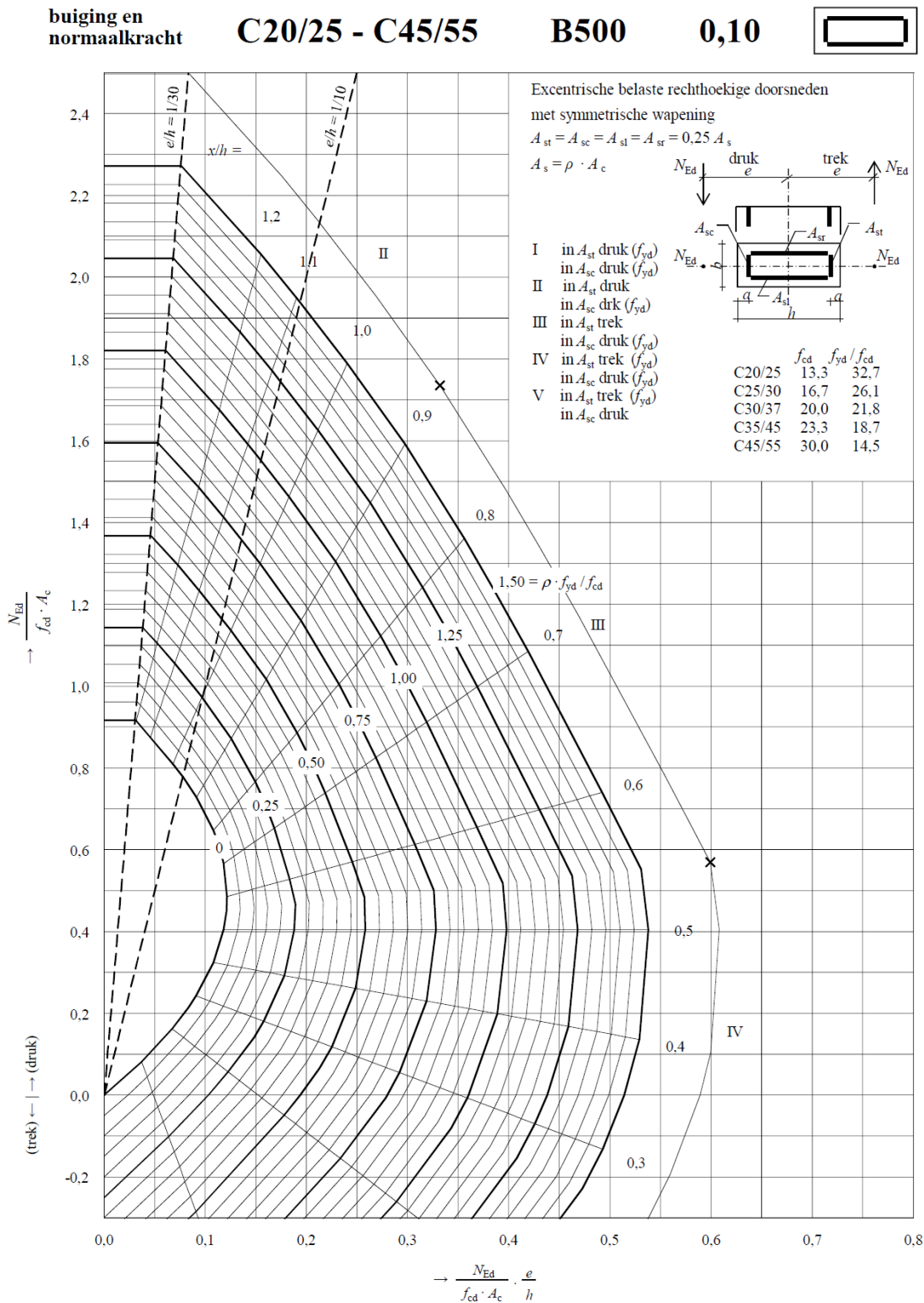


Figure D.2: Design graph 103.a from GTB 2013 for determining the required reinforcement of the concrete columns. A similar design graph is used for C55/67.

b_{min}	350	450
a_{min}	57	51

Table D.2: Requirements to the minimum width and cover of columns for fire safety in mm.

D.3. Reinforcement design core

The design of the reinforcement of the core is approached by splitting the core walls into two categories when subjected to lateral loading. The front and back wall are subjected to pure compression and tension forces due to the acting bending moment on the core. The side walls are subjected to pure shear due to the shear forces on the core. This approach is also generally applied in steel beam cross-sections. A graphic representation of this approach is shown in figure D.3.

There are no requirements regarding the minimum amount of vertical and horizontal reinforcement according to the Eurocode. However, due to practical reasons a minimum reinforcement net of Ø8-150/250 is present, where 150 mm is the spacing for vertical reinforcement and 250 mm the spacing for horizontal reinforcement. Reinforcement is placed at the two sides of the walls with a minimum cover of 35 mm for fire safety reasons.

For the determination of the vertical reinforcement, also normal forces due to vertical loads are taken into account. LC3 is considered in this case as this load case results in the highest amount of tensile stress in the core. Considered is a one meter wide strip of the core wall, only subjected to normal forces. Forces are retrieved from the Karamba model and a n value is calculated for every story. Then, a ψ value is calculated, using the column approach explained in the previous section. This ψ value is used to determine the required reinforcement, which is then exported to an Excel file where the applied vertical reinforcement is determined.

The determination of the horizontal reinforcement approaches the side walls as beams. The required shear reinforcement is determined using the same formula as is used with the beams. Here z is taken as the centre to centre distance of the front and back wall, which are subjected to normal forces. $A_{s,w}/s_{req}$ is also exported to the Excel file where the applied horizontal reinforcement is also determined.

$$A_{s,w}/s_{req} = \frac{V_{Ed}}{z * \cot(\theta) * f_{ywd}} \quad (D.25)$$

The Excel file is shown in figures D.4 and D.5. Automatic checks to check the applied reinforcement are incorporated. Furthermore, material quantities are also automatically determined when reinforcement is applied.

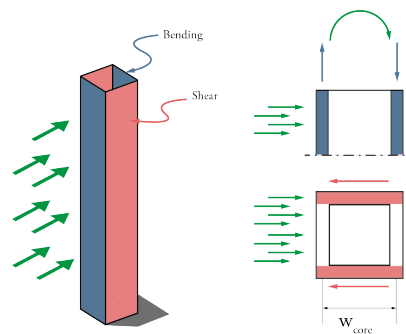


Figure D.3: Sketch showing the way of modelling for designing the reinforcement of the core.

150M_3.TUBE_PF_10cl_f11

Cross-section [-]	W [mm]	t [mm]	k [-]	Wouter [mm]	Winner [mm]	A [mm ²]	I [mm ²]
CoreA	12000	650	1,129	12650	11350	31200000	7,50997E+14
CoreB	12000	330	1,129	12330	11670	15840000	3,80447E+14
CoreC	12000	300	1,129	12300	11700	14400000	3,45816E+14
CoreD	12000	0	1,129	12000	12000	0	0
CoreE	12000	0	1,129	12000	12000	0	0

fck 35,00 N/mm2
 fcd 23,33 N/mm2
 fyd 435 N/mm2

H 3,800 m

Vconcrete 3067,56 m3
 Vs rebar 22,30 m3
 MEAN 57,1 kg/m3

Spacing [mm]	Bars/meter	Total area per Diameter [mm ²]
100	10,00	282,74
150	6,67	188,50
200	5,00	141,37
250	4,00	113,10
300	3,33	94,25
350	2,86	80,78

Diameter [mm]	Total area [mm ²]	number of bars
6	28,27	56,55
8	50,27	100,53
10	78,54	157,08
12	113,10	226,19
16	201,06	402,12
20	314,16	628,32
25	490,87	981,75
32	804,25	1608,50

Wall [-]	As:req [mm ² /m]	As:req:1side [mm ² /m]	A bnet [mm ² /m]	A vert [mm ² /m]	A extra req [mm ² /m]	A extra [mm ² /m]	As vert total [mm ² /m]	Check [-]	Asw/s [mm ² /mm]	Asw/s:1side [mm ² /m]	A net hor [mm ² /m]
1	8716	4358,00	502,65	2010,62	1844,73	2010,62	4523,89	1	0.543486	271,74	335,10
2	8716	4358,00	502,65	2010,62	1844,73	2010,62	4523,89	1	0.532414	266,21	335,10
3	6973	3486,50	502,65	2010,62	973,23	1130,97	3644,25	1	0.515366	257,68	335,10
4	6973	3486,50	502,65	2010,62	973,23	1130,97	3644,25	1	0.498279	249,14	335,10
5	6973	3486,50	502,65	2010,62	973,23	1130,97	3644,25	1	0.481213	240,62	335,10
6	5229	2614,50	502,65	2010,62	101,23	141,37	2654,65	1	0.464679	232,34	335,10
7	5229	2614,50	502,65	2010,62	101,23	141,37	2654,65	1	0.448704	224,35	335,10
8	5229	2614,50	502,65	2010,62	101,23	141,37	2654,65	1	0.433264	216,63	335,10
9	3486	1743,00	502,65	1130,97	109,37	141,37	1775,00	1	0.417978	208,99	335,10
10	3486	1743,00	502,65	1130,97	109,37	141,37	1775,00	1	0.402768	201,38	335,10
11	3486	1743,00	502,65	1130,97	109,37	141,37	1775,00	1	0.387827	193,91	335,10
12	3486	1743,00	502,65	1130,97	109,37	141,37	1775,00	1	0.373077	186,54	335,10
13	3486	1743,00	502,65	1130,97	109,37	141,37	1775,00	1	0.359515	179,76	335,10
14	1770	885,00	502,65	502,65	-120,31	0,00	1005,31	1	0.347561	173,78	335,10
15	1770	885,00	502,65	502,65	-120,31	0,00	1005,31	1	0.331279	165,64	335,10
16	885	442,50	502,65	0,00	-60,15	0,00	502,65	1	0.313886	156,94	335,10
17	885	442,50	502,65	0,00	-60,15	0,00	502,65	1	0.296569	148,28	335,10
18	885	442,50	502,65	0,00	-60,15	0,00	502,65	1	0.279482	139,74	335,10
19	0	0,00	335,10	0,00	-335,10	0,00	335,10	1	0.262663	131,33	335,10
20	0	0,00	335,10	0,00	-335,10	0,00	335,10	1	0.246113	123,06	335,10
21	0	0,00	335,10	0,00	-335,10	0,00	335,10	1	0.22983	114,92	335,10
22	0	0,00	335,10	0,00	-335,10	0,00	335,10	1	0.213778	106,89	335,10
23	0	0,00	335,10	0,00	-335,10	0,00	335,10	1	0.197955	98,98	335,10
24	0	0,00	335,10	0,00	-335,10	0,00	335,10	1	0.182554	91,28	335,10
25	0	0,00	335,10	0,00	-335,10	0,00	335,10	1	0.168111	84,06	335,10
26	0	0,00	335,10	0,00	-335,10	0,00	335,10	1	0.155276	77,64	335,10
27	0	0,00	335,10	0,00	-335,10	0,00	335,10	1	0.154625	77,31	335,10
28	0	0,00	335,10	0,00	-335,10	0,00	335,10	1	0.141752	70,88	335,10
29	0	0,00	335,10	0,00	-335,10	0,00	335,10	1	0.127386	63,69	335,10
30	0	0,00	335,10	0,00	-335,10	0,00	335,10	1	0.112329	56,16	335,10
31	0	0,00	335,10	0,00	-335,10	0,00	335,10	1	0.097043	48,52	335,10
32	0	0,00	335,10	0,00	-335,10	0,00	335,10	1	0.08168	40,84	335,10
33	0	0,00	335,10	0,00	-335,10	0,00	335,10	1	0.06624	33,12	335,10
34	0	0,00	335,10	0,00	-335,10	0,00	335,10	1	0.049843	24,92	335,10
35	0	0,00	335,10	0,00	-335,10	0,00	335,10	1	0,0	0,00	335,10
36	0	0,00	335,10	0,00	-335,10	0,00	335,10	1	0,0	0,00	335,10
37	0	0,00	335,10	0,00	-335,10	0,00	335,10	1	0,0	0,00	335,10
38	0	0,00	335,10	0,00	-335,10	0,00	335,10	1	0,0	0,00	335,10
39	0	0,00	335,10	0,00	-335,10	0,00	335,10	1	0,0	0,00	335,10
40	0	0,00	335,10	0,00	-335,10	1,00	336,10	1	0.035668	17,83	335,10

Figure D.4: The left side of the spreadsheet that is used to determine the applied reinforcement of the core.

meter width [mm2/m]			
8	10	12	16
502,65	785,40	1130,97	2010,62
335,10	523,60	753,98	1340,41
251,33	392,70	565,49	1005,31
201,06	314,16	452,39	804,25
167,55	261,80	376,99	670,21
143,62	224,40	323,14	574,46

3	4	5	6	7	8	9	10	11	12	13	14	15
84,82	113,10	141,37	169,65	197,92	226,19	254,47	282,74	311,02	339,29	367,57	395,84	424,12
150,80	201,06	251,33	301,59	351,86	402,12	452,39	502,65	552,92	603,19	653,45	703,72	753,98
235,62	314,16	392,70	471,24	549,78	628,32	706,86	785,40	863,94	942,48	1021,02	1099,56	1178,10
339,29	452,39	565,49	678,58	791,68	904,78	1017,88	1130,97	1244,07	1357,17	1470,27	1583,36	1696,46
603,19	804,25	1005,31	1206,37	1407,43	1608,50	1809,56	2010,62	2211,68	2412,74	2613,81	2814,87	3015,93
942,48	1256,64	1570,80	1884,96	2199,11	2513,27	2827,43	3141,59	3455,75	3769,91	4084,07	4398,23	4712,39
1472,62	1963,50	2454,37	2945,24	3436,12	3926,99	4417,86	4908,74	5399,61	5890,49	6381,36	6872,23	7363,11
2412,74	3216,99	4021,24	4825,49	5629,73	6433,98	7238,23	8042,48	8846,72	9650,97	10455,22	11259,47	12063,72

A extra req [mm2/m]	A extra [mm2/m]	As hor total [mm2/m]	Check [-]	As vert total [mm2/m]	rho vert [-]	Vs vert [m3]	As hor total [mm2/m]	rho hor [-]	Vs hor [m3]	Vconcrete [m3]	[kg/m3]
-63,36	0,00	335,10	1	9047,79	0,0139	1,65	670,21	0,0010	0,12	116,79	119,1
-68,90	0,00	335,10	1	9047,79	0,0139	1,65	670,21	0,0010	0,12	116,79	119,1
-77,42	0,00	335,10	1	7288,49	0,0112	1,33	670,21	0,0010	0,12	117,11	97,3
-85,96	0,00	335,10	1	7288,49	0,0112	1,33	670,21	0,0010	0,12	117,11	97,3
-94,49	0,00	335,10	1	7288,49	0,0112	1,33	670,21	0,0010	0,12	117,11	97,3
-102,76	0,00	335,10	1	5309,29	0,0082	0,97	670,21	0,0010	0,12	117,47	72,9
-110,75	0,00	335,10	1	5309,29	0,0082	0,97	670,21	0,0010	0,12	117,47	72,9
-118,47	0,00	335,10	1	5309,29	0,0082	0,97	670,21	0,0010	0,12	117,47	72,9
-126,11	0,00	335,10	1	3550,00	0,0055	0,65	670,21	0,0010	0,12	117,79	51,3
-133,72	0,00	335,10	1	3550,00	0,0055	0,65	670,21	0,0010	0,12	117,79	51,3
-141,19	0,00	335,10	1	3550,00	0,0055	0,65	670,21	0,0010	0,12	117,79	51,3
-148,56	0,00	335,10	1	3550,00	0,0055	0,65	670,21	0,0010	0,12	117,79	51,3
-155,35	0,00	335,10	1	3550,00	0,0055	0,65	670,21	0,0010	0,12	117,79	51,3
-161,32	0,00	335,10	1	2010,62	0,0061	0,37	670,21	0,0020	0,12	59,70	64,3
-169,46	0,00	335,10	1	2010,62	0,0061	0,37	670,21	0,0020	0,12	59,70	64,3
-178,16	0,00	335,10	1	1005,31	0,0030	0,18	670,21	0,0020	0,12	59,89	40,1
-186,82	0,00	335,10	1	1005,31	0,0030	0,18	670,21	0,0020	0,12	59,89	40,1
-195,36	0,00	335,10	1	1005,31	0,0030	0,18	670,21	0,0020	0,12	59,89	40,1
-203,77	0,00	335,10	1	670,21	0,0020	0,12	670,21	0,0020	0,12	59,95	32,0
-212,05	0,00	335,10	1	670,21	0,0020	0,12	670,21	0,0020	0,12	59,95	32,0
-220,19	0,00	335,10	1	670,21	0,0020	0,12	670,21	0,0020	0,12	59,95	32,0
-228,21	0,00	335,10	1	670,21	0,0020	0,12	670,21	0,0020	0,12	59,95	32,0
-236,13	0,00	335,10	1	670,21	0,0020	0,12	670,21	0,0020	0,12	59,95	32,0
-243,83	0,00	335,10	1	670,21	0,0020	0,12	670,21	0,0020	0,12	59,95	32,0
-251,05	0,00	335,10	1	670,21	0,0020	0,12	670,21	0,0020	0,12	59,95	32,0
-257,47	0,00	335,10	1	670,21	0,0020	0,12	670,21	0,0020	0,12	59,95	32,0
-264,23	0,00	335,10	1	670,21	0,0022	0,12	670,21	0,0022	0,12	54,48	35,2
-271,41	0,00	335,10	1	670,21	0,0022	0,12	670,21	0,0022	0,12	54,48	35,2
-278,94	0,00	335,10	1	670,21	0,0022	0,12	670,21	0,0022	0,12	54,48	35,2
-286,58	0,00	335,10	1	670,21	0,0022	0,12	670,21	0,0022	0,12	54,48	35,2
-294,26	0,00	335,10	1	670,21	0,0022	0,12	670,21	0,0022	0,12	54,48	35,2
-301,98	0,00	335,10	1	670,21	0,0022	0,12	670,21	0,0022	0,12	54,48	35,2
-310,18	0,00	335,10	1	670,21	0,0022	0,12	670,21	0,0022	0,12	54,48	35,2
-335,10	0,00	335,10	1	670,21	0,0022	0,12	670,21	0,0022	0,12	54,48	35,2
-335,10	0,00	335,10	1	670,21	0,0022	0,12	670,21	0,0022	0,12	54,48	35,2
-335,10	0,00	335,10	1	670,21	0,0022	0,12	670,21	0,0022	0,12	54,48	35,2
-335,10	0,00	335,10	1	670,21	0,0022	0,12	670,21	0,0022	0,12	54,48	35,2
-335,10	0,00	335,10	1	670,21	0,0022	0,12	670,21	0,0022	0,12	54,48	35,2
-317,27	1,00	336,10	1	672,21	0,0022	0,12	672,21	0,0022	0,12	54,47	35,3

Figure D.5: The right side of the spreadsheet that is used to determine the applied reinforcement of the core.

D.4. Data visualisation

The determination of the required reinforcement for the columns, beams and core all happens within the Grasshopper environment. Therefore, data can be visualised, meaning that it can be shown what reinforcement ratios are required in certain elements. This is shown in figure D.6. The reasoning behind the required beam reinforcement is discussed in appendix E. For the columns, reinforcement is largely defined by the minimum required reinforcement due to big cross-sections that are required for stiffness. Reinforcement is needed when normal forces decrease resulting in relatively high moments.

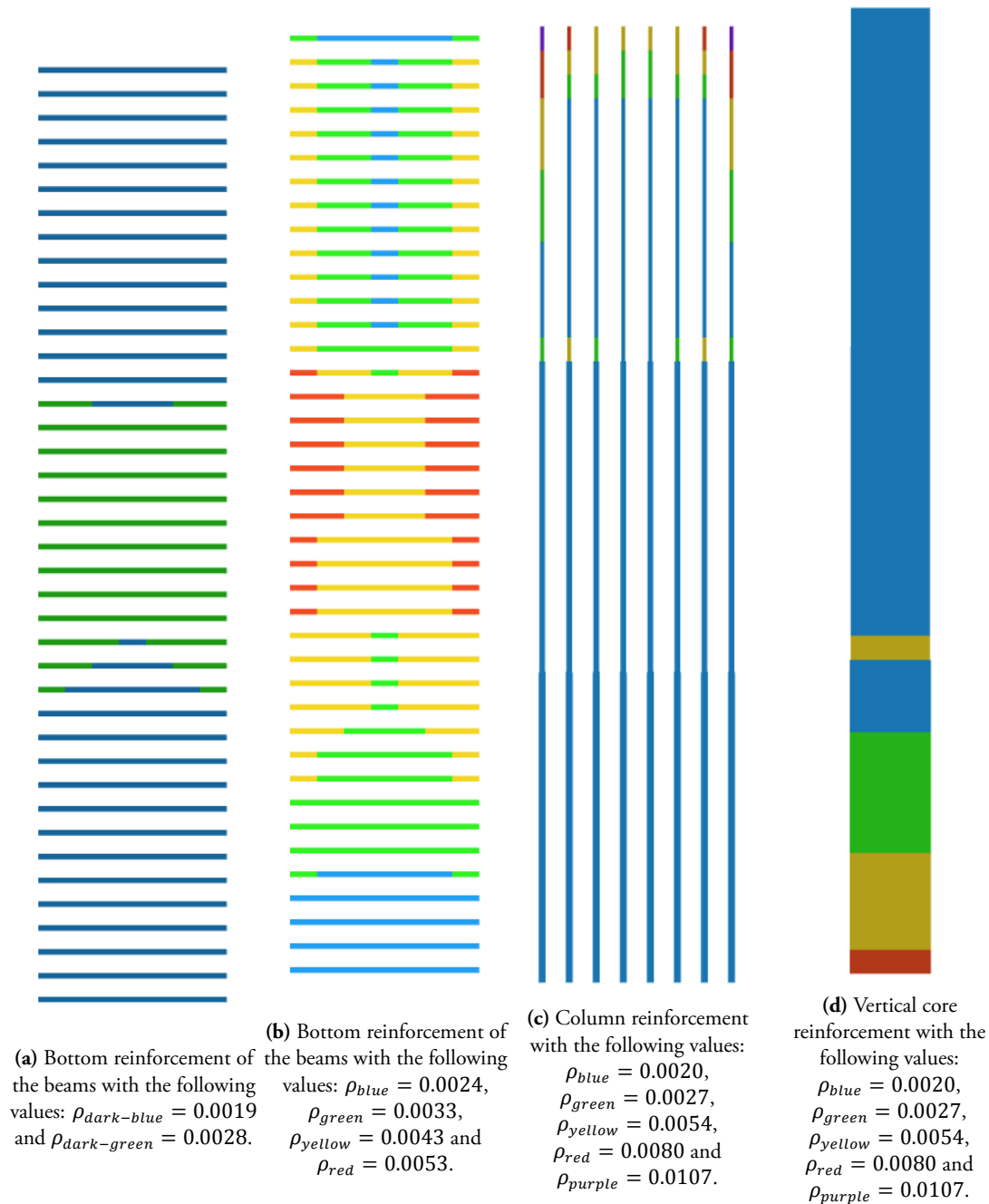
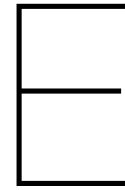


Figure D.6: Visual representation of the required reinforcement in concrete elements for a 150-meter frame model.



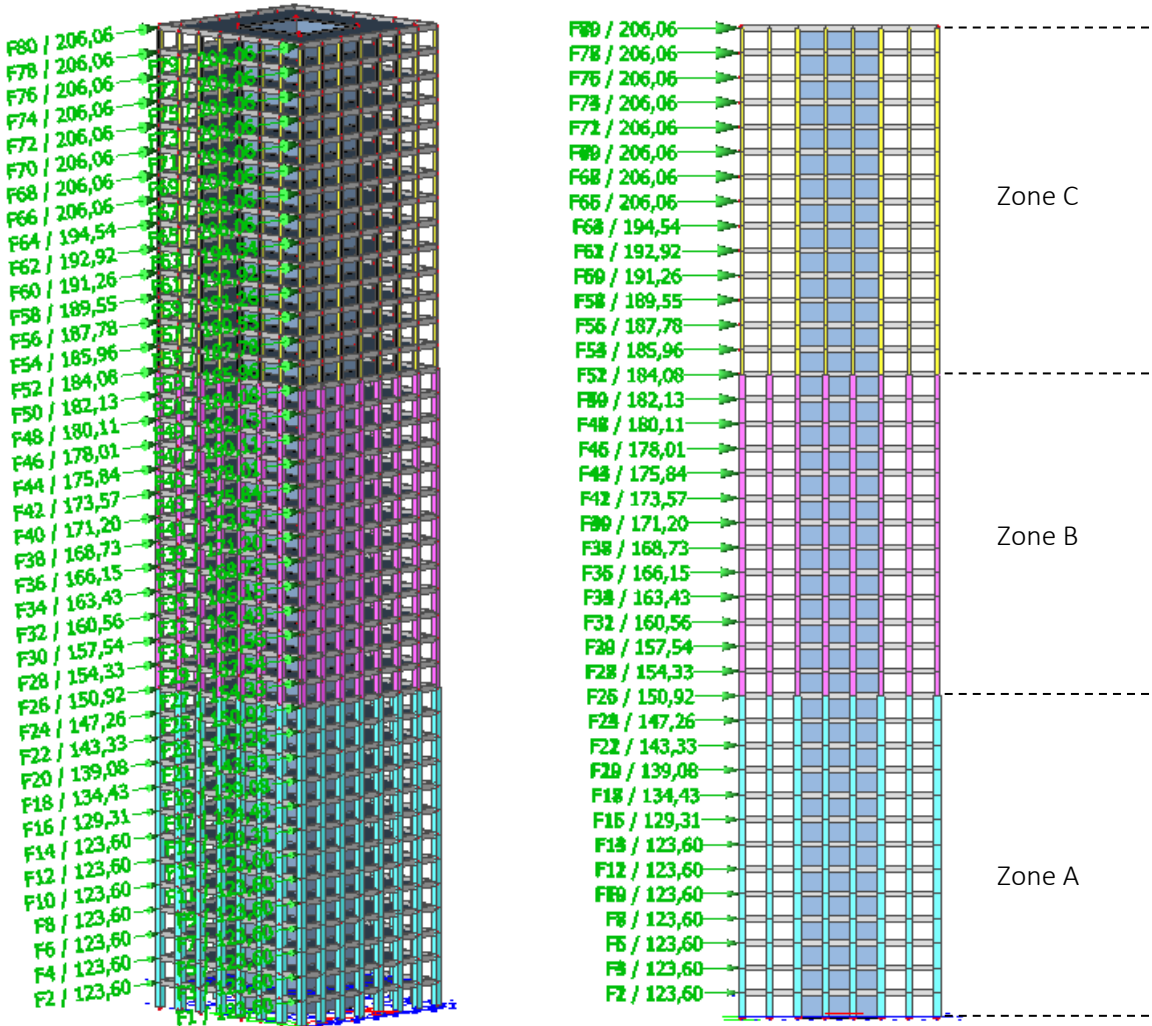
Frame and tube behaviour

This appendix elaborates on the behaviour of the frame and tube structural systems combined with the core. The core primarily acts as a bending beam and the frame/tube structure as shear beam, this results in interaction forces which cause a particular moment distribution. Important to note here is that when moving to more detailed design stages, the core would move more towards shear beam behaviour due to openings in the core which could lead slightly different moment distributions. However, due to the 2-dimensional models in this thesis, this behaviour could not be simulated and therefore it was decided to stick to the behaviour explained in this appendix.

FRAME AND TUBE MODEL BEHAVIOUR - G.J. Lankhorst - 20-01-18

This document elaborates on the behaviour of the frame and tube models that are used. The purpose is to explain the behaviour of the structural system as a whole; and local bending moments in the beams and columns, due to lateral wind loads.

The frame and tube models both consist of a core, acting as a bending beam, and a shear frame, acting as a shear beam. The used model for this purpose is a 40 storey building of 152 meter in height and 30 by 30 meter in width and depth. The core dimensions are 12 by 12 meter and there are 8 columns placed at each façade. The model is showed in the figures down below.



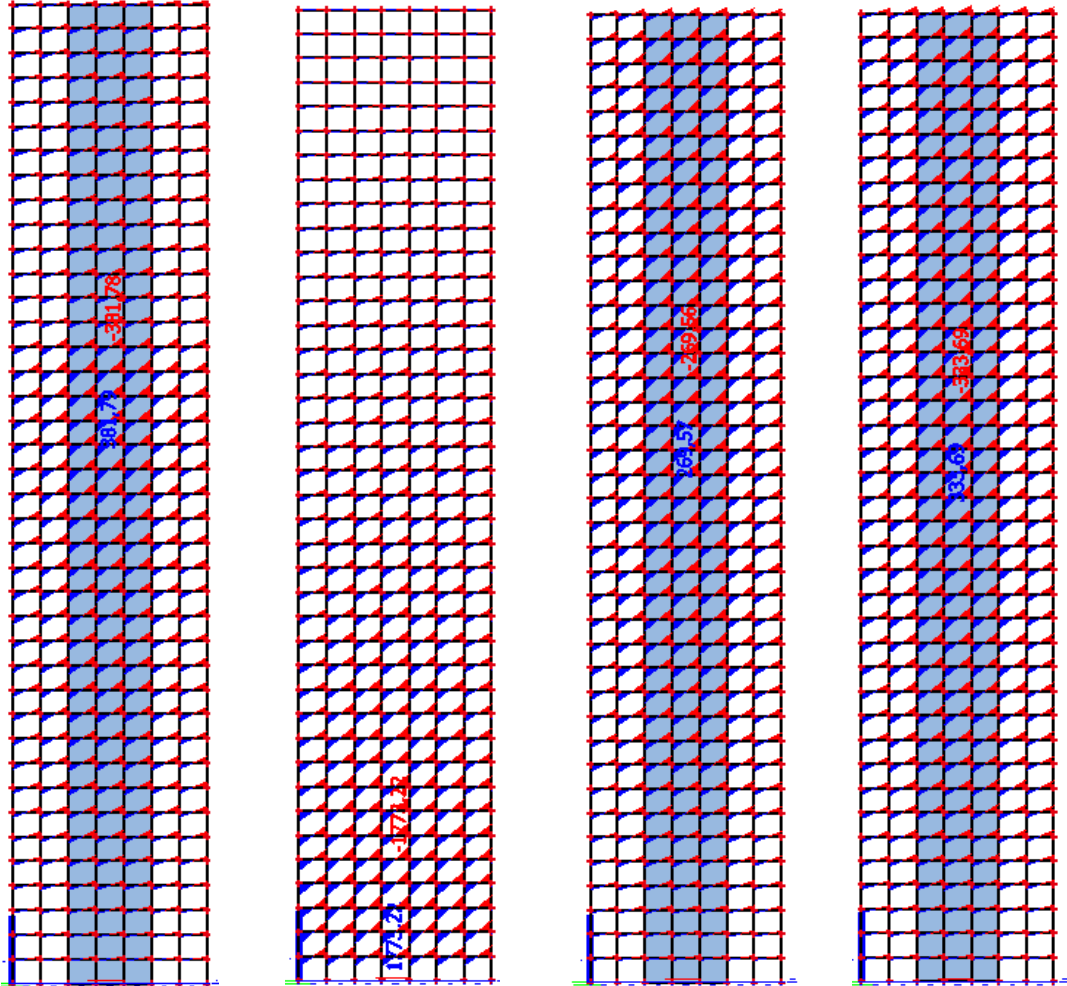
ORIGINAL MODEL	Dimensions [mm]	Thickness [mm]	Material	E-modulus [N/mm ²]
Column zone A	1100 x 1100	-	C35/45	11.000
Column zone B	900 x 900	-	C35/45	11.000
Column zone C	600 x 600	-	C35/45	11.000
Core wall zone A	12000 x 12000	680	C35/45	34.000
Core wall zone B	12000 x 12000	380	C35/45	34.000
Core wall zone C	12000 x 12000	300	C35/45	34.000
Beam	900 x 500	-	C35/45	11.000

The wind loads are calculated according to the Eurocode and placed on the corner columns of the loaded façade. The floors act as rigid diaphragms and distribute the lateral load over the façade columns and core. The thickness of the floors in this model is reduced by a factor of 1/10 while the E-modulus is increased by a factor of 10. In this way, the EA properties of the floors are not compromised while the bending stiffness is greatly reduced and therefore do not contribute to the overall stiffness of the building.

In order to explain the behaviour of the model, 3 other slightly different models in addition to the original model were evaluated:

- Model 1: **original model** with varying core wall thicknesses and varying column cross sections
- Model 2: model without core and equal column cross sections (900 x 900 mm)
- Model 3: model with equal core wall thickness (680 mm) and equal column cross sections
- Model 4: model with original core wall thicknesses and equal column cross sections
- Model 5: model with varying core wall thicknesses and without any rigid frame

In the figures underneath, the bending moments in the beams are shown due to lateral wind loads.



Model 1 (original)
Varying thickness core
Varying column dim

Model 2
No core
Equal column dim

Model 3
Equal thickness core
Equal column dim

Model 4
Varying thickness core
Equal column dim

Lateral loads

Model 2 & model 3

It can clearly be seen in *Model 2* that the system without core behaves as a pure shear beam. *Model 3* consists of both a core and a shear frame. The two systems want to deform differently from each other, but are restricted to undergo the same deformation. This is illustrated in the figure underneath (Ali & Moon, 2007). The upper part of the core is restrained by the rigid frame, while the lower part of the rigid frame is restrained by the core.

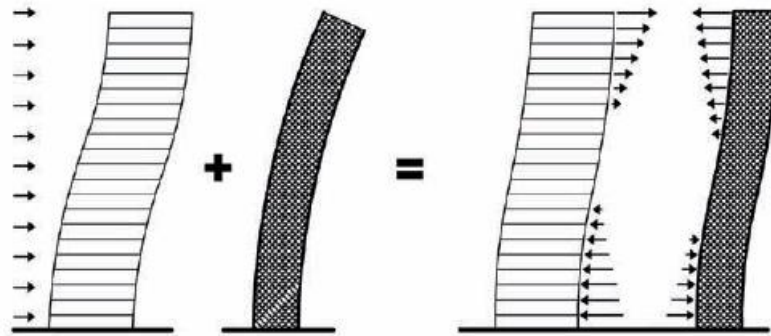


Figure 5: Shear wall (or shear truss)-frame interaction system.

The core is more dominant in the global stiffness in the lower storeys of the building; therefore bending moments due to wind loads are almost not present in the beams here. The rigid frame needs a bigger deflection than the core to be 'activated'.

The mid area of the building is where the rigid frame is more dominant in the global stiffness of the building. The bending moments in the beams increase gradually when the height increases. The maximum bending moments can be found just below 2/3 of the height of the building.

The upper part of the building is where core is restrained by the rigid frame, resulting in interaction forces. This causes additional bending moments in the rigid frame, which can be seen in the figure. The bending moments in the beams gradually decrease while the height increases.

Model 4

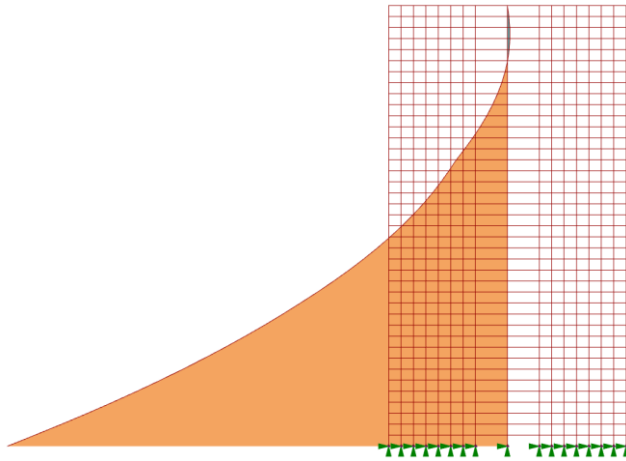
Model 4 shows the model with varying core thicknesses. There is almost no difference in moment distribution in the beams compared to *model 3*. This shows that the upper core walls have less influence on the global stiffness of the building.

Model 1 (original)

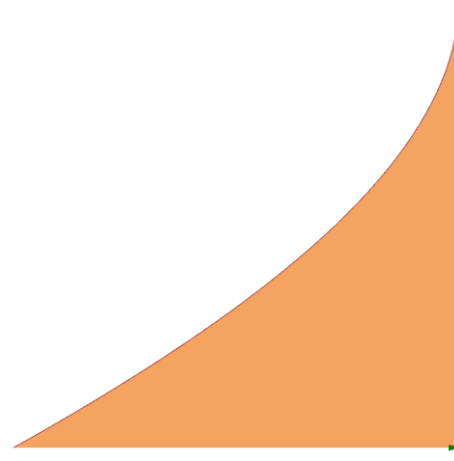
When considering the original model, *model 1*, a jump can be seen in the bending moments in the beams at 2/3 of the height. The only change, in comparison with *model 4*, is the varying cross sections for the columns. The dimensions of the columns in zone B are 900 x 900 mm, while the dimensions of the columns in zone C are 600 x 600 mm. This results in a less stiff frame at the top of the building, resulting in lower bending moments in the upper part of the rigid frame.

Bending moments core model 1 (original) and model 5

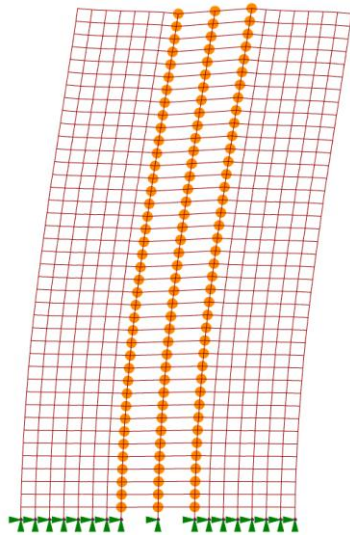
When looking at the bending moment diagram of the core of *model 1* (original) and *model 5* page 4, it can be seen that the bending moment at the bottom of the core is reduced by adding the rigid frame. Additionally, at the top a negative moment occurs due to the rigid frame that is restraining the core.



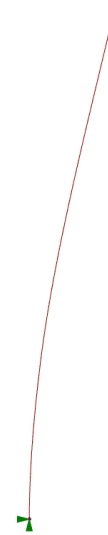
Maximum bending moment core model 1
886.333 kNm



Maximum bending moment core model 5
1.147.988 kNm



Maximum deformation model 1
214 mm



Maximum deformation model 5
313 mm

Vertical loads

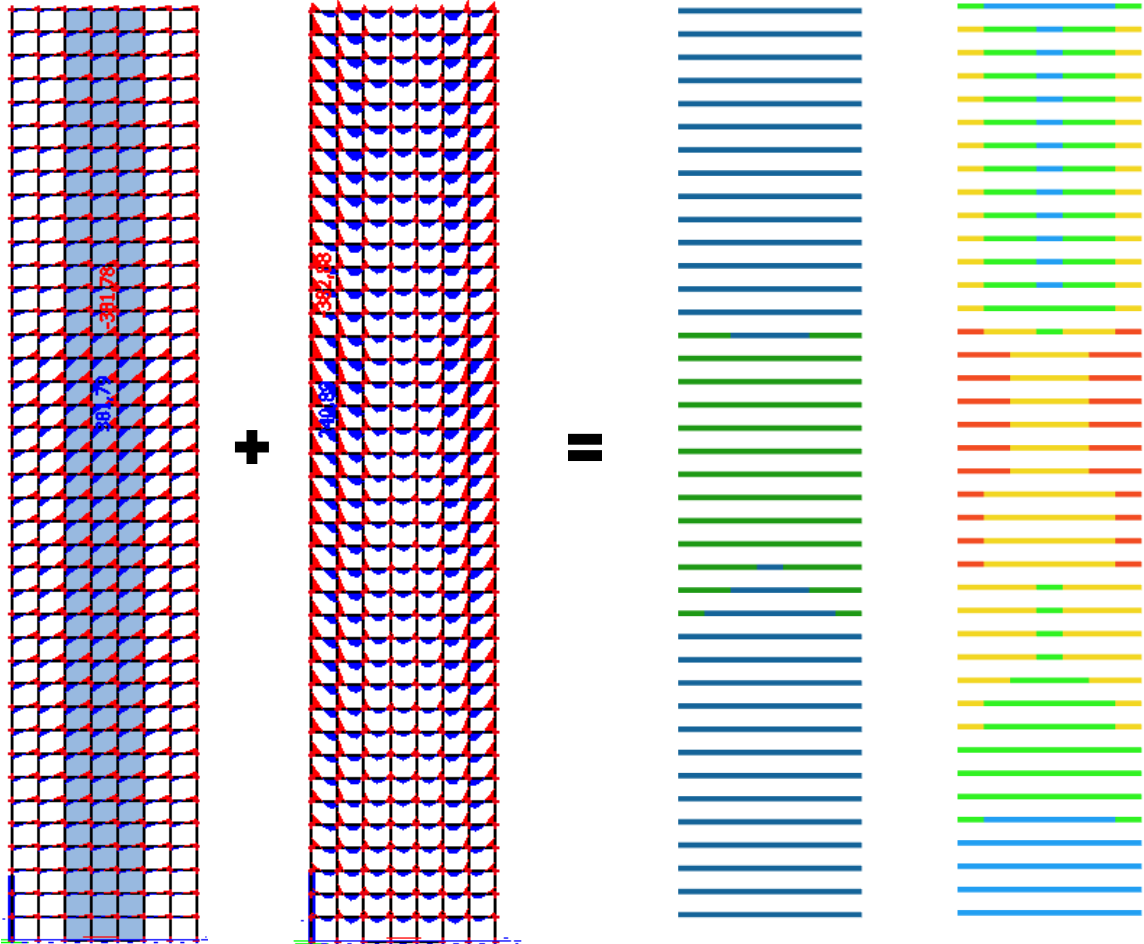
Additionally to the bending moments due to *lateral wind loading*, also bending moments due to *area loads* on the floors occur. However, due to unequal distribution of the floor load over the columns, differences in normal forces will be present. This causes differential settlements between the columns, because the cross sections are the same over the storey. This results that the middle columns want to ‘hang’ on the corner columns which then results in a change in bending moment diagrams of the beams. This effect gradually increases towards the top of the building where the differential settlements also increase. In the figure underneath, the bending moments in the beams due to vertical area loads are shown.

To retrieve the design moments for the beam, the bending moments due to *vertical loads* are added to the bending moments due to *lateral loads*. When considering the fact that the cross sections of the beams are the same over the height of the building, the required reinforcement will follow the same pattern as the final bending moment ($M_{\text{final}} = M_{\text{wind}} + M_{\text{vertical}}$).

The considered load cases that are used are listed below. From these load cases, the maximum field and support moment per beam are retrieved and used for the determination of the reinforcement.

- LC1: $1,32 * G + \Psi_{0,o} * 1,65 * Q_o + 1,65 * Q_w$
- LC2: $1,49 * G + \Psi_{0,o} * 1,65 * Q_o$
- LC3: $0,90 * G + 1,65 * Q_w$

The required reinforcement is generally higher in the mid height region of the building. This follows from the bending moments due to wind loads. In addition, the required reinforcement increases when considering the corners of the buildings in comparison with the mid area of the building. This follows from the ‘hanging’ effect of the middle columns on the corner columns due to vertical area loads. The required bottom reinforcement is generally less than the required top reinforcement, because the maximum field moments due to vertical area loads are generally lower than the maximum support moments.



Bending moments due to wind load

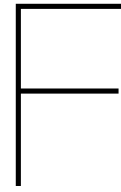
Bending moments due to vertical area load

Required bottom reinforcement

Required top reinforcement

$\rho_{blue} = 0,0019$
 $\rho_{green} = 0,0028$

$\rho_{blue} = 0,0024$
 $\rho_{green} = 0,0033$
 $\rho_{yellow} = 0,0043$
 $\rho_{red} = 0,0053$



Validation of calculation models

Due to time limitations and a high amount of models, it was chosen to perform 2-dimensional frame calculations. This appendix elaborates on the validation of these models with 3-dimensional analysis models in verified structural analysis software.

In this thesis it was chosen to perform structural analyses with 2-dimensional models instead of 3-dimensional models. This decision was made based on the fact that calculation time and complexity could significantly be reduced, enabling to create and analyse a high number of parametric models. Moreover, since a square floor-plan was chosen and geometry was kept simple and repetitive, 2-dimensional models could represent the 3-dimensional behaviour quite closely.

The 2-dimensional models of the stability systems were retrieved from a reader from Delft University of Technology (TU Delft) by Terwel and Ham[22]. Here, models for the rigid frame, tube, outrigger and braced tube were found, excluding core. The 2-dimensional model for the diagrid was developed by the author, based on the tube model. All of these models are combined with the core, which leads to a combined behaviour, as is explained for the frame and tube models in appendix E.

It was chosen to only validate the frame/tube and diagrid models. The outrigger model was believed to be already a fairly good representation of reality as it was also found in literature. The behaviour of the braced tube model without core was relatively simple and the deformation would be governed by bending, just as the core. Therefore, no difficulties and/or errors were suspected. The combined behaviour of the frame/tube+core models was uncertain, especially with respect to rules from Schueller[46] concerning the shear-lag effect. Also the behaviour of the diagrid+core was uncertain and it was unclear what kind of factor for the area increase of the corner columns should be used.

3-dimensional models in SCIA and ETABS were used, both finite element analysis (FEA) software packages. SCIA was the main package that is used, ETABS served as verification to check if the 3-dimensional model was properly modelled in SCIA, as there was little reference.

A couple of approaches for the 3-dimensional models were analysed concerning the modelling approach of the floors. It was found in the results of the 3-dimensional models that the floors would contribute to the global stiffness of the building. Bending would occur in the floors between the core and structure in the façade when wind loads were applied to the building structure. It was chosen to neglect this additional stiffness caused by the floors as no proper way could be found to approach this behaviour in 2-dimensional models. Additionally, this would require rigid connections between the floor, the core and façade structure, introducing additional bending moments in the floors and local bending moments in the core. By neglecting the stiffness by the floors, a conservative approach was chosen.

To neglect the bending stiffness of the floors within the 3-dimensional models, the Young's modulus of the floors was reduced to 10.000 MPa and stiffness modifiers ($M_{11} = M_{22} = M_{33} = 0.01$) were used to minimize bending in the slabs.

F.1. Frame and tube models

The 2-dimensional frame and tube models are modelled in the same way and therefore it was chosen to consider them as one type of model in the validation. A 200-meter frame model (as discussed in section 3.3.1) with 8 columns was used with the dimensions that are found in table F.1. C45/55 was used in this case with a Young's modulus of 36000 MPa.

First, the 3-dimensional models were modelled in SCIA and ETABS. An impression of the SCIA model can be found in figure F.1. The model contains only wind loads, corresponding to the 200-meter wind loads

Elements	Dimensions [mm]	Parameter
Columns	800*800	h^*w
Beams	750*500	h^*w
Core wall	300	t
Floor	300	t

Table F.1: Dimensions that are used in the frame/tube validation models.

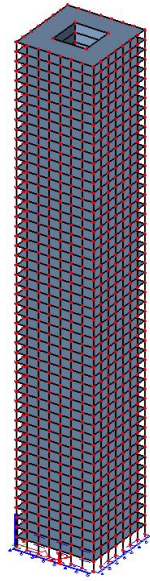


Figure F.1: The 3-dimensional validation model in SCIA.

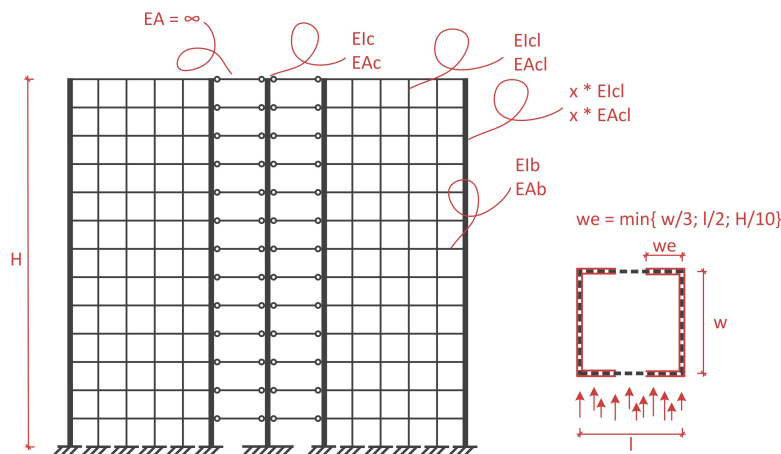


Figure F.2: The 2-dimensional validation model with the rule by Schueller[46] to cover for the shear lag aspect.

used in this thesis, modelled as point loads on the corners of the façade every floor. The models were analysed and compared, results were compared.

Then a 2-dimensional model was created in SCIA, seen in figure F.2, with axially infinite stiff hinged elements connecting the core and façade structures. The areas of the corner columns were increased by the factor proposed by Schueller[46]. Two possible approaches were considered, the rounded down value of the factor and the actual value of the factor (for 8 columns this resulted in values of 3 and 3.3). Wind loads are also modelled as point loads, attached to the core. The same model was created from the parametric Grasshopper model.

The deflections due to wind load of the discussed models are shown in figure F.3. It can be seen that the 2-dimensional models approximate the global deflection quite accurately. Next, three models, including the discussed one, were created and evaluated on the global deflection and support reaction of the corner columns. This concerned models with 6, 8 and 10 columns in the façade (for one side). Both approaches for the Schueller factor were evaluated. The results are shown in figure F.4.

From the results it can be seen that the 2-dimensional models approach the 3-dimensional models quite accurately, within a 5% margin. This is considered accurate enough for the purpose of this thesis as only

		2 - REDUCED E + STIFFNESS MODIFIERS		
		E _{floor} = 10.000 MPa; M11=M22=M33= 0.01		
		2D model: floors connected to core with hinges		
		SCIA	ETABS	Grasshopper
3D	u [mm]	268,8 100%	263,9 98%	
2D	u [mm]	269,6 100%		269,9 100%
Schueller rounded down				
2D	u [mm]			263,5 98%
Schueller exact				

Figure F.3: Comparison of global deflection of the 3- and 2-dimensional models for 8 columns.

200m TUBE

Summary	All columns	GH1 2D
6 columns	Displacement Corner column	103% 98%
8 columns	Displacement Corner column	100% 102%
10 columns	Displacement Corner column	99% 104%

6 columns

	Sum corner column Σ[kN]	Corner column [kN]	Second column [kN]	Third column [kN]	Horizontal core reaction [kN]	Displacement [mm]
3D 1	7444	3572	1546	468	11399	350,7
Schueller rounded down						
GH1 2D 2x	7307 98%	3506 98%	1588	483	11427 100%	361 103%
Schueller exact	7871	3777	1234	379	11213	342,6
All columns	8079	3877	1104	340	11098	335,7
			71%	74%		

8 columns

	Sum corner column Σ[kN]	Corner column [kN]	Second column [kN]	Third column [kN]	Fourth column [kN]	Horizontal core reaction [kN]	Displacement [mm]
3D 1	8718	3253,68	1757	832	283	10981	268,8
Schueller rounded down							
GH1 2D 3x	8908 102%	3328 102%	1601	884	284	10773 98%	269,9 100%
Schueller exact	9157	3417	1463	811	260	10656	263,5
All columns	9557	3567	1241	693	223	10413	253,2
			71%	74%	76%		

10 columns

	Sum corner column Σ[kN]	Corner column [kN]	Second column [kN]	Third column [kN]	Fourth column [kN]	Fifth column [kN]	Horizontal core reaction [kN]	Displacement [mm]
3D 1	9557	2932	1770	1122	527	202	10580	215,9
Schueller exact/rounded								
GH1 2D 4x	9976 104%	3061 104%	1498	998	571	187	10101 95%	213,7 99%
All columns	10525	3228	1230	827	475	156	9733	202,2
			69%	47%	27%	9%	82%	84%

Figure F.4: Comparison of global deflection and corner column support reaction of the 3- and 2-dimensional frame/tube models for 6, 8 and 10 columns.

concept design is considered. Therefore, it was concluded that the 2-dimensional models were accurate enough and could be used for calculations.

F.1.1. Verification with hand calculation

A simple hand calculation was also made to get some feeling with the numbers and to verify the digital models. For this purpose, a 150-meter prefab concrete tube structure was used without a core in order to simplify the required calculations.

The tube structure was modelled as a single cantilevered beam, shown in figure E5. Column and beam dimension were kept constant over the height with a width/height of 1.5 meters and a thickness of 0.4 meters. A constant wind load was applied to the structure of 50 kN/m (which comes down to a pressure of 1.67 kN/m²). The centre to centre distance of the columns is 3 meters, the total width of the building is 30 meters.

The tube structure is simplified as a bending beam where the materials of the columns and beams are spread out over the entire perimeter of the building. By doing this, gaps for windows are removed. Due to shear-lag, not the whole cross-section of the flanges can be taken into account when determining the stiffness. In this calculation, the contribution to the stiffness by the webs is neglected, as the contribution of these to the total moment of inertia was negligible. The total moment of inertia and the resulting deflection can be calculated as follows:

$$t = 0.4/3 = 0.1333m \quad (\text{E.1})$$

$$w_e = \min(w/3, l/2, H/10) = 10m \quad (\text{E.2})$$

$$I_{total} = 2 * I_{flange} = 2 * z^2 * A_{flange;eff} = 2 * 15^2 * (10 * 2 * 0.1333) = 1200m^4 \quad (\text{E.3})$$

$$\delta_{hand} = \frac{q * H^4}{8 * EI} = \frac{50 * 152000^4}{8 * 12000 * 1200 * 10^{12}} = 231.7mm \quad (\text{E.4})$$

The digital model that was used to compare the results with was a 2-dimensional tube Grasshopper model with the same specifications. Here, the total deflection was $\delta_{pc} = 208.9mm$ which falls within the same range. Therefore it was concluded that the 2-dimensional representation of the tube models was sufficient.

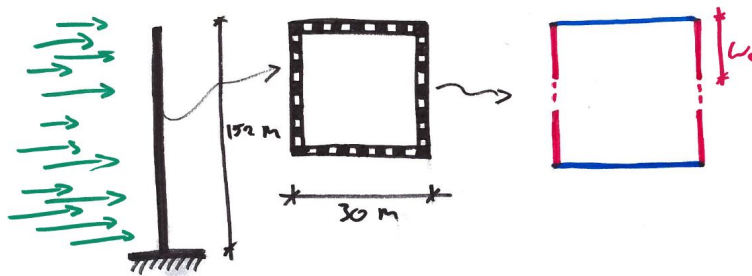


Figure E5: Simplification of the tube structure for the purpose of a hand calculation.

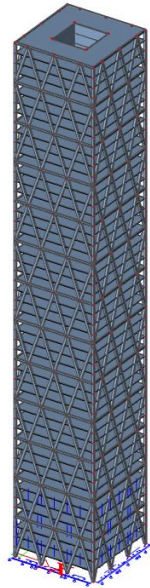


Figure F.6: The 3-dimensional validation model in SCIA.

F.2. Diagrid models

The diagrid models were modelled following the same approach as the frame/tube models. The inclined columns and primary beams were put in the model as explained in section 3.5.1, secondary beams were excluded due to the fact that they do not contribute to global stiffness. Again, the geometry of the 200 model was used. The dimensions of the cross-sections are listed in F.2 and C45/55 was used here also.

The approach here was a little bit different as building up the SCIA model was more time consuming. Therefore, also a parametric 3-dimensional Grasshopper model was build, to validate the results. The 2-dimensional model that was build is shown in figure F.7. The area of the corner columns was also increased to model the additional stiffness by the perpendicular façade. However, it was not known whether a shear-lag effect would be present and what kind of factor should be used to represent the additional elements that contribute to the global stiffness.

The first evaluated models contained diagrid members spanning 4 floors and 6 inclined members per horizontal plane (4FL-3TR). Results showed that the 3-dimensional Grasshopper model represented the behaviour of the 3-dimensional SCIA model very accurately, there was only 1% difference in deflection. Therefore, the 3-dimensional Grasshopper model was used to validate other variations of the diagrid models.

It was evident from the 3-dimensional models that the diagrid members in the perpendicular façade also contributed to the global stiffness. Shear-lag did not seem to be present as the system was primarily loaded with axial forces. However, because of the inclination the reasoning was that simply increasing the corner columns with the half of the number of diagrid members would overestimate the contribution of these members. Therefore, a reduction factor was used for the number of these members which resulted in the following

Elements	Dimensions [mm]	Parameter
Columns	800*800	$h*w$
Braces (diagrid)	800*800	$h*w$
Beams	750*500	$h*w$
Core wall	300	t
Floor	300	t

Table F.2: Dimensions that are used in the diagrid validation models.

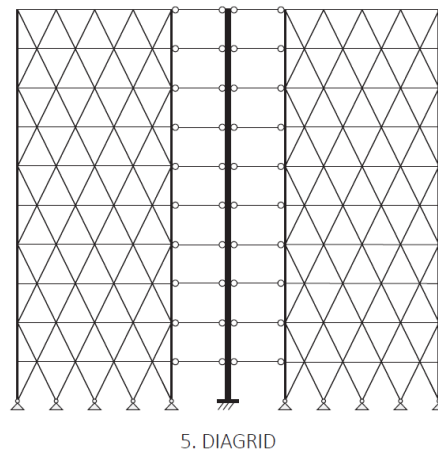


Figure F.7: The 2-dimensional validation model with increased areas of the corner columns.

formula, where Z represented the factor that should be determined, n half of the number of inclined diagrid members in one façade and 1 the factor for the corner column:

$$x_{diagrid} = Z * n + 1 \quad (\text{F.5})$$

At first it was suspected that Z would be related to the angle of the diagrid elements, however, no clear relationship could be identified. Therefore it was chosen to determine a constant value for all the diagrid variations. $Z = 0.8$ had the best overall performance, except for the 2 floors - 8 diagonals model (2FL-4TR) with an inclination angle of 63° . Results are shown in figure F.8.

After interpreting the results, it was chosen to use a value of 0.75 for Z to be on the conservative side. This implies that the stiffness of the models with inclination angles around 63° are slightly overestimated. This results in the following formula that is used in section 3.5.1:

$$x_{diagrid} = 0.75 * n + 1 \quad (\text{F.6})$$

200m DIAGRID

Summary	All columns	GH1 2D	GH 3D	SCIA 3D
4 floors 6 diagonals	Displacement	100%	101%	100%
	Corner column	100%	100%	100%
4 floors 8 diagonals	Displacement	102%	-	-
	Corner column	101%	-	-
2 floors 12 diagonals	Displacement	99%	-	-
	Corner column	102%	-	-
2 floors 8 diagonals	Displacement	89%	-	-
	Corner column	105%	-	-

4 floors - 6 diagonals - 70,9 degrees

	Sum corner support Σ [kN]	Corner support [kN]	Second support [kN]		Horizontal core reaction [kN]	Displacement [mm]	
3	ETABS						
D	13590	8760	1733	-1733	7227	141,6	
2	SCIA						
	13529	8740	1755	-1755	7353	142,8	
	100%	100%	101%	101%	102%	101%	
G	All -1 diagonals 1+x*0,8						
	GH1 2D 2,6x	12991	8374	1969	-2008	7471	161,1
	-	100%	100%	113%	116%	114%	
H	All -1 diagonals 1+x*1,0						
	GH1 2D 3x	13343	8601	1789	-1851	7515	150,6
	-	100%	100%	107%	107%	103%	
1	All diagonals 1+x*0,8						
	GH1 2D 3,4x	13640	8792	1638	-1718	7554	141,8
	-	100%	100%	99%	105%	100%	

4 floors - 8 diagonals - 75,5 degrees

	Sum corner support Σ [kN]	Corner support [kN]	Second support [kN]		Horizontal core reaction [kN]	Displacement [mm]
3	SCIA					
D	13150	7387	2195	-2195	8045	125,9
2	GH 3D					
	13123	7372	2172	-2241	8182	130,5
	-	100%	100%	102%	102%	103%
G	All -1 diagonals 1+x*1,0					
	GH1 2D 4x	13233	7434	2099	2172	8197
	-	101%	101%	-99%	102%	102%
H	All diagonals 1+x*0,8					
	GH1 2D 4,2x	13433	7546	1968	-2046	8225
	-	100%	100%	93%	102%	102%
1	All diagonals 1+x*0,9					

2 floors - 12 diagonals - 70,9 degrees

	Sum corner support Σ [kN]	Corner support [kN]			Horizontal core reaction [kN]	Displacement [mm]
3	SCIA					
D	14361	6340			5577	88,7
2	GH 3D					
	14280	6304			7129	94,8
	-	100%	100%		128%	107%
G	All -1 diagonals 1+x*0,8					
	GH1 2D 5x	14787	6528		7137	86
	-	100%	100%		128%	100%
H	All -1 diagonals 1+x*1,0					
	GH1 2D 6x	14696	6488		7134	87,6
	-	102%	102%		128%	99%
1	All diagonals 1+x*0,8					

2 floors - 8 diagonals - 63 degrees

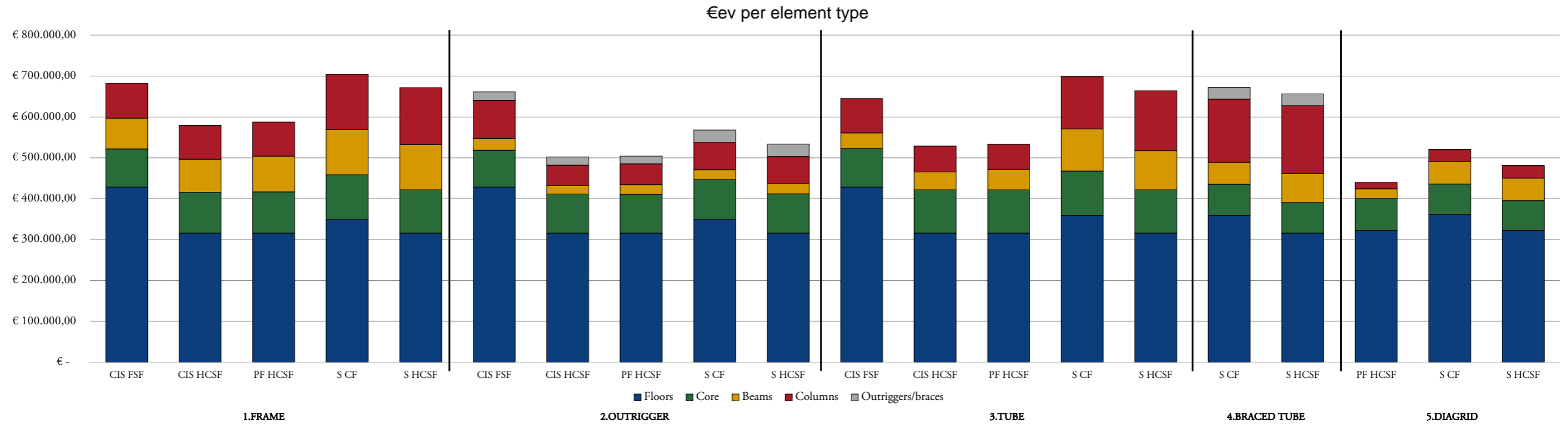
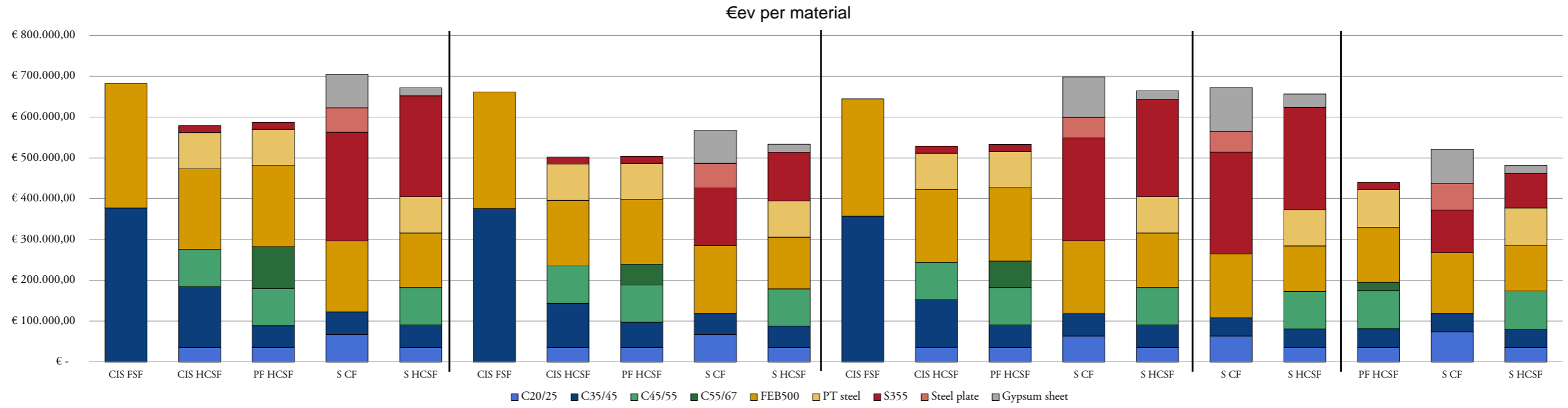
	Sum corner support Σ [kN]	Corner support [kN]			Horizontal core reaction [kN]	Displacement [mm]
3	SCIA					
D	14422	8248			6000	125,3
2	GH 3D					
	14474	8278			6798	127
	-	100%	100%		113%	101%
G	All diagonals 1+x*0,6					
	GH1 2D 3,4x	14801	8465		6771	119
	-	100%	100%		113%	95%
H	All -1 diagonals 1+x*1,0					
	GH1 2D 3,8x	15082	8625		6749	112,1
	-	105%	105%		112%	89%
1	All diagonals 1+x*0,8					

Figure F.8: Comparison of global deflection and corner column support reaction of the 3- and 2-dimensional diagrid models.

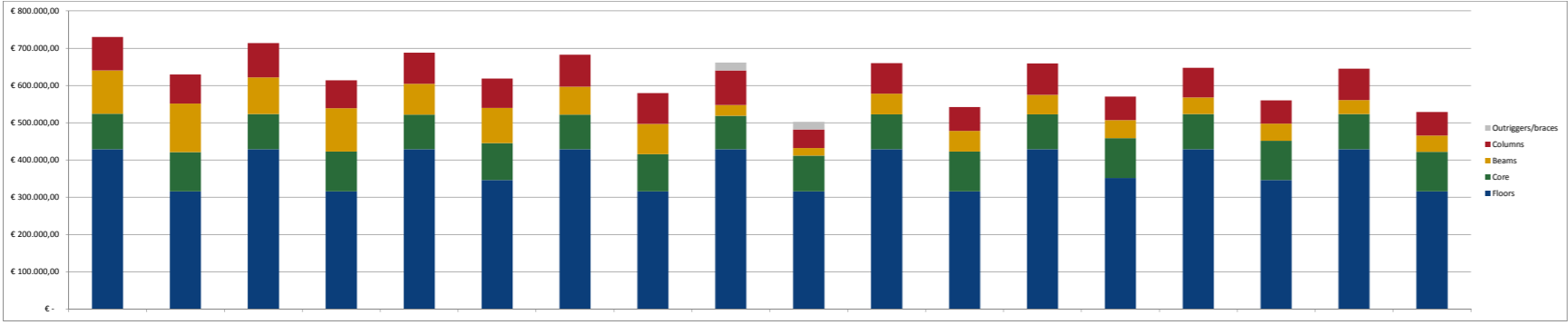
G

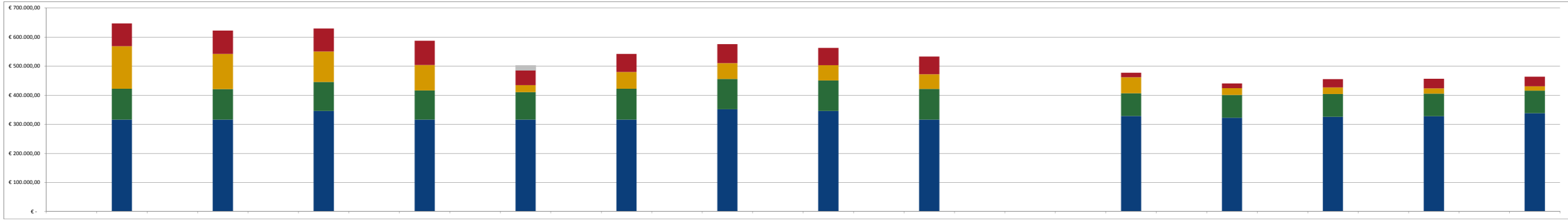
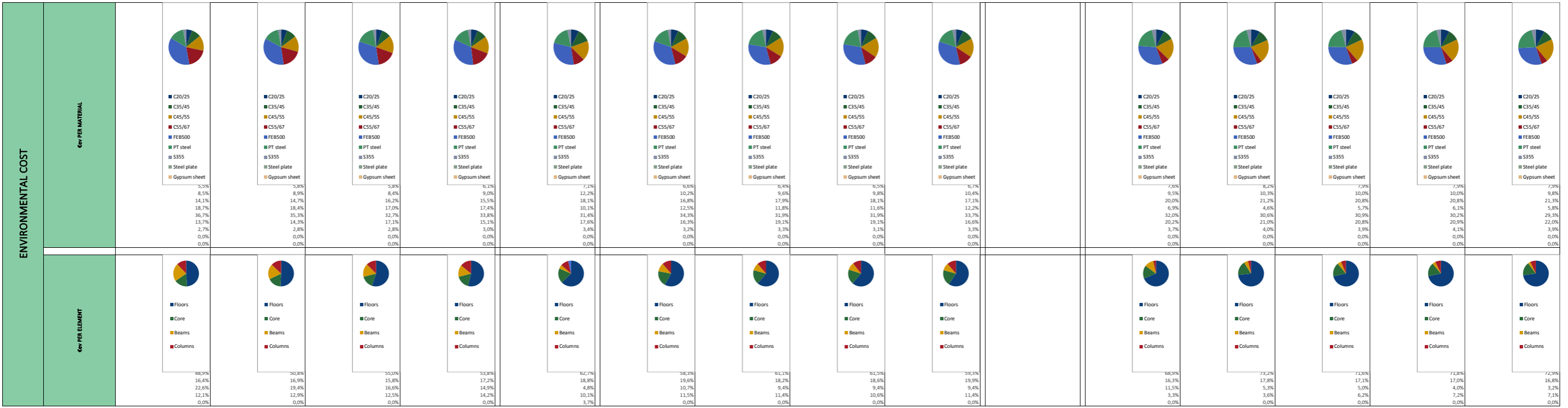
Results

This appendix contains all of the life-cycle analysis results of all the designed models of this thesis. Additionally, it also contains structural information as cross-section sizes and amount of applied reinforcement.



ENVIRONMENTAL COST	€ per MATERIAL	Material Breakdown Data (Columns 2-17)																Empty Columns																									
		Material 1	Material 2	Material 3	Material 4	Material 5	Material 6	Material 7	Material 8	Material 9	Material 10	Material 11	Material 12	Material 13	Material 14	Material 15	Material 16	Material 17	Material 18	Material 19	Material 20																						
ENVIRONMENTAL COST	€ per ELEMENT	Pie charts showing material composition for each element																Empty Columns																									
		Element 1	Element 2	Element 3	Element 4	Element 5	Element 6	Element 7	Element 8	Element 9	Element 10	Element 11	Element 12	Element 13	Element 14	Element 15	Element 16	Element 17	Element 18	Element 19	Element 20																						
		0.0%	5.7%	0.0%	5.8%	0.0%	5.9%	0.0%	6.2%	0.0%	7.1%	0.0%	6.6%	0.0%	6.3%	0.0%	6.0%	0.0%	6.8%	0.0%	6.8%																						
		54.2%	26.4%	54.9%	25.8%	55.0%	24.3%	55.3%	25.7%	56.8%	21.5%	55.0%	22.3%	55.0%	20.7%	55.1%	20.9%	55.4%	22.1%	56.8%	21.5%	55.0%	22.3%																				
		0.0%	14.5%	0.0%	14.9%	0.0%	16.5%	0.0%	15.8%	0.0%	18.2%	0.0%	16.8%	0.0%	18.1%	0.0%	18.2%	0.0%	17.3%	0.0%	18.2%	0.0%																					
		0.0%	0.0%	0.0%	0.0%	0.0%	0.0%	0.0%	0.0%	0.0%	0.0%	0.0%	0.0%	0.0%	0.0%	0.0%	0.0%	0.0%	0.0%	0.0%	0.0%	0.0%																					
		45.8%	36.6%	45.1%	36.2%	45.0%	33.1%	44.7%	34.1%	43.2%	32.1%	45.0%	34.7%	45.0%	32.1%	44.9%	32.0%	44.6%	33.8%	45.0%	32.1%	45.0%																					
		0.0%	14.1%	0.0%	14.4%	0.0%	17.4%	0.0%	15.3%	0.0%	17.7%	0.0%	16.4%	0.0%	19.3%	0.0%	19.2%	0.0%	16.8%	0.0%	19.2%	0.0%																					
		0.0%	2.8%	0.0%	2.8%	0.0%	2.8%	0.0%	3.0%	0.0%	3.0%	0.0%	3.2%	0.0%	3.4%	0.0%	3.1%	0.0%	3.3%	0.0%	3.3%	0.0%																					
		0.0%	0.0%	0.0%	0.0%	0.0%	0.0%	0.0%	0.0%	0.0%	0.0%	0.0%	0.0%	0.0%	0.0%	0.0%	0.0%	0.0%	0.0%	0.0%	0.0%	0.0%																					
		0.0%	0.0%	0.0%	0.0%	0.0%	0.0%	0.0%	0.0%	0.0%	0.0%	0.0%	0.0%	0.0%	0.0%	0.0%	0.0%	0.0%	0.0%	0.0%	0.0%	0.0%																					
		58.7%	50.2%	60.1%	51.5%	62.3%	55.9%	62.8%	54.6%	64.8%	62.9%	64.9%	58.3%	65.1%	61.7%	66.2%	61.8%	66.5%	59.7%	64.9%	62.9%	64.9%																					
		13.1%	16.7%	13.2%	17.3%	13.5%	16.0%	13.7%	17.3%	13.6%	19.0%	14.3%	19.7%	14.3%	18.7%	14.6%	18.8%	14.6%	20.0%	14.3%	19.0%	14.3%																					
		15.9%	20.6%	13.8%	19.0%	12.0%	15.2%	11.0%	14.0%	4.4%	4.1%	8.4%	10.2%	7.8%	8.5%	7.0%	8.3%	5.9%	8.3%	14.0%	19.0%	14.3%																					
		12.3%	12.4%	12.9%	12.2%	12.1%	12.8%	12.5%	14.2%	14.0%	9.9%	12.4%	11.8%	12.8%	11.0%	12.3%	11.0%	13.0%	12.0%	14.0%	9.9%	12.4%																					
		0.0%	0.0%	0.0%	0.0%	0.0%	0.0%	0.0%	0.0%	3.2%	4.0%	0.0%	0.0%	0.0%	0.0%	0.0%	0.0%	0.0%	0.0%	3.2%	4.0%	0.0%																					

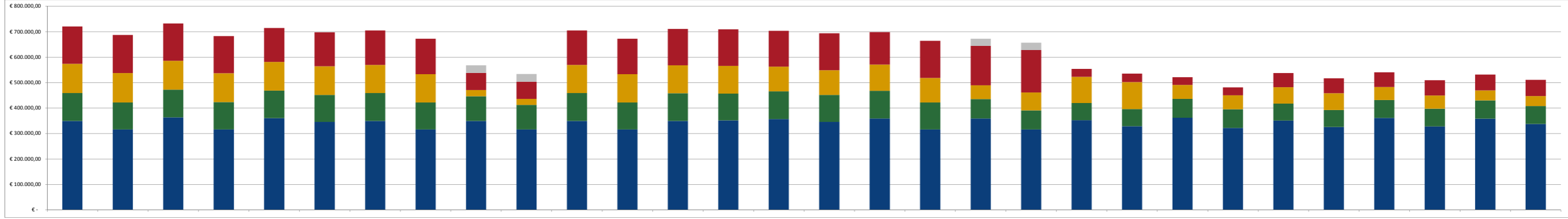


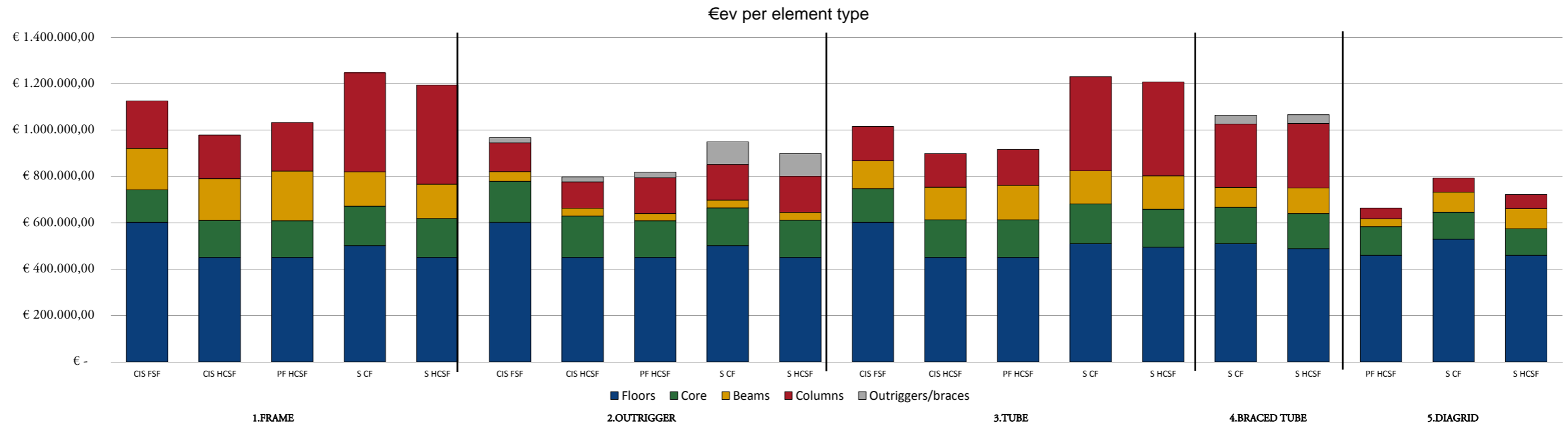
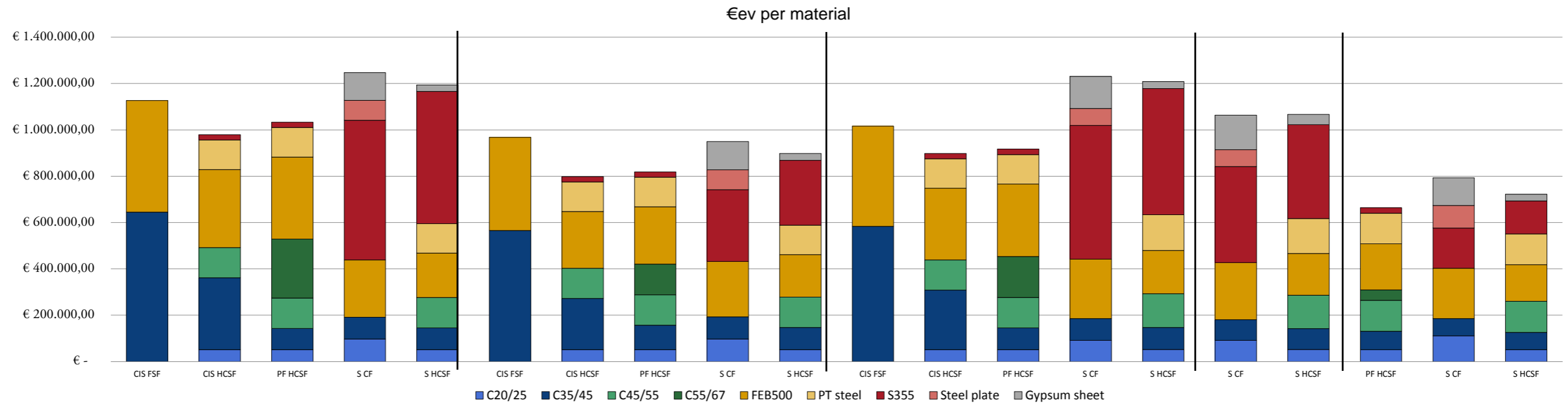


ENVIRONMENTAL COST - 150 M - STEEL

Parameters table with columns: Amount of floors, Surface area / floor, Reinforcement factor, and material properties for Weight materials and Env materials.

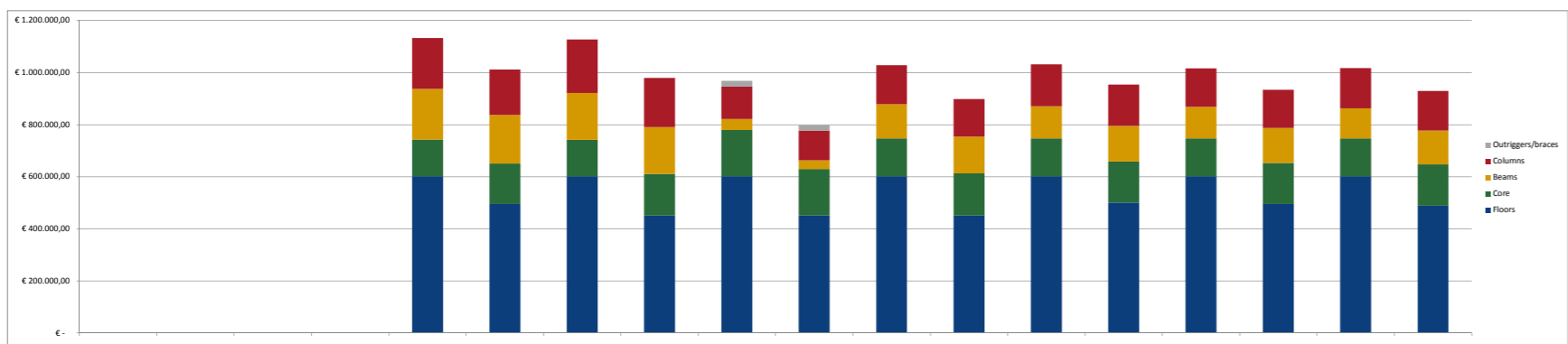
Main environmental cost table with columns for system types (Floors, Core, Beams, Columns, Outriggers/braces) and elements (1.FRAME, 2.OUTRIGGER, 3.TUBE, 4.BRACED TUBE, 5.DIAGRID), and rows for various materials and their environmental costs in €/kg.

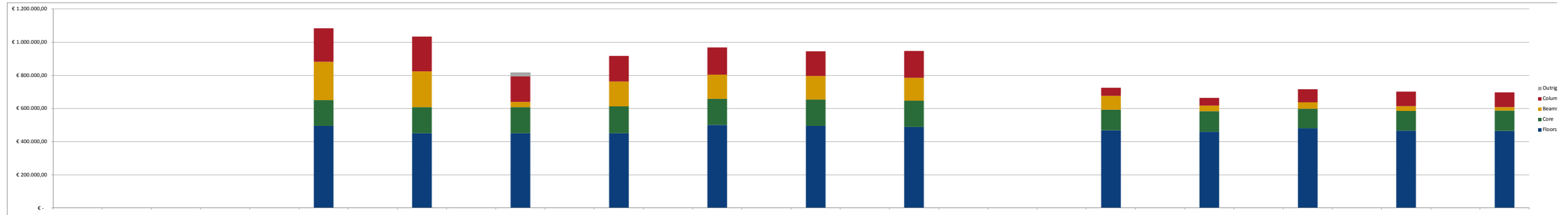




ENVIRONMENTAL COST	€m PER MATERIAL	Material Breakdown Data															
		1	2	3	4	5	6	7	8	9	10	11	12	13	14	15	16
		<ul style="list-style-type: none"> C20/25 C35/45 C45/55 C55/67 FE8500 PT steel S355 Steel plate Gypsum sheet 	<ul style="list-style-type: none"> C20/25 C35/45 C45/55 C55/67 FE8500 PT steel S355 Steel plate Gypsum sheet 	<ul style="list-style-type: none"> C20/25 C35/45 C45/55 C55/67 FE8500 PT steel S355 Steel plate Gypsum sheet 	<ul style="list-style-type: none"> C20/25 C35/45 C45/55 C55/67 FE8500 PT steel S355 Steel plate Gypsum sheet 	<ul style="list-style-type: none"> C20/25 C35/45 C45/55 C55/67 FE8500 PT steel S355 Steel plate Gypsum sheet 	<ul style="list-style-type: none"> C20/25 C35/45 C45/55 C55/67 FE8500 PT steel S355 Steel plate Gypsum sheet 	<ul style="list-style-type: none"> C20/25 C35/45 C45/55 C55/67 FE8500 PT steel S355 Steel plate Gypsum sheet 	<ul style="list-style-type: none"> C20/25 C35/45 C45/55 C55/67 FE8500 PT steel S355 Steel plate Gypsum sheet 	<ul style="list-style-type: none"> C20/25 C35/45 C45/55 C55/67 FE8500 PT steel S355 Steel plate Gypsum sheet 	<ul style="list-style-type: none"> C20/25 C35/45 C45/55 C55/67 FE8500 PT steel S355 Steel plate Gypsum sheet 	<ul style="list-style-type: none"> C20/25 C35/45 C45/55 C55/67 FE8500 PT steel S355 Steel plate Gypsum sheet 	<ul style="list-style-type: none"> C20/25 C35/45 C45/55 C55/67 FE8500 PT steel S355 Steel plate Gypsum sheet 	<ul style="list-style-type: none"> C20/25 C35/45 C45/55 C55/67 FE8500 PT steel S355 Steel plate Gypsum sheet 	<ul style="list-style-type: none"> C20/25 C35/45 C45/55 C55/67 FE8500 PT steel S355 Steel plate Gypsum sheet 		
		0,0%	5,2%	0,0%	5,3%	0,0%	6,4%	0,0%	5,7%	0,0%	6,4%	0,0%	5,7%	0,0%	5,6%	0,0%	5,6%
		56,9%	27,5%	57,2%	31,7%	58,4%	27,7%	57,3%	28,6%	57,5%	27,7%	57,4%	27,3%	57,8%	27,9%	57,8%	27,9%
		0,0%	14,4%	0,0%	13,4%	0,0%	16,4%	0,0%	14,6%	0,0%	14,6%	0,0%	15,5%	0,0%	15,5%	0,0%	15,5%
		0,0%	0,0%	0,0%	0,0%	0,0%	0,0%	0,0%	0,0%	0,0%	0,0%	0,0%	0,0%	0,0%	0,0%	0,0%	0,0%
		43,1%	35,2%	42,8%	34,4%	41,6%	30,7%	42,7%	34,4%	42,5%	32,2%	42,6%	32,3%	42,2%	32,3%	42,2%	32,3%
		0,0%	15,2%	0,0%	13,0%	0,0%	15,9%	0,0%	14,1%	0,0%	16,4%	0,0%	16,4%	0,0%	16,2%	0,0%	16,2%
		0,0%	2,5%	0,0%	2,4%	0,0%	2,9%	0,0%	2,6%	0,0%	2,7%	0,0%	2,8%	0,0%	2,5%	0,0%	2,5%
		0,0%	0,0%	0,0%	0,0%	0,0%	0,0%	0,0%	0,0%	0,0%	0,0%	0,0%	0,0%	0,0%	0,0%	0,0%	0,0%
		0,0%	0,0%	0,0%	0,0%	0,0%	0,0%	0,0%	0,0%	0,0%	0,0%	0,0%	0,0%	0,0%	0,0%	0,0%	0,0%

ENVIRONMENTAL COST	€m PER ELEMENT	Element Breakdown Data															
		1	2	3	4	5	6	7	8	9	10	11	12	13	14	15	16
		<ul style="list-style-type: none"> Floors Core Beams Columns 	<ul style="list-style-type: none"> Floors Core Beams Columns 	<ul style="list-style-type: none"> Floors Core Beams Columns 	<ul style="list-style-type: none"> Floors Core Beams Columns 	<ul style="list-style-type: none"> Floors Core Beams Columns 	<ul style="list-style-type: none"> Floors Core Beams Columns 	<ul style="list-style-type: none"> Floors Core Beams Columns 	<ul style="list-style-type: none"> Floors Core Beams Columns 	<ul style="list-style-type: none"> Floors Core Beams Columns 	<ul style="list-style-type: none"> Floors Core Beams Columns 	<ul style="list-style-type: none"> Floors Core Beams Columns 	<ul style="list-style-type: none"> Floors Core Beams Columns 	<ul style="list-style-type: none"> Floors Core Beams Columns 	<ul style="list-style-type: none"> Floors Core Beams Columns 	<ul style="list-style-type: none"> Floors Core Beams Columns 	<ul style="list-style-type: none"> Floors Core Beams Columns
		53,2%	49,0%	53,5%	46,0%	62,2%	56,5%	58,0%	50,2%	58,4%	52,5%	59,3%	53,1%	59,2%	52,6%	59,2%	52,6%
		12,4%	15,4%	12,4%	16,3%	18,3%	22,4%	14,1%	18,1%	14,1%	16,5%	14,3%	16,9%	14,3%	17,1%	14,3%	17,1%
		17,2%	18,5%	15,9%	18,4%	4,3%	4,2%	12,7%	15,6%	11,9%	14,4%	11,8%	14,4%	11,1%	14,0%	11,1%	14,0%
		17,2%	17,2%	18,2%	19,3%	12,8%	14,2%	14,6%	16,1%	15,6%	16,6%	14,6%	15,6%	15,2%	16,3%	15,2%	16,3%
		0,0%	0,0%	0,0%	0,0%	2,3%	2,7%	0,0%	0,0%	0,0%	0,0%	0,0%	0,0%	0,0%	0,0%	0,0%	0,0%



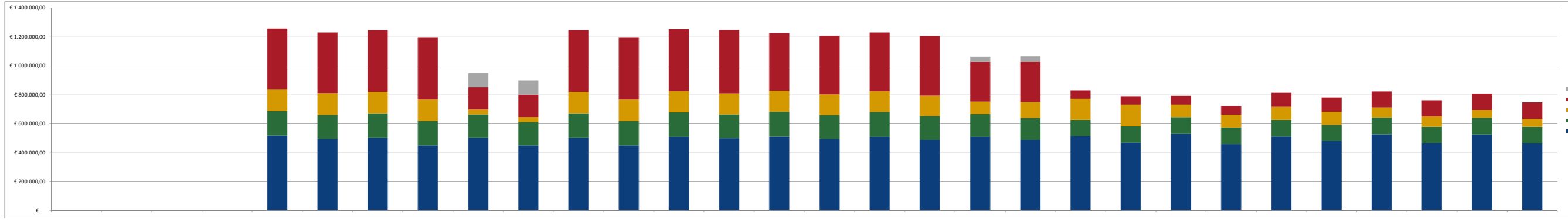


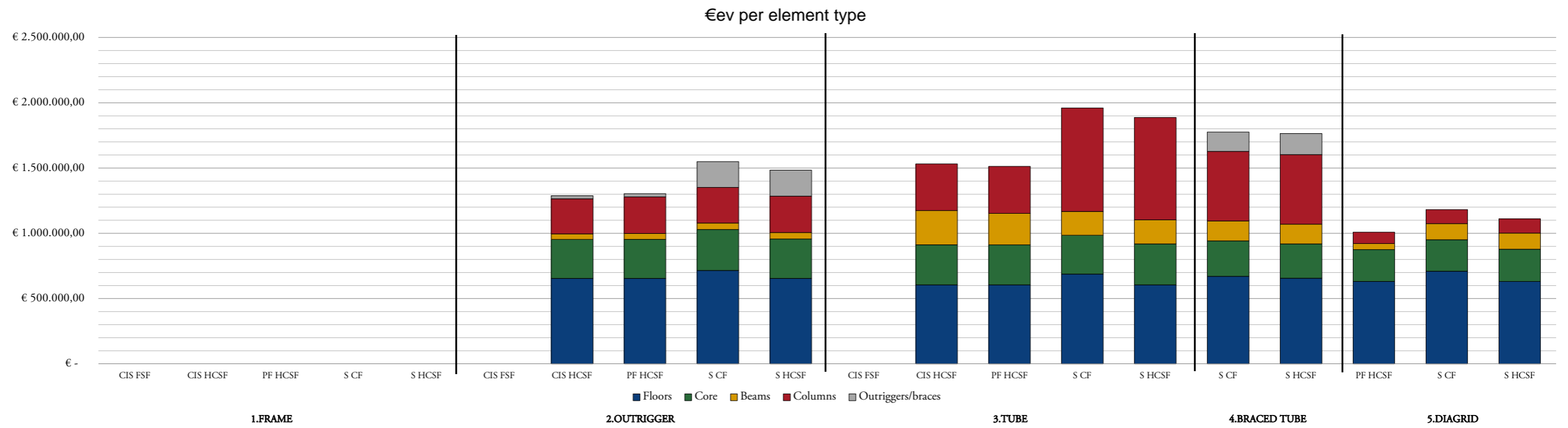
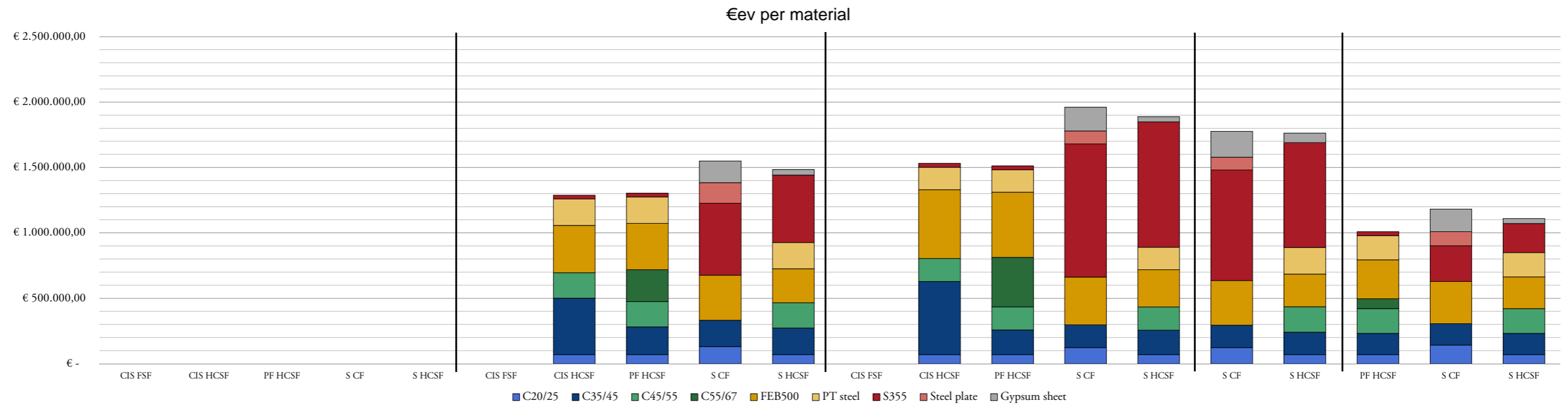
ENVIRONMENTAL COST - 200 M - STEEL

Parameters
 Amount of floors 52 -
 Surface area /floor 992,25 m2
 Additional reinforcement 1,15 -

	Weight materials		Env materials	
C20/25	2400	kg/m3	0,007322	Env/kg
C35/45	2400	kg/m3	0,007500	Env/kg
C45/55	2400	kg/m3	0,008238	Env/kg
C55/67	2400	kg/m3	0,008975	Env/kg
FE800	7800	kg/m3	0,247110	Env/kg
PT steel	7800	kg/m4	0,656817	Env/kg
S355	7800	kg/m3	0,067500	Env/kg
Steel plate	7800	kg/m3	0,161500	Env/kg
Gypsum sheet	870	kg/m3	0,269281	Env/kg

Stability system	1.FRAME				2.OUTRIGGER				3.TUBE				4.BRACED TUBE				5.DIAGRID			
	BC		HCSP		BC		HCSP		BC		HCSP		BC		HCSP		BC		HCSP	
Floor system	CF	HCSP	CF	HCSP	CF	HCSP	CF	HCSP	CF	HCSP	CF	HCSP	CF	HCSP	CF	HCSP	CF	HCSP	CF	HCSP
kg/floor FLOOR	...																			
C20/25	...																			
C35/45	...																			
C45/55	...																			
C55/67	...																			
FE800	...																			
PT steel	...																			
S355	...																			
Steel plate	...																			
Gypsum sheet	...																			
kg FLOOR	...																			
C20/25	...																			
C35/45	...																			
C45/55	...																			
C55/67	...																			
FE800	...																			
PT steel	...																			
S355	...																			
Steel plate	...																			
Gypsum sheet	...																			
env FLOOR	...																			
C20/25	...																			
C35/45	...																			
C45/55	...																			
C55/67	...																			
FE800	...																			
PT steel	...																			
S355	...																			
Steel plate	...																			
Gypsum sheet	...																			
m3 CORE	...																			
C35/45	...																			
FE800	...																			
kg CORE	...																			
C35/45	...																			
FE800	...																			
env CORE	...																			
C35/45	...																			
FE800	...																			
m3 BEAMS	...																			
C35/45	...																			
C55/67	...																			
FE800	...																			
S355	...																			
Gypsum sheet	...																			
kg BEAMS	...																			
C35/45	...																			
C55/67	...																			
FE800	...																			
S355	...																			
Gypsum sheet	...																			
env BEAMS	...																			
C35/45	...																			
C55/67	...																			
FE800	...																			
S355	...																			
Gypsum sheet	...																			
m3 COLUMNS	...																			
C35/45	...																			
C55/67	...																			
FE800	...																			
S355	...																			
Gypsum sheet	...																			
kg COLUMNS	...																			
C35/45	...																			
C55/67	...																			
FE800	...																			
S355	...																			
Gypsum sheet	...																			
env COLUMNS	...																			
C35/45	...																			
C55/67	...																			
FE800	...																			
S355	...																			
Gypsum sheet	...																			
m3 OUTRIGGERS/BRACES	...																			
C35/45	...																			
FE800	...																			
S355	...																			
Gypsum sheet	...																			
kg OUTRIGGERS/BRACES	...																			
C35/45	...																			
FE800	...																			
S355	...																			
Gypsum sheet	...																			
env OUTRIGGERS/BRACES	...																			
C35/45	...																			
FE800	...																			
S355	...																			
Gypsum sheet	...																			
env PER MATERIAL	...																			
C20/25	...																			
C35/45	...																			
C45/55	...																			
C55/67	...																			
FE800	...																			
PT steel	...																			
S355	...																			
Steel plate	...																			
Gypsum sheet	...																			
env PER ELEMENT TYPE	...																			
Columns	...																			
Core	...																			
Beams	...																			
Columns	...																			
Outriggers/Braces	...																			
env TOTAL	...																			
TOTAL/floor	...																			
envTOTAL/m2	...																			





DIMENSIONS		1.FRAME				2.OUTRIGGER		3.TUBE			4.BRACED TUBE		5.DIAGRID					
		5C	6C	7C	8C	8C	9C	10C	11C	11C	4FL-2TR	4FL-3TR	2FL-4TR	2FL-5TR	2FL-6TR			
Core	IA IB IC ID IE					1500 980 650 400 300			1400 980 600 300 300			1400 980 600 300 300						
Column	HxW A / profile A HxW B / profile B HxW C / profile C HxW D / profile D HxW E / profile E					1550*1500 1400*1400 1250*1250 950*950 450*450			1350*1350 1350*1350 1300*1350 1250*1350 1100*1350			1200*1200 1200*1200 1150*1200 1100*1200 1050*1200						
Sec column	profile																	
Beam	HxW / profile					600*300			2000*500			2000*500						
Sec beam	HxW / profile																	
Outrigger	HxW / profile					7600*400												
Mega beam	profile																	
Mega brace	profile																	
REBAR KG/M3																		
Core	mean kg/m3					35,1			45,4			45,0						
Column	mean kg/m3					25,1			23,5			24,6						
Beam	mean kg/m3					77,8			117,4			114,6						
Outrigger	mean kg/m3					124,4												
FLOORS																		
CORE																		
BEAMS																		
COLUMNS																		
OUTRIGGERS/BRACES																		

ENVIRONMENTAL COST - 250 M - PREFAB CONCRETE

Parameters
 Amount of floors 64 -
 Surface area /floor 1089 m2
 Additional reinforcement 1.15 -

	Weight materials	Env materials
C20/25	2400 kg/m3	0,007322 €/kg
C35/45	2400 kg/m3	0,007500 €/kg
C45/55	2400 kg/m3	0,008238 €/kg
C55/67	2400 kg/m3	0,008975 €/kg
FE800	7800 kg/m3	0,247110 €/kg
PT steel	7800 kg/m3	0,656817 €/kg
S355	7800 kg/m3	0,067500 €/kg
Steel plate	7800 kg/m3	0,167500 €/kg
Gypsum sheet	870 kg/m3	0,069241 €/kg

	1.FRAME						2.OUTRIGGER						3.TUBE						4.BRACED TUBE						5.DIAGRID					
	BC		HCSP		7C		BC		HCSP		9C		10C		11C		11C		4FL-2TR		4FL-3TR		2FL-4TR		2FL-5TR		2FL-6TR			
Stability system	BC		HCSP		7C		BC		HCSP		9C		10C		11C		11C		4FL-2TR		4FL-3TR		2FL-4TR		2FL-5TR		2FL-6TR			
Nr columns/diagonals	BC		HCSP		7C		BC		HCSP		9C		10C		11C		11C		4FL-2TR		4FL-3TR		2FL-4TR		2FL-5TR		2FL-6TR			
Floor system	BC		HCSP		7C		BC		HCSP		9C		10C		11C		11C		4FL-2TR		4FL-3TR		2FL-4TR		2FL-5TR		2FL-6TR			
kg/floor FLOOR																														
C20/25							150985				148322		151464						148899		149477		149284		150305		150247			
C35/45																														
C45/55							367503				335412		372846						342429		355572		347107		359744		358803			
C55/67																														
FE800							10054				10054		10054						10054		10054		10054		10054		10054			
PT steel							4797				4935		4935						4241		4397		4345		4625		4604			
S355							6806				7532		7532						6951		6951		7048		7048		7048			
Steel plate																														
Gypsum sheet																														
kg FLOOR							9663019				9492595		9693668						9529558		9566522		9554201		9619529		9618006			
C20/25							0				0		0						0		0		0		0		0			
C35/45							0				0		0						0		0		0		0		0			
C45/55							23520222				21466368		23862188						2195472		22756615		22214874		23023638		22961380			
C55/67							0				0		0						0		0		0		0		0			
FE800							643443				643443		643443						643443		643443		643443		643443		643443			
PT steel							300982				261485		214557						271434		281383		278066		295982		294647			
S355							435600				448294		448294						448294		448294		451088		451088		451088			
Steel plate							0				0		0						0		0		0		0		0			
Gypsum sheet							0				0		0						0		0		0		0		0			
€/FLOOR							€ 654.541,64				€ 606.491,00		€ 665.694,47						€ 617.623,46		€ 631.357,55		€ 625.044,70		€ 643.952,74		€ 642.552,35			
C20/25							€ 70.754,12				€ 69.506,25		€ 70.978,53						€ 69.776,90		€ 70.435,55		€ 69.952,33		€ 70.435,68		€ 70.408,42			
C35/45							€ -				€ -		€ -						€ -		€ -		€ -		€ -		€ -			
C45/55							€ 193.751,77				€ 176.832,81		€ 196.588,61						€ 180.532,37		€ 187.461,43		€ 182.998,75		€ 189.661,08		€ 189.164,69			
C55/67							€ -				€ -		€ -						€ -		€ -		€ -		€ -		€ -			
FE800							€ 159.001,37				€ 159.001,37		€ 159.001,37						€ 159.001,37		€ 159.001,37		€ 159.001,37		€ 159.001,37		€ 159.001,37			
PT steel							€ 201.631,38				€ 171.748,18		€ 206.606,63						€ 178.282,55		€ 184.816,93		€ 182.638,81		€ 194.406,17		€ 193.529,43			
S355							€ 29.403,00				€ 32.539,32		€ 32.539,32						€ 30.030,26		€ 30.030,26		€ 30.448,44		€ 30.448,44		€ 30.448,44			
Steel plate							€ -				€ -		€ -						€ -		€ -		€ -		€ -		€ -			
Gypsum sheet							€ -				€ -		€ -						€ -		€ -		€ -		€ -		€ -			
m3 CORE							11239,74				10489,70		10490,69						9088,63		9083,27		9088,35		9088,35		9088,72			
C35/45							50,57				60,97		59,85						36,37		42,24		36,40		36,40		35,97			
FE800							0				0		0						0		0		0		0		0			
kg CORE							26975381				25175281		25177665						21807919		21799839		21812039		21812039		21812027			
C35/45							0				0		0						0		0		0		0		0			
FE800							394480				475586		466677						299304		329501		283905		283905		282585			
€/CORE							€ 299.799,26				€ 306.340,29		€ 304.156,96						€ 237.523,46		€ 244.925,05		€ 233.749,18		€ 233.749,18		€ 232.935,53			
C35/45							€ 202.316,15				€ 188.818,14		€ 188.836,02						€ 163.562,46		€ 163.501,85		€ 163.593,35		€ 163.593,35		€ 163.600,02			
FE800							€ 97.480,11				€ 117.522,15		€ 115.320,54						€ 73.961,01		€ 81.423,19		€ 70.155,83		€ 70.155,83		€ 69.335,52			
m3 BEAMS							1168,12				4453,55		4454,28						1748,89		627,48		857,24		608,79		428,61			
C35/45							10,23				74,87		73,67						41,96		17,26		21,14		16,69		12,04			
C55/67							0				0		0						0		0		0		0		0			
FE800							2803486				10688530		10690374						4197311		1505940		2057979		1461084		1028657			
S355							79834				583956		574627						327314		134649		164860		130191		93925			
Gypsum sheet							0				0		0						0		0		0		0		0			
kg BEAMS							2803486				10688530		10690374						4197311		1505940		2057979		1461084		1028657			
C35/45							0				0		0						0		0		0		0		0			
C55/67							0				0		0						0		0		0		0		0			
FE800							2803486				10688530		10690374						4197311		1505940		2057979		1461084		1028657			
S355							79834				583956		574627						327314		134649		164860		130191		93925			
Gypsum sheet							0				0		0						0		0		0		0		0			
€/BEAMS							€ 44.887,16				€ 240.233,13		€ 237.943,55						€ 118.554,60		€ 46.780,17		€ 59.203,88		€ 45.284,94		€ 32.442,19			
C35/45							€ -				€ -		€ -						€ -		€ -		€ -		€ -		€ -			
C55/67							€ 25.161,83				€ 95.931,64		€ 95.947,30						€ 37.671,87		€ 13.516,10		€ 18.465,38		€ 13.113,51		€ 9.232,40			
FE800							€ 19.725,33				€ 144.301,49		€ 141.996,25						€ 80.882,74		€ 33.273,06		€ 40.738,50		€ 32.171,42		€ 23.209,80			
S355							€ -				€ -		€ -						€ -		€ -		€ -		€ -		€ -			
Gypsum sheet							€ -				€ -		€ -						€ -		€ -		€ -		€ -		€ -			
m3 COLUMNS							10123,33				13132,91		11233,00						3118,26		2926,89		5223,63		6000,89		5958,43			
C35/45							32,71				39,99		34,75						11,70		12,11		23,47		25,48		28,09			
C55/67							0				0		0						0		0		0		0		0			
FE800							24295997				31518989		26959200						7483813		7024538		12536717		14402126		14300225			
S355							2																							

DIMENSIONS		1.FRAME				2.OUTRIGGER	3.TUBE			4.BRACED TUBE	5.DIAGRID					
		5C	6C	7C	8C	8C	9C	10C	11C	11C	4FL-2TR	4FL-3TR	2FL-4TR	2FL-5TR	2FL-6TR	
Core	IA					1500										
	IB					980										
	IC					650										
	ID					300										
	IE					300										
Column	HxW A / profile A					1500*1500				1200*1200						
	HxW B / profile B					1350*1350				1150*1150						
	HxW C / profile C					1200*1200				1000*1000						
	HxW D / profile D					850*850				800*800						
	HxW E / profile E					450*450				650*650						
Sec column	profile															
Beam	HxW / profile					600*300				200*500						
Sec beam	HxW / profile															
Outrigger	HxW / profile					7600*400										
Mega beam	profile															
Mega brace	profile															
REBAR KG/M3																
Core	mean kg/m3					35,1				45,3						
Column	mean kg/m3					25,2				24,1						
Beam	mean kg/m3					68,3				129,0						
Outrigger	mean kg/m3					126,7										
FLOORS																
CORE																
BEAMS																
COLUMNS																
OUTRIGGERS/BRACES																

ENVIRONMENTAL COST TRANSPORTATION - 200M OUTRIGGER

Material	€ev materials
C20/25	0,007322 €/kg
C35/45	0,007500 €/kg
C45/55	0,008238 €/kg
C55/67	0,008975 €/kg
FEB500	0,247110 €/kg
PT steel	0,656817 €/kg
S355	0,067500 €/kg
Steel plate	0,167500 €/kg
Gypsum sheet	0,069241 €/kg

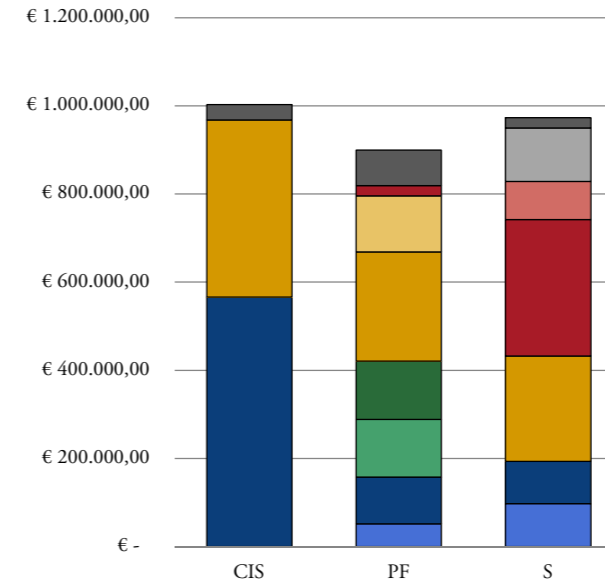
Shadow price € 0,01518 €/tkm

	Material quantities			Actual distance [km]	Actual distance		
	CIS [t]	PF [t]	S [t]		CIS [€ev]	PF [€ev]	S [€ev]
C20/25	0	7.028	13.250	30	€ -	€ 3.201,28	€ 6.035,89
C35/45	75.444	14.095	12.796	30	€ 34.367,48	€ 6.420,99	€ 5.828,94
C45/55	0	15.892	0	150	€ -	€ 36.196,53	€ -
C55/67	0	14.802	0	150	€ -	€ 33.714,62	€ -
FEB500	1.628	1.003	968	30	€ 741,63	€ 456,67	€ 440,90
PT steel	0	194	0	150	€ -	€ 440,92	€ -
S355	0	344	4.595	150	€ -	€ 783,47	€ 10.464,88
Steel plate	0	0	514	30	€ -	€ -	€ 233,93
Gypsum sheet	0	0	1.756	30	€ -	€ -	€ 799,84

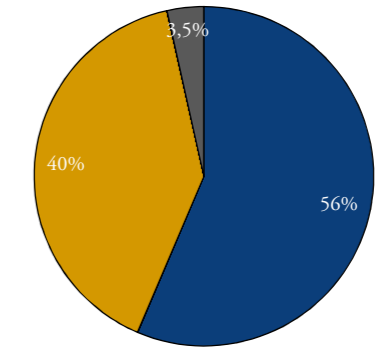
TOTAL €ev transport	€ 35.109,11	€ 81.214,49	€ 23.804,38
TOTAL €ev material	€ 968.147,57	€ 819.034,09	€ 949.884,93
TOTAL €ev	€ 1.003.256,68	€ 900.248,58	€ 973.689,32
% transport of total	3,5%	9,0%	2,4%

	Material quantities		
	CIS [t]	PF [t]	S [t]
C20/25	€ -	€ 51.456,52	€ 97.019,35
C35/45	€ 565.842,05	€ 105.718,13	€ 95.970,34
C45/55	€ -	€ 130.911,99	€ -
C55/67	€ -	€ 132.852,69	€ -
FEB500	€ 402.305,52	€ 247.728,34	€ 239.170,33
PT steel	€ -	€ 127.147,77	€ -
S355	€ -	€ 23.218,65	€ 310.131,82
Steel plate	€ -	€ -	€ 86.017,05
Gypsum sheet	€ -	€ -	€ 121.576,04
Transport	€ 35.109,11	€ 81.214,49	€ 23.804,38
TOTAL	€ 1.003.256,68	€ 900.248,58	€ 973.689,32

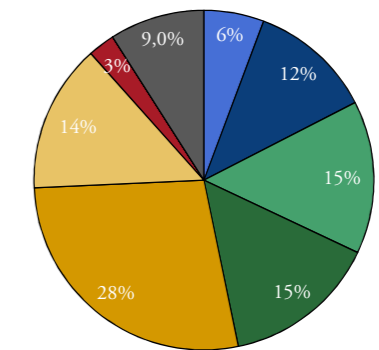
Total €ev including transport



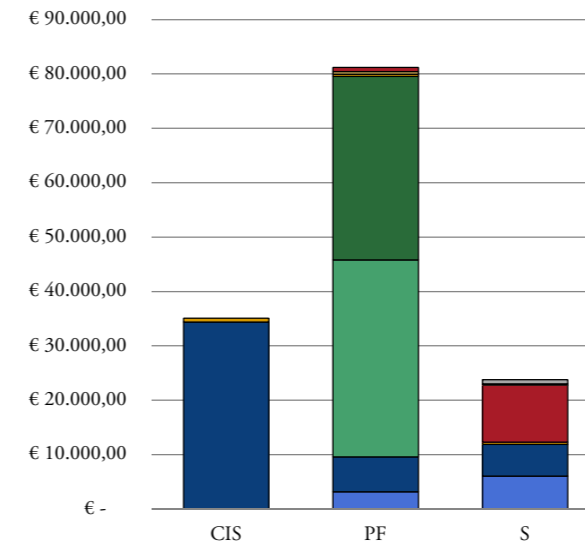
Environmental impact CIS



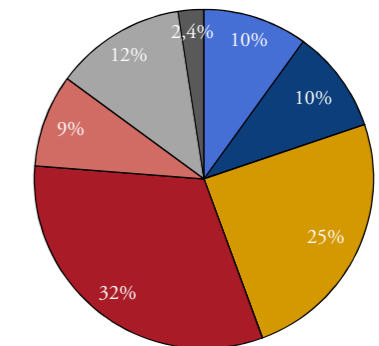
Environmental impact PF



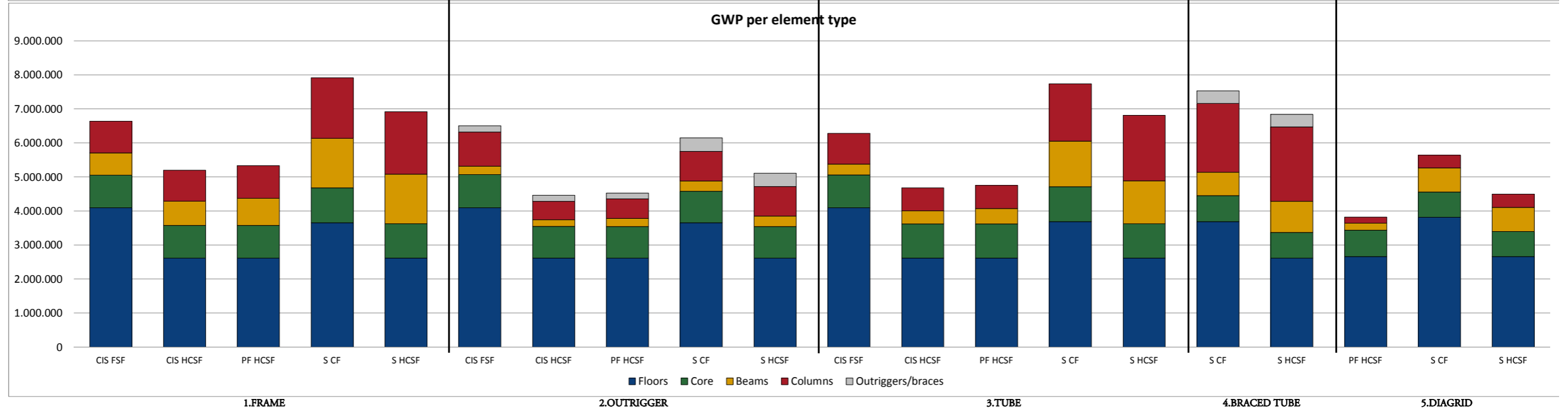
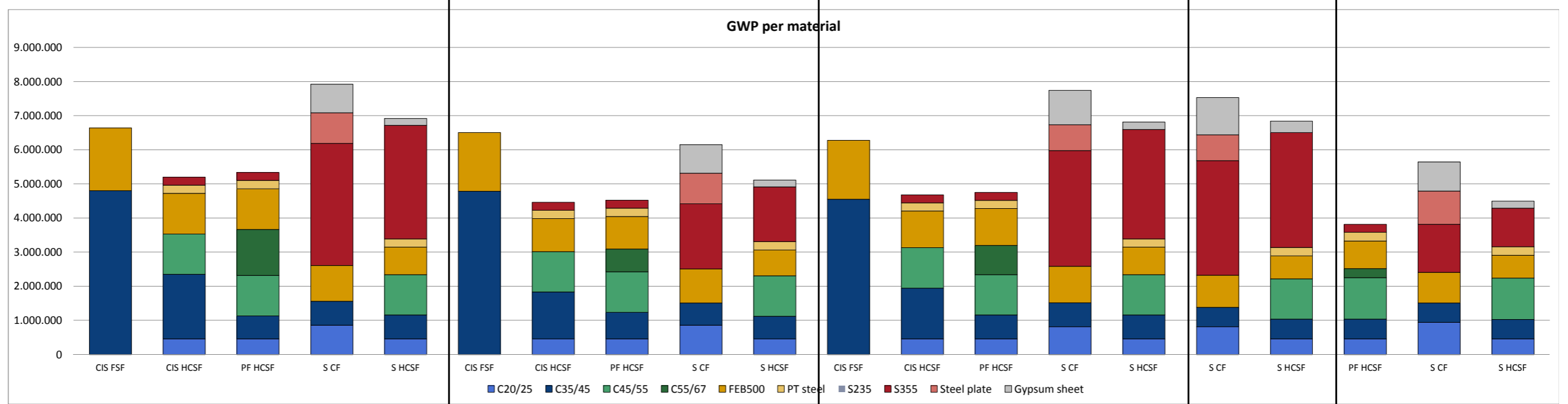
€ev from transport per material



Environmental impact S



■ C20/25 ■ C35/45 ■ C45/55
■ C55/67 ■ FEB500 ■ PT steel
■ S355 ■ Steel plate ■ Gypsum sheet



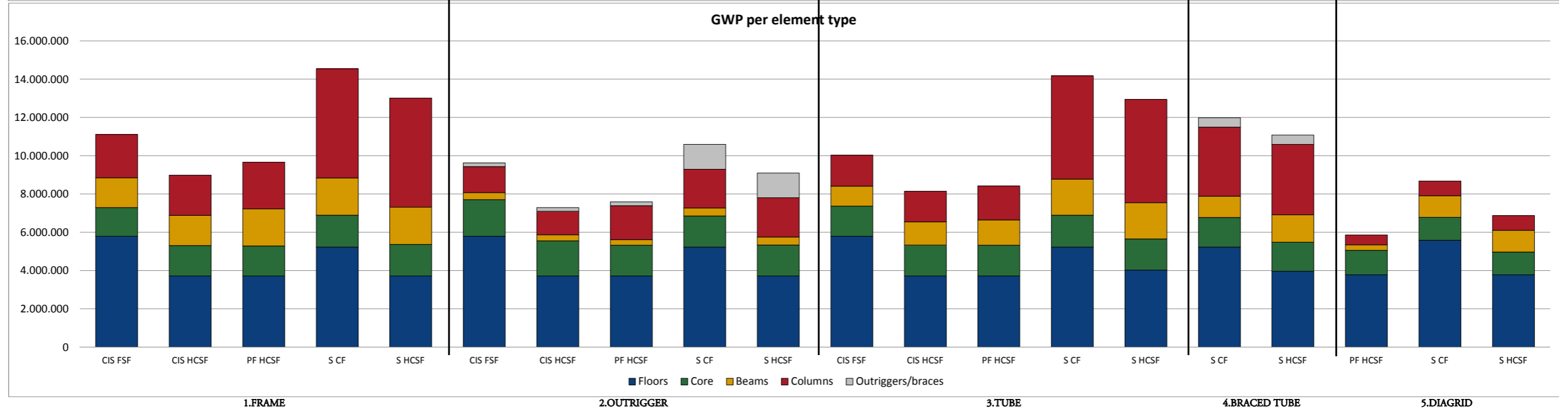
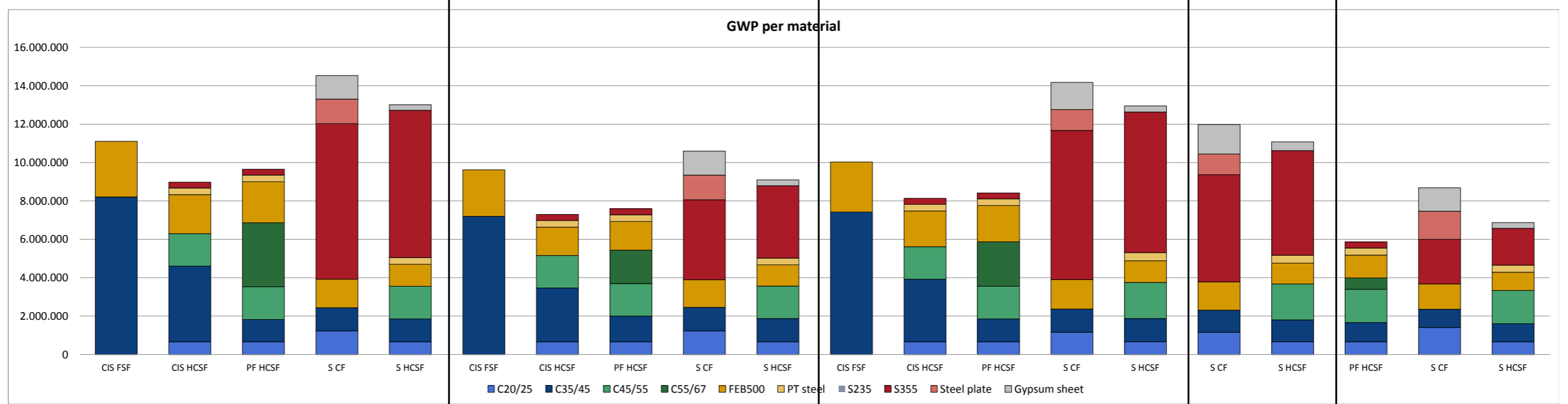
1.FRAME

2.OUTRIGGER

3.TUBE

4.BRACED TUBE

5.DIAGRID



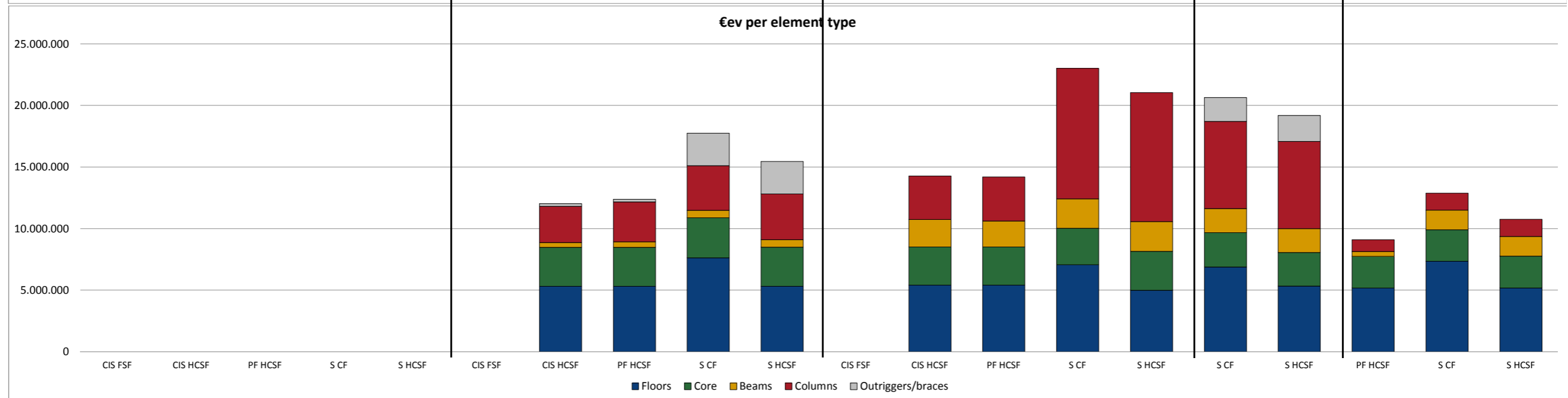
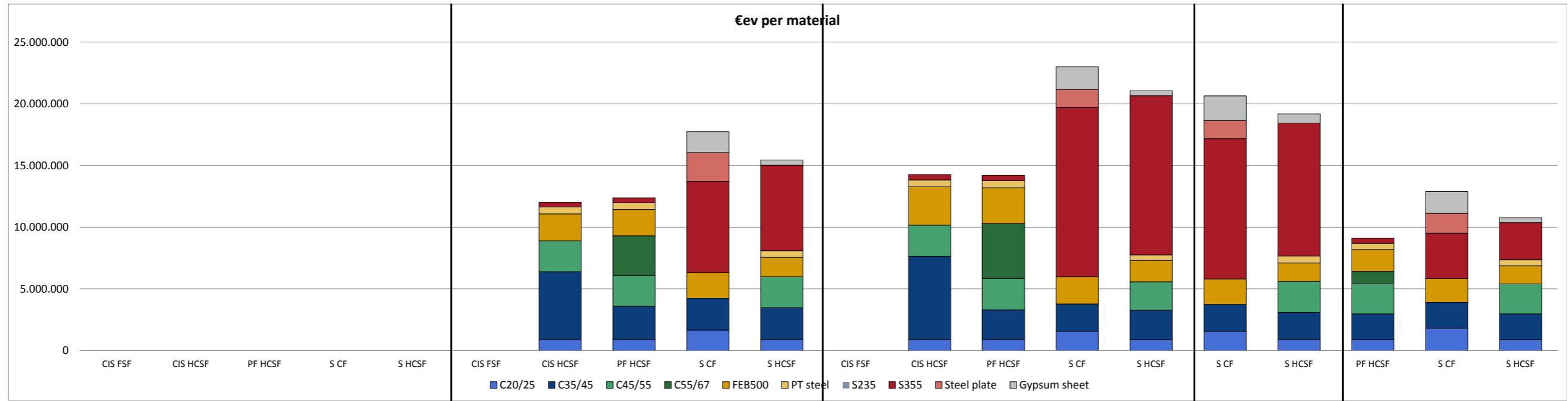
1.FRAME

2.OUTRIGGER

3.TUBE

4.BRACED TUBE

5.DIAGRID



1.FRAME

2.OUTRIGGER

3.TUBE

4.BRACED TUBE

5.DIAGRID